

**Response of Shallow Aquatic Ecosystems to Different
Nutrient Loading Levels**



Promotor: Dr. L. Lijklema, Hoogleraar Waterkwaliteitsbeheer

Robert Portielje

Response of Shallow Aquatic Ecosystems to Different Nutrient Loading Levels

Respons van ondiepe aquatische oecosystemen op verschillende nutriëntenbelastingnivo's

PROEFSCHRIFT

ter verkrijging van de graad van doctor
in de landbouw- en milieuwetenschappen,
op gezag van de rector magnificus,
dr. C.M. Karssen,
in het openbaar te verdedigen
op woensdag 19 oktober 1994
des namiddags te vier uur in de Aula
van de Landbouwniversiteit te Wageningen.

150 366171

CIP-DATA KONINKLIJKE BIBLIOTHEEK, DEN HAAG

Portielje, Robert

Response of shallow aquatic ecosystems to different
nutrient loading levels/ Robert Portielje.

- [S.l.:s.n.]. - Ill

Thesis Wageningen. - With ref. - With summary in Dutch.

ISBN 90-5485-275-5

Subject headings: eutrophication.

BIBLIOTHEEK
LANDBOUWUNIVERSITEIT
WAGENINGEN

The research described in this thesis was carried out at the Department of Nature Conservation, Water Quality Management Section, of the Wageningen Agricultural University, P.O. 8080, 6700 DD, Wageningen, The Netherlands.

Parts of the research were done in cooperation with the DLO-Winand Staring Centre for integrated Land, Soil and Water Research in Wageningen, The Netherlands, and with the DLO-Institute for Forestry and Nature Research in Leersum, The Netherlands

Aan mijn ouders

CONTENTS

	page
Chapter 1 Response of shallow aquatic ecosystems to different nutrient loading levels: - general introduction	9
Chapter 2 The accumulation of phosphorus in test ditches in relation to external loading from mass balances	35
Chapter 3 Primary succession of aquatic macrophytes in experimental ditches in relation to nutrient input	61
Chapter 4 The effect of reaeration and benthic algae on the oxygen balance of an artificial ditch	83
Chapter 5 Estimation of productivity from continuous oxygen measurements in ditches dominated by benthic algae	113
Chapter 6 Estimation of primary production in macrophyte dominated ditches from continuous dissolved oxygen signals	143
Chapter 7 Sorption of phosphate by sediments as a result of enhanced external loading	171
Chapter 8 Kinetics of luxury uptake of phosphate by algae dominated benthic communities	201
Chapter 9 Carbon dioxide fluxes across the air-water interface and its impact on carbon availability in aquatic systems	221
Chapter 10 Summary	247
Samenvatting	257
Abstract	265
Dankwoord	267
List of Publications	269
Curriculum Vitae	271

Chapter 1

Response of shallow aquatic ecosystems to different
nutrient loading levels:

- general introduction

1. INTRODUCTION

1.1 *Eutrophication, a general definition*

Although algal blooms had been reported long before, eutrophication became widely recognized as a water quality problem during the sixties (Vollenweider, 1968).

Eutrophication has been defined by the OECD (1982) as 'the nutrient enrichment of waters which results in the stimulation of an array of symptomatic changes, among which increased production of algae and macrophytes and deterioration of water quality, which are found to be undesirable and to interfere with water uses'.

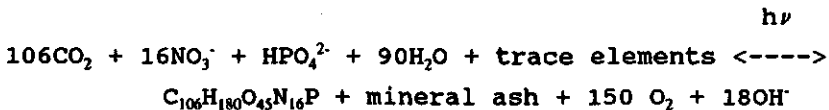
One can distinguish between natural and cultural eutrophication. Natural eutrophication is the natural aging of an aquatic system due to the inflow of eroded materials and atmospheric deposition, and results in the slow change from an aquatic to a terrestrial system. It is a slow, largely irreversible process. The time-scale depends on morphological and environmental factors controlling the inflow of allochthonous material, and is usually in the order of hundreds of thousands of years for large lakes (Ryding and Rast, 1989: p2). Generally natural water bodies are characterized by a good water quality and a diverse biological community throughout their existence. Cultural eutrophication, on the other hand, is the excessive inflow of nutrients into an aquatic system due to human activities. It is a relatively fast process that deteriorates the water quality and reduces the biological diversity of the system to a variable, but frequently large extent. In a number of cases it has been shown to be reversible (Cullen and Forsberg, 1988).

Cultural eutrophication has since decades been of major concern to water quality managers. Excessive nutrient availability has resulted in an increased primary productivity, manifesting itself in algal or macrophyte blooms. The resulting enhanced dissolved oxygen fluctuations in turn may cause

occasional fish kills. A general feature of a higher trophic state is the intensification of internal cycles within an aquatic ecosystem. As pointed out by Rohde (1969), the trophic state of a system is characterised by rates rather than by biomass: higher primary production rates, and, as a result of adaptation to an enhanced availability of organic matter, also higher decay rates.

The trophic state and the saprobic state of an ecosystem, both reflected in indicator organisms (Leentvaar, 1980), may change in time and are interrelated (Caspers and Karbe, 1966).

The initial response of an aquatic ecosystem following enhanced nutrient availability is an enhanced autotrophic activity. The autotrophic activity of an ecosystem will be limited by constraints imposed by any of the ingredients of the photosynthesis reaction, of which the stoichiometry can be roughly represented by (from Uhlmann, 1975):



whereas the photosynthesis rate is:

$$P_{T^{\circ}\text{C}} = P_{\text{max},T^{\circ}\text{C}} \cdot F(I) \cdot F(N) \cdot F(T) \quad (1)$$

with $P_{T^{\circ}\text{C}}$ the actual photosynthesis rate, $P_{\text{max},T^{\circ}\text{C}}$ the maximum rate at temperature T , and $F(I)$ and $F(N)$ (both between 0 and 1) the limitation factors with respect to light and nutrients: phosphorus, nitrogen and inorganic carbon. $F(T)$ is a correction factor for the rate at the actual temperature in comparison with a reference temperature. In small waters competition for space also may become important, especially in dense near-surface vegetations of aquatic macrophytes. A widely accepted view, based on observations (Droop, 1973; Rhee, 1978) is that in any system with nutrient limitation essentially only one of the nutrients is actually growth-limiting. Therefore $F(N)$ is determined by the minimum of limitations imposed by any of the

nutrients C,N and P:

$$F(N) = \min \{ F_C , F_N , F_P \} \quad (2)$$

Rhee (1978) found an atomic N:P ratio of 30 to be the transition from N to P limitation in *Scenedesmus* sp., and found no evidence for a multiplicative effect of limitation by both N and P. However, other authors (Kunikane et al., 1984; Kunikane and Kaneko, 1984) reported a multiplicative effect of both nutrients on growth of *Scenedesmus dimorphus* under a wide range of total-N : total-P ratios from 4-110.

Phosphorus has generally been acknowledged as the limiting factor in natural fresh water systems, but alternating limitation of photosynthesis in lakes by P, N and light have been reported (Zevenboom, 1980). The limiting nutrient concept seems only valid at steady-state conditions, but is not very useful in transient state situations resulting from irregular nutrient inputs (Odum, 1971).

The availability of the individual nutrients in a particular system usually are not independent. Agricultural run-off and effluent of waste water treatment plants are responsible for an influx of N as well as P and C, although the ratios of the different nutrients may vary. Another example is the enhanced atmospheric carbon dioxide influx into a water body following a pH increase due to a higher primary production, which in turn results from a higher trophic state with respect to N and P (see chapter 9).

A simple method to indicate the actual rate-limiting nutrient is through the analysis of the ratios of bioavailable C,N and P and comparison with the ratios indicated by the stoichiometry of the photosynthesis reactions. In practice however this is an oversimplification, since the optimum N:P ratio may vary significantly (Forsberg and Ryding, 1980) and even the exact stoichiometry of the photosynthesis reaction is still debated and depends e.g. on the nitrogen source used (Stumm and Morgan, 1981). A better assessment can be obtained from bioassays

(Klapwijk, 1988), if properly conducted and interpreted (Ryding and Rast, 1989).

The extent to which a system is limited by nutrient availability cannot be determined from concentrations only. The fluxes through the biotic compartment are in this sense more important, as low concentrations do not exclude relatively high fluxes. This depends on the rate constants of nutrient release and uptake. Moreover, due to luxury storage of phosphorus low external concentrations can be accompanied by high intracellular concentrations in the primary producers.

1.2 Developments in eutrophication research

Insight in the effect of an input variable on the response of large scale natural systems has at first been obtained from steady state models relating a state variable to an input variable through empirical relationships. An example of such a statistical approach in the field of eutrophication are the well known OECD relationships (Vollenweider and Kerekes, 1980) that relate the observed P-concentrations to the areal P-loading rate L , the hydraulic load q_s , and the hydraulic detention time τ of the basin:

$$P = \frac{1}{1 + \sqrt{\tau}} \frac{L}{q_s} \quad (3)$$

In such an approach, the underlying physical, chemical and biological mechanisms are not considered. For instance, the dimensions in the equation are not correct. The model provides an estimation of the trophic state of lakes without the requirement of an extensive data base, and has been shown to be of some practical use. The confidence intervals of the output variables are however very wide. The value of this approach is therefore restricted to a global insight in the trophic state of a system, and application to one specific lake has many pitfalls (Reckhow and Chapra, 1979).

In order to obtain more specific information eutrophication

research has focussed more and more on providing a conceptual basis. This is a prerequisite for prediction of the long-term development of a system in relation to a variable level of external nutrient loading, when the assumption of steady-state is not valid. The behaviour of a water system as a whole depends on the dynamic interactions between all of its components, and therefore has a high degree of complexity. Modelling implies a reduction of the number of state variables and interactions, by taking into account only those that determine the behaviour of the system to the largest extent. A firm reduction may suffice for short term analysis, but extrapolation to long term predictions often is difficult, as those interactions that may be negligible initially, may become significant later on. The sensitivity of the output signal for a state variable is usually the criterium for incorporation of that state variable in a model structure. For the purpose of dynamic modelling three main features need consideration (Ryding and Rast, 1989: p107):

- 1) physical system boundaries and boundary conditions
- 2) hydrological and hydrodynamic characteristics
- 3) chemical and biological transformations

ad 1) the terms describing inputs and outputs across the boundaries of the system determine the external mass balance of a variable. This indicates the direction of the long term change of the trophic state of a system.

ad 2) the hydrodynamic conditions determine whether a system can be assumed ideally mixed or that a spatial variability exists. The latter is the case when transport processes are slow in comparison with the transformations determining the sources and sinks of a state variable. Implementation in models obliges a spatial segmentation, that can be done with respect to 0 (completely mixed), 1, 2 or 3 dimensions.

ad 3) the internal (re)distribution of nutrients determines the actual trophic state, and therefore the transformations

need to be implemented. The sediment can be treated either as a black-box, in which case the sediment-water interface is the system boundary, or as a part of the system, in which case a definition and quantitative formulation of the biological and chemical interactions within the sediment is required. This requires a thorough understanding of sedimentary processes and their kinetics. Transport processes, which are much slower in the sediment than in the overlying water, play a dominating role in the determination of sediment fluxes. Due to the vertical attenuation of turbulence and the presence of particles, transport may become rate limiting. In the absence of vertical advective flow due to seepage or infiltration, vertical transport within the sediment is determined by diffusive mechanisms. These are difficult to calibrate, but determine to a large extent the actual fluxes. Advective flow is relatively easy to measure, and in case advective transport dominates, the uncertainties in sedimentary transport processes are relatively small. Inclusion of the sediment in the model structure always obliges a vertical spatial segmentation due to the slowness of interstitial and solid-phase transport in comparison with biological and chemical transformations.

1.3 State variables

Knowledge of the kinetics of dynamic interactions is a prerequisite for a proper decision whether a certain state variable or interaction should be included in the systems description, i.e. the model structure. Problems usually arise when processes that are recognized to be important cannot be measured with enough accuracy, or when their dependency on environmental factors can not be quantified. Although simplification is unavoidable, oversimplification may often result in erroneous results. An example in the field of eutrophication modeling is the use of fixed conversion factors for biomass and nutrient contents by assuming photosynthesis and nutrient uptake to be synchronous processes. The P content of cells can

vary an order of magnitude due to the fact that phosphorus uptake and storage on one hand and photosynthesis on the other are processes, that are only coupled with each other through the internal phosphorus content of the cells. Photosynthesis causes a flux from internally stored P to organic compounds, for which the photosynthesis stoichiometry can be assumed, but this represents thereby only a fraction of the total P content of the cells.

The role of the sediments and sedimentary processes occurring in the sediments also have often been simplified by using instantaneous equilibria or fixed boundary conditions (fluxes) instead of taking into account the kinetics of the processes and their mutual interactions.

Steady-state conditions will hardly ever occur, and when considering dynamic interactions, attention should be paid to the rate constants of individual interactions.

In eutrophication research most attention has been paid to the occurrence of algal blooms. Algae are commonly seen as the organisms that cause the nuisances related to eutrophication (Van Straten, 1986). This holds particularly for shallow lakes, in which the original vegetation of rooted and/or submerged macrophytes is in an unfavourable competitive position with respect to light in comparison with epiphytic algae, resulting in a decline of macrophytes, and giving way to phytoplankton blooms (Philips et al., 1978). In tropical, but also in small shallow water bodies in temperate regions, nuisances may also be attributed to macrophytes. As eutrophication implies the alleviation of nutrient limitation, the competition for light and space becomes the main factor determining the success of a species. Therefore macrophyte species capable of locating their photosynthetic active sites as close to or even above the water surface are in an advantageous position. In hypertrophic, small, shallow water bodies often a dense vegetation of floating or emergent macrophytes may develop. Floating macrophytes may cover the whole water surface. They obtain their required nitrogen and phosphorus from

the water phase, and a substantial part of the carbon directly from the atmosphere. The deteriorating effect on the water quality is evident: the water phase is reduced to a compartment where mainly decomposition takes place, resulting in severe oxygen deficiencies.

1.4 Measures for eutrophication control.

The best solution to any problem, or at least the first to consider, is the removal of the basic cause of the problem. In eutrophication control this simply means a reduction of the nutrient load to surface waters. Analysis of the contributions by various sources through watershed models yields information on how this can be achieved, as insight into the quantitative contributions of all diffusive and non-diffusive sources is obtained. Thus insight is provided into what measures most efficiently reduce the total load. Quality models for the receiving water however have to provide information on what reduction is actually needed to achieve a desired improvement in water quality.

The success of these models in predicting the future water quality depends on the accuracy of the description of the internal interactions. Practical experiences have shown that the recovery of the water quality after a reduction of the nutrient load to surface waters may vary considerably (Cullen and Forsberg, 1988; Sas, 1989), as internal factors and resilience in a system play an important role.

Besides reduction of the external load also other management tools for controlling eutrophication have been applied, e.g.:

- Chemical or physical treatment

Chemical treatment usually involves the use of a phosphate sorbing or precipitating agent to immobilize the dissolved phosphorus pool. It has been applied in various situations in different ways, for example by injecting FeCl_3 in the upper sediment layers (Boers, 1991), thereby enhancing the adsorpti-

ve capacity of the sediment. Aluminum salts have also been used for this purpose, and the effects on sediment P-release were long-lasting (Cooke et. al, 1993): they are brought into the water, and while settling of the flocs formed these can remove a considerable part of the dissolved phosphorus by precipitation. Alternatively, salts can be injected directly into the sediments. Oxidation of the sediment and precipitation of P has also been attempted by injection with $\text{Ca}(\text{NO}_3)_2$ (Ripl, 1976)

In case of severely polluted sediments dredging of the loose nutrient-rich surface layer of the sediment can be a tool for the restoration of a lake (Björk, 1978)

Flushing of a eutrofied water body with allochthonous water relatively poor with nutrients has also been applied (Hosper, 1985; Jagtman et al., 1992). When the concentrations in the supply water are lower than that of the water itself, the enhanced flushing rate causes both a dilution and an enhanced loss of nutrients through discharge, and will accelerate the recovery of lakes in which internal loading is high. Moreover, the inlet of allochthonous water can also cause the inlet of P-immobilizing components, such as Fe-(hydr)oxides or CaCO_3 .

- Biomanipulation

The decline of the macrophyte community due to competition by epiphytic algae and the resulting phytoplankton blooms, also reduces the possibilities of survival of fish that depends on submerged macrophytes for spawning or as a refuge for young fish. Moreover, the sediment structure is altered severely by the vanishing of macrophytes, and a further increase in turbidity follows from enhanced sensitivity for resuspension by wind action and/or by benthivorous fish. Biomanipulation implies an intervention in the food-web in favour of piscivorous fish, zooplankton and submerged macrophytes, and against benthivorous or planktivorous fish and phytoplankton (Gulati et al., 1990).

1.5 *Experimental ditches for eutrophication research*

The primary measure for eutrophication control is a reduction of the external nutrient load. Quantitative assessment of the relation between the external nutrient load and the trophic state of a water body, as indicated by several state variables, has to be obtained from research on the chemical and biological transformations within a system.

To allow a proper establishment of the effects of the external nutrient load on the trophic state, other input variables that influence the behaviour of the system should be controlled, or at least known, as much as possible. A proper estimation of these effects in natural waters is often blurred by differences in morphology, environmental conditions and uncertainties in the other input variables. Resuming, the three categories of terms on which quantitative information has to be available, and that determine system behaviour are (Ryding and Rast, 1989: p107):

- 1) physical system boundaries and boundary conditions
- 2) hydrological and hydrodynamic characteristics
- 3) chemical and biological transformations

An experimental design is needed, which allows research on the biological and chemical transformations as they are occurring under natural conditions. These transformations then can be related to the input across the systems boundaries. This means to study 3) while manipulating 1) and controlling 2).

For this purpose an experimental system of ditches has been constructed. In spring 1988 the construction was completed under the supervision of the DLO Winand Staring Centre for Integrated Land, Soil and Water Research in Wageningen, the Netherlands. The project was financed by the Directorate for Agricultural Research of the Ministry of Agriculture, Nature Management and Fisheries.

There are 20 ditches, 12 of which are used for ecotoxicolo-

gical research and 8 for eutrophication research. The ditches used for eutrophication research comprise four ditches with a clayish sediment and four ditches with sand as the bottom material. In the clay ditches, a sediment layer, with a thickness of 0.25 m, taken from a mesotrophic fen near Wijchen in The Netherlands, has been brought in. In the sand-ditches a bottom layer with a thickness of 0.2 m has been applied.

The ditches are located near Renkum in the central part of The Netherlands. The ditches have a length of 40 m and a width of 1.6 m at the bottom. On both sides is a gravel bank with a slope of 30°. The water depth can be regulated with an overflow funnel, but during the research reported in this thesis it was maintained at 0.50 m in the middle of the ditch. The average depth therefore is 0.38 m. The ditch system is separated from the environment by a water-impermeable foil, to preclude seepage or infiltration, or diffusive exchange with the soil and groundwater. The ditches are fed by precipitation, and, during dry periods, the inlet of local groundwater to maintain the desired water level.

An experimental design was chosen in which the four ditches of both sediment types were exposed to four different levels of external nutrient (N and P) input, while all other input variables were kept the same for all ditches. The hydrological conditions, and thus the individual terms of the water balance, thus were similar for all individual test systems. The water balance W ($L^3.T^{-1}$) is:

$$W = \text{Precipitation} + \text{Groundwater inlet} - \text{Evaporation} - \text{Discharge} \quad (4)$$

Precipitation and discharge are measured. The inlet of groundwater, which serves to maintain a constant water level, is dosed and measured as the automatically counted number of tipping-buckets with a known volume. Evaporation is the rest term of the water balance. Checks have been carried out and these showed that the water balances were correct within acceptable

margins (Drent and Kersting, 1993).

A detailed description of the instrumentation for collection and analysis of precipitation and discharge samples, and of the hydrological possibilities of the ditches, are given by Drent and Kersting (1993).

The hydrodynamic conditions depend on the geometry of the system and their exposure to meteorological conditions (wind action, solar irradiance etc.). Differences in the hydrodynamic conditions between individual test systems, that bias the assessment of the effect of the particular input variable to be investigated, are eliminated to a large extent by the design of the ditches. They are all identical with respect to shape, geometry, and orientation in the wind-field. The distance from one side of the ditch plant to the other is about 200 m, so a spatial variability in meteorological conditions can be neglected. The ditch plant is situated in a flat and open terrain without irregularities that can locally influence the wind field. However, due to the development of differences in vegetation types at different trophic levels in time, the dissipation of wind-generated turbulence will tend to deviate among the different test systems. For example, a dense vegetation of submerged macrophytes near the water surface will cause different hydrodynamic conditions in the near bottom region than in case of an open water column. The same applies to a cover of floating macrophytes.

The development of a system depends to a large extent on the initial conditions, especially during the first period after the construction. A proper investigation of the effects of the level of external nutrient input on the response of a system is therefore only possible if the initial conditions are to a large extent equal. This was true due to the construction and the introduction of homogenized sediment material etc. (Drent and Kersting, 1993)

1.6 Assessment of the levels of external nutrient loading to the ditches.

Four different levels of external nutrient loading were implemented. The nutrient loading programme was started in May 1989 and maintained for a period of four years.

An a priori choice was made for the first ditch (A, reference) to receive a level of nutrient input as low as possible. The background loading rate, originating from dry and wet atmospheric input and inlet of groundwater, was originally estimated at $0.03 \text{ g P.m}^2.\text{yr}^{-1}$ and $3.3 \text{ g N.m}^2.\text{yr}^{-1}$, based on total P and total N analyses of precipitation samples from a nearby meteorological station at Deelen. Later on, after analysis of the dry and wet atmospheric P deposition at the site itself during the running of the programme, the actual background level of phosphorus input was shown to be $0.11 \text{ g P.m}^2.\text{yr}^{-1}$.

The second level was based upon guidelines provided by the Dutch advisory committee CUWVO (Lijklema et al., 1989). They developed empirical relationships between the observed total P and total N concentrations in a large number of Dutch surface waters and the external P input, as a function of the mean retention time of the water and the average water depth. For the second level of external nutrient loading a loading rate was chosen that corresponds through these relationships with an expected total P concentration of 0.15 g P.m^{-3} and 2.2 g N.m^{-3} . These concentrations are considered as 'basic quality' in the Dutch water quality policy. The relationships yielded a desired input of $0.43 \text{ g P.m}^2.\text{yr}^{-1}$ and $1.59 \text{ g N.m}^2.\text{yr}^{-1}$. Because of the shallowness of the ditches in comparison with the waters from which the empirical relationships were derived, extrapolation of these relationships to an average depth of 0.38 m was necessary. This second level of external loading rate is referred to as the B (1x CUWVO) level. The background loading rate with N was already twice the desired input for the B level, but the background P loading rate was low. It was therefore decided to supply an additional, manually added P-input of $0.4 \text{ g P.m}^2.\text{yr}^{-1}$. No extra N was supplied.

The third level assigned is at a level that is three times the second. In this ditch (C, 3x CUWVO) an additional N input has

to be supplied, and the choice has been made for an N:P ratio in the external loading rate of 6:1 by weight.

The last ditch (D) was to receive a very high level of external nutrient input. Besides the wish to cover a wide trophic range, another argument for the latter was to accomplish sufficient P-accumulation in the sediment during the four years of the loading programme. This enables future research on the recovery of heavily eutrophied systems, with a large sedimentary P-pool, after a reduction of the external nutrient load in the near future. The highest loaded ditch receives about 25x the input of that of the second ditch, with again an N:P ratio of 6:1 by weight. The dosages to the second (B) and third (C) ditch are given in two portions per year, in May and late October. The highest loaded ditch originally (in 1989 and 1990) received monthly dosages, but due to problems with ice cover during the winter, this has been changed into 10 portions per year since 1991: from early March until the end of November. Table 1.1 summarizes the manually added levels of external nutrient input.

Table 1.1. Manually added N- and P-input ($\text{g}\cdot\text{m}^2\cdot\text{yr}^{-1}$).

level	description	N	P	remarks
A	Reference	-	-	
B	1x CUWVO	-	0.4	2x per year
C	3x CUWVO	4.5	1.2	2x per year
D	highest	72.0	12.0	10x per year

The first dosages were given in May 1989. Nutrients are added as K_2HPO_4 and NH_4NO_3 , dissolved in tap water and homogeneously distributed over the water surface through a sprinkler from a transportable apron just above the water surface.

1.7 Continuous measurements of water quality and environmental variables.

A number of variables, which are considered necessary for the study, are continuously measured and stored. These include water quality and environmental variables.

In the middle of the ditches dissolved oxygen (2 depths, 10 cm and 40 cm below the water surface), pH (25 cm below the water surface) and temperature (3 depths: 10, 25 and 40 cm below water surface) are measured every 30 seconds, and registered in a data-logger as fifteen minute averages.

Environmental variables that are continuously measured by a weather station from Campbell Scientific Ltd. (Shepshed Leicestershire, UK) are: light irradiance, wind speed, wind direction, air pressure, relative air humidity, air temperature and precipitation. A detailed description of the measuring instruments at the weather station is provided by Drent and Kersting (1993).

1.8 Sediment composition in the ditches

The sand and the clay that were used as sediment were low in nutrient content and uncontaminated.

The sediment of the clay-ditches originated from a mesotrophic fen, the 'Wezelse Plas', near Wijchen in the Netherlands. The procedure for sampling and transport and finally the deposition of the sediment in the test ditches was designed in such a way that a well mixed homogeneous sediment was obtained, with an equal composition in all ditches.

Sediment was collected from the fen with a suction-pipe and placed in a depot. After settling, the overlying water was removed. The sediment was mixed again, loaded on a truck and transported to the site of the ditches, where it was stored in a depot. It was homogenized well just before it was brought into the ditches as a layer with a constant thickness of 0.25 m. The ditches were filled with local groundwater with low nutrient concentrations. During an incubation period of one year, without any human interference, the ditches developed an ecosystem that in all four clay-ditches consisted of a

homogeneous Chara vegetation with an areal coverage of over 90 %.

In the sand-ditches no vegetation of aquatic macrophytes had developed, due to the absence of a seedbank. On top of the sand a distinct layer mainly consisting of settled algae had started to develop.

The eutrophication experiments started after one year with the start of the external loading program.

Just before the first nutrient dosage an extensive sampling and analytical program was carried out for the determination of the initial sediment composition. This included:

- a- Particle size distribution of the sediment;
- b- Vertical profiles of porosity and dry weight concentrations;
- c- P-content of the sediment and P-fractionization according to the extraction scheme by Hieltjes and Lijklema (1980);
- d- A number of other parameters;

ad a) The particle size distribution of the clay ditches is given in table 1.2.

ad b) The results of the determination of the vertical profiles of porosity ϵ and dry weight content DW (kg dry weight.m³) are given in table 1.3. The high standard deviations in the dry weight content of the top 5 mm layers may result from the difficulty of a separation at exactly 5 mm, and the sharp decrease in the porosity with depth in the top layer.

ad c) The initial P-content at the start of the loading programme was determined as the average P content of the whole sediment column. Results of the extractions are summarized in table 1.4. The table shows that the P-content of the clayish sediment is low and that the variation is small. The slightly higher P-concentration in the 3x CUWVO clay-ditch is mainly due to a higher NaOH-extractable fraction.

Table 1.2. Particle size distribution of the sediment of the clay- and sand-ditches (% of dry weight)

ditch	< 2	2-16	16-50 (μm)	50-105	105-2000
clay-ditches					
A, reference	10.9	4.3	5.3	4.0	74.1
B, 1x CUWVO	10.0	3.7	4.6	4.5	76.2
C, 3x CUWVO	9.8	3.4	4.5	4.0	77.3
D, highest	10.4	3.7	5.9	4.2	74.0
average	10.3	3.8	5.1	4.2	75.4
st. dev.	0.4	0.3	0.6	0.2	1.4
sand-ditches					
A, reference	1.3	0.1	0.0	0.5	98.0
B, 1x CUWVO	1.0	0.3	0.0	0.4	98.0
C, 3x CUWVO	1.1	0.1	0.0	0.3	98.5
D, highest	1.3	0.1	0.0	0.8	97.7
average	1.2	0.2	0.0	0.5	98.1
st. dev.	0.1	0.1	-	0.2	0.3

Table 1.3. Average porosity and dry weight content of sublayers in the clay-ditches (n=16) and sand-ditches (n=4) and the relative standard deviations RSD.

depth in sediment	ϵ ($\text{m}^3 \cdot \text{m}^{-3}$)	RSD (%)	DW ($\text{kg} \cdot \text{m}^{-3}$)	RSD (%)
clay-ditches				
0- 5 mm	0.794	8.8	281	43.6
5-10 mm	0.633	17.6	887	29.7
10-20 mm	0.448	14.1	1349	11.6
20-30 mm	0.391	11.4	1562	5.5
30-50 mm	0.367	7.1	1556	4.3
sand-ditches				
0- 5 mm	0.710	7.7	710	24.3
5-10 mm	0.431	7.5	1484	8.5
10-20 mm	0.314	3.7	1699	1.7
20-30 mm	0.315	4.6	1817	4.9
30-50 mm	0.295	6.6	1705	3.1

Table 1.4. Extractable P-fractions according to the scheme by Hieltjes and Lijklema (1980).

ditch:	fraction: NH ₄ Cl a	NaOH-ort	NaOH-tot b	HCl c	tot a+b+c
	(mg P. [g DW] ⁻¹)				
clay-ditches					
A, reference	0.03	0.16	0.18	0.03	0.24
B, 1x CUWVO	0.02	0.12	0.17	0.03	0.22
C, 3x CUWVO	0.02	0.17	0.22	0.05	0.29
D, highest	0.01	0.10	0.18	0.05	0.24
sand-ditches					
A, reference	0.02	0.03	0.08	0.01	0.11
B, 1x CUWVO	0.02	0.03	0.07	0.02	0.11
C, 3x CUWVO	0.01	0.03	0.08	0.02	0.10
D, highest	0.01	0.03	0.08	0.02	0.10

ad d) Some other sediment characteristics are given in table 1.5.

Table 1.5. Chemical characteristics of the sediment in May 1989.

parameter:	ditch:	highest	3x CUWVO	1x CUWVO	Reference
clay-ditches					
total N (mg/g DW)		0.41	0.45	0.60	0.54
Org. Mat. (% of DW)		0.8	0.7	0.7	0.8
CaCO ₃ (% of DW)		0.4	0.3	0.3	0.6
Fe total (mg/g DW)		12	10	11	12
sand-ditches					
total N (mg/g DW)		0.07	0.03	0.05	0.04
Org. Mat. (% of DW)		0.1	0.1	0.2	0.1
CaCO ₃ (% of DW)		<0.1	<0.1	<0.1	<0.1
Fe total (mg/g DW)		1.7	1.6	1.8	1.8

The total N and organic matter concentrations in the sediment are all low. Only a minor fraction of total Fe is in the oxalate-extractable form, which is of importance for the P-sorption capacity of the sediments: ca. 3 mg Fe.[g DW]⁻¹ in the clay-ditches, and ca. 0.07 mg Fe.[g DW]⁻¹ in the sand-ditches.

1.9 Outline of this thesis

The overall scope of this thesis is the study of the effects of different levels of external nutrient loading on small scale aquatic ecosystems with respect to their functioning and structure.

The emphasis is on the chemical and biological transformations that control the cycling of phosphorus, and the relationships between the level of nutrient input and the primary productivity of the receiving ecosystem.

The study is done in cooperation with the DLO-Winand Staring Centre for Integrated Land, Soil and Water Research in Wageningen, the Netherlands, which concentrate on N budgets and transformations, and the DLO-Institute for Forestry and Nature Research in Leersum, the Netherlands, which cooperated on the study of primary productivity.

Chapter 2 addresses the P-accumulation in sediment, water and vegetation, and the loss of P through the outflow. The aim of this chapter is to provide insight into the internal distribution of the phosphorus input into the system, and the recovery of P from these pools. This then can be compared with the external P mass balances.

Chapter 3 discusses the development of the aquatic macrophytes community in the clay ditches. It is interpreted both in terms of species composition and dominant growth form in relation to the level of external N and P loading.

Chapter 4 addresses the modelling of the oxygen budgets of the reference sand-ditch based on measured process parameters. The emphasis is on primary production by a benthic community dominated by algae and reaeration. It serves as a basis for chapters 5 and 6.

Chapters 5 and 6 deal with the estimation of primary production and oxygen consumption from continuous dissolved oxygen concentrations over a two years period for the sand and the clay ditches respectively. The highest loaded ditches were not considered in this study, as very frequent and long-

lasting anaerobia inhibited the use of the method.

Chapter 7 treats a descriptive model for the transport and subsequent sorption of phosphate in the sediment of the highest loaded sand-ditch. Emphasis is put on physical transport processes and on the kinetics and time-scales of fast and slow sorption processes.

Chapter 8 deals with the kinetics of phosphorus uptake by the benthic communities of the sand-ditches. These communities were dominated by algae. The highest loaded ditch was again excluded in this study.

Chapter 9 describes a model for the exchange of carbon dioxide across the air-water interface and its application on the ditches, using continuously measured pH and wind measurements. The aim of this chapter is to provide insight into the extent to which atmospheric exchange can cover the carbon requirements of the primary producers and to study the dependency of carbon dioxide exchange on environmental conditions.

A summary (in Dutch and in English) of the results of the individual chapters and the main conclusions is given in chapter 10.

REFERENCES

- Björk, S., 1978. Redevelopment of lake ecosystems. A case-study approach. *Ambio* 17, 90-98.
- Boers, P.C.M., 1991. The release of dissolved phosphorus from lake sediments. PhD Dissertation, Agricultural University Wageningen, The Netherlands, 138 pp.
- Carignan R. and J. Kalff, 1980. Phosphorus sources for aquatic weeds: water or sediments ? *Science* 207, 987-988.
- Caspers, H. and L. Karbe, 1966. Trophie und Saprobität als stoffwechselfeldynamischer Komplex. *Arch. Hydrobiol.* 61, 453-470.
- Cooke, G.D., E.B. Welch, A.B. Martin, D.G. Fulmer, J.B. Hyde & G.D. Schriever, 1993. Effectiveness of Al, Ca and Fe salts

- for control of internal phosphorous loading in shallow and deep lakes. *Hydrobiologia* 253, 323-335.
- Cullen, P & C. Forsberg, 1988. Experiences with reducing point sources of phosphorus to lakes. *Hydrobiologia* 170, 321-336.
- Drent, J. and K. Kersting, 1993. Experimental research in ditches under natural conditions. *Water Res.* 27 (9), 1497-1500.
- Droop, M.R., 1973. Some thoughts on nutrient limitation in algae. *J. Phyc.* 9, 264-277.
- Forsberg, C. and S.O. Ryding, 1980. Eutrophication parameters and trophic state indices in 30 Swedish waste-receiving lakes. *Arch. Hydrobiol.* 89, 189-207.
- Gulati, R.D., E.H.R.R. Lammens, M.-L. Meijer and E. van Donk, 1990. Biomanipulation, Tool for Water Management. Proceedings of an International Conference held in Amsterdam, the Netherlands, 8-11 August, 1989. Kluwer Academic Publishers, Dordrecht [etc.], 628 pp.
- Hieltjes, A. and L. Lijklema, 1980. Fractionation of inorganic phosphates in calcareous sediments. *J. Envir. Qual.* 9, 405-407.
- Hosper, S.H., 1985. Restoration of Lake Veluwe, The Netherlands, by reduction of phosphorous loading and flushing. *Water Sci. Tech.* 17, 757-786.
- Jagtman, E, D.T. Van der Molen and S. Vermij, 1992. The influence of flushing on nutrient dynamics, composition and densities of algae and transparency in Veluwemeer, The Netherlands. *Hydrobiologia* 233, 187-196.
- Klapwijk, S.P., 1988. Eutrophication of surface waters in the Dutch polder landscape. Dissertation Technical University Delft. 227 pp.
- Kunikane, S., M. Kaneko and R. Maehara, 1984. Growth and nutrient uptake of green alga, *Scenedesmus dimorphus*, under a wide range of nitrogen/phosphorus ratio-I. *Water Res.* 18 (10), 1299-1311.

- Kunikane, S. and M. Kaneko, 1984. Growth and nutrient uptake of green alga, *Scenedesmus dimorphus*, under a wide range of nitrogen/phosphorus ratio-II. *Water Res.* 18 (10), 1313-1326.
- Leentvaar, P., 1980. Comparison of hypertrophy on a seasonal scale in Dutch inland waters. In: J. Barica and L.R. Mur (eds.), *SIL Workshop on Hypertrophic Ecosystems*, Vaxjö, September 10-14, 1979, p 45-55.
- Lijklema, L., J.H. Jansen and R.M.M. Roijackers, 1989. Eutrophication in the Netherlands. *Wat. Sci. and Technol.* 21, 1899-1902.
- Novozamsky, I., V.J.G. Houba, R. van Eck and W van Vark, 1983. A novel digestion technique for multi-element plant analysis. *Comm. Soil Sci. Plant Anal.* 14, 239-249.
- Odum, E.P., 1971. *Fundamentals of Ecology*, 3rd edition. W.B. Saunders Co., Philadelphia, Pennsylvania, USA, 574 pp., p. 106.
- OECD, 1982. *Eutrophication of waters., Monitoring, Assessment and Control. Final report. OECD Cooperative programme on monitoring of inland waters (Eutrophication control)*, Environment Directorate, OECD, Paris, 154 pp.
- Patrick, W.H. and R.A. Khalid, 1974. Phosphate release and sorption by soils and sediments: effect of aerobic and anaerobic conditions. *Science* 186, 53-55.
- Philips, G.L., D. Eminson and B. Moss, 1978. A mechanism to account for macrophyte decline in progressively eutrophicated freshwaters. *Aquatic Bot.* 4, 103-126.
- Reckhow, K.H. and S.C. Chapra, 1979. A note on error analysis for a phosphorus retention model. *Water Resources Res.* 15, 1643-1646.
- Rhee, C.-Y, 1978. Effects of N:P atomic ratios and nitrate limitation on algal growth, cell composition and nitrate uptake. *Limnol. & Oceanogr.* 23, 10-25.
- Ripl, W., 1976. Biochemical oxidation of polluted lake sediment with nitrate - a new lake restoration method. *Ambio* 5, 132-135.

- Rodhe, W., 1969. Crystallization of eutrophication concepts in northern Europe. In: Eutrophication: Causes, Consequences, Correctives, Nat. Acad. Sci. Washington, D.C., 50-64.
- Ryding, S-O. and W. Rast, 1989. The control of eutrophication of lakes and reservoirs. Paris, UNESCO, 314 pp.
- Sas, H., 1989. Lake restoration by reduction of nutrient loading: Expectations, experiences, extrapolations. St. Augustin, Academia verlag Richarz, 497pp., p. 1-9.
- Stumm, W. and J.J. Morgan, 1981. Aquatic chemistry, 2nd Ed. John Wiley and Sons, New York [etc.], 780 pp.
- Uhlmann, D., 1975. Hydrobiologie, ein Grundriß für Ingenieure und Naturwissenschaftler (in German). VEB Gustav Fischer Verlag Jena, 345 pp.
- Van Straten, G., 1986. Identification, uncertainty assessment and prediction in lake eutrophication. Ph.D.Dissertation Technical University Twente, The Netherlands, 240 pp.
- Vollenweider, R.A., 1968. Scientific fundamentals of the eutrophication of lakes and flowering waters with particular reference to nitrogen and phosphorus as factors in eutrophication. Paris: OECD, 193 pp.
- Vollenweider, R.A. and J.J. Kerekes, 1980. The loading concept as basis for controlling eutrophication. Philosophy and preliminary results of the OECD programme on eutrophication; Progress in Water Technology 12, 5-38.
- Zevenboom, W., 1980. Growth and nutrient uptake kinetics of *Oscillatoria agardhii*. Dissertation University of Amsterdam, 178 pp.

Chapter 2

The accumulation of phosphorus in test ditches in relation to external loading from mass balances

2. THE ACCUMULATION OF PHOSPHORUS IN TEST DITCHES IN RELATION TO EXTERNAL LOADING FROM MASS BALANCES

2.1 Introduction

Internal and external mass balances were calculated on a yearly basis to provide insight into the build-up of different nutrient pools in the ditches, and into the significance of these different pools in relation to the level of external nutrient loading.

Internal mass balances provide information on the total amount of a component present in a system, and the internal distribution over the different compartments. They were in this study obtained from an annual inventory of these different compartments. This comprises analysis of the total phosphorus pool in the water phase (WAT), in the sediments (SED) and in the vegetation. The vegetation has been divided into the aquatic macrophytes (AV), including all submersed, free-floating and emergent species that root in the sediment or in the water phase, and the vegetation on the banks (BV), that also derives its nutrient requirements from the ditch system. The procedures for sampling of the vegetation and the sediments, and the analytical procedures used for the analyses are given in appendix A.

The internal P mass balances of the clay- and sand-ditches are discussed in paragraphs 2.3 and 2.6 respectively.

The external mass balance is the change in the total amount of phosphorus in a system, ΔP , calculated from the total input and output across the system boundaries. It is a global indicator for the direction of change of the trophic state of the system:

$$\Delta P = \sum \text{input} - \sum \text{output}$$

The input into the ditches consists of dry and wet atmospheric deposition (A), phosphate input through the inlet of groundwa-

ter (S) and manually supplied P (M). The output results from discharge (D) and occasional harvesting of vegetation from the banks (H). Harvesting is done as little as possible, but occasionally it is necessary for management purposes.

Atmospheric deposition (A) of P is measured as the total P concentration in regularly, generally biweekly, collected precipitation samples, multiplied by the precipitated volume. Rainwater falling on the banks is also considered as input into the ditch system, since the banks are separated from the environment by an impermeable foil that precludes exchange with the subsoil, and run-off from the banks discharges into the ditches. The catchment area therefore is 200 m^2 , while the water surface is 132 m^2 . The intake of groundwater is recorded automatically and registered through the number of tipping-buckets with a known volume. This groundwater originates from a local well and its composition is approximately constant, so occasional analysis of its total-P concentration is satisfactory. The P-concentrations are low anyway and the supplied volume is small, so groundwater inlet (S) contributes only a minor fraction to the external P input. The manually added phosphorus (M) is supplied as a known amount of K_2HPO_4 , dissolved in tap water, and homogeneously distributed over the water surface. Discharged P (D) is measured as the total P concentration times the total discharged volume. Discharge samples are collected volume proportionally and analyzed as biweekly averages, unless of course no discharge did take place.

The external mass balance of the clay- and sand-ditches are described in paragraphs 2.2 and 2.5 respectively.

Paragraphs 2.4 and 2.7 give a comparison between internal and external P mass balances of clay- and sand-ditches respectively. Paragraph 2.8 give a discussion on the results and some conclusions.

2.2 External phosphorus mass balances of the clay-ditches

Table 2.1 presents the external balances of the clay ditches

Accumulation of P from mass balances

over a two and a half years period, and the contributions of the individual terms. The table shows that the variation in input between the four ditches is for the major part determined by the manually added phosphorus, and that the other input terms are only of minor relative importance for the external P-balance. The discharge of P from ditch D has increased significantly resulting from increased total P concentrations in the water phase, but equilibrium between input and output had not yet been reached by October 1991.

Table 2.1. External P mass balances of the clay ditches during the period May '89 - October '91

	A	S	M	D	H	Net
	(g P/ ditch)					
A, reference						
May'89 - Oct'89	5	4	-	0		9
Oct'89 - Oct'90	13	3	-	2		14
Oct'90 - Oct'91	11	7	-	23		-5
Total	29	14	-	25		18
B, 1x CUWVO						
May'89 - Oct'89	5	2	25	2		30
Oct'89 - Oct'90	13	1	50	10		54
Oct'90 - Oct'91	11	5	50	24		42
Total	29	8	125	36		126
C, 3x CUWVO						
May'89 - Oct'89	5	2	80	0		87
Oct'89 - Oct'90	13	1	161	8		166
Oct'90 - Oct'91	11	6	161	15		163
Total	29	9	402	23		416
D, highest loaded						
May'89 - Oct'89	5	2	496	1		502
Oct'89 - Oct'90	13	1	1612	178		1448
Oct'90 - Oct'91	11	6	1438	443	79	933
Total	29	9	3546	622	79	2883

2.3 Internal phosphorus mass balances of the clay-ditches

- sediment P-pool

The accumulation of P in the sediments (SED) after the start of the loading programme in May 1989 has been followed from

annual analysis of the P-content of the sediments. The sedimentary P-pool is calculated as the P-content on a dry weight basis times the total amount of dry weight. Inaccuracies and spatial variability in both terms have to be taken into account. To provide insight into the vertical distribution of P within the sediment, three horizontal sublayers (0-1, 1-5 and >5 cm) were separated, and the P analyses were applied to each layer, according to the scheme by Hieltjes and Lijklema (1980). This procedure comprises subsequent extraction in solutions with 1 M NH_4Cl at pH=7, 0.1 M NaOH and 0.5 M HCl. The fractions represent loosely bound, Fe- and Al-associated phosphorus and Ca-bound P respectively. The dry weight content of each sublayer was calculated from the averaged solids concentrations within a layer of all sixteen clay ditches (see table 1.3).

The total amount of dry weight per ditch in the sediment layers between 0-1 cm and 1-5 cm are 374 ± 93 and 3855 ± 143 kg dry weight per ditch. The standard deviation in the measured dry weight concentration is especially high in the top centimeter. As the P-contents in the top layer are affected most by the external phosphorus loading, this causes a fairly large inaccuracy in the calculation of the total amount of P in the ditches. The standard deviation of the dry weight content of the 1-5 cm layer is smaller, but this layer represents a much larger amount of dry weight. It should also be noted, that as a vertical concentration gradient develops in the top of the sediment, small inaccuracies in the separation at 1 cm depth may lead to a dilution or concentration artefact in the calculated P content. As the sediment P-pool contributes the major fraction to the internal P-balance, inaccuracies in the calculation of the sedimentary P-pool will affect the agreement between the internal and external P mass balances.

- Results of chemical extractions

In appendix B-D the results of the extractions according to the scheme by Hieltjes and Lijklema (1980) are given for the clay-ditches. The different fractions in the individual sub-layers and their changes in time, as averages of duplo's, are presented in figures 2.1 A-D. The figures show that the extractable P-concentrations have increased enormously in the top centimeter of the sediment of ditch D. The major part of the increase is recovered in the NaOH-extractable fraction, indicating a large relative importance of Fe- and Al-(hydr)-oxides for the fixation of P in the clay-ditches and a large contribution of organic P (appendix D). After 2.5 years only a slight increase could be observed in the intermediate layer between 1 and 5 cm, showing the slowness of vertical penetration. At a depth > 5 cm no increase could yet be discovered. In ditches B and C the extractable phosphorus content of the top layer initially increased, resulting in an enhanced vertical stratification of phosphorus in the sediment. The increment during the period May 1989 - October 1989 was larger in the ditch C than in ditch B. Between October 1990 and October 1991 the extractable P-content in the top layers of these two ditches has decreased considerably, while the P-content of the intermediate layers remained virtually unchanged.

The sequence of first an increase and later a decrease in extractable P-content in the top layer can also to a lesser extent be detected in the ditch A. This phenomenon can be attributed to a number of factors:

- a) it may result from the dissolution of Fe-OH-P complexes following changed redox conditions;
- b) it may be attributed to P-uptake by roots and subsequent transport to above ground plant parts;
- c) it may result from the sedimentation of material with a lower P-content than that of the top sediment layer;
- d) it may represent the equilibration of the sediment to the

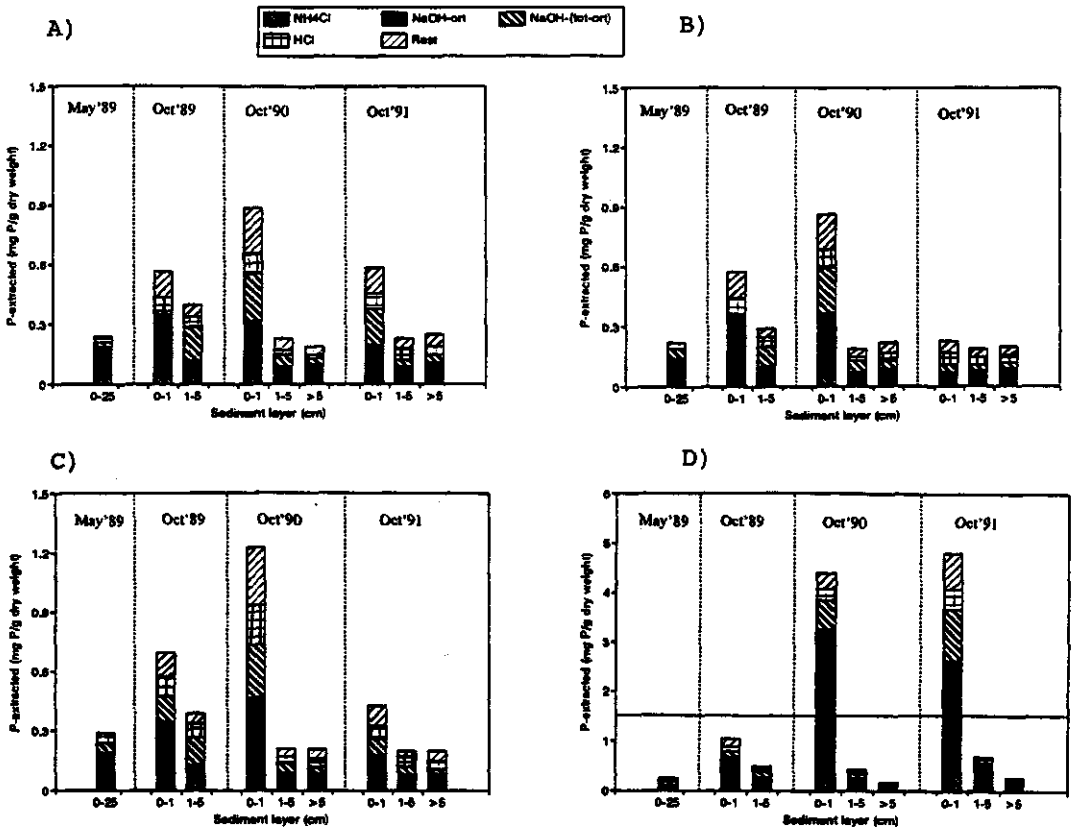


Figure 2.1. Extractable P in the steps of the extraction scheme in May 1989, Oct. 1989, Oct. 1990 and Oct. 1991 in different horizontal sediment layers. A) reference; B) 1x CUWVO; C) 3x CUWVO; D) highest loaded.

changed composition of the overlying water in the ditches in comparison with that in the fen from which the sediment originated;

- e) microbially mediated P-release under anoxic conditions;
- f) inaccuracies in the sampling and analysis procedure

ad a) In the ditches B and C anaerobic conditions regularly occur in the near bottom region during the summer, as measured from the dissolved oxygen concentration measured at an elevation of 10 cm above the sediment-water interface. Anoxic conditions in the sediment therefore are likely to prevail for

longer periods, resulting in a (partly) reduction of Fe^{3+} to Fe^{2+} . As Fe(II)-P complexes have a higher solubility, dissolution will result in increased Fe-concentrations in the interstitial water with respect to the overlying water. This vertical concentration gradient results in an upward diffusion of Fe^{2+} and a subsequent oxidation and precipitation just below the sediment-water interface. When anoxic conditions prevail at or even above the sediment-water interface, a synchronisation of Fe- and P-release can occur.

The oxalate-extractable Fe in the sediment of the clay ditches in October 1990 and 1991 are given in table 2.2. The table shows that only in the top sediment layer of ditch B a decrease in the oxalate-extractable Fe has occurred, whereas it remained about constant in the ditch C, and increased in the ditches A and D. A synchronisation of P- and Fe- release from the top sediment layer to the overlying water has, based on the data in table 2.2, occurred in ditch B. Moreover, the decrease in total extractable P-content in the top layers of ditches A, B and C is caused by a decrease in all fractions, and not just in the NaOH-extractable fraction (see appendix B).

The data from table 2.2 suggest an upward diffusion of Fe within the sediment in the ditches A and C, resulting in increasing Fe-contents in the top centimeter and lowered Fe contents at larger depths. It should be noted that at the moment that the sediment was brought into the ditches, it was a homogeneous mixture, and that the observed vertical gradients and differences between ditches therefore originate from processes taking place after that moment.

The molar P:Fe ratios in the top layers decreased in all ditches between October 1990 and October 1991. This applies to the NaOH-extractable P-fraction as well as to the total P.

The high oxalate-extractable Fe-content of the 0-1 and 1-5 cm layer of ditch D, which suffers from long periods of anaerobiosis, may result from the sedimentation of Fe(II)-P complexes from the anaerobic water column. Although sorption of P on

Fe(II) is more labile than that of P on Fe(III), it may be significant due to the higher specific surface area of reduced ferrous compounds (Patrick and Khalid, 1974).

Table 2.2. Ammonium-oxalate extractable Fe (mg.[g DW]⁻¹) in the clay-ditches in October 1990 and October 1991.

ditch	layer (cm)	Oct'90	Oct'91
A, reference	0-1	6.9	14.5
	1-5	4.2	3.7
	> 5	3.5	3.5
B, 1x CUVVO	0-1	5.6	2.3
	1-5	3.6	3.9
	> 5	4.2	3.4
C, 3x CUVVO	0-1	7.5	8.1
	1-5	3.6	4.4
	> 5	3.7	2.6
D, highest	0-1	10.0	12.9
	1-5	3.9	7.3
	> 5	3.7	4.0

ad b) The extent to which submerged aquatic macrophytes depend on the sediments for their nutrient supply may vary, depending on the relative availability of nutrients from the sediment and the water column. Although submerged species are capable of significant foliar uptake during periods of enhanced nutrient concentrations (Philips et al., 1978), and thereby may significantly contribute to the fast decrease of the dissolved inorganic phosphorus concentration during the first days after a dosage, uptake from the sediments probably will prevail during the rest of the year. Due to nutrient uptake through the roots and subsequent transport to above ground plant parts, aquatic macrophytes may serve as a nutrient pump (Carignan and Kalff, 1980). Thereby they can contribute to the observed decrease of P in the top centimeters of the sediment, where the major fraction of the root mass is located.

ad c) The possible explanation of dilution of sedimentary P in

the top layer due to sedimentation of material with a lower P-content is not likely, as the settling material has a higher P-content than the sediment on a dry weight basis. Only after microbially mediated P-release from organic matter (see e-) a significant decrease of the P-content of the top layer can be expected.

ad d) The exposure of the sediment to various types of overlying water may affect the sediment composition on a long term. The composition of the interstitial water is mainly controlled by the characteristics of the sediment. Thus concentration gradients at the sediment-water interface may develop, causing fluxes across this interface. Equilibration of the sediment composition with respect to the overlying water will be a slow process, and is limited by vertical transport in the sediment. It also depends on the retention time of the overlying water, which determines the loss of a constituent through discharge. On a time-scale of years, however, it cannot be precluded.

ad e) Under anaerobic conditions biologically mediated release of phosphorus from the sediments occurs, as shown by Fleischer (1978), who found that P release from particulate matter did not occur in poisoned anaerobic sediment cores. The P-content of settled organic matter can be significantly lowered by biologically mediated P-release (mineralisation).

ad f) Inaccuracies in the sampling and analysis procedure originate mainly from difficulties in the separation of exactly one centimeter; separation of a layer of more than one centimeter will lower the average P-content in the samples. Further steps in the procedure include the taking of well homogenized subsamples and the separation of the supernatant from the different extraction steps, and ultimately the analysis of P.

From the extractable P-contents and the dry weight contents in the various sediment layers the total P-pool in the sediment is calculated. From the results of the extractions it

can be seen that the penetration of phosphorus into the sediments did not yet extend past a depth of 5 cm in all four ditches. The composition of the deeper sediment with respect to P in all ditches had remained constant until October 1991. Therefore for calculation of the sedimentary P-pool only the top 5 cm layer has been considered.

The overall mass balance of P in the sediment is complicated by accumulation at the top of the sediment, which leads to a certain burial rate of phosphorus at the lower boundary of the 1-5 cm layer. A general equation for the long term accumulation of phosphorus in the sediment, analogous to Lijklema (1986) is :

$$\frac{dC}{dt} = \frac{S}{L} - \frac{\Delta L \cdot c}{L}$$

with ΔL the accumulation rate (m.yr^{-1}) and S the P-sedimentation rate ($\text{g P.m}^2.\text{yr}^{-1}$). L was originally interpreted as the mixing depth of the sediment, but the equation is also valid if L is an arbitrarily chosen depth, which is in this case 5 cm. The loss of phosphate due to burial in the deeper sediment is not known. Attempts to measure directly the sedimentation rate with sediment traps failed (results are not included in this thesis), due to the very large inaccuracies that are inherent to this kind of measurements in shallow, macrophyte dominated systems. Therefore the sedimentation rate has to be estimated. With a supposed, rather high, accumulation rate of 0.5 cm.yr^{-1} and a P-content at 5 cm of $0.20 \text{ mg P.}[\text{g dry weight}]^{-1}$ the burial rate would be ca. 100 g P.yr^{-1} per ditch. In ditch D this loss rate may be relatively higher due to a higher sedimentation rate.

Table 2.3 presents the total amounts of phosphorus in the sediment (0-5 cm). Comparison of the standard deviation in the sedimentary P-pool with the net external mass balances over the whole period of 2.5 years (table 2.1) shows that these are of the same order of magnitude for ditch A and B. The net external P balance significantly exceeds the inaccuracy in the

sedimentary P-pool for ditches C and D.

The large total amount of P in the 1-5 cm layers in October 1989 was due to a remarkably high NaOH-extractable P-fraction in all samples.

Table 2.3. Phosphorus pool (g P/ditch) in the sediment. Standard deviations are derived from the standard deviations of the dry weight concentration measurements and of the P analyses.

ditch		May'89	Oct'89	Oct'90	Oct'91
A, reference	0-1 cm	108	215± 58	331± 82	220± 56
	1-5 cm	1118	1530± 57	875± 50	883±154
	Total	1226	1745± 81	1206± 97	1103±164
B, 1x CUWVO	0-1 cm	94	220± 63	325± 82	85± 21
	1-5 cm	964	1120±184	734± 30	740±104
	Total	1058	1340±194	1059± 86	825±106
C, 3x CUWVO	0-1 cm	123	263± 67	460±115	162± 41
	1-5 cm	1272	1492± 72	806± 34	761± 49
	Total	1395	1755± 98	1266±120	923± 64
D, highest	0-1 cm	112	396±101	1645±411	1805±450
	1-5 cm	1157	1868±105	1656± 65	2656±112
	Total	1269	2263±146	3304±416	4461±464

- Total internal P mass balance

Table 2.4 presents the internal P-pool in water, vegetation and top 5 cm of the sediment during the 2.5 years period. The sediment P-pool is by far the largest, and the water phase contributes a negligible fraction except for ditch D. The increase of the P-storage in the vegetation is due to increased internal P-concentrations in the aquatic macrophytes (see chapter 3) and not the consequence of an increase in biomass. Although the relative inaccuracies in the biomass estimations of aquatic macrophytes communities are large (relative standard deviations in recovered biomass from cylin-

ders are in the order of 15 %, with n=3), the absolute inaccuracies in the estimation of the sedimentary P-pools are much larger. The observed increase in the sediment pool during the period May'89 - Oct'89 and the decrease during the following year in ditches A, B and C seems improbable.

Table 2.4. Total internal P-pools (g P/ditch) of SEDiment, WATERphase and Water Vegetation + Banks Vegetation

ditch:		WAT	SED	WV+BV	TOT
A, reference	May'89	2	1226	51	1279
	Oct'89	2	1745	73	1820
	Oct'90	1	1206	38	1245
	Oct'91	1	1103	33	1137
B, 1x CUWVO	May'89	2	1058	46	1106
	Oct'89	2	1340	58	1400
	Oct'90	3	1059	68	1130
	Oct'91	2	825	107	934
C, 3x CUWVO	May'89	2	1395	48	1445
	Oct'89	3	1755	46	1804
	Oct'90	3	1266	84	1353
	Oct'91	4	923	107	1034
D, Highest	May'89	2	1269	43	1314
	Oct'89	42	2263	94	2399
	Oct'90	154	3304	474	3932
	Oct'91	217	4461	493	5171

2.4 Comparison between internal and external P mass balances

Comparison of the internal P mass balance (table 2.4) with the external mass balance (table 2.1) shows that the net input into ditch A is very small compared to the total amount of P in the system. It is scanty with respect to the range of the uncertainties in the estimation of the internal P mass balance.

In ditch B the internal P mass balance suggests a decrease of ca. 200 g P in the total amount of P in the system, while the external P mass balance predicts an increase of ca. 100 g P.

The inaccuracy in the internal P-pool, both at the start and at the end of the considered period, is however of the same order of magnitude. A burial rate of 100 g P.yr^{-1} at a depth of 5 cm in the sediment, which corresponds to a rather high sedimentation rate of 0.5 cm.yr^{-1} (see section 2.3), can also explain part of the difference.

In ditch C the internal P mass balance shows a decrease of ca. 400 g P in the total amount of P present in the system, while the external P balance suggests an increase of ca. 400 g P. This discrepancy of 800 g P over a 2.5 years period can partly be explained by burial of P at the lower boundary of the top 5 cm sediment layer (at maximum ca. 250 g P). This leaves still a fairly large unexplained difference c.q. error.

In ditch D the net external P mass balance is large, even compared to the total amount of P that was initially present in the system. In this ditch the increase in total P in the system suggested by the internal P mass balance was higher than that predicted by the external P mass balance: 3850 g P and 2900 g P respectively. The burial rate of P at the lower boundary of the top 5 cm sediment layer may be higher than in the other ditches due to an enhanced sedimentation rate, but not so much due to increased P-concentrations in the sediment, as the penetration of P into the sediment had not reached a depth of 5 cm in the sediment yet. The inaccuracy in the internal P-pool is high: $> 400 \text{ g P}$ in October 1991.

2.5 External P mass balances for the sand-ditches

The terms of the external P mass balances of the sand-ditches are the same as for the clay-ditches. The procedures used for measuring input through groundwater intake and output through discharge are also the same. Table 2.5 presents the external P mass balances over the period May 1989 - October 1991.

Due to high total P concentrations in the water phase, discharge has become an important term of the external P balance of ditch D. In this ditch more than 50 % of the external P

input during the period October 1990 - October 1991 was lost through the discharge. In the highest loaded clay-ditch this was significantly less: only 30 % of the external P input over the same period was lost again.

Table 2.5. External P mass balances of the sand ditches during the period May '89 - October '91

	A	S	M	D	H	Net
	(g P/ ditch)					
A, reference						
May'89 - Oct'89	5	2	-	1		6
Oct'89 - Oct'90	13	1	-	5		9
Oct'90 - Oct'91	11	6	-	4		13
Total	29	9	-	10		28
B, 1x CUWVO						
May'89 - Oct'89	5	2	25	1		31
Oct'89 - Oct'90	13	1	50	9		54
Oct'90 - Oct'91	11	5	50	7		59
Total	29	8	125	17		144
C, 3x CUWVO						
May'89 - Oct'89	5	2	80	2		85
Oct'89 - Oct'90	13	1	161	16		159
Oct'90 - Oct'91	11	5	161	10		167
Total	29	8	402	28		411
D, highest						
May'89 - Oct'89	5	1	496	9		493
Oct'89 - Oct'90	13	1	1612	421		1205
Oct'90 - Oct'91	11	4	1438	747	180	526
Total	29	6	3546	1177	180	2224

2.6 Internal P mass balances of the sand-ditches

In the sand-ditches aquatic macrophytes were negligible during the whole period in ditches A, B and C. In ditch C a temporary bloom of the filamentous alga *Cladophora* occurred in 1990, but this vanished in early spring 1991. In ditch D a *Lemna minor* cover developed in late 1989 and has since remained dominant. The P-pool in *Cladophora* in October 1990 and in the *Lemna minor* cover was estimated analogous to that in the aquatic macrophytes of the clay-ditches.

In all four sand-ditches a distinct organic layer containing mainly settled algae developed on top of the sand. The P-pool of this layer (B) was analyzed from areal dry weight content and the P-concentrations (g P.[g DW]⁻¹). Three sediment cores per ditch, each with a diameter of 5.3 cm, were pushed into the sand to a depth of about 10 cm. The benthic layer was separated from the sand by repeated resuspension and decantation of the organic material until only the plain sand remained in the sediment core. The algal suspension was filled up to a volume of 1 l and dry weight (105°C) was measured after evaporation of a subsample of this suspension. Upon drying (40°C) of another subsample the internal P-concentration was measured after digestion of the dried material in a H₂SO₄ - Se mixture, using H₂O₂ as an oxidator (Novozamsky et al., 1983).

Table 2.6 presents the internal P mass balance of the sand ditches.

Table 2.6. Total internal P-pools (g P/ditch) of **SED**iment, **WAT**erphase, **WATER** Vegetation + **BANKS** Vegetation and **BENTHIC** layer

ditch:		WAT	SED	WV+BV	B	TOT
A, reference	May'89	2	534	-	-	536
	Oct'89	3	449	-	3	455
	Oct'90	3	272	2	8	285
	Oct'91	1	326	2	7	334
B, 1x CUWVO	May'89	2	534	-	-	536
	Oct'89	3	585	-	3	591
	Oct'90	3	219	2	14	238
	Oct'91	1	364	1	23	389
C, 3x CUWVO	May'89	2	534	-	-	536
	Oct'89	4	536	-	4	544
	Oct'90	4	323	24	29	380
	Oct'91	12	370	2	114	498
D, highest	May'89	2	534	-	-	536
	Oct'89	85	441	-	23	549
	Oct'90	219	457	382	56	1114
	Oct'91	434	491	298	149	1372

The accumulation of P in the benthic layer shows a positive relation with the level of external P input. The difference between ditches A and B is mainly reflected in the benthic layer. Only after the P storage capacity of this benthic layer has approached saturation, as ditches C and D, an increase of the P-pool in the water column can be observed. In ditch D the continuous external nutrient input has caused a steady increase in the dissolved P concentrations in the water phase, indicating that the losses through sedimentary uptake and discharge are insufficient to compensate for the addition. This is illustrated in figures 2.2 a and b, which present the dissolved P concentration over a 3 years period (May 1989 - July 1992) in the clay-ditch D and sand-ditch D respectively. The figures show the decrease in dissolved P concentrations after the nutrient dosages and reflect the gradual decline of the P uptake capacity, which is more pronounced in the sand-ditch.

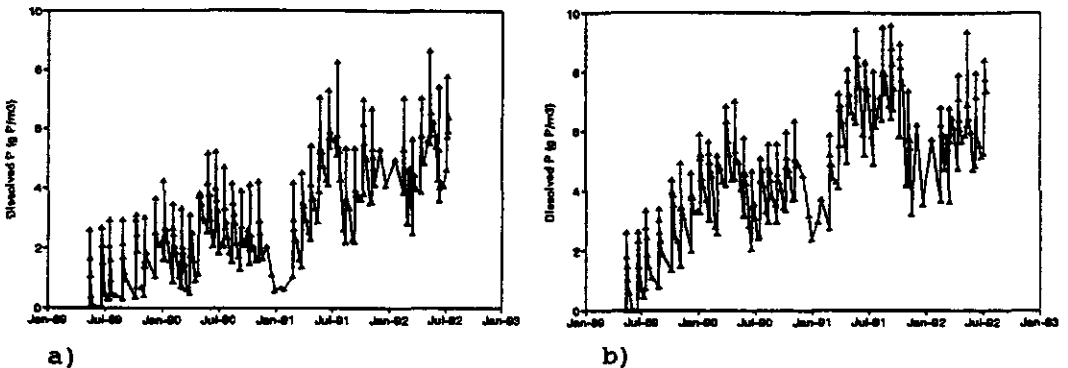


Figure 2.2. Dissolved $\text{PO}_4\text{-P}$ ($\text{g P}\cdot\text{m}^{-3}$) concentrations in:
a) clay-ditch D; b) sand-ditch D

The sedimentary P-pool, calculated as the sum of the individual fractions of the extraction scheme according to Hieltjes and Lijklema (1980) times the solids concentration in the top 5 cm layer of the sand, shows an irregular pattern (table 2.6). This may be mainly due to a low amount of extractable P in all fractions, with large relative errors. The sorption

capacity with respect to P of the sand on a dry weight basis is much smaller than that of the clay sediment. Moreover, settled organic matter remains on top of the sand as a distinct layer, and does not mix with the sand to any appreciable extent, so the build-up of the organic sedimentary P-pool is reflected in the benthic layer (B). To reduce the error in the measured total P content of the sand due to the summation of the errors in the individual fractions, the extractions were repeated with freeze-dried samples from May '89, October '90 and October '91, that had been stored. This time only a 24 hours extraction in 0.5 M HCl was performed. The results are shown in table 2.7. The samples from May '89 concerned sand that was homogeneously mixed over the whole depth of the cores (ca. 20 cm), and therefore these cannot be compared directly with the other sampling data. However, as aluminum is the main P sorbing element in the sediment of the sand ditches (see chapter 7), the sorption is probably rather insensitive to redox conditions. As the sand was homogeneously mixed before it was brought into the ditches, it can be assumed that vertical stratification of P in the sediments before the start of the loading program was not significant.

Table 2.7 shows that a clear increase in the P-content of the top 5 cm sediment layer of ditch D could be retrieved, which was not present in the results of the original extraction scheme (see table 2.6). Below 5 cm no increase in HCl extractable P could yet be discovered. Table 2.8 presents the sedimentary P pool of the top 5 cm and the total P pool in the ditches, using the extractable amounts of P from table 2.7 and the other terms of the internal P mass balance (water phase, water + banks vegetation, benthic layer) from table 2.6.

The total P pool has remained virtually unchanged in the ditches A and B. In ditch C an increase in the total amount of P in the system of 126 g between May'89 and October'91 has been recovered. In ditch D this increase was 1055 g P.

Table 2.7. 0.5 M HCl extractable P ($\mu\text{g P} \cdot [\text{g DW}]^{-1}$) in stored sediment samples (sand ditches) from May 1989, Oct 1990 and Oct 1991.

ditch	layer (cm)	May'89	Oct'90	Oct'91
A, reference	0-1	24	19	14
	1-5	24	24	22
	>5			25
B, 1x CUWVO	0-1	24	19	19
	1-5	24	23	20
	>5			17
C, 3x CUWVO	0-1	18	23	24
	1-5	18	15	17
	>5			18
D, highest	0-1	17	81	72
	1-5	17	41	48
	>5			15

Table 2.8. Sediment P-pool and total P-pool (g P/ditch) calculated from 0.5 M HCl sediment extraction.

	May'89	Oct'90	Oct'91
Sediment P pool			
A, reference	123	120	107
B, 1x CUWVO	123	115	102
C, 3x CUWVO	92	83	92
D, highest	87	239	263
Total P pool			
A, reference	125	133	117
B, 1x CUWVO	125	134	127
C, 3x CUWVO	94	140	220
D, highest	89	896	1144

2.7 Comparison of internal and external P mass balances of the sand ditches.

Comparison of the internal and external P mass balances shows that the net change of P calculated from the internal mass balance is smaller than that calculated from the external mass balances for all ditches (see table 2.9).

Table 2.9. Comparison of net internal and net external P mass balance between May '89 and October '91.

	$\Delta(\text{internal})$ (grammes P)	$\Delta(\text{external})$
A, reference	-8	28
B, 1x CUWVO	2	144
C, 3x CUWVO	126	411
D, highest	1055	2224

In ditch A the magnitudes of these changes are very small and within experimental errors. In the ditches B, C and D the recovered amount of P is substantially less than the quantity added, indicating that the applied sampling and analytical methods are not adequate and/or accurate enough to recover the whole internal P pool. This is most probably due to the sediment compartment.

2.8 CONCLUSIONS AND DISCUSSION

In the clay ditches a reasonable agreement between internal and external P mass balances, within the range of experimental errors, was obtained in all systems except ditch C (3x CUWVO level).

In the sand ditches the total amount of P in the system, as calculated from the sum of the individual P pools, was in all ditches smaller than the value estimated from external P mass balances. This is most probably due to underestimation of the sedimentary P pool, when extractable P contents are considered.

The P mass balances provide some insight in the internal distribution of the external P input over the various compartments. Thereby they provide information on the transformations that may be important and need further research to assess the nutrient cycling in the ditches. However, the dynamics of the transformations cannot be revealed by annual snap-shots, certainly not within these fairly large experimental errors.

Sedimentary uptake in the sand ditches, which has been shown

to be a process that cannot be analyzed adequately from simple mass balances, is studied in detail in chapter 7.

REFERENCES

- Fleischer, S., 1978. Evidence for the anaerobic release of phosphorus from lake sediments as a biological process. *Naturwissenschaften* 65, 109-110.
- Hieltjes, A. and L. Lijklema, 1980. Fractionation of inorganic phosphates in calcareous sediments. *J. Envir. Qual.* 9, 405-407.
- Lijklema, L., 1986. Phosphorus accumulation in sediments and internal loading. *Hydr. Bulletin* 20 (1/2), 213-224.
- Murphy J. and J.P. Riley, 1962. A modified single solution method for the determination of phosphate in natural waters. *Anal. Chim. Acta* 27, 31-36.
- Novozamsky, I., V.J.G. Houba, R. van Eck and W. van Vark, 1983. A novel digestion technique for multi-element plant analysis. *Comm. Soil Sci. Plant Anal.* 14, 239-249.

APPENDIX A

Sampling of vegetation

Submersed Vegetation: The submersed vegetation was sampled after the placement of a cylinder with a radius of 18.5 cm in a homogeneous part of the dominant species of the vegetation. The plant material within the cylinder was quantitatively harvested. Per ditch three cylinders were harvested.

Floating vegetation (Lemnids): Floating vegetation (*Lemna minor*) was harvested with a 1 mm sieve of 10 x 20 cm (five samples per ditch).

Banks vegetation: The vegetation on the banks was sampled from complete harvesting of three segments per ditch, each with a length of 1 m.

The plant material was dried at 40°C for three days and weighted. Total biomass of the dominant species in the ditch was estimated from the average areal dry weight in the cylinder and the areal coverage of the species in the ditch.

After grinding, weighted samples (usually 300 mg) of the grinded plant material were, in duplo, digested in a H_2SO_4 - Se mixture, using H_2O_2 as an oxidator (Novozamsky et al., 1983).

Water analysis

Dissolved phosphate analyses were performed after filtering through a 0.45 μm Schleicher & Schuell ME 25 membranefilter. Total P analyses were performed after digesting of maximum 50 ml of ditchwater in 0.1 M H_2SO_4 , using potassiumperoxodisulphate as oxidator.

Sediment sampling

Per ditch five sediment cores with a diameter of 5.3 cm were collected and transported to the laboratory. The cores were frozen at -18°C and the layers of 0-1, 1-5 and >5 cm were separated. Corresponding layers of the five sediment cores were homogeneously mixed. From these mixtures subsamples were taken to which the extraction scheme according to Hieltjes and Lijklema (1980; see text) were applied (in October 1989 the layer >5 cm was not analyzed).

Sampling of benthic layer in sand-ditches

Three sediment cores, with a diameter of 5.3 cm per ditch, were pushed into the sand to a depth of about 10 cm. The benthic layer was quantitatively separated from the sand by repeated resuspension and decantation of the organic material. The algal suspension was filled up to a volume of 1 l and dry weight (105°C) was measured after evaporation of a subsample of this suspension. Upon drying (40°C) of another subsample the P-concentration was measured after digestion (Novozamsky et al., 1983).

All phosphate analyses were performed on a Scalar SA-40 Autoanalyser with the modified molybdate-blue method (Murphy and Riley, 1962).

APPENDIX B

October 1989

Results of sediment phosphate extractions (mg P. [g DW]⁻¹)

ditch	layer (cm)	NH ₄ Cl	NaOH	extraction step		total
				HCl	rest	
A	0-1	0.043	0.278	0.065	0.127	0.513
		0.034	0.389	0.069	0.144	0.637
	1-5	0.021	0.250	"	0.083	0.399
		0.036	0.270	0.045	0.046	0.397
B	0-1	0.032	0.454	0.071	0.113	0.670
		0.034	0.241	0.081	0.152	0.508
	1-5	0.000	0.160	0.040	0.044	0.244
		0.032	0.200	0.060	0.045	0.337
C	0-1	0.028	0.413	0.097	0.133	0.671
		0.029	0.488	0.097	0.123	0.737
	1-5	0.070	0.210	0.079	0.042	0.401
		0.037	0.230	0.064	0.047	0.377
D	0-1	0.091	0.651	0.098	0.153	0.993
		0.119	0.768	0.099	0.136	1.122
	1-5	0.067	0.300	0.075	0.022	0.464
		0.082	0.330	0.049	0.044	0.505

" = not available, but value of duplo used for calculation of total

Accumulation of P from mass balances

APPENDIX C

October 1990

Results of sediment phosphate extractions (mg P.[g DW]⁻¹)

ditch	layer (cm)	NH ₄ Cl	NaOH	extraction step		total	
				HCl	rest		
A	0-1	0.026	0.527	0.108	0.232	0.892	
		0.038	0.546	0.099	0.197	0.880	
	1-5	0.016	0.128	0.020	0.054	0.217	
		0.015	0.140	0.025	0.057	0.237	
	>5	0.011	0.113	0.022	0.044	0.189	
		0.012	0.116	0.022	0.035	0.185	
	B	0-1	0.038	0.550	0.100	0.163	0.872
			0.051	0.562	0.082	0.170	0.865
		1-5	0.016	0.116	0.016	0.046	0.194
0.014			0.101	0.032	0.040	0.187	
>5		0.010	0.116	0.033	0.044	0.203	
		0.016	0.111	0.059	0.048	0.235	
C		0-1	0.049	0.763	0.178	0.278	1.268
			0.037	0.652	0.222	0.281	1.192
		1-5	0.020	0.119	0.034	0.039	0.213
	0.015		0.123	0.024	0.043	0.205	
	>5	0.017	0.107	0.052	0.048	0.224	
		0.020	0.107	0.022	0.045	0.193	
	D	0-1	0.215	3.564	0.204	0.307	4.290
			0.186	3.755	0.235	0.330	4.506
		1-5	0.052	0.285	0.038	0.059	0.435
0.037			0.296	0.034	0.056	0.424	
>5		0.018	0.104	0.024	0.042	0.188	
		0.015	0.107	0.020	0.037	0.178	

APPENDIX D

October 1991

Results of sediment phosphate extractions (mg P.[g DW]⁻¹)

ditch	layer (cm)	NH ₄ Cl	NaOH	extraction step		total	
				HCl	rest		
A	0-1	0.019	0.320	0.083	0.134	0.555	
		0.013	0.387	0.081	0.142	0.623	
	1-5	0.007	0.087	0.023	0.073	0.190	
		0.019	0.125	0.086	0.039	0.268	
	>5	0.028	0.123	"	0.067	0.262	
		0.017	0.142	0.043	0.042	0.245	
	B	0-1	0.009	0.092	"	0.072	0.230
			0.015	0.108	0.058	0.044	0.224
		1-5	0.013	0.116	0.047	0.043	0.218
0.009			0.086	0.036	0.034	0.166	
>5		0.006	0.104	0.034	0.054	0.198	
		0.015	0.100	0.050	0.038	0.203	
C		0-1	0.010	0.245	0.076	0.081	0.413
			0.017	0.246	0.065	0.123	0.451
		1-5	0.012	0.115	"	0.036	0.208
	0.007		0.095	0.045	0.041	0.187	
	>5	0.007	0.088	0.032	0.042	0.170	
		0.018	0.103	0.052	0.050	0.223	
	D	0-1	0.368	3.653	0.324	0.562	4.908
			0.295	3.057	0.520	0.875	4.746
		1-5	0.028	0.538	0.056	0.053	0.675
0.028			0.553	0.060	0.063	0.703	
>5		0.010	0.142	0.046	0.067	0.265	
		0.022	0.145	0.052	0.055	0.274	

" = not available, but value of duplo used for calculation of total

Chapter 3

Primary succession of aquatic macrophytes in experimental ditches in relation to nutrient input

Key-words:

Submersed aquatic macrophytes - Pleustophytes - Ditch
vegetations - Eutrophication - Primary succession

Based on: Primary succession of aquatic macrophytes in experimental ditches
in relation to nutrient input, by R. Portielje and R.M.M. Roijackers,
submitted to Aquatic Botany

3. PRIMARY SUCCESSION OF AQUATIC MACROPHYTES IN EXPERIMENTAL DITCHES IN RELATION TO NUTRIENT INPUT

ABSTRACT

In four experimental ditches, receiving four different levels of external nutrient input, the development of the species composition of the aquatic macrophyte communities was monitored during a period of 3.5 years (May 1989 - October 1992). The rate of primary succession was positively related to the level of external loading with nutrients (N and P).

At the start of the nutrient loading program, one year after the creation of the ditches, the vegetation was in a pioneer stadium. It consisted for the greatest part of Characeae, with an abundance, expressed as areal coverage, of > 90 % in all four ditches.

After the start of the program the Characeae disappeared and were replaced by *Elodea nuttallii* in all four ditches. The rate of the transition was positively related to the level of external nutrient loading.

In a ditch receiving a very high nutrient input, *Elodea nuttallii* was in turn replaced by *Lemna minor*. At two intermediate levels of nutrient loading *Elodea* has remained stable towards the end of the research period, performing a horizontal growth strategy, and forming a dense near-surface biomass with an areal coverage of almost 100 % during the summer. At the lowest level of nutrient input *Elodea nuttallii* reached an areal coverage of almost 50 % in October 1992, still performing a vertical growth strategy.

INTRODUCTION

The effect of eutrophication on aquatic communities has been studied extensively for decades. Most attention has been paid to phytoplankton blooms, as they are considered to cause most of the nuisances related to cultural eutrophication (Van Straten, 1986). However, nuisances caused by excessive growth of aquatic macrophytes also occur. Especially free-floating and emergent species may cause severe inconveniences by obstructing navigation or other forms of water usage (Sculthorpe, 1967).

In lakes eutrophication usually causes a decline of submersed aquatic macrophytes, caused by excessive growth of periphytic and filamentous algae. This then gives way to phytoplankton

blooms (Philips et al., 1978). Competition with species with floating or emergent leaves may also cause the disappearance of submersed species, especially in small water bodies. This results in a decline of the ecosystem diversity, as concomitantly the secondary producers that depend on submersed macrophytes for various purposes disappear.

In shallow waters the sediment plays an important role in the nutrient supply of rooted macrophytes (Carignan and Kalff, 1980; Barko and Smart, 1980). In case of low nutrient concentrations in the water column, macrophytes capable of extracting their nutrient requirements from the sediments are in an advantageous position. In stagnant waters, where a root system is not necessary for anchoring, the function of the roots is mainly restricted to nutrient uptake. The water column is clear so that light can sufficiently penetrate to the bottom zone (see figure 3.1 A).

Aquatic macrophytes can also be capable of significant nutrient uptake from the water phase (Philips et al., 1978). This can be either foliar uptake or uptake by a part of the root system that is suspended in the water (Agami and Waisel, 1986). At intermediate trophic states, with varying concentrations of dissolved nutrients, uptake from the sediments and the water column can occur alternately. During periods of higher concentrations of dissolved nutrients in the water column, nutrient uptake from the water column prevails. The necessity for an energetically unfavourable underground root system decreases with increasing trophic state.

Once the restriction of nutrient limitation with respect to nitrogen and phosphorus has been alleviated, the survival of an autotrophic species mainly depends on its ability to compete for light, carbon and space. This results in a movement of the production zone towards or above the water surface. For submersed species a switch from a vertical to a horizontal growth strategy is beneficially. Optimal occupation of the zone just below the water surface is of competitive advantage, both with respect to light interception and carbon availa-

bility. Enhanced primary production induces a higher pH, which in turn enhances the CO_2 flux from the atmosphere (Portielje and Lijklema, *subm.*). The atmospheric C-flux can be high enough to sustain a considerable net primary production during the growth season (see figure 3.1 B).

Sedimentary uptake can compensate for a part of the excess phosphorus after enhanced external loading and this fraction is not available for non-rooted plants. The uptake capacity of the sediment is limited, and may determine to a large extent the occurrence of pleustophytic life forms.

At high trophic states, with constant high concentrations of dissolved nutrients in the water column, pleustophytic life forms (Den Hartog and Segal, 1964) that derive their N and P requirements solely from the water column are in an advantageous position. Carbon dioxide is taken up directly from the atmosphere (see figure 3.1 C).

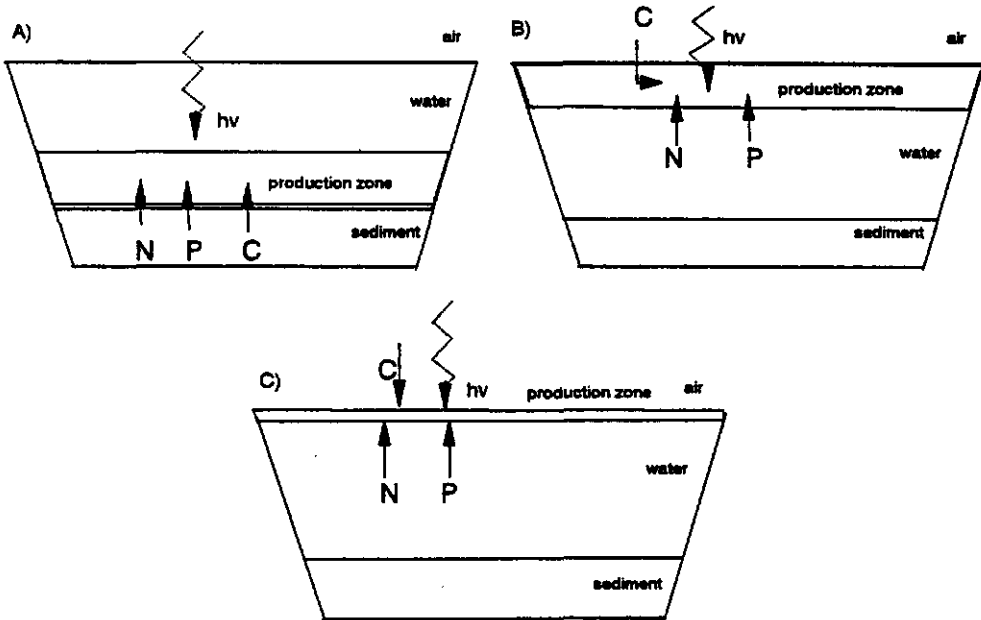


Figure 3.1. Global overview of different trophic states in aquatic macrophytes communities (for explanation see text).

In experimental ditches research is conducted on the effect of different levels of external nutrient loading on the response of the system with respect to its structure and functioning. A shift in species composition of the aquatic macrophyte community is a direct effect of eutrophication. In turn it can result in various indirect effects, related to the interactions between different components of the ecosystem (Brock et al., submitted). The effect of nutrient availability on the species composition and the dominant growth form of the macrophyte community is therefore an important aspect of eutrophication.

This paper deals with the change in species composition of the community of aquatic macrophytes in four experimental ditches during a period of 3.5 years. Four different levels of external nutrient loading were applied. The development of the vegetation after the start of the nutrient loading program reflects the effect of eutrophication on the primary succession of the vegetation. Abundance of individual species is estimated on the basis of areal coverage, and is analyzed in time.

In this study all species have been included that extract their nutrient requirements from the water or the sediment. These are, besides the rooted and non-rooted submersed species, also pleustophytes (lemnids) and helophytes. The vegetation on the banks was not included in this study.

To assess the importance of microphytes in the systems, the growth of periphytic algae on artificial substratum was monitored.

SITES STUDIED

The location of the ditch plant and the characteristics of the ditches are described in chapter 1.5 (p.20-22).

The ditches were constructed in March 1988, one year before the start of the nutrient loading program. During this year a vegetation had developed that was typical for a pioneer stadi-

um: it consisted mainly of Characeae, with a coverage of more than 90% in all four ditches.

The external nutrient loading rates of the ditches and the method for nutrient addition are described in chapter 1.6 (p. 22-24).

The concentrations of dissolved phosphorus remained low in ditches A, B and C, with in the latter two only a temporary increase following each dosage. In ditch D the dissolved phosphorus concentrations have gradually increased since the start of the loading program. Ortho-P concentrations of ditch D are displayed in figure 2.2 a.

The particle size distribution and other characteristics of the sediment, as measured before the start of the nutrient loading program in May 1989, are given in tables 3.1 and 3.2.

Table 3.1. Particle size distribution at the start of the nutrient loading program (May 1989).

ditch:	A	B	C	D
fraction (μm):				
< 2	10.9	10.0	9.8	10.4
2 - 16	4.3	3.7	3.4	3.7
16 - 50	5.3	4.6	4.5	5.9
50 - 105	4.0	4.5	4.0	4.2
105 - 2000	74.1	76.2	77.3	74.0

Table 3.2. Chemical characteristics of the sediment in May 1989

ditch:	A	B	C	D
variable:				
total P ($\text{mg.}[\text{g DW}]^{-1}$)	0.24	0.21	0.29	0.25
total N ($\text{mg.}[\text{g DW}]^{-1}$)	0.54	0.60	0.45	0.41
Org. Matter (% of DW)	0.8	0.7	0.7	0.8
CaCO ₃ (% of DW)	0.6	0.3	0.3	0.4
Fe total (% of DW)	1.2	1.1	1.0	1.2

Table 3.3 presents the composition of the ditch water with respect to a number of variables during the growth season of

1990. The table shows that the ditches have similar concentrations of Mg^{2+} and Na^+ . Ditch D had higher concentrations of Ca^{2+} and K^+ compared to the other three. The high K^+ -concentrations in ditch D are caused by the monthly K_2HPO_4 dosages. Ditches A, B and C have a similar alkalinity and EC_{25} , but EC_{25} is higher in ditch D.

Table 3.3. Composition of ditch water, ranges of variables during 1990.

	A	B	C	D
Alkalinity (meq.l ⁻¹)	1.0-1.6	0.9-1.5	0.9-1.8	0.7 - 2.5
EC_{25} ($\mu S.cm^{-1}$)	110-150	120-180	110-170	200 - 270
Na^+ (g.m ⁻³)	5.2-8.1	5.4-8.0	3.7-7.5	7.3 - 8.8
K^+ (g.m ⁻³)	0.8-1.7	0.8-2.2	0.9-2.8	15.7-22.2
Ca^{2+} (g.m ⁻³)	11 - 15	10 - 15	8 - 17	20 - 29
Mg^{2+} (g.m ⁻³)	1.7-2.0	1.7-2.1	1.0-2.1	1.5 - 2.1

Figures 3.2 a-d display the pH-range during the period 1989-1992, presented as the monthly minimum and maximum values for the four ditches.

MATERIALS AND METHODS

The ditches were longitudinally divided in 20 equidistant segments, each with a length of 2 m. In each segment the areal coverage was estimated for individual species. Results are presented as the mean of the whole ditch.

Internal P-concentrations of the plant material in the four ditches were measured on four occasions: May 1989, October 1989, October 1990 and October 1991. These only provide a global estimation of their development over time, and do not reflect short term dynamics.

Samples were obtained from quantitative harvesting of the vegetation within a cylinder with a diameter of 37.5 cm placed in a homogeneous part of the vegetation, on three sites per ditch. Dry weight was measured after drying at 40°C.

Primary succession of macrophytes

The internal P concentration of the plant material was measured after complete digestion of a weighted amount of dry matter in a H_2SO_4 - Se mixture, using H_2O_2 as an oxidator (Novozamsky et al., 1983). Phosphate analyses were performed with the modified molybdate-blue method according to Murphy and Riley (1962).

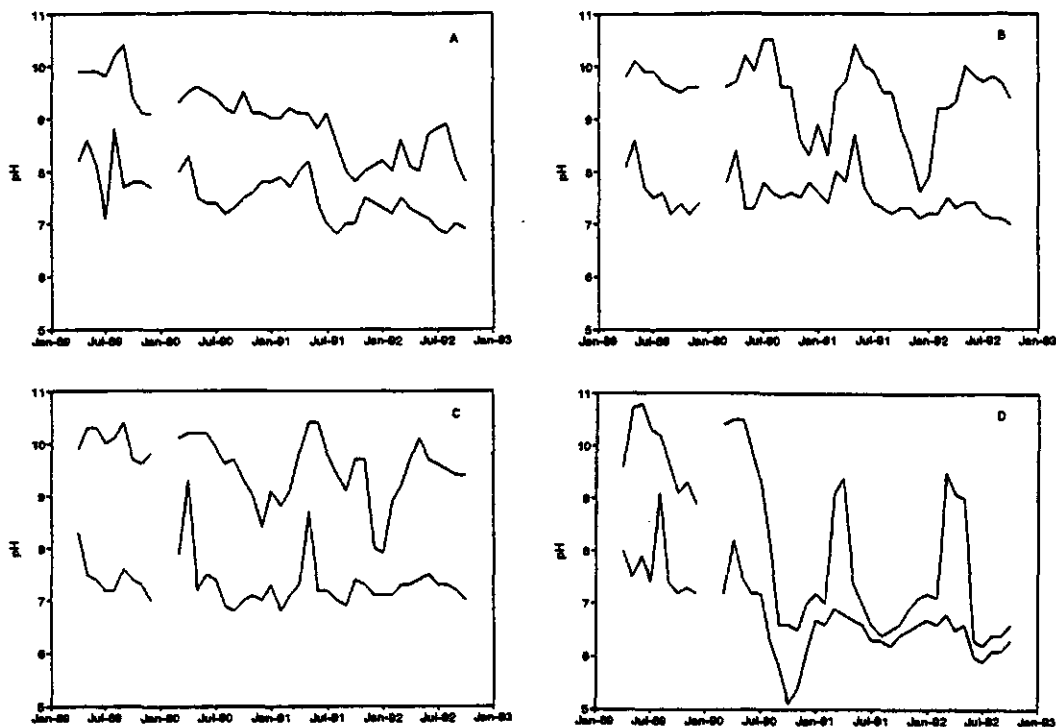


Figure 3.2. Monthly pH minima and maxima.
a) ditch A; b) ditch B; c) ditch C; d) ditch D;

The growth of periphytic algae was measured as the areal chlorophyll-a content on artificial substratum after one month incubation in the ditches. As artificial substratum microscope glass slides were used. Chlorophyll-a was estimated according to the hot ethanol method (Roijackers, 1981).

Sedimentary P was measured as the sum of the fractions of the extraction scheme according to Hieltjes and Lijklema (1980), followed by digestion with H_2SO_4 .

RESULTS

The total number of species that has been observed is 14 (including filamentous algae as a group). Table 3.4 gives a complete overview of the species that have been encountered in one or more of the ditches and a global indication of their maximum areal coverage during the period May 1989 - October 1992. *Senecio congestus* generally a terrestrial species, was included because in ditch D it showed up as a pleustophytic life form. This is probably due to the anchoring effect of a *Lemna minor* bed and the high concentrations of dissolved nutrients in the water.

At the start of the nutrient loading program the species composition was almost identical in all four ditches. Characeae were dominant, with an areal coverage of > 90% in all four ditches. Figure 3.3 presents the relative areal coverage of Characeae in time. It shows that they disappeared from all four ditches, but that the rate of decline is positively related to the external nutrient loading. In ditch D the Characeae completely disappeared during the first year after the start of the program, while in ditch A it took about 2.5 years.

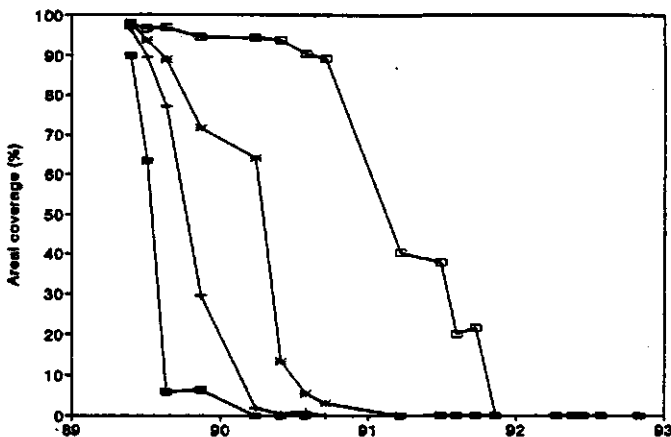


Figure 3.3. Relative areal coverage of Characeae (\square = ditch A; * = ditch B; + = ditch C; \blacksquare = ditch D).

Table 3.4. Overview of species present in the ditches and a global indication of their maximum areal coverage (%) during the period May 1989 - October 1992.

species	ditch:	A	B	C	D
<i>Alisma plantago-aquatica</i> L.		xx	x	x	xxx
Characeae		xxxx	xxxx	xxxx	xxxx
<i>Elodea nuttallii</i> (Planch.) St. John		xxx	xxxx	xxxx	xxxx
<i>Lemna minor</i> L.		x	x	x	xxxx
<i>Luronium natans</i> (L.) Raf.		x	x	-	-
<i>Myriophyllum verticillatum</i> L.		-	-	x	-
<i>Polygonum amphibium</i> L.		-	x	-	x
<i>Potamogeton crispus</i> L.		xx	x	xx	xx
<i>Potamogeton pusillus</i> L.		xx	x	x	-
<i>Ranunculus circinatus</i> Sibth.		xxx	xxx	xxx	xxx
<i>Sagittaria sagittifolia</i> L.		xxx	xx	x	xxx
<i>Eleocharis palustris</i> L.		xxx	-	-	-
<i>Senecio congestus</i> (R.Br.) DC.		-	-	-	xxx
filamentous algae		xxx	xxx	xxx	xx

) - : not found ; x : max. < 2 % ;
 xx : max. 2-10 % ; xxx : max 10-50 % ;
 xxxx : max. > 50 % ;

Figure 3.4 displays the areal coverage of *Elodea nuttallii* in time. It shows an enormous expansion in ditch D during the growing season of 1989. In ditch C and B the expansion was much less, while in ditch A it did not become abundant until medium 1991. At the start of the nutrient loading program there was a slight gradient in the abundance of *Elodea nuttallii*: the areal coverage was 0, 0.5, 2 and 9 % in ditches A, B, C and D respectively.

Figure 3.5 presents the development of *Lemna minor* in ditch D, where it became the dominant species during the summer of 1990. After that its areal coverage varied considerably, but this is mainly due to wind action. In the other ditches *Lemna minor* never reached an areal coverage of > 0.1%.

Figures 3.6 a-c display the areal coverage of *Sagittaria sagittifolia*, *Ranunculus circinatus* and *Alisma plantago-aquatica* respectively. *Sagittaria sagittifolia* reaches higher

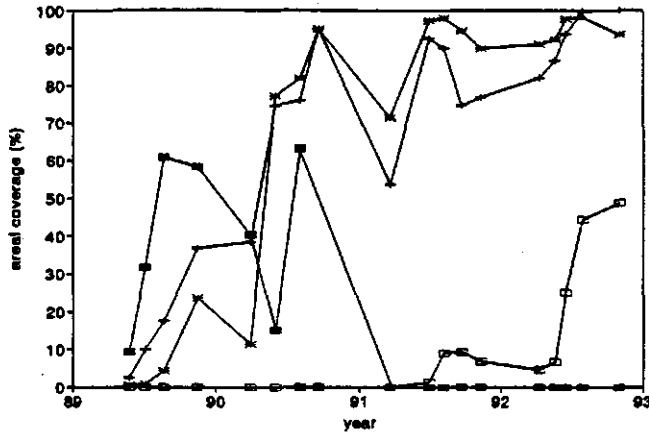


Figure 3.4. Relative areal coverage of *Elodea nuttallii*. (\square = ditch A; * = ditch B; + = ditch C; \blacksquare = ditch D).

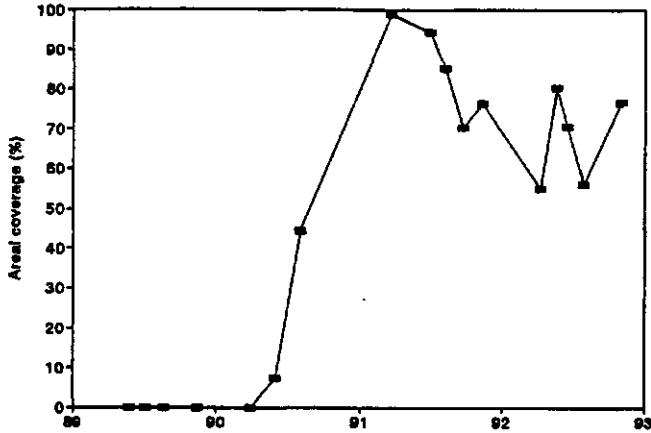


Figure 3.5. Relative areal coverage of *Lemna minor* in ditch D.

coverages in ditch A and D than in the ditches with the two intermediate trophic states. During the first year after the start of the loading program, the abundance of *Ranunculus circinatus* indicated a positive relationship with the trophic state, but after that declined in ditch B, C and D. *Alisma plantago-aquatica* shows an increase in coverage in ditch D,

but here a shift from rooting in the sediment to rooting near the banks of the ditch has occurred.

The internal P-concentrations of the dominant species are given in table 3.5.

Table 3.5. Internal P-concentrations (mg P.[g dry weight]⁻¹) in the dominant taxa Characeae (C), *Elodea* (E) and *Lemna* (L)

ditch:	A	B	C	D
May 1989	1.3 C	1.3 C	1.4 C	1.5 C
Oct 1989	1.9 C	2.1 E,C	2.7 E,C	6.8 E
Oct 1990	1.4 C	2.1 E	3.2 E	14.2 L
Oct 1991	1.2 C	3.6 E	4.5 E	14.4 L

Table 3.5 shows that *Lemna minor* is capable of accumulating much higher internal P-concentrations than *Elodea* and Characeae. The internal P-concentrations of *Elodea nuttallii* vary considerably, and are higher in ditch C than in ditch B. In both ditches they increase in time. In ditch D the internal P-concentrations in *Elodea nuttallii* reached a high value within five months after the start of the nutrient loading program. The internal P-concentrations of Characeae are continuously low and fairly constant.

Growth of epiphytic algae is presented in figures 3.7 a-d. The figures show that the areal chlorophyll-a content in ditches A, B and C varies considerably. No clear seasonal pattern can be detected. The values in ditches B and C are generally higher than those in ditch A. In ditch D very high values were measured during the first half of 1990, and after that they decreased. In 1991 and 1992 relative high chlorophyll-a contents were measured in spring; during the summer and autumn they were low.

Table 3.6 presents total sedimentary P in the top 5 centimeters. For reasons of comparison with the external loading rates (see chapter 1.5), sedimentary P is presented as g P.[m² water surface area]⁻¹. Deeper sediment layers showed no change in sedimentary P-content after 2.5 years after the start of

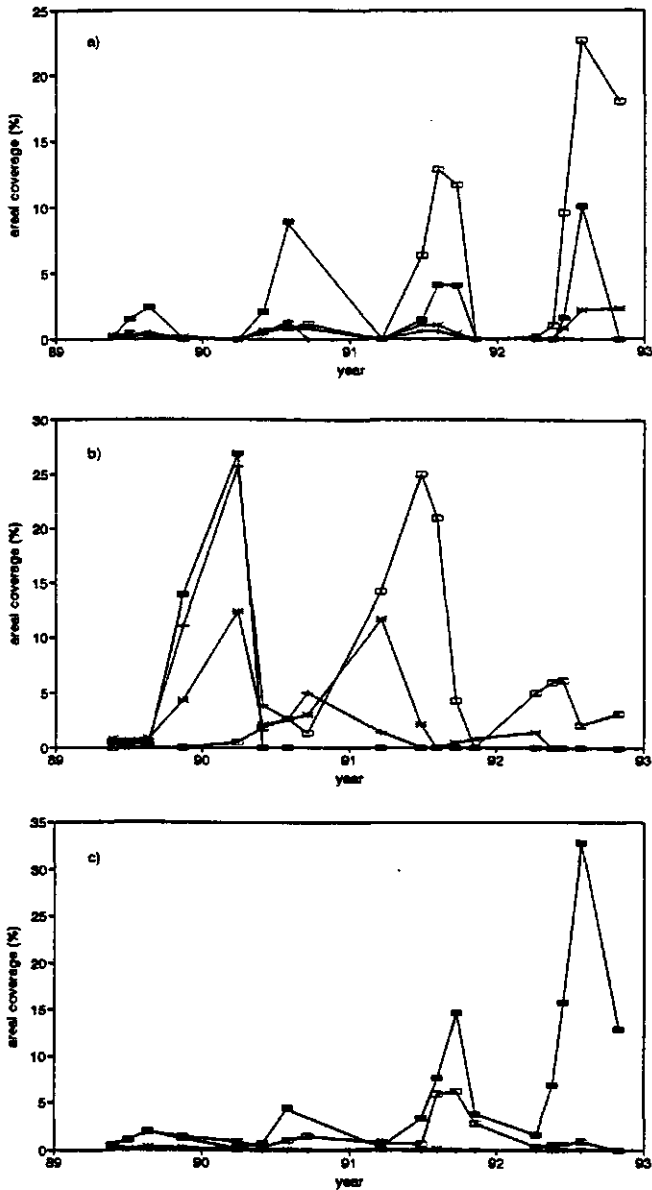


Figure 3.6. Relative areal coverage of a) *Sagittaria sagittifolia*; b) *Ranunculus circinatus*; c) *Alisma plantago-aquatica* (\square = ditch A; * = ditch B; + = ditch C; \blacksquare = ditch D).

Primary succession of macrophytes

the loading program, even at the highest loading rate, and therefore have not been taken into account. This indicates that vertical transport within the sediment is very slow. Table 3.6 shows that in ditch A, B and C there is even a slight decrease in sedimentary P-pool after 2.5 years, but the pattern is irregular. The values from October 1989 are all high, and a systematic analysis error can be considered. In ditch D the sedimentary P-pool increased steadily. The average sedimentary P-uptake rate after 2.5 years in ditch D was $10.7 \text{ g P} \cdot [\text{m}^2 \text{ water surface area}]^{-1}$, which is slightly smaller than the external P loading rate (see chapter 1.5).

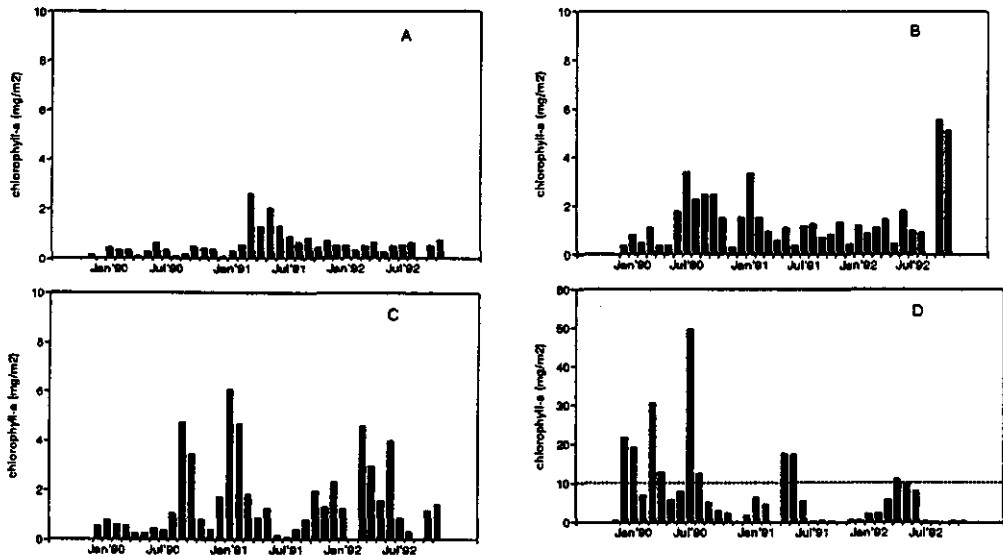


Figure 3.7. Growth of periphytic algae on artificial substratum from November 1989 to October 1992.

(A = ditch A; B = ditch B; C = ditch C; D = ditch D).

Table 3.6. Sedimentary P-pool ($\text{g P} \cdot [\text{m}^2 \text{ water surface}]^{-1}$).

ditch	May '89	Oct '89	Oct '90	Oct '91
A	9.9	14.1 ± 0.7	9.7 ± 0.8	8.9 ± 0.5
B	8.5	10.8 ± 1.6	8.5 ± 0.7	6.7 ± 0.9
C	11.3	14.2 ± 0.8	10.2 ± 1.0	7.4 ± 0.5
D	10.2	18.3 ± 1.1	26.6 ± 3.4	36.0 ± 3.7

CONCLUSIONS AND DISCUSSION

The rate of primary succession in four experimental ditches was positively related to the level of external nutrient input. The first step was the replacement of Characeae by *Elodea nuttallii*. In ditch A, which receives the lowest external nutrient input, it took 2.5 years after the start of the loading program and 3.5 years after the creation of the ditches before the Characeae had vanished completely. In ditches B and C it was respectively a little over and a little under 1.5 years after the start of the nutrient loading program. In ditch D the Characeae vegetation already collapsed during the first growth season, and disappeared within ten months. In ditches B, C and D the disappearance of the Characeae can be directly attributed to displacing by *Elodea nuttallii*. During the transition period *Elodea* filled up the top part of the water column, and overgrew the Characeae vegetation that was present in the bottom part. In ditch A *Elodea* only became significant after the Characeae had already vanished almost completely. The conclusion that the level of nutrient loading causes the differences in primary succession rates is, however, slightly biased by differences in the initial coverage of *Elodea*.

In ditches B and C the *Elodea* vegetation has remained stable, with an almost 100 % coverage during the summer and autumn. At the end of the research period ditch C was virtually a monoculture. Ditch B had a low abundance of *Sagittaria* with a maximum areal coverage of 1 and 2 % in 1991 and 1992 respectively, and a larger coverage with filamentous algae than ditch C.

In ditch D *Elodea nuttallii* was displaced by *Lemna minor* and was completely gone at the end of 1990. The growth of *Lemna minor* during the summer of 1990 resulted in a pH drop from 7 till 9 in June to 5 till 6 in September and generally anoxic conditions throughout the whole water column. Dominance of

Lemna minor reduces the water column to a compartment where the biological activity is mainly restricted to decomposition. The development of phytoplankton or epiphytic algae is possible only during periods when the *Lemna minor* cover is not complete: on a large time-scale this is due to seasonal effects, whereas on a short time scale it results from wind stress, when *Lemna minor* is pushed towards the banks. Growth of periphytic algae was high during the first half of 1990, and declined after the transition to dominance by *Lemna minor* had occurred. In 1991 and 1992 growth of periphytic algae in ditch D was high during spring, and declined to very low values during the second half of the year. In the other ditches this decline was not observed.

Phytoplankton blooms have not occurred to any appreciable extent during the period of transition from a Characeae to an *Elodea* dominated system. One of the reasons could be the release of allelopathic compounds by the macrophytes. This has not been tested in our studies. From literature we know that allelopathic effects of Characeae extracts on phytoplankton have can occur in bio-assay experiments (Wium-Andersen et al., 1982). It has not been shown that this phenomenon also occurs in situ with intact Characeae cells (Forsberg et al., 1990). However, during periods of massive die-off of Characeae, allelopathic compounds may be released and cause the suppression of phytoplankton blooms.

Lemna minor remained the dominant species in ditch D until the end of the research period in October 1992. Due to the anchoring function of the *Lemna* bed and high concentrations of dissolved nutrients, *Senecio congestus*, generally a terrestrial species, manifested itself as a pleustophytic species. It reached considerable areal coverages during 1991 and 1992.

The measured internal P-concentrations of *Lemna minor* are consistent with those given by Riemer and Toth (1968), who found that among 37 investigated species of angiosperms *Lemna minor* had the highest internal P-concentrations. The internal P-concentrations of *Elodea nuttallii* vary considerably, depen-

ding both on the level and duration of the phosphorus loading. The areal coverage by *Elodea nuttallii* followed a similar pathway in ditches B and C, but the difference in external loading rate is reflected in the internal P-concentrations.

Lemna minor derives its P requirements solely from the water column. The transition from dominance by *Elodea nuttallii* to dominance by *Lemna minor* will only take place after the system has lost its ability to store the added P, either through storage in the sediments or internal storage in the vegetation.

The sediment uptake capacity is limited by a maximum, which was slightly exceeded in the highest loaded ditch, resulting in increasing nutrient concentrations in the water column. This is probably a precondition for the occurrence of pleustophytic life forms. At lower external nutrient loading rates, on the other hand, a decrease of the sedimentary P-pool was observed. In this case the sediments released P, which sustained the growth of macrophytes.

The internal storage in the vegetation is also limited by a maximum in both biomass and internal P concentration. In ditches A, B and C *Lemna minor* was found occasionally with a low coverage that never exceeded 0.1 %. In these ditches the nutrient concentrations obviously were not high enough to allow the development of a *Lemna minor* bed.

Analysis of continuous oxygen measurements (from March 1990 to March 1992) revealed that the gross production rate is higher in ditch C than in ditch B (Portielje et al., *subm.*). Net production on the other hand, was initially also higher in ditch C, but became negative after 1990, while it remained generally positive in ditch B. The gradual build-up of an organic pool consisting of mainly dead plant material will result in a higher internal P-release from decomposition. This further reduces the available P storage capacity of the system.

The measured internal P-concentrations of Characeae are close to the critical concentration, which is defined as the trans-

ition point at which storage without additional growth starts to occur (Hutchinson, 1975). This critical concentration is ca. $1.3 \text{ mg P. [g dry weight]}^{-1}$ for a wide range of species (Gerloff and Krombholz, 1966).

Sagittaria sagittifolia was most abundant at both extremes of the trophic gradient, and this is most probably due to the negative effect of the dense *Elodea* vegetation in the two ditches with intermediate trophic levels. A dense *Elodea* vegetation might hamper the penetration of shoots of *Sagittaria* towards the water surface. A cover of *Lemna minor* apparently did not obstruct *Sagittaria*. A great variety in leaf forms can be performed by *Sagittaria sagittifolia* (Hutchinson, 1975). In ditch D *Sagittaria sagittifolia* manifests as larger plants with larger and brighter leaves compared to those in ditch A.

ACKNOWLEDGEMENTS

The authors thank dr. Kees Kersting for the continuous pH measurements and Fred Bransen for chlorophyll-a measurements.

REFERENCES

- Agami, M. and Y. Waisel, 1986. The ecophysiology of roots of submerged vascular plants. *Physiol. Veg.* 24, 607-624.
- Barko, J.W. and R.M. Smart, 1980. Mobilization of sediment phosphorus by submersed freshwater macrophytes. *Freshwater Biol.* 10. 229-238.
- Brock, T.C.M., R.M.M. Roijackers, R. Rollon, F. Bransen and L. van der Heyden (subm.). Effects of nutrient loading and insecticide application on the ecology of *Elodea*-dominated freshwater microcosms. II. Responses of macrophytes, periphyton and macroinvertebrate grazers. submitted to *Arch. Hydrobiol.*
- Carignan, R. and J. Kalff, 1980. Phosphorus sources for aquatic weeds: Water or sediments? *Science* 207, 987-988.

- Den Hartog, C. and S. Segal, 1964. A new classification of water-plant communities. *Act. Botan. Neerl.* 13, 367-393.
- Drent, J. and K. Kersting, 1993. Experimental research in ditches under natural conditions. *Water Res.* 27 (9), 1497-1500.
- Forsberg, C., S. Kleiven and T. Willén, 1990. Absence of allelopathic effects of *Chara* on phytoplankton in situ. *Aquat. Bot.* 38, 289-294.
- Gerloff, G.C. and P.H. Krombholz, 1966. Tissue analysis as a measure of nutrient availability for the growth of aquatic plants. *Limnol. Oceanogr.* 11, 529-537.
- Hieltjes, A. and L. Lijklema, 1980. Fractionation of inorganic phosphates in calcareous sediments. *J. Envir. Qual.* 9, 405-407.
- Hutchinson, G.E., 1975. A treatise on Limnology, Volume III. John Wiley and Sons, New York etc., 660 pp.
- Lijklema, L., J.H. Jansen and R.M.M. Roijackers, 1989. Eutrophication in The Netherlands. *Wat. Sci. and Technol.* 21, 1899-1902.
- Murphy J. and J.P. Riley, 1962. A modified single solution method for the determination of phosphate in natural waters. *Anal. Chim. Acta* 27, 31-36.
- Novozamsky, I., V.J.G. Houba, R. van Eck and W. van Vark, 1983. A novel digestion technique for multi-element plant analysis. *Comm. Soil Sci. Plant Anal.* 14, 239-249.
- Philips, G.L., D. Eminson and B. Moss, 1978. A mechanism to account for macrophyte decline in progressively eutrophicated freshwaters. *Aquatic Bot.* 4, 103-126.
- Portielje R. and L. Lijklema (subm.). Carbon dioxide fluxes across the air-water interface and its impact on carbon availability in aquatic systems. (submitted to *Limnology and Oceanography*)
- Portielje R., K. Kersting and L. Lijklema (subm.). Estimation of primary production in macrophyte dominated ditches from continuous dissolved oxygen signals. (submitted to *Water Research*)

- Riemer, D.N. and S.J. Toth., 1968. A survey of the chemical composition of aquatic plants in New Jersey. New Brunswick, 14 pp.
- Roijackers, R.M.M., 1981. A comparison between two methods of extracting chlorophyll-a from different phytoplankton samples. *Hydrobiol. Bull.*, 15: 179-183.
- Sculthorpe, C.D., 1967. The biology of aquatic vascular plants. Edward Arnold Publishers Ltd., London, 610 pp.
- Van Straten, G., 1986. Identification, uncertainty assessment and prediction in lake eutrophication. Ph.D.Thesis Technical University Twente, The Netherlands, 240 pp.
- Wium-Andersen, S., U. Anthoni, C. Christophersen and G. Houen, 1982. Allelopathic effects on phytoplankton by substances isolated from aquatic macrophytes (Charales). *Oikos* 39, 187-190.

Chapter 4

The effect of reaeration and benthic algae on the oxygen balance of an artificial ditch

key-words:

Dissolved oxygen - Reaeration - Tracer experiments -
Benthic algae

Based on: The effect of reaeration and benthic algae on the oxygen balance of an artificial ditch, by R. Portielje and L. Lijklema. Accepted for publication by Ecological Modelling.

4. THE EFFECT OF REAERATION AND BENTHIC ALGAE ON THE OXYGEN BALANCE OF AN ARTIFICIAL DITCH

ABSTRACT

In an artificial ditch, receiving a low nutrient input, processes affecting DO (dissolved oxygen) were measured. Estimated process parameters were implemented in a dynamic model to simulate continuously measured DO. The processes modeled were primary production, respiration, sediment oxygen demand and reaeration.

Primary production by a benthic layer of algae was found to dominate the oxygen balance. The contribution of reaeration was also large, even at the observed oxygen concentrations which were close to equilibrium.

Adaptation to ambient light conditions was introduced in the description of benthic primary production. The reaeration-coefficient was related to the continuously measured wind velocity. This resulted in a good agreement between simulated and measured DO concentrations, with a model efficiency of 89%.

INTRODUCTION

In artificial ditches research on eutrophication is conducted. The effects of the level of external nutrient loading (N and P) on the structure and functioning of the system is studied, with emphasis on the underlying processes.

A consequence of enhanced nutrient supply to nutrient limited systems is an increase in the productivity and concomitantly a change in the oxygen balance. High productivity can result in large DO fluctuations, with high oversaturation during daytime. The intensification of the nutritional cycle also causes an increased respiration and decomposition of organic matter, resulting in DO depletion at night. In aquatic systems with low productivity, DO generally will be close to the equilibrium, with a daily amplitude that is relatively small compared to this equilibrium.

In this chapter the oxygen balance of a ditch with a low nutrient input, originating from dry and wet atmospheric deposi-

tion and occasional supply of groundwater with low N and P concentrations, is discussed. DO is simulated using measured process parameters. In this study the attention is specifically on the exchange of oxygen across the water-air interface and on the role of benthic algae.

Due to a low external input, the concentrations of dissolved phosphorus are low: on average about 10 $\mu\text{g PO}_4\text{-P/l}$. Concentrations of suspended particular P are about 20 $\mu\text{g P/l}$. Near the water-sediment interface the availability of nutrients will generally be higher. A layer of mainly benthic algae, some dead organic matter and bacteria has developed. This interface provides a preferred habitat to algae and bacteria in systems with low nutrient concentrations in the overlying water.

The rationale for the study of the oxygen balance is the close relationship between nutrient dynamics and primary production. Whereas nutrient fluxes cannot be measured directly with sufficient accuracy, analysis of continuous DO recordings enables the reconstruction of net and gross production rates through an adequate model. Gross production rates then can be used to estimate the fluxes of nutrients through the biotic compartment.

THEORY

Modelling concepts

A balance for the oxygen concentration C [$\text{g}\cdot\text{m}^{-3}$] is:

$$\frac{dC}{dt} = \text{PROD} - \text{RESP} - \text{SOD} + \text{REAER} \quad (1)$$

with PROD and RESP primary production and respiration by both benthic algae and phytoplankton, SOD=sediment oxygen demand and REAER=reaeration. The relative importance of the different processes varies within the diurnal and the seasonal cycle. Figure 4.1 presents a conceptual diagram of the model.

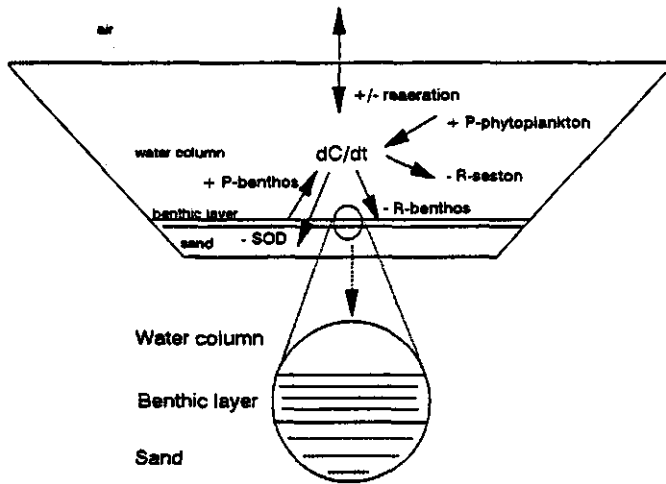


Figure 4.1. Conceptual diagram of the model and its application to the artificial ditch.

Reaeration

Information on reaeration in stagnant waters is relatively scarce as compared to that in streams. In the latter the mass transfer coefficient at the water-air interface depends on the turbulence generated by the bottom shear stress of the flowing water. In stagnant water wind generates the turbulence at the surface. Existing relationships between wind velocity and the mass transfer coefficient are not suitable for small systems. Hence in situ measurement of this relationship is necessary.

Techniques for the measurement of reaeration can be divided in three groups:

- 1) direct measurement
- 2) calculation as the restpost of a DO mass balance after all other terms have been measured.
- 3) calculation from measurements on a tracer gas.

1) usually involves the placement of a cap on the water surface, thereby enclosing a volume of air which is then flushed with N_2 to drive out oxygen. The rate of replenishment with oxygen from the water is measured, and the mass transfer coefficient can be calculated. The cap can locally influence turbulence, and thereby affect reaeration, especially in small water bodies where the size of the cap is not negligibly small as compared to the water surface. It is not clear at what scale of turbulence a loss of turbulence may be induced but it can be assumed that the dissipation of energy from the waves downwards to smaller eddies and ultimately to Brownian movement (heat) will be affected, especially at the scales of the cap and the depth of submersion of the instrument. Only comparison with independent measurements can give an estimate of the potential reduction in mass transfer rates. Measurements with a cap have the disadvantage with respect to 3) that it measures reaeration at one spot, while a spatial variability might exist. This is especially the case in the ditches, where significantly higher waves can be generated on the lee-side.

2) has the clear disadvantage of accumulating all the inaccuracies in the other terms of the oxygen balance into the calculated reaeration rate.

3) has neither of the above mentioned disadvantages, but puts some demands on the tracer gas to be used :

- it must be conservative and have no other sources or sinks except exchange across the air-water interface.

- the method for analysis of the tracer must have a sufficient accuracy and a sufficiently low detection limit.

- as with oxygen, the solubility must be low, and the resistance towards gas exchange must be at the water-side of the interface.

- for application in natural waters it must, of course, be a non-toxic.

- its molecular diffusion coefficient should be close to that of O_2 . According to different theories, e.g. the film model (Whitman, 1923) or the penetration model (Higbie, 1935) the

mass transfer coefficient K_L is proportional to D^n , with $n=0.5$ in the penetration model and $n=1.0$ in the film model. In reality n lies between these two theoretical values, but is not known and varies apparently with the hydrodynamic conditions. Experimental evidence suggests values of about 0.6-0.7. If $D_{\text{tracer}} \approx D_{\text{O}_2}$ then $K_{L,\text{tracer}} \approx K_{L,\text{O}_2}$, irrespective of the value of n .

Tsivoglou et al. (1965) did tracer experiments to measure reaeration in the laboratory and later in the field as well (Tsivoglou et al, 1968). Krypton-85 was used as the gas tracer and tritium as dispersion/dilution tracer. Rathbun et al. (1978) introduced low molecular weight hydrocarbon gases as gas tracer. In laboratory and field studies chlorinated hydrocarbons such as methylchloride have also been used (Wilcock, 1984a,b).

In this study ethylene was chosen as gas tracer. It is non-toxic at low concentrations and its diffusion coefficient is close to that of oxygen ($D_{\text{C}_2\text{H}_4, 20^\circ\text{C}} = 1.87 \cdot 10^{-9} \text{ m}^2 \cdot \text{s}^{-1}$ (Reid, 1977) and $D_{\text{O}_2, 20^\circ\text{C}} = 2.55 \cdot 10^{-9} \text{ m}^2 \cdot \text{s}^{-1}$). Microbial conversion can be neglected compared to the flux across the water-air interface, although repeated use of the gas in the same water body on a longer term may cause the development of a microbial population that is capable of breaking down ethylene. In a small isolated water body the use of a dilution-/dispersion tracer is not needed, as the time to achieve complete mixing of the tracer after dosing is small compared to the time-scale of the exchange across the water-air interface.

The flux F ($\text{g} \cdot \text{m}^{-2} \cdot \text{hr}^{-1}$) across the air-water interface is given by:

$$F = K_L(C_g - C) \quad (2)$$

with K_L the mass transfer coefficient ($\text{m} \cdot \text{hr}^{-1}$). The equilibrium concentration C_g [$\text{g} \cdot \text{m}^{-3}$] of oxygen in freshwater, assuming a

constant partial pressure in the atmosphere, is a function of temperature, and is given by (Rich,1973):

$$C_s = 14.652 - 0.410T + 7.99 \cdot 10^{-3}T^2 - 7.78 \cdot 10^{-5}T^3 \quad (3)$$

with T in °C.

The mass transfer coefficient of oxygen is derived from that of the tracer from:

$$K_{L,O_2} = K_{L,t} \left(\frac{D_{O_2}}{D_t} \right)^n \quad (4)$$

(Subscript t refers to the tracer)

With $n=0.6$ this yields $K_{L,O_2} = 1.20 K_{L,t}$ and with $n=0.7$ $K_{L,O_2} = 1.24 K_{L,t}$.

Rathbun et al. (1978) derived from laboratory experiments on sorption rates of oxygen and ethylene in a temperature traject of 20-30°C, that $K_{L,O_2} = 1.15 K_{L,t}$ ($n=81, \sigma=0.11$, standard deviation supplied by Rainwater and Holley (1984) using the original data from Rathbun).

In this study the mass transfer coefficient of oxygen is calculated from the measured ethylene K_L -value using this experimentally derived ratio of 1.15. The partial pressure of the tracer in the atmosphere can be assumed zero.

Since measurement of one $K_{L,t}$ value takes a few days the wind velocity unfortunately has to be averaged over that period, A non-linear relationship therefore is forced into a linear framework. $K_{L,t}$ also depends on temperature:

$$K_{L,t} = K_{L,t_{30^\circ C}} \Theta_A^{(T-20)} \quad (5)$$

Θ_A is the temperature coefficient, and a value of 1.024 (-) has been estimated by Downing and Truesdale (1955).

The relationship between wind velocity and the mass transfer coefficient will differ between individual water bodies. The dissipation of turbulence generated by wind depends on the

geometry of the system. Therefore it has to be determined experimentally.

Banks (1975) distinguished three different trajects of wind speed in relation to K_L : at low wind speed $K_L \approx W^{1/2}$, at intermediate wind speed $K_L \approx W$ and at high wind speed $K_L \approx W^2$. The transition from the intermediate wind speed traject to the high wind speed traject seems to correspond to the initiation of breaking waves and the resulting surface enlargement. In the ditches the fetch is too short to cause this phenomenon, and therefore consideration of a quadratic wind-reaeration relation at high wind speeds may be undue.

Primary production

In the test ditch primary production by macrophytes can be neglected, so only algae are included in the model concept. The algae are divided in phytoplankton and phytobenthos, for which the primary production rates can be modelled with the same equations. The values of the model parameters will differ:

$$PROD = Pr_{\max, w/b_{20^\circ C}} F(N) F(I) F(T) \quad (6)$$

in which $F(N)$ and $F(I)$ represent limitation by nutrients and light and $F(T)$ the temperature effect relative to the reference temperature. Subscripts w and b refer to water column and benthic layer respectively. The nutrient availability in the ditch is low and is mainly determined by internally stored P (Portielje and Lijklema, 1993). As the relative change in biomass is small during a period of a few days, it can be considered constant for the simulation period. Therefore $F(N)$ can be included in the maximum gross production rate $Pr_{\max, w/b}$ of the phytoplankton or phytobenthos.

The photosynthesis-light function $F(I)$ used is that of Steele (1962), which takes into account photo-inhibition at high irradiance:

$$F(I_z) = \frac{I_z}{I_{s,w}} e^{(1 - \frac{I_z}{I_{s,w}})} \quad (7)$$

with I , the optimum light intensity (W.m^{-2}). Subscripts z and w refer to depth and phytoplankton respectively. To account for the attenuation of light equation (7) is averaged over depth:

$$F(I) = \frac{e}{\epsilon_w B} [e^{(\frac{-I_s}{I_{s,w}})} - e^{(\frac{-I_0}{I_{s,w}})}] \quad (8)$$

with $e=2.71$. ϵ_w is the total extinction coefficient of the water (m^{-1}) and subscripts 0 and B refer to water surface ($z=0$) and bottom ($z=B$) respectively.

Light attenuation is much larger in the benthic layer than in the water column. The extinction coefficient has to be determined experimentally. The material is flaky and the distribution of material in the layer is vertically inhomogeneous, with lower densities in the top part. Therefore the extinction coefficient ϵ_b is defined as the attenuation of light per dry weight per area ($\text{m}^2.[\text{g dry weight}]^{-1}$). For this purpose the benthic layer has been divided into a number of horizontal sublayers, each representing an equal amount of dry weight. The light intensity I_n in the middle of a layer n is:

$$I_n = I_B e^{-\epsilon_b M \frac{n-1/2}{n_{\text{tot}}}} \quad (9)$$

with I_B the light intensity at the interface of the water-benthic layer interface and n_{tot} the number of sublayers. M is the total amount of dry weight per unit of area. For the individual sublayers the light function can be calculated as :

$$F(I)_n = \frac{I_n}{I_{s,b}} e^{(1 - \frac{I_n}{I_{s,b}})} \quad (10)$$

The overall light response function for the benthic layer is attained from averaging the $F(I)$ -values of the individual sublayers. The optimum light intensities $I_{s,w}$ and $I_{s,b}$ vary in

time due to adaptation to incident light conditions. Therefore $I_{s,w}$ and $I_{s,b}$ are calculated for each day with:

$$I_{s,w} = c \sum_{\lambda} \frac{I_0}{\lambda} \quad (11a)$$

$$I_{s,b} = c \sum_{\lambda} \frac{I_z}{\lambda} \quad (11b)$$

with λ the length of the light period. c is a constant, to which Smith (1980) assigned a value of 0.3 (-). Van Straten (1986) found $c=0.45$. It is based on the observation that in lakes the maximum productivity occurs roughly at a depth z where $I_z \approx 0.3I_0$. Equations 11a,b imply an instantaneous adaptation to the light conditions of the actual day.

The exchange of oxygen between the benthic layer and the overlying water may be limited by transport across the interface. During periods of high productivity a concentration gradient, with higher DO concentrations in the benthic layer than in the overlying water, may be generated. Revsbech et al. (1983) measured steep gradients within a microbial mat using microelectrode techniques. The effective vertical diffusion coefficient D_{eff} at the benthic layer-water interface is determined by turbulence and pressure gradients in the overlying water. Portielje and Lijklema (1993) estimated for phosphate that D_{eff} at the lower boundary of the benthic layer (the sediment-benthic layer interface) in a ditch identical to that considered in this study was on average about 25 times the molecular diffusion coefficient D_{mol} . At the benthic layer-water interface D_{eff} may therefore well be in the order of several hundreds times D_{mol} . The exact value is not known, and varies in time depending on environmental conditions. The sensitivity of the simulated DO course in the overlying water to the value of D_{eff} however has to be considered.

Respiration

Respiration by algae and DO consumption by bacteria is modeled solely as a function of temperature, again analogous to (5), with the temperature coefficient $\theta_R = 1.08$ (-), (Van Duin and Lijklema, 1989). Photo-respiration, which has been shown to respond rapidly to the gross photosynthesis rate (Harris & Piccinin, 1977), has not been taken into account, but manifests in primary production measurements as a lowered net production rate.

Sediment oxygen demand

Sediment oxygen demand is the result of several oxygen consuming processes in the sediment, each with its own characteristic kinetics (Wang, 1980). A detailed description would be cumbersome and might not contribute significantly to a better simulation.

A simplified model, that describes the flux of oxygen across the water-sediment interface as a function of the overlying water DO concentration, is:

$$SOD(T) = SOD(20^\circ C) \theta_s^{(T-20)} \frac{C}{K_s + C} \quad (12)$$

McDonnell and Hall (1969) have reported values for θ_s between 1.065 and 1.075 from their own experiments and literature data. Van Duin and Lijklema (1989) reported a value for K_s of $0.7 \text{ g O}_2 \cdot \text{m}^{-3}$. In this study, the oxygen concentration in the water is permanently high enough ($> 9 \text{ g O}_2 \cdot \text{m}^{-3}$) to allow zero-order kinetics, and therefore the Monod term has been omitted. The measured sediment oxygen demand can be related to a volumetric oxygen demand rate in the sediment porewater. A simplified mass balance for the oxygen concentration in the porewater yields:

$$\frac{\partial C}{\partial t} = D_{eff, O_2} \frac{\partial^2 C}{\partial x^2} - R \quad (13)$$

with R the zero order oxygen demand in the interstitial water ($g\ O_2 \cdot m^{-3} \cdot hr^{-1}$) which has been assumed constant.

For discretization with respect to the depth, the sediment has been divided into horizontal sublayers with equal thickness. SOD is directly related to the concentration gradient at the sediment-water interface $dC/dx|_{x=0}$. R has been estimated from fitting the simulated flux across the sediment-water to the measured flux.

Model efficiency

The Model efficiency η was calculated as:

$$\eta = \frac{\sum_{i=1}^n (C_{i,m} - \bar{C}_m)^2 - \sum_{i=1}^n (C_{i,s} - C_{i,m})^2}{\sum_{i=1}^n (C_{i,m} - \bar{C}_m)^2} * 100\% \quad (14)$$

Subscript m refers to measured and s to simulated oxygen concentrations. n is the total number of measurements.

It relates the sum of squares of the deviations between measured and simulated data to the variation in the measured signal.

MATERIALS AND METHODS

The ditch

The research is conducted in the reference sand-ditch (A). The location and characteristics of the ditch are described in chapter 1.5 (p. 20-22) and the external nutrient loading rate in chapter 1.6 (p. 22-24).

In the center of the ditch dissolved oxygen, pH and temperature are measured continuously and transferred to a

data-logger and registered as fifteen minute averages. DO is measured at two depths (10 and 40 cm), pH at one depth (25 cm) and temperature at three depths (10, 25 and 40 cm).

Light irradiance and wind velocity at an elevation of 2 m are continuously measured and registered by a data-logger as fifteen minute averages. The instrumentation is described in detail by Drent and Kersting (1993).

The sand is poor in nutrients with an extractable phosphorus content of about $0.10 \text{ mg P. [g dry weight]}^{-1}$ as the sum of the different fractions of the selective extraction procedure according to Hieltjes and Lijklema (1980). This procedure involves subsequent extraction with 1 M NH_4Cl , 0.1 M NaOH and 0.5 M HCl and destruction of the remaining material.

Reaeration measurements

In the lab a vessel containing about 30 l of demineralised water is saturated with ethylene (C_2H_4) by flushing it for 30 minutes. The vessel is closed air-tight and transported to the ditch. Here the ethylene saturated water is homogeneously distributed and mixed with the ditchwater.

During three days samples were collected in sixfold, at two different positions and at three different depths. 10 ml samples were injected into a septum-tied bottle with a volume of 30 ml. The samples were transported to the laboratory where they were stored for a few days at 20°C to allow equilibration between dissolved and gaseous ethylene.

100 μl of the gas phase of each sample was injected in a gaschromatograph (Packard 430, column type Porapack R) and analysed for ethylene. Since only the relative ethylene concentration was of importance, the calculations were based on peak heights.

Sediment oxygen demand

The oxygen demand of the sand was measured in an enclosure

under a pyramid-shaped cap (0.45 X 0.45 X 0.45 m) placed on top of the sandy sediment. The benthic layer of algae and detritus was carefully removed by gentle stirring, without causing resuspension of the sand. Due to the large density difference between the benthic layer and the sand this was accomplished readily. The cap was equipped with a stirring propeller and DO was measured continuously for 4 hrs with an oxygen electrode.

Primary production and respiration

Primary production and respiration were measured in light and dark bottles according to Vollenweider (1974) at two locations and at two depths (5 cm below the water surface and 10 cm above the sediment). Two light and two dark bottles were filled with water from that depth and incubated for 4 hrs. The initial concentration was measured in fourfold. All DO measurements were performed according to the Winkler-method.

Oxygen consumption in dark bottles comprises both bacterial oxygen demand and algal respiration. To measure primary production and respiration by benthic algae and bacteria six sediment cores with a diameter of 5.3 cm were collected. The benthic layer was separated from the sand by subsequent resuspension and decantation. The material from all six cores was well mixed and ditchwater was added to a volume of 5 l. From this 9 bottles were filled. Three were used for analysis of the initial concentration, three for measurement of respiration and three for gross primary production measurement. The latter six were placed on top of the sediment and incubated for 4 hrs. The mixture was analyzed for dry weight.

Measurement of extinction coefficients

The extinction coefficient of the water was calculated from light intensities measured at two depths (z_1, z_2) with two

Bottemanne sensors attached to a support. The signals were transferred to a data-logger. The extinction coefficient ϵ_w was calculated from :

$$\epsilon_w = \frac{\ln(I_{z1}) - \ln(I_{z2})}{z2 - z1} \quad (15)$$

and averaged over time. The incubation time was about three hours.

To measure light attenuation within the benthic layer, three sediment cores (diameter 5.3 cm) were collected, and the benthic layers were separated and mixed. The suspension was analysed for dry weight. In the lab a glass tube with a flat bottom of constant thickness and a diameter of 2.2 cm was placed on a Bottemanne sensor. The side walls were taped with black plastic to prevent light scattering. A light source was placed above the tube.

Different volumes of the suspension were added to the tube which after that was filled up with demineralised water to a marked level. The extinction coefficient ϵ_b ($\text{m}^2 \cdot [\text{g dry weight}]^{-1}$) was calculated as the slope of the logarithm of the light intensity plotted versus the areal dry weight content of the tube.

RESULTS

Extinction coefficients

The results of the two measurements of ϵ_w were:

1:	$\epsilon_w = 1.592 \pm 0.262$	(n=21)	m^{-1}
2:	$\epsilon_w = 1.554 \pm 0.068$	(n=17)	m^{-1}
average:	$\epsilon_w = 1.575 \pm 0.200$	(n=38)	m^{-1}

In the model simulations a value for ϵ_w of 1.58 m^{-1} has been used.

The result of the measurement of ϵ_b is presented in figure 4.2, that displays $\ln(I)$ plotted versus the areal dry weight content of the tube. Linear regression resulted in :

$$\epsilon_b = 0.0455 \text{ (m}^2 \cdot [\text{g dry weight}]^{-1}) \quad n=11 \quad r^2 = 0.978$$

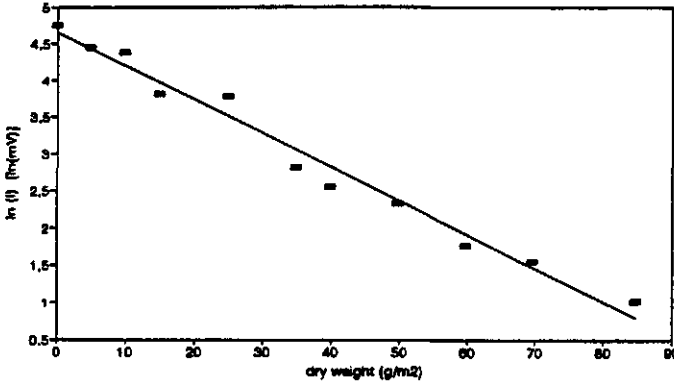


Figure 4.2. Light attenuation by benthic algae as a function of areal dry weight.

Primary production

Primary production of phytoplankton was measured on two occasions in the simulation period. Data were corrected for the average water temperature during the incubation period. The temperature did not deflect more than 2°C from the reference temperature of 20°C. Results are ($\text{gO}_2 \cdot \text{m}^{-3} \cdot \text{hr}^{-1}$):

day	$\text{Pr}_{\text{max},w}(20^\circ\text{C}) * F(I)$	$F(I)$	$\text{Pr}_{\text{max},w}(20^\circ\text{C})$
2/7	0.043	0.41	0.105
3/7	0.076	0.56	0.136

The average $\text{Pr}_{\text{max},w}(20^\circ\text{C})$ was $0.121 \text{ g O}_2 \cdot \text{m}^{-3} \cdot \text{hr}^{-1}$.

Primary production by the benthic algae was measured on three occasions. Data were also corrected for temperature and experimental light conditions (in the bottles the areal dry weight content was smaller than that in the ditch). Results in

$\text{g O}_2 \cdot \text{m}^{-2} \cdot \text{hr}^{-1}$ are:

date	Prod(20°C)*F(I)	F(I)	Pr _{max,b} (20°C)
2/7	0.537	0.67	0.80
3/7	0.416	0.66	0.63
4/7	0.485	0.58	0.84

The average value for Pr_{max,b}(20°C) was $0.76 \text{ g O}_2 \cdot [\text{m}^2 \cdot \text{hr}]^{-1}$ (n=3, $\sigma=12\%$). The overall primary production by phytoplankton was small compared to that by the benthic algae.

Respiration

Measured temperature corrected respiration rates of the seston ($\text{g O}_2 \cdot \text{m}^{-3} \cdot \text{hr}^{-1}$) and the benthic layer ($\text{g O}_2 \cdot \text{m}^{-2} \cdot \text{hr}^{-1}$) were:

date	R _{seston}	R _{benthos}
2/7	0.0514	-
3/7	0.0277	0.094
4/7	0.0156	0.063
15/7*		0.103
16/7*		0.053
average	0.0316	0.078
σ	0.0149	0.021

* Additional measurements used for estimation of R_{benthos}

The coefficient of variation in the measured respiration rates of the seston is high due to small DO changes during the incubation periods. The oxygen consumption is low compared to that by the benthic layer. For calculation of the respiration rate by the benthos additional data from outside the simulation period (two weeks later) were used.

Reaeration

In table 4.1 the measured values for K_{L,C_2H_4} and the resulting temperature corrected reaeration coefficients $K_{L,O_2}(20^\circ\text{C})$ are given. Figure 4.3 displays K_{L,O_2} plotted versus the average wind velocity. Linear regression yields:

$$K_{L,O_2}(20^\circ\text{C}) = 0.0387 W - 0.0377 \quad (n=4, r^2=0.89)$$

Table 4.1. Mass transfer coefficients for ethylene and oxygen.

exp.	$K_{L,t}$ (hr ⁻¹)	n	r ²	temp ^a (°C)	$K_{L,t}(20^{\circ}\text{C})$ (hr ⁻¹)	$K_{L,O_2}(20^{\circ}\text{C})$ (hr ⁻¹)
1	0.0417	26	0.98	22.2	0.0396	0.0450
2	0.0390	24	0.98	17.9	0.0410	0.0467
3	0.0558	26	0.99	21.0	0.0540	0.0614
4	0.0298	24	0.98	21.4	0.0291	0.0331

^a temperature averaged over incubation period

This relationship would yield a negative mass transfer coefficient at low wind velocities. As the lower limit for $K_{L,O_2}(20^{\circ}\text{C})$ a value of 0.006 hr⁻¹ has been chosen arbitrarily. The solid line in figure 4.3 represents the overall wind function F(W).

Sediment oxygen demand

The oxygen demand of the plain sand was measured on two occasions. In both cases the oxygen consumption rate was very low compared to that of the other processes, and as a consequence the sensitivity of the model for the SOD is small. Measured rates were 0.037 and 0.010 g O₂ m⁻².hr⁻¹ respectively.

Taking into account the vertical porosity profile in the sand, this corresponds to an average volumetric consumption rate R in the interstitial water of 0.75 g O₂.m⁻³.hr⁻¹. The contribution of SOD to the oxygen balance is small.

Model simulation

The DO concentration was simulated over a four days period and compared to the measured DO course. As the initial concentration in the simulation the measured concentration was used. Values of model parameters and their sources are summarized in table 4.2.

Figures 4.4 a-c present the wind velocity at an elevation of 2 m, the average water temperature and the irradiance during the simulation period.

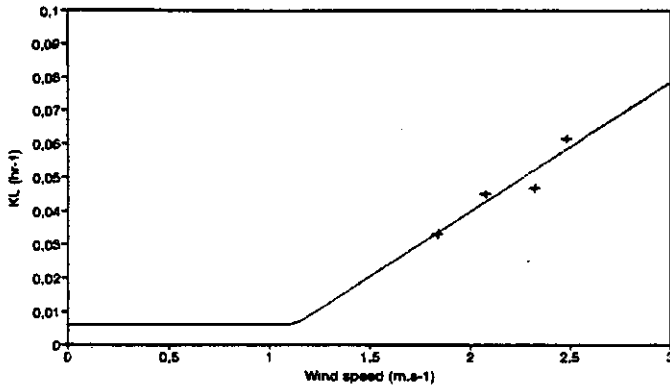


Figure 4.3. Reaeration coefficient $K_{L,O_2}(20^\circ\text{C})$ as a function of wind speed (dots = measured, line = overall wind-function).

Table 4.2. Parameter values used in the simulation of DO.

parameter	unit	value	source*
$K_{L,O_2}(20^\circ\text{C})$	hr^{-1}	0.006	($W < 1.1 \text{ m/s}$)
		0.0387W - 0.0377	($W > 1.1 \text{ m/s}$)
$Pr_{\max,w}(20^\circ\text{C})$	$\text{g O}_2 \cdot \text{m}^{-3} \cdot \text{hr}^{-1}$	0.12	E
$Pr_{\max,b}(20^\circ\text{C})$	$\text{g O}_2 \cdot \text{m}^{-2} \cdot \text{hr}^{-1}$	0.76	E
$Resp_w(20^\circ\text{C})$	$\text{g O}_2 \cdot \text{m}^{-3} \cdot \text{hr}^{-1}$	0.032	E
$Resp_b(20^\circ\text{C})$	$\text{g O}_2 \cdot \text{m}^{-2} \cdot \text{hr}^{-1}$	0.078	E
R	$\text{g O}_2 \cdot \text{m}^{-3} \cdot \text{hr}^{-1}$	0.75	E
θ_A	-	1.024	L
θ_p	-	1.030	L
θ_r	-	1.081	L
θ_s	-	1.070	L
ϵ_w	m^{-1}	1.58	E
ϵ_b	$\text{m}^2 \cdot [\text{g DW}]^{-1}$	0.0455	E
C	-	0.3	L

*) L = literature, E = experimental, own results

The result of the simulation is given in figure 4.5. There is a good agreement between simulated and measured DO during the first three days, but a somewhat higher deviation during the first half of the fourth day. C in equations 11a and 11b has been assigned values of 0.3 and 0.45 (-), the latter giving slightly better simulation results. Model efficiencies over

Reaeration and benthic algae

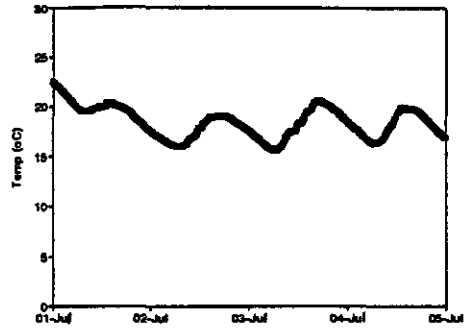
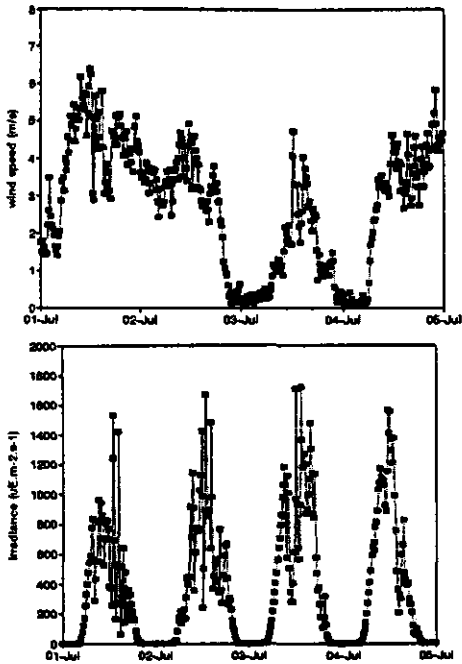


Figure 4.4.
 a) Wind velocity (m.s^{-1}) at an elevation of 2 m.,
 b) average water temperature ($^{\circ}\text{C}$), and
 c) light irradiance ($\mu\text{E.m}^{-2}.\text{s}^{-1}$), all during the simulation period.

the four days period were 87% and 89% respectively. In the simulations D_{eff} at the interface between benthic layer and overlying water has been set at $100.D_{\text{mol}}$.

The sensitivity of the simulation result to the value of D_{eff} is demonstrated in figure 4.6, with values for D_{eff} of 10, 100 and 500 times D_{mol} . It is evident that the result is virtually independent of D_{eff} at values larger than $100 D_{\text{mol}}$. A value for D_{eff} of $10 D_{\text{mol}}$ is obviously too small.

Figure 4.7 displays the DO concentration inside the benthic layer for different values of D_{eff} , and demonstrates the enormous daily DO fluctuations at low values for D_{eff} .

Figure 4.8 displays the contributions of the individual terms to the oxygen balance. The dominating processes are primary production and reaeration. Benthic algae contributed about 70% of the total gross primary production over the four days period and phytoplankton about 30%.

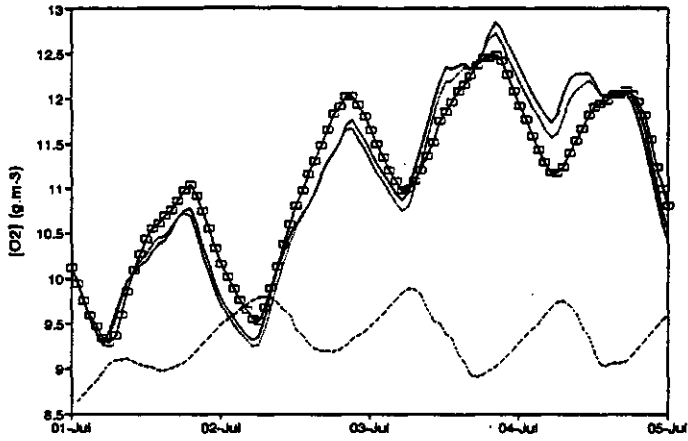


Figure 4.5. Results of the simulation for $c=0.3$ and $c=0.45$, equilibrium concentration C_B and measured DO course over four days. (\square = measured; —: $c=0.45$;: $c=0.30$; - - - -: C_B).

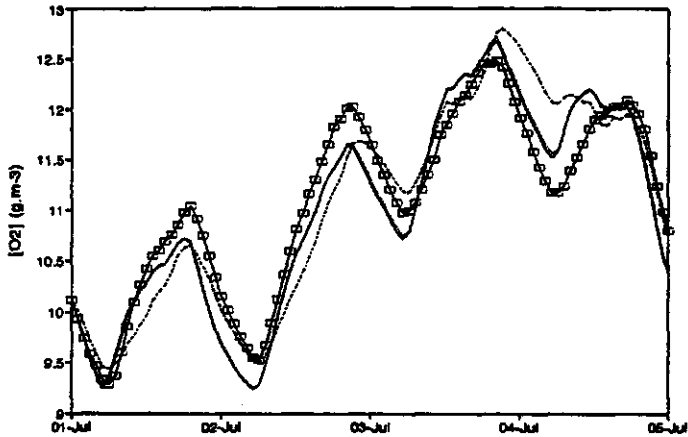


Figure 4.6. Measured DO course and simulation results for three values of D_{eff} . (\square = measured; —: $D_{eff} = 500 D_{mol}$;: $D_{eff} = 100 D_{mol}$; - - - -: $D_{eff} = 10 D_{mol}$).

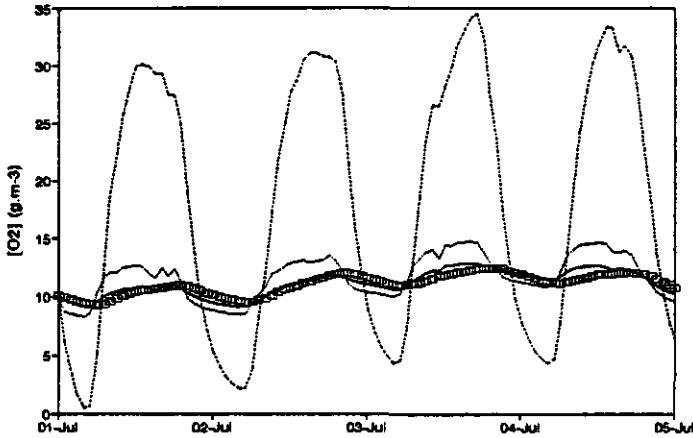


Figure 4.7. Simulated DO concentration inside the benthic layer. (□ = measured in overlying water; — : $D_{eff} = 500.D_{mol}$; : $D_{eff} = 100.D_{mol}$; - - - - : $D_{eff} = 10.D_{mol}$).

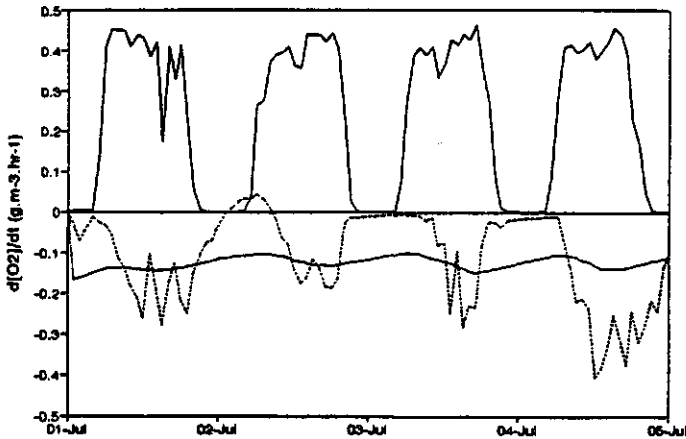


Figure 4.8. Contribution of processes on dC/dt in time. — : Prod.; = Resp.; - - - - = Reaer.; - - - - = SOD, (SOD is close to zero).

A mass balance over the four days period yields:

	4 days cumulative ($g O_2.m^{-3}$)
Benthic gross production	16.0
Sestonic gross production	6.6
Respiration	-12.0
Reaeration	-10.3
Sediment Oxygen Demand	-0.1
Total (= $DO_{end} - DO_{t=0}$)	0.2

Differences in primary production between individual days are small compared to the variations in the daily light irradiances:

date	Tot. Light irradiance (E.m ² .day ⁻¹)	Tot. Gross Prod. (g O ₂ .m ⁻³)
1/7/90	25.4	5.9
2/7/90	29.7	5.7
3/7/90	37.4	5.6
4/7/90	33.2	5.4

The large attenuation of light in the benthic layer may be an explanation for the relatively small differences in total gross production between individual days. Photo-inhibition in the top of the benthic layer is compensated by a higher production in a lower region, so the average production approaches a maximum at high light intensities.

DISCUSSION AND CONCLUSIONS

The use of a tracer gas to measure exchange over the water-air interface is a well applicable method for small water bodies. A disadvantage is that the length of an experiment compels to average the input variables wind and temperature over longer periods. This can hamper the determination of a system specific wind-reaeration relation, because differences between the averaged wind velocities in different experiments will be relatively small. Still a fairly good correlation was found ($r^2=0.89$, $n=4$). The reaeration at low wind velocities has been assumed constant with a K_L of 0.006 hr^{-1} . This may over- or underestimate K_L , but the sensitivity of the model for the reaeration coefficient at low wind velocities is small anyway. Furthermore, the wind direction and the resulting fetch length have not been taken into account, but may influence the reaeration coefficient.

In a shallow water with a large surface to volume ratio reaeration has been shown to be an important term in the oxygen balance, even when the oxygen concentrations are close

to equilibrium. The oxygen demand by the sand was only of minor importance.

The benthic layer of algae was responsible for 70 % of the gross primary production. A better availability of nutrients near the sediment surface causes better growth conditions. Therefore a major part of the total biomass is located in the benthic layer.

During periods of high irradiance, the deeper parts of the layer become photosynthetically active while the productivity in the upper parts may be lowered by photo-inhibition. Photo-inhibition has been taken into account by using the productivity-light function according to Steele (1962). It has been shown by Harris & Piccinin (1977) that photo-inhibition is induced only after a longer period of exposure to high light conditions. In their experiments short-term photosynthesis measurements (10-20 minutes) did not reveal photo-inhibition, while long-term measurements (4 hrs) did. Because of vertical turbulence and the generation of Langmuir cells by wind action and the resulting periodic vertical movement of phytoplankton in the water column, the residence time in the upper layer with oversaturating light conditions may often be too short to induce photo-inhibition. In case of benthic algae however no significant vertical mixing exists. Due to adaptation to lower average light intensities, photo-inhibition at high light irradiance is likely to occur in the top of the benthic layer.

The use of light and dark bottles may lead to underestimation of photosynthesis by phytoplankton due to induction of photo-inhibition by fixation at a low depth. This applies especially for systems with low productivity which require longer incubation periods. In this case however primary production by phytoplankton was low compared to that by benthic algae, and the contribution to the oxygen balance is relatively small.

Irregularities in the simulated DO course on the middle of day 182 and 185 (see figure 4.6) coincide with high wind velocities. Therefore they may be caused by overestimation of

the reaeration rate at high wind speeds, and not by simulated photo-inhibition.

I_g has been assigned a constant value throughout one day, and is related to the total irradiance of the actual day. Thereby instantaneous adaptation is assumed. This 'feed-forward' mechanism is based on practical applicability. Van Straten (1986) used a value for c of 0.45 for warm water phytoplankton and Vollenweider (1965) gave a range of 0.25-0.5.

Hysteresis in the diel photosynthesis-irradiance efficiency, with higher efficiencies during periods of increasing light intensities than during periods of decreasing light intensities, has not been taken into account in the model simulations. The mechanism(s) causing hysteresis are still subject to discussion. Photo-respiration, which is proportional to the amount of recently formed photosynthate (Jassby and Platt, 1976; Harris and Piccinin, 1977), may be one cause. In this study only a temperature dependent dark respiration rate has been considered. The incubation of the dark bottles usually started towards noon with freshly sampled algae. At this time of the day usually no considerable production has occurred. The contribution of photo-respiration is still small. Other mechanisms that may be responsible for hysteresis are for example a shrinkage of chloroplasts during periods of high irradiance, to reduce the area of photon interception. Recovery from chloroplast shrinkage may be a process with a time-scale of at least several hours (Harris and Piccinin, 1977). Inhibition by end products is an additional cause for hysteresis (Falkowski, 1984).

The introduction of a wind-reaeration relationship and the development of a model structure for benthic primary production provide a basis for the long-term description of net production through parameter estimation from measured diurnal DO courses. Combined with knowledge on the kinetics of phosphate uptake it provides a basis for dynamic modelling of the phosphorus household of the biotic compartment. This is the subject of ongoing research in the test ditches.

ACKNOWLEDGEMENTS

The authors thank Clair Holland and Ingrid Bremmer for their experimental contributions, and Hans Aalderink for critically reviewing the manuscript.

REFERENCES

- Banks, R.B., 1975. Some features of wind action on shallow lakes. *Journal of Env. Engin. Div.*, 101, 813-827.
- Banks, R.B. and F.F.Herrera, 1977. Effect of wind and rain on surface reaeration. *Journal of Env. Engin. Div.*, 103, 489-504.
- Downing, A.L. and G.A. Truesdale, 1955. Some factors affecting the rate of solution of oxygen in water. *J. Appl. Chem.*, 5, 570-581.
- Drent, J. and K. Kersting, 1993. Experimental ditches for research under natural conditions. *Water Research* 27 (9), 1497-1500.
- Falkowski, P.G., 1984. Physiological responses of phytoplankton to natural light regimes. *J. Plankton Research*, 6, 295-307.
- Harris, G.P. and B.B. Piccinin, 1977. Photosynthesis by natural phytoplankton communities. *Arch. Hydrobiol.*, 50, 405-457.
- Hieltjes, A. and L. Lijlema, 1980. Fractination of inorganic phosphates in calcareous sediments. *J. Envir. Qual.*, 9, 405-407.
- Jassby, A.D. and T. Platt, 1976. Mathematical formulation of the relationship between photosynthesis and light for phytoplankton. *Limnol. & Oceanogr.* 21, 540-547.
- McDonnell A.J. and S.D. Hall, 1969. Effects of environmental factors on benthic oxygen uptake. *J. Wat. Poll. Con. Fed.* 41, R353-R363.
- Portielje, R. and L. Lijklema, 1994. Kinetics of uptake of phosphate by benthic algal communities. *Hydrobiologia*

- 275/276, 349-358.
- Portielje R. and L. Lijklema, 1993. Sorption of phosphate by sediments as a result of enhanced external loading. *Hydrobiologia* 253, 249-261.
- Rainwater, K.A. and E.R. Holley, 1984. Laboratory studies on hydrocarbon tracer gases. *Journal of Env. Engin. Div.*, 110, 27-41.
- Rathbun, R.E., D.W. Stephens, D.W. Schultz and D.Y. Tai, 1978. Laboratory studies of gas tracers for reaeration. *Journal of Env. Engin. Div.*, 104, 215-229.
- Reid, R.C., J.M. Prausnitz and T.K. Sherwood, 1977. The properties of gases and liquids, 3rd ed, McGraw-Hill, Inc, New York, New York.
- Revsbech, N.P., B.B. Jørgensen and T.H. Blackburn, 1983. Microelectrode studies of the photosynthesis and O_2 , H_2S and pH profiles of a microbial mat. *Limnol. & Oceanogr.* 28, 1062-1074.
- Rich, L.G., 1973. Environmental Systems engineering. McGraw-Hill, New York, pp 138-154.
- Smith, R.A., 1980. The theoretical basis for estimating phytoplankton production and specific growth rate from chlorophyll, light and temperature data. *Ecol. Modelling*, 10, 243-264.
- Steele, J.H., 1962. Environmental control of photosynthesis in the sea. *Limnol. & Oceanogr.* 7, 137-150.
- Tsivoglou, E.C., R.L. O'Connell, R.L. Walter, P.J. Godsil and G.S. Logson, 1965. Tracer measurement of atmospheric reaeration: I, Laboratory studies. *J. Wat. Poll. Con. Fed.*, 37, 1343-1362.
- Tsivoglou, E.C. et al., 1968. Tracer measurements of stream reaeration: II, Field studies. *J. Wat. Poll. Con. Fed.*, 40, 285-305.
- Van Duin, E.H.S. and L. Lijklema, 1989. Modelling photosynthesis and oxygen in a shallow hypertrophic lake. *Ecol. Modelling*, 45, 243-260.
- Van Straten, G., 1986. Identification, uncertainty assessment

and prediction in lake eutrophication. Dissertation
University of Twente. 240 pp.

- Vollenweider, R.A., 1965. Calculation models of photosynthesis-depth curves and some implications regarding day rate estimates in primary production measurements. In: C.R. Goldman (ed.), Primary production in aquatic environments. Univ. of California, p 425-457.
- Vollenweider, R.A., 1974. A manual of methods measuring primary production in aquatic environments. IBP Handbook, 12. London.
- Wang, W., 1980. Fractionation of sediment oxygen demand. *Wat. Res.*, 14, 603-612.
- Wilcock, R.J., 1984a. Methyl-chloride as a gas-tracer for measuring stream reaeration coefficients-I Laboratory studies. *Water Res.*, 18, 47-52.
- Wilcock, R.J., 1984b. Methyl-chloride as a gas-tracer for measuring stream reaeration coefficients-II Stream studies. *Water Res.*, 18, 53-57.

APPENDIX

SYMBOL	DESCRIPTION	UNIT
PROD	Production rate	$\text{gO}_2 \cdot \text{m}^{-3} \cdot \text{hr}^{-1}$
RESP	Respiration rate	$\text{gO}_2 \cdot \text{m}^{-3} \cdot \text{hr}^{-1}$
SOD	Sediment oxygen demand	$\text{gO}_2 \cdot \text{m}^{-3} \cdot \text{hr}^{-1}$
REAER	Reaeration rate	$\text{gO}_2 \cdot \text{m}^{-3} \cdot \text{hr}^{-1}$
A	Area of sediment	m^2
C	Dissolved oxygen concentration	$\text{g O}_2 \cdot \text{m}^{-3}$
C_m	Measured DO	$\text{g O}_2 \cdot \text{m}^{-3}$
$C_{\text{avg},m}$	Average measured DO	$\text{g O}_2 \cdot \text{m}^{-3}$
C_s	Saturating DO at ambient T	$\text{g O}_2 \cdot \text{m}^{-3}$
C_{sim}	Simulated DO	$\text{g O}_2 \cdot \text{m}^{-3}$
D	Molecular diffusion coefficient	$\text{m}^2 \cdot \text{hr}^{-1}$
D_{eff}	Effective diffusion coeff. in sediment	$\text{m}^2 \cdot \text{hr}^{-1}$
F	Flux across air-water interface	$\text{g} \cdot \text{m}^{-2} \cdot \text{hr}^{-1}$
F(I)	Light function	-
F(N)	Function for nutrient concentration	-
F(T)	Function for temperature	-
H	Henry's constant	$\text{g} \cdot \text{m}^{-3} \cdot \text{atm}^{-1}$
I_0	Light at watersurface	$\text{W} \cdot \text{M}^{-2}$
I_b	Light at top of benthic layer	$\text{W} \cdot \text{M}^{-2}$
I_n	Light in n^{th} sublayer of benthos	$\text{W} \cdot \text{M}^{-2}$
I_s	Saturating light intensity	$\text{W} \cdot \text{M}^{-2}$
I_z	Light at depth z	$\text{W} \cdot \text{M}^{-2}$
K_L	Mass transfer coefficient/depth	hr^{-1}
K_s	Monod constant for SOD	$\text{g O}_2 \cdot \text{m}^{-3}$
η	Model efficiency	%
Pr_{max}	Maximum productivity	$\text{gO}_2 \cdot \text{m}^{-3} \cdot \text{hr}^{-1}$
R	O_2 consumption rate in porewater	$\text{gO}_2 \cdot \text{m}^{-3} \cdot \text{hr}^{-1}$
T	Temperature	$^{\circ}\text{C}$
V	Watervolume	m^3
W	Windvelocity	$\text{m} \cdot \text{s}^{-1}$
b	Average water depth	m
d	Thickness of laminair boundary layer	m
l	Length of light period	hr
n	Number of sublayers of benthos	-
t	Time	hr
ϵ_w	Extinction coefficient of water	m^{-1}
ϵ_{bn}	Extinction coefficient of benthos	$\text{m}^3 \cdot [\text{g DW}]^{-1}$
θ_A	Temperature coeff. for reaeration	-
θ_p	Temperature coeff. for production	-
θ_r	Temperature coeff. for respiration	-
θ_s	Temperature coeff. for SOD	-

subscripts

n	Number of sublayer in benthos	-
i	Number of sublayer in sediment	-

Chapter 5

Estimation of productivity from continuous oxygen measurements in ditches dominated by benthic algae

key-words:

benthic algae - eutrophication - parameter estimation -
diurnal oxygen balance

Based on : Estimation of productivity from continuous oxygen measurements in ditches dominated by benthic algae in relation to the level of external nutrient input, by R. Portielje, K.Kersting and L. Lijklema. submitted to Water Research.

5. ESTIMATION OF PRODUCTIVITY FROM CONTINUOUS OXYGEN MEASUREMENTS IN DITCHES DOMINATED BY BENTHIC ALGAE

ABSTRACT

Processes governing the diurnal dissolved oxygen fluctuations in three artificial ditches, dominated by a layer of benthic algae and receiving three different levels of external nutrient loading (levels A, B and C) were estimated for individual days and evaluated over a two-years period.

Both cumulative gross and net primary production were positively related to the level of external nutrient supply. At all three levels a continuous increase in cumulative net production was observed.

The accumulation of biomass, expressed as dry weight, was calculated from cumulative net production and the O_2 :dry weight conversion factor based on the stoichiometry of the photosynthesis reaction. The calculated accumulation was compared with the occasionally measured areal dry weight content of the benthic layer. It showed good agreement in the ditch with the lowest level of external nutrient supply (ditch A). In the ditches receiving the intermediate and the highest level of external nutrient supply (ditches B and C), the measured increase was lower than calculated.

Reaeration was related to the incident wind velocity, which was measured continuously. Analysis of wind data showed a daily cycle in the wind speed, with higher average wind speeds during the afternoon than during the night. As high wind speeds thereby generally coincide with higher oxygen saturations, the use of a variable reaeration coefficient during a diurnal cycle is necessary, and results in higher gross and net production rates than the use of a constant reaeration coefficient throughout a day.

Analysis of temperature corrected daily gross production rates in relation to the total light irradiance of the same day showed a saturation at higher total irradiances, that resembles Smith's photosynthesis-light relationship. The maximum daily gross production rate increases with increasing level of nutrient supply. After a transition from dominance by benthic algae to phytoplankton the maximum gross production rate increased further, while the light parameter decreased.

INTRODUCTION

Eutrophication is a widely recognized problem in water quality management. Excessive availability of nutrients usually leads to impoverishment of the species assemblage of aquatic ecosystems.

Enhanced nutrient supply to a nutrient limited system results

in increased primary production rates and can lead to algal blooms. As a result of the intensification of the nutritional cycles, respiration and decomposition concomitantly increase, and the effects are clearly reflected in the diurnal dissolved oxygen fluctuations. In extreme situations, the daily amplitude of the dissolved oxygen course may become so large that also a further deterioration of the ecosystem can occur, for example by causing fish kills.

In test ditches research is conducted on the effects of the level of external N- and P-loading on the structure and functioning of the system. The analysis of the diurnal dissolved oxygen course provides a good insight into the effect of the level of nutrient input on the productivity of the system. The interactions between primary production and nutrient cycling have a dynamic character, as the productivity of a system affects the availability of nutrients through storage and mineralization. The net storage of nutrients in organic matter can be estimated from primary production and oxygen consumption rates by means of photosynthesis stoichiometry, combined with knowledge on mechanisms and kinetics of nutrient uptake and storage by photo-autotrophs.

In stagnant and isolated systems like the test ditches in the present study, the net production over longer periods is equal to the cumulative diffusive flux of oxygen across the water-air interface, when anaerobic losses through CH_4 volatilization are disregarded. In parameter estimation routines the reaeration coefficient is often estimated as an independent parameter. In this study we calculated the reaeration coefficient from an empirical relationship describing mass transfer across the air-water interface as a function of incident wind velocity. This allows for variation of the reaeration coefficient within a day.

Light is a main factor governing primary production (for a review see Kirk, 1983). Simultaneous recorded light irradiance allows determination of the parameters governing the photosyn-

thesis-light relationship (Cosby and Hornberger, 1984; Cosby et al., 1984). These parameters and a parameter determining the oxygen consumption rate can be well identified from the diurnal oxygen cycle and have physical significance as well.

This chapter deals with the estimation of primary production and oxygen consumption in ditches dominated by benthic algae from curve-fitting to continuous oxygen measurements. Parameters are estimated for individual days and evaluated over a two-years period (March 1st, 1990 - Feb 28th, 1992) and related to the level of external nutrient loading. The relationship between gross production and light irradiance was analyzed on a daily basis.

From the estimated cumulative net primary production over a two-years period the accumulation of dry weight is calculated from the O₂ : dry weight stoichiometry of the photosynthesis and respiration reaction, and compared to measurements.

MATERIAL AND METHODS

Site studied

The location and characteristics are described in chapter 1.5 (p. 20-22).

The three ditches analyzed in this chapter are the sand-ditches A, B and C (for explanation see chapter 1.6, p. 22-24). Before the start of the nutrient loading programme all ditches were virtually identical with respect to nutrient concentrations in both sediment and water column. The initial concentrations were all low. A layer of benthic algae with a growing thickness is the main location of primary production. In ditch C a transition to phytoplankton dominance occurred in the second year.

Measurements

Dissolved oxygen is measured at two water depths, 10 cm below

the surface, and 10 cm above the bottom. Water temperature is also measured at these depths and in addition at mid depth. Incident irradiation is measured with a quantum sensor in the air. Wind speeds are obtained from a weather station at the experimental site. All measurements are taken at 30 second intervals and averaged over 15 minutes prior to storage in a data logger. A detailed description of the experimental ditches and the measuring equipment is given by Drent and Kersting (1993).

Nutrient addition

The levels of external nutrient loading and the method of nutrient addition are described in chapter 1.6 (p.22-24). The nutrient loading programme was started in May 1989, ten months before the start of the simulation period considered in this chapter.

Dry weight measurements

The dry weight content of the benthic layer of algae was measured on a few occasions, usually in autumn. Three sediment cores with a diameter of 5.3 cm were collected from each ditch. The core tubes were pushed into the sand to a depth of at least 10 cm. The benthic layer was removed by means of resuspension in demineralised water and decantation of the algal suspension after settling of the sand. This was repeated several times until all the algal material was removed. The benthic material from the three cores was mixed for each ditch and filled up to 1 l with demineralized water. Dry weight (105°C) was determined after evaporation of a subsample of the mixture.

THEORY

model structure

The model and the method of parameter estimation are adapted and modified from that described by Aalderink (1994).

The time-concentration course over a one-day period is calculated from the analytical solution of the mass balance equation. The differential equation describing the oxygen concentration is:

$$\frac{dC}{dt} = k_A(C_s - C) + G_m F(I) - R_{20^\circ C} \theta^{(T-20)} \quad (1)$$

G_m	: maximum O_2 production	$[g\ O_2 \cdot m^{-3} \cdot hr^{-1}]$
k_A	: reaeration coefficient	$[hr^{-1}]$
$F(I)$: light-production function	$[-]$
$R_{20^\circ C}$: oxygen consumption rate	$[g\ O_2 \cdot m^{-3} \cdot hr^{-1}]$
θ	: temperature coefficient	$[-]$
C_s	: saturation concentration	$[g\ O_2 \cdot m^{-3}]$

θ has been assigned a value of 1.08 (Van Duin and Lijklema, 1989).

From an initial condition $t=0 : C=C_0$, C is calculated at each time interval i from:

$$C_i = C_0 + \sum_{j=1}^i k_{A,j} (C_{s,j} - C_j) + G_m \sum_{j=1}^i F(I)_j - R_{20^\circ C} \sum_{j=1}^i \theta^{(T_j-20)} \quad (2)$$

Parameters estimated are the oxygen consumption rate $R_{20^\circ C}$, the maximum gross primary production rate G_m and the parameter determining the light-production (P-I) function. For the latter we used that of Smith (1936), assuming saturation at high light intensities:

$$F(I) = \frac{\frac{I}{I_k}}{\sqrt{1 + \left(\frac{I}{I_k}\right)^2}} \quad (3)$$

with I_k the light parameter according to Smith ($E.m^{-2}.s^{-1}$)

The best-fit was obtained from minimization of the sum of squares (SS) of the differences between measured and simulated oxygen concentrations:

$$SS = \sum_{i=1}^n (C_{i,m} - C_{i,s})^2 \quad (4)$$

Subscript m refers to measured and s to simulated oxygen concentrations. n is the number of samples per day.

The model is linear in G_m and $R_{20^\circ C}$, but not in I_k . A search routine (Aalderink, 1994) is applied on I_k , and for each value of I_k the optimum values for G_m and $R_{20^\circ C}$ (which yield the minimum sum of squares at that particular value of I_k) are calculated from solving the normal equations:

$$\frac{dSS}{dR_{20^\circ C}} = 0 \quad \frac{dSS}{dG_m} = 0 \quad (5)$$

The reaeration coefficient k_A is calculated from the measured wind speed at each time step from an empirical wind-reaeration relationship, determined from in situ measurements. The experiments are described in detail by Portielje and Lijklema (1994). The function that relates k_A (hr^{-1}) to wind-speed at $20^\circ C$ is:

$$\begin{aligned} k_{A,20^\circ C} &= 0.006 && (W < 1.4 m/s) \\ &= 0.0377.W - 0.0387 && (W > 1.4 m/s) \end{aligned} \quad (6)$$

Temperature correction is done with:

$$k_{A,T} = k_{A,20^{\circ}C} \theta_D^{(T-20)} \quad (7)$$

with $\theta_D = 1.024$ [-] (Van Duin and Lijklema, 1989).

During periods with an ice cover the reaeration coefficient is arbitrarily set at zero.

The initial concentration C_0 is obtained by linear regression and subsequent extrapolation to $t=0$ of the first five data points for each day, which cover a period of 1.25 hours. As the oxygen course at night mainly depends on the oxygen consumption rate, it is approximately linear in the period during which the first five data are collected.

In the ditches a benthic layer of algae is the main source of oxygen production and consumption (Portielje and Lijklema, 1994), except for ditch C during the second year (March 1991 - March 1992), in which a transition to a phytoplankton dominated system occurred in early spring 1991. The P-I relationship is integrated over the thickness of the benthic layer, in which the attenuation of light is determined by the specific extinction coefficient of the dry matter ($0.0455 \text{ m}^2 \cdot [\text{g dry matter}]^{-1}$; Portielje and Lijklema, 1994). Attenuation of light by the water within the benthic layer is negligible.

The light intensity at the surface of the benthic algal layer I_b is calculated from the incident light irradiance at the water surface I_0 using Lambert-Beer's law:

$$I_b = I_0 \exp(-\epsilon H) \quad (8)$$

with H the water depth, and ϵ the extinction coefficient [m^{-1}] of the water column.

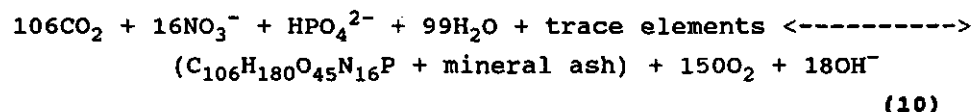
After phytoplankton had become dominant in ditch C in spring 1991, a model has been used in which primary production is homogeneously distributed over the water column instead of being restricted to the benthic layer. For this period the P-I function has been integrated over the depth of the water column.

The quality of the fit of the simulated to the measured oxygen course is expressed in terms of a model efficiency η , which is defined as:

$$\eta = \frac{\sum_{i=1}^n (C_{i,m} - \bar{C}_m)^2 - \sum_{i=1}^n (C_{i,s} - C_{i,m})^2}{\sum_{i=1}^n (C_{i,m} - \bar{C}_m)^2} \quad (9)$$

\bar{C}_m is the daily averaged measured concentration. Subscript m refers to measured and s to simulated oxygen concentrations. n is the number of samples per day.

Conversion of oxygen to dry weight is based on an assumed stoichiometry (Uhlmann, 1975) of the photosynthesis reaction:



in which the forward reaction represents photosynthesis and the reverse respiration. A net O_2 production of 1 g yields a production of 0.68 g dry weight.

Confidence contours for the parameters describing daily gross production as a function of total daily light irradiance are calculated from (Draper and Smith, 1981):

$$SS_{\text{cont}} = SS_{\text{min}} \left[1 + \frac{p}{n-p} F(n, n-p, \alpha\%) \right] \quad (11)$$

with SS_{cont} the sum of squares at the $\alpha\%$ confidence contour, SS_{min} the minimum sum of squares, p the number of parameters, n the number of independent data and $F(n, n-p, \alpha\%)$ the F-distribution according to Fischer.

RESULTS

Analysis of the wind data over the two year period showed that there is a daily cycle in the wind speed. This is illustrated in figure 5.1, where the average ($n=732$) wind speed is plotted versus the hour of the day. Wind speeds are significantly lower during the night and reach a maximum in the afternoon.

As high wind speeds thus coincide with higher oxygen saturations, the use of incident wind velocities will therefore systematically yield higher calculated cumulative diffusive fluxes across the water-air atmosphere than the use of a constant average wind speed or reaeration coefficient throughout a day. Comparison of both approaches on the present data sets revealed that the use of a constant wind speed throughout a day resulted in an underestimation of the cumulative diffusive flux over two years of 20-25 % compared to the use of incident wind speeds.

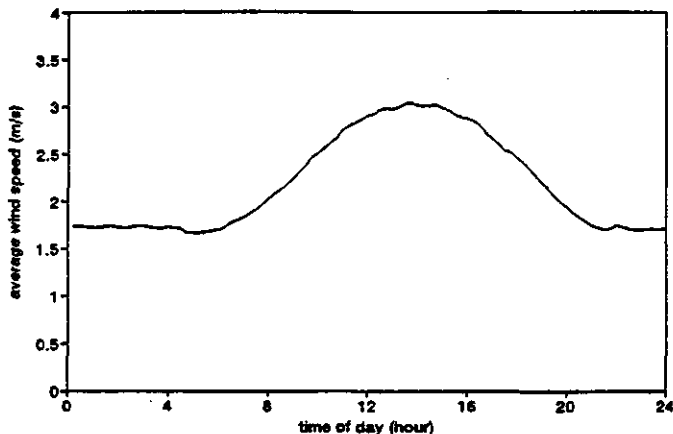


Figure 5.1. Average wind speed versus hour of the day ($n=732$).

Generally the water column was homogeneous and therefore the measured oxygen concentrations at 10 cm and 40 cm were averaged.

Figure 5.2 presents the daily amplitudes of the dissolved oxygen concentrations in the three ditches over the two years

period. The figure shows that there is a clear relationship between the level and duration of nutrient input and the amplitude, with amplitudes of about $10 \text{ g O}_2 \cdot \text{m}^{-3}$ in ditch C during the summer of 1991.

The daily amplitudes are only a crude indication of the metabolic activity of the ditches. Parameter estimation of the mass balance equation provides us with an estimate of gross photosynthetic production and oxygen consumption rates.

The model explained the data fairly well. The frequency distributions of the model efficiencies of the individual days are presented in figure 5.3, for all three ditches. A model efficiency of 0.9 is exceeded on 38, 64 and 71 % of the individual days for ditch A, B and C respectively. The increase of these percentages with increasing level of external nutrient loading is due to the larger amplitudes in the diurnal dissolved oxygen course at higher trophic states, which gives a better signal to noise ratio. The low model efficiencies in ditch A are especially due to very small oxygen amplitudes during the winter periods.

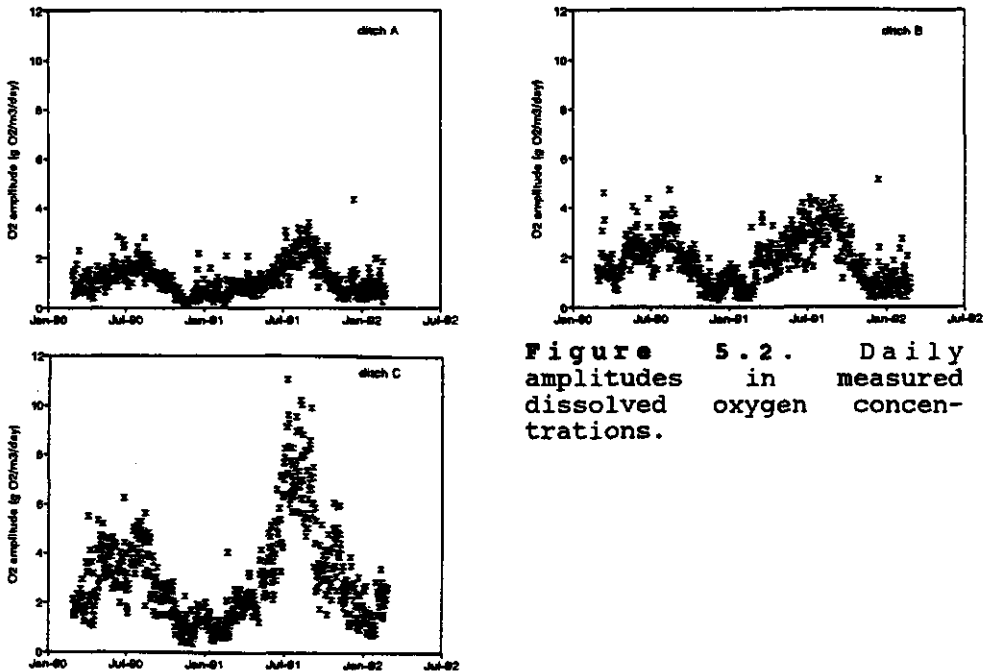


Figure 5.2. Daily amplitudes in measured dissolved oxygen concentrations.

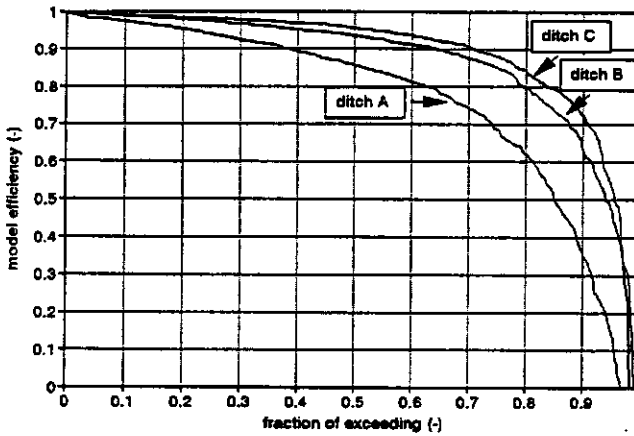


Figure 5.3. Frequency distribution of model efficiency values.

Figure 5.4 presents the estimated daily gross production rates. The photosynthetic activity has increased in 1991 as compared to 1990, especially in ditch C. In this ditch the summer maxima increased with about 50 %. The production rates are clearly related to the nutrient loads. Similar trends are found for the estimated daily oxygen consumption rates (figure 5.5).

The daily net production rates, calculated as the differences between daily gross production and oxygen consumption rates, are displayed in figure 5.6. These are also positively related to the external nutrient supply, but exhibit a high variability between individual days. The seasonal fluctuations are apparent, but net production remains generally positive in all ditches during the whole period of two years. Due to the high variability of net production rates between days, the data are evaluated over longer periods and as cumulatives.

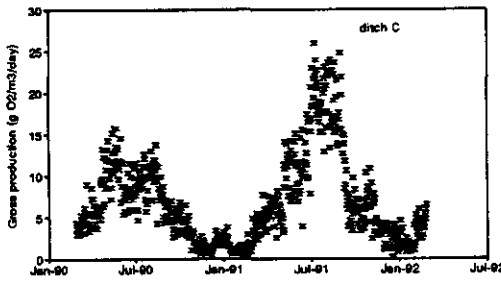
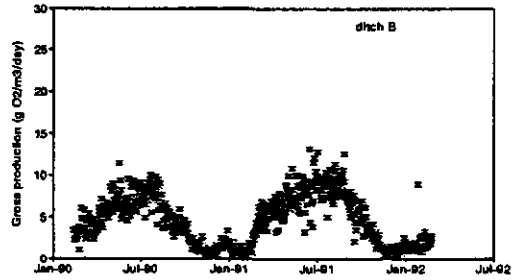
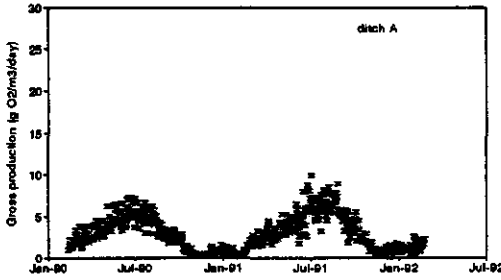


Figure 5.4. Estimated daily gross production rates ($\text{g O}_2 \cdot \text{m}^3 \cdot \text{d}^{-1}$).

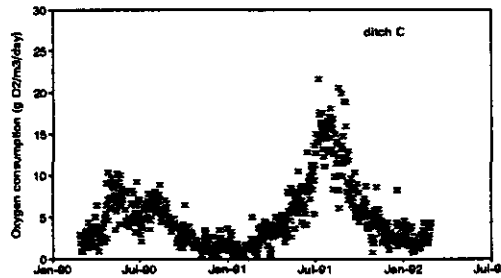
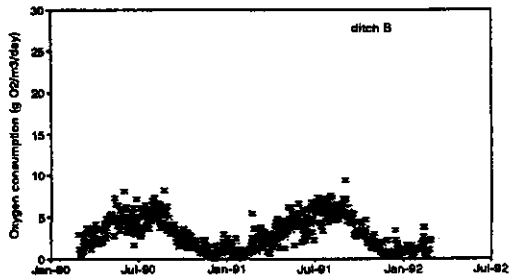
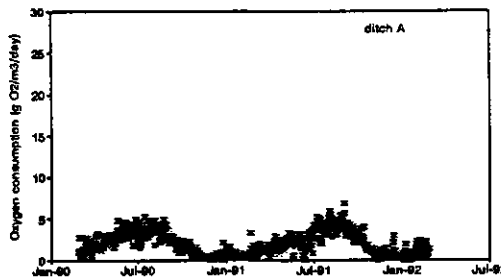


Figure 5.5. Estimated daily oxygen consumption rates ($\text{g O}_2 \cdot \text{m}^3 \cdot \text{d}^{-1}$).

Estimation of productivity by benthic algae

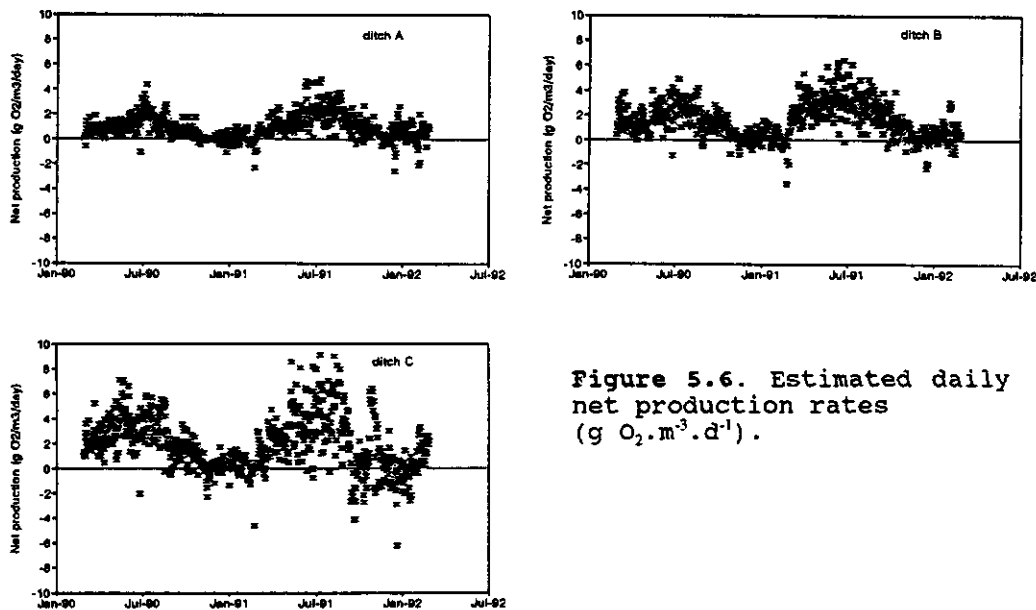


Figure 5.6. Estimated daily net production rates ($\text{g O}_2 \cdot \text{m}^3 \cdot \text{d}^{-1}$).

Figure 5.7 displays the cumulatives of gross production, oxygen consumption and net production over the two years period. All cumulated processes are related to the level of external nutrient input. The total annual gross productions and oxygen consumptions are given in table 5.1.

Table 5.1 shows that the relative increase in both annual gross production and annual oxygen consumption was much larger in ditch C than in the other two ditches. As especially the oxygen consumption increased, the relative increase in the total net production is much smaller in ditch C. The P/R ratio decreased only in this ditch, while it increased in the other two.

The cumulative net production indicates a continuous increase

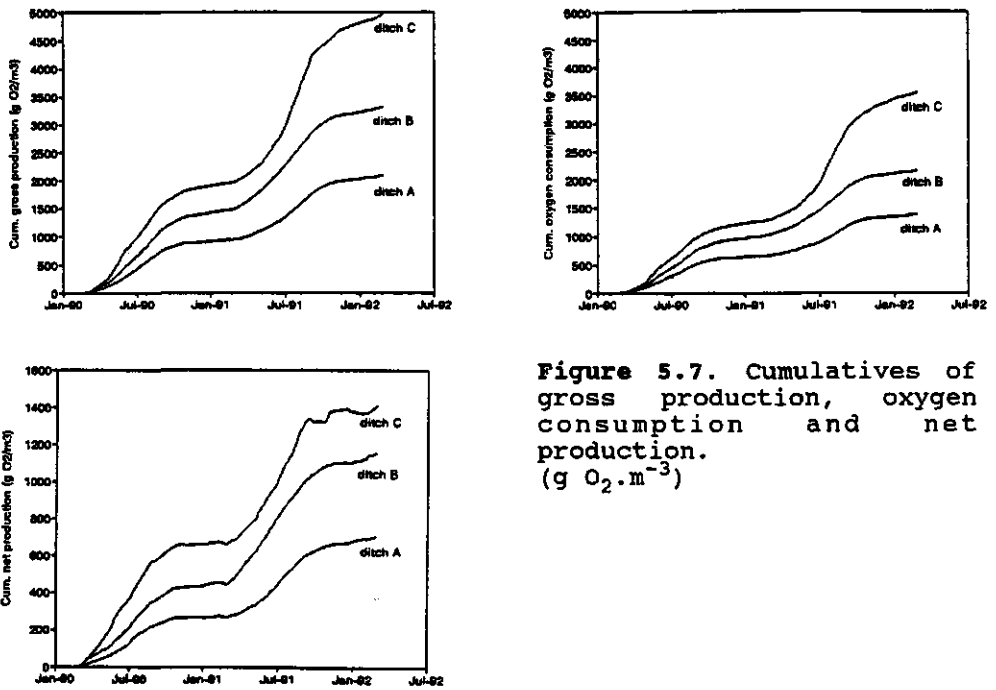


Figure 5.7. Cumulatives of gross production, oxygen consumption and net production. ($\text{g O}_2 \cdot \text{m}^{-3}$)

Table 5.1. Annual (March 1 - Febr 28) gross production (P), oxygen consumption (R), P/R ratio and net production (NP) [$\text{g O}_2 \cdot \text{m}^{-3}$]. The percentage change in 1991 compared to 1990 is given between brackets.

ditch		1990	1991	
A, reference	P	938	1156	(23)
	R	669	719	(7)
	P/R	1.40	1.61	
	NP	269	437	(62)
B, medium	P	1482	1833	(24)
	R	1035	1127	(9)
	P/R	1.43	1.63	
	NP	447	706	(58)
C, highest	P	1968	2999	(52)
	R	1301	2257	(73)
	P/R	1.51	1.33	
	NP	667	742	(11)

of stored organic matter. From the O_2 :dry weight stoichiometry of the photosynthesis reaction the accumulation of organic matter is calculated from the cumulative net oxygen production. This calculation is compared with the occasional measurements of the dry weight content of the benthic layer (figure 5.8). In ditch A the observed accumulation of dry matter in the benthic layer shows a reasonable agreement with that calculated from the cumulative net production. In ditches B and C the observed accumulation is smaller than calculated. The production characteristics of the ditches can be represented by plotting daily gross productions for individual days, converted to productions at $20^\circ C$ with a temperature coefficient of $6\% \text{ } ^\circ C^{-1}$ (Van Duin and Lijklema, 1989), versus the daily light irradiance (Figure 5.9).

As ditch C was dominated by phytoplankton in the second year and showed much higher gross production rates than in the preceding year, for this ditch the first and second year are plotted in separate graphs in figure 5.9. For ditches A and B the two years are plotted together, as no obvious differences in daily gross productions were found between the two consecutive years. The data are scattered but show that a maximum is reached at higher light intensities, and that the data resemble Smith's light-production relationship. This relationship was fitted to the daily productions at $20^\circ C$. The maximum daily gross production $P_{\max, 20^\circ C}$ ($g \text{ } O_2 \cdot m^{-3} \cdot day^{-1}$) and the light parameter I_k ($E \cdot m^{-2} \cdot day^{-1}$) were estimated from least-squares fitting. The results are given in table 5.2.

Figure 5.10 shows the 95% confidence contours for both parameters. $P_{\max, 20^\circ C}$ is related to the level and history of nutrient input. Ditches A and B have a similar value for I_k , but the maximum gross production rate is significantly higher in ditch B. In ditch C a significant decrease in I_k took place after transition from a system dominated by benthic algae and filamentous algae to a dominance by phytoplankton. This coincided with an increase in $P_{\max, 20^\circ C}$. The data are not corrected for biomass, but the attenuation of light within the

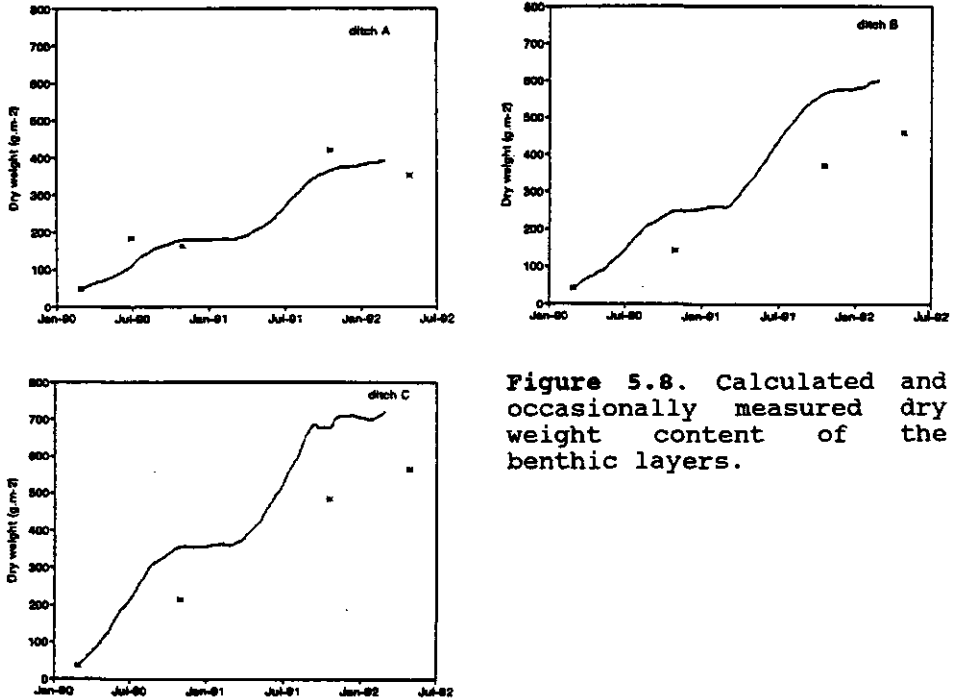


Figure 5.8. Calculated and occasionally measured dry weight content of the benthic layers.

benthic layer is so large that the euphotic zone does not extend to the bottom of this layer during most of the period. Initially the dry weight content was about 50 g.m^{-2} . With a specific extinction coefficient of $0.0455 \text{ m}^2.[\text{g dry weight}]^{-1}$ this means that the light intensity at the bottom of the layer is still 10% of that at the top of this layer. During most of the period, with dry weight contents $>100 \text{ g.m}^{-2}$, the light that penetrates through the layer is negligible. The amount of dry weight actually participating in primary production may increase in time, but reaches a maximum after the dry weight content has passed a critical value.

Estimation of productivity by benthic algae

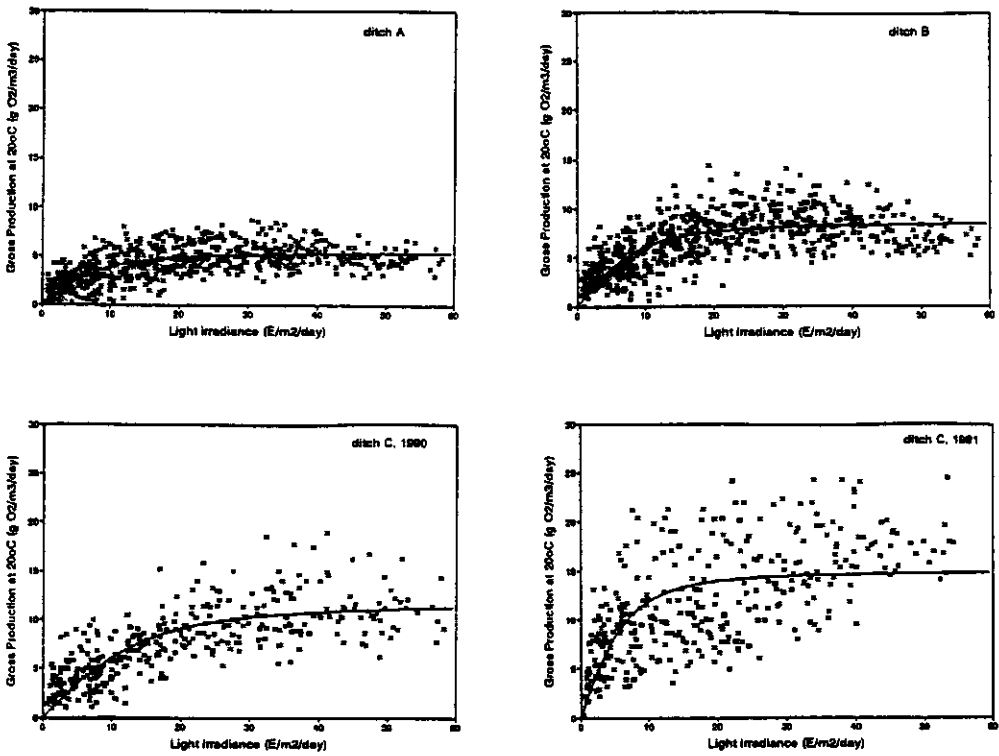


Figure 5.9. Daily gross production at 20°C versus daily light irradiance. Solid lines represent least-squares fit.

Table 5.2. $P_{\max,20^{\circ}\text{C}}$ ($\text{g O}_2 \cdot \text{m}^{-3} \cdot \text{day}^{-1}$) and I_k ($\text{E} \cdot \text{m}^{-2} \cdot \text{day}^{-1}$) obtained from least square fitting of data to Smith function.

ditch	$P_{\max,20^{\circ}\text{C}}$	I_k
A, reference	5.4	9.8
B, medium	8.5	9.9
C, highest (1990)	11.6	16.2
C, highest (1991)	14.9	7.6

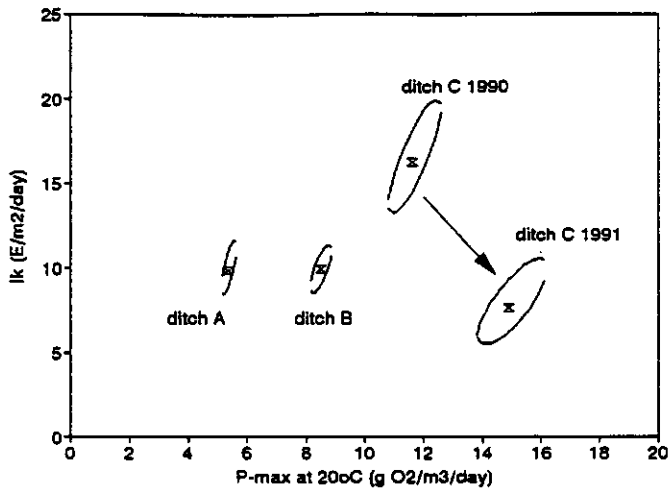


Figure 5.10. 95 % confidence contours of I_k versus the maximum daily production rate at 20°C.

DISCUSSION

The choice for the use of Smith' photosynthesis-light relationship in the model of the mass balance equation was based on preliminary tests with three photosynthesis-light relationships: the first a linear relation-ship, the second including photo-saturation at higher light intensities (Smith, 1936) and the third including both photo-saturation and photo-inhibition (Steele, 1962). The relationship according to Smith gave the best results for all three ditches in terms of model efficiencies. This is consistent with the results of Jassby & Platt (1976) who tested eight different mathematical formulations and rated Smith' second best. Their best was a hyperbolic tangent function, but for this function an analytical solution of the depth integrated production cannot always be obtained. Therefore it has the disadvantage of substantially increasing computational time due to the

showed that the hyperbolic tangent function can be approximated by taking a higher order of Smith' relationship, with a more abrupt transition to light-saturation with increasing irradiation.

Cosby et al. (1984) used an extended Kalman filter routine to identify the P-I model for a Danish river, but all eight P-I relationships tested (including the three mentioned above) were rejected as inadequate, indicating that the real P-I relationship is more complex than expressed in the present mathematical formulations. A basic problem in our model as well as in the models discussed by Cosby et al. (1984) is the assumption of constant parameters for the simulation period (mostly one day). The parameters of the photosynthesis-light relationship may vary during a day. Hysteresis effects, with higher efficiencies in the morning than in the afternoon have been reported by various authors (Van Duin, 1992). Harris (1978) discusses several mechanisms that could be responsible for these variations.

Photo-inhibition of microbenthic algae was found by Hunding (1971) in samples taken in November but not in samples taken in June. He suspended the benthic algae in water in the laboratory for measurement of the photosynthetic capacity at different light intensities. In this way he destroyed the layering of the benthic algae and exposed them to light intensities much higher than the ones in the field. Incubation of light bottles at a small depth often induces photo-inhibition due to the fixation of the algae at this depth. Photo-inhibition is however often absent in real field situations because of vertical movement. The residence time in the near-surface zone thereby often is too short to induce photo-inhibition (Harris & Piccinin, 1977). Fraleigh et al. (1981) did not find a depression of photosynthesis, measured in suspended bottles near the surface of Lake Ohrid. They explained this as adaptation to high light intensities as a result of a very strong and stable stratification at the lake surface. The algae thus did not experience low light

intensities due to movements through the water column.

Revsbech et al. (1983), using microelectrode techniques, found during the diurnal cycle of a sunny summer day that after a fast increase at low light intensities a linear increase in the areal photosynthesis rate with increasing light occurred. No signs of photo-inhibition could be detected, even at an irradiance of $1670 \mu\text{E}\cdot\text{m}^{-2}\cdot\text{s}^{-1}$.

Photo-inhibition during periods of high light intensities can be caused by various mechanisms (Falkowski, 1984; Vincent 1990). The induction of photo-inhibition is a process with a time scale in the range of 10 to 30 minutes. The incorporation of photo-inhibition as in Steele's P-I function, has a negative effect on the performance of the model at light intensities below the optimum (Jassby & Platt, 1976). A proper incorporation of photo-inhibition would require a parameter describing the time dependency of the induction of photo-inhibition at light conditions above the optimum, and the recovery afterwards (Van Duin, 1992).

Oxygen consumption was corrected for temperature, with a temperature coefficient of $8\% \text{ } ^\circ\text{C}^{-1}$ (Van Duin and Lijklema, 1989). In a review on phytoplankton productivity Harris (1978) discussed other mechanisms that also alter the respiration rates. Photo-respiration leads to higher oxygen consumption rates at high light intensities. Respiration of phytoplankton has been shown to depend on the light history by a relationship with the carbohydrate pool (Gibson, 1975, Kamp-Nielsen 1981).

The parameters G_m and I_k of the Smith light function are estimated for the integrated benthic layer. In case of a non mixed benthic layer, algae present at different depths within this layer adapt to different light conditions, and will assume different values for the parameters. The lower parts of the benthic layer will be exposed to very low light intensities (≈ 0) and contribute hardly to the overall primary production. This part will thus be subject to mainly

respiration or decomposition. Thereby the fraction of living algae compared to bacteria and dead organic matter will decrease with depth. With a specific light attenuation coefficient in the benthic layer of $0.0455 \text{ m}^2 \cdot [\text{g dry matter}]^{-1}$ (Portielje and Lijklema, 1994), and a porosity of about 99 %, the light intensity at a depth of 1 cm in the benthic layer is about 1 % of that at the surface. This value of 1 % is usually considered as a rough criterium for the depth of the euphotic zone (Sand-Jensen, 1989), but productivity has been reported at much lower values (Richardson et al., 1983). Jørgensen et al. (1979) measured in a dense sediment mat of cyanobacteria that the light intensity at a depth of 1.2 mm in the mat was 7 % of that at the surface during the summer, and only 0.02 % during the winter. In their study the vertical light attenuation was probably much larger than in the present study. Another approach is to use a fixed depth for the euphotic zone within the benthic layer. In this case the choice for a value of the fixed depth will be arbitrary. Another alternative is to consider the benthic layer as flat and to relate productivity to the incident light intensity at the surface of the layer. This approach also suffers from the same imperfection as integration over the whole depth or the choice of a fixed depth: the values for G_m and I_k will not be representative for the whole column of benthic flora, although the mathematical formulation is easier. The estimated total production however is virtually independent of the chosen approach in the model formulations.

In the model complete horizontal and vertical mixing of the water phase is assumed. Horizontal concentration gradients are not likely to occur, because the benthic algal layer is homogeneously distributed over the whole ditch, and the mixing rate is fast. Vertical gradients are negligible most of the time, but during periods of low wind-speed and high temperature and irradiance (high productivity) a difference between the oxygen concentration at 10 and 40 cm depth can be

observed, with higher DO concentrations at greater depth, near the productive benthic layer. Fitting to averaged oxygen concentrations influenced the reaeration calculation and consequently also the estimated magnitude of the other processes during these (short) periods.

During periods with an ice cover the photosynthetic activity of the microbenthic community continued. The absence of reaeration sometimes resulted in a gradual increase of the DO concentrations to values of $>25 \text{ mg O}_2 \cdot \text{l}^{-1}$. As for periods with ice cover the reaeration was set at zero, the net productivity during these periods may have been underestimated due to a locally induced reaeration at the measuring site. Here a small area was kept ice-free through the horizontal movement of the sensors. During these periods the concentration measured at larger depth was considered more reliable, since here the influence of the local exchange through the air-water interface is smaller. In the literature evidence is provided that algal populations can survive photo-autotrophically under an ice cover for longer periods (Richardson et al., 1983; Boylen and Brock, 1974).

When the loss of gaseous reduced carbon components (CH_4) is negligible, the net production is equal in magnitude but opposite in sign to the diffusion over longer periods.

The choice of the wind-reaeration relationship is crucial to the calculation of net production. Under super saturation an increase in the reaeration coefficient has a positive effect on the calculated net production. To obtain the same agreement between measured and simulated oxygen course, the enhanced calculated flux of oxygen from the water to the atmosphere has to be compensated for by an increased net production. In this chapter we have used a relationship obtained from independent measurements. Unfortunately this relationship is based on a limited range of wind speeds and assumptions had to be made to extend the relationship over the full range of wind speeds

(equation 6). This can be a source of error. However, 50% of the measured wind speeds was within the range of the linear part of the wind-re-aeration relationship. This relationship was based on measurements performed in ditch A, and was also used for the other ditches. As all ditches are of identical geometry, and all have an open water surface, significant differences in the re-aeration-wind relationship are not likely.

An alternative is to estimate the re-aeration coefficient k_A together with the other parameters. Application on the present data sets however resulted in k_A values with a very wide scatter when plotted versus the wind speed, and also a wide variation between individual ditches on a particular day. In this approach k_A is an extra free parameter that contributes to a better fit, but the obtained values may not be realistic.

The daily gross productions plotted versus the daily light irradiances over two years (figure 5.9) indicate that a maximum is reached at high light irradiance. The long term photosynthesis-light relation resembles the Smith (1936) curve with photo-saturation. The 95% confidence contours (see figure 5.10) for $P_{\max,20^\circ\text{C}}$ and I_k show a clear relationship between $P_{\max,20^\circ\text{C}}$ and the level and duration of nutrient input. Although Smith' P-I function originally has not been developed for interpretation over long periods, it provides a criterium for the P-I characteristics at the level of the whole system. This approach does not take into account the adaptation to low light intensities in winter and to high light intensities in summer, but assumes constancy of the light parameter. There is no evidence for inhibition of the daily gross production at high daily light irradiances.

The production in ditch A was phosphorus limited as an increase in productivity was observed in ditch B receiving just phosphate (table 5.1). Further addition of phosphorus in combination with nitrogen gave a still higher metabolic

activity. At the nutrient load of ditch B the phosphorus input was 4.6 times the load in ditch A. Both cumulative gross and net production had increased with a factor 1.6. Ditch C received 2.8 times as much phosphorus and 2.3 times as much nitrogen as ditch B. This resulted in a 1.5 times increase in cumulative gross production and a 1.2 times increase in net production. The productions increased less than proportional with the nutrient loads. The dissolved phosphorus concentrations are low during the major part of the year in all three ditches, the observed relationship between external loading and both gross and net primary production (see figures 5.7 a and c) can better be explained by the observed differences in intracellular nutrient concentrations (Portielje and Lijklema, 1994). In ditch A, with a very low external P-input, the amount of dry matter in the benthic layer increased as a result of positive cumulative net primary production. Concomitantly there was a slight decrease in internal P-concentration. The limit of the internal P-concentration below which primary production will be seriously hampered by nutrient deficiencies apparently had yet not been reached, at the end of the simulation period. Bierman (1976) gives for green algae and non N-fixing blue-green algae a value for the minimum stoichiometric level of total phosphorus in the cells of 2.3 and 0.7 mg P.[g dry matter]⁻¹ respectively. Concentrations measured in the benthic layer of ditch A have reached lower values : 0.6 mg P.[g dry matter]⁻¹ in May 1992. Although microscopic examination revealed that the layer consisted for the major part of living algae, it also included some dead organic material.

In ditches B and C the increase in biomass of the benthic layer at the end of the simulation period was lower than that calculated from net oxygen production by roughly 30% and 40% in ditch B and C respectively. In ditch C the filamentous algae, which were present during 1990, will explain part of the difference, but will only affect the measured value in autumn 1990. There are several other possible explanations for

the discrepancies. First, grazing might have played a role, but it is not known whether this is more significant in ditches B and C than in ditch A. The biomass stored in grazers is not known, but it is most likely that it can be neglected. Anoxic or anaerobic decomposition might also explain part of this difference, when it results in the volatilization of methane. Another uncertainty can be found in the mineral ash content of the benthic material. A mineral ash content of 25 % w/w for freshly formed algae has been assumed from the stoichiometry of the photosynthesis reaction. The mineral residue after decomposition of dead organic material, and the extent to which this residue dissolves again on the long term are not known. A different stoichiometry with respect to mineral ash content of the short and long term reaction is likely. The method used for sampling of the benthic layer is based on large differences in settling rate between the organic material and the underlying sand. The mineral residue of the benthic layer therefore may not have been removed from the sand.

In spite of all uncertainties, the primary production calculated from oxygen regimes show a comparable pattern as the accumulation of organic matter. Moreover, trends related to nutrient loading are observable with both techniques.

CONCLUSIONS

- The model and method used for estimation of the parameters determining primary production from continuous dissolved oxygen measurements showed to be well applicable, both with respect to its capability to fit measured data as with respect to computation time.
- Both net and gross production are strongly related to the level of external nutrient input. The increase in production is less than proportional in relation to the nutrient load.
- In all three ditches a considerable positive cumulative net primary production occurred over a two years period. It showed

a good agreement with the measured increase of dry weight in the benthic layer in ditch A, but was larger in ditch B and C. - The use of a constant reaeration coefficient throughout a day gives an underestimation of the cumulative diffusive flux across the air-water interface and therefore of net production over longer periods.

REFERENCES

- Aalderink, R.H., subm. Estimation of parameters describing primary production from continuously measured dissolved oxygen. (submitted to *Ecol. Modelling*)
- Bannister, T.T., 1979. Quantitative description of the steady-state, nutrient-saturated algal growth, including adaptation. *Limnol. Oceanogr.* 24, 76-96.
- Bierman, V.J., 1976. Mathematical model of the selective enhancement of blue-green algae by nutrient enrichment. In: R.P. Canale (ed), *Modeling biochemical processes in aquatic ecosystems*, 1-31. Ann Arbor Science Publ. Michigan, USA.
- Boylen, C.W. and T.D. Brock, 1974. A seasonal diatom in a frozen Wisconsin lake. *Journal of Phycology* 10, 210-213.
- Cosby, B.J. and G.M. Hornberger, 1984. Identification of photosynthesis-light models for aquatic systems. I. Theory and simulations. *Ecol. Modelling* 23, 1-24.
- Cosby B.J., G.M. Hornberger and M.G. Kelly, 1984. Identification of photosynthesis-light models for aquatic systems. II. Application to a macrophyte dominated stream. *Ecol. Modelling* 23, 25-51.
- Draper, N.R. and H. Smith, 1981. *Applied regression analysis*, 2nd edition. John Wiley and Sons, New York, pp 458-474.
- Drent, J. and K. Kersting, 1993. Experimental ditches for research under natural conditions. *Water Research* 27 (9), 1497-1500.
- Falkowski, P.G., 1984. Physiological responses of phytoplankton to natural light regimes. *J. Plankton Research* 6,

295-307.

- Fraleigh, P.C., B.T. Ocevski, I.E. Cado and H.L. Allen, 1981. Primary production (oxygen) and chlorophyll relationships in Lake Ohrid, Yugoslavia. Verh. Internat. Verein. Limnol. 21, 492-499.
- Gibson, C.E., 1975, A field and laboratory study of oxygen uptake by planktonic blue-green algae, J. Ecol., 42: 867-880.
- Harris, G.P, and B.B. Piccinin, 1977. Photosynthesis by natural phytoplankton populations. Arch. Hydrobiol. 80, 405-457.
- Harris, P.G., 1978. Photosynthesis, productivity and growth: the physiological ecology of phytoplankton. Arch. für Hydrobiol. Beih. 10. Schweizerbart, Stuttgart. 171 pp.
- Hunding, C., 1971. Production of benthic microalgae in the littoral zone of a eutrophic lake. Oikos 22, 389-397.
- Jassby, A.D. and T. Platt, 1976. Mathematical formulation of the relationship between photosynthesis and light for phytoplankton. Limnol. Oceanogr. 21, 540-547.
- Jorgensen, B.B., N.P. Revsbech, T.H. Blackburn and Y.Cohen, 1979. Diurnal cycle of oxygen and sulfide microgradients and microbial photosynthesis in a cyanobacterial mat sediment. Appl. Environm. Microbiol., 38, 46-58.
- Kamp-Nielsen, L., 1981, Diurnal variation in phytoplankton oxygen metabolism, Verh. Internat. Verein. Limnol., 21:431-437.
- Kirk, J.T.O., 1983. Light and photosynthesis in aquatic ecosystems. Cambridge University Press.
- Lijklema, L., J.H. Jansen and R.M.M. Roijackers, 1989. Eutrophication in the Netherlands. Wat. Sci. and Technol. 21, 1899-1902.
- Portielje, R. and L. Lijklema, 1994. The effect of reaeration and benthic algae on the oxygen balance of an artificial ditch. (accepted for publication by Ecol. Modelling)
- Revsbech, N.R., B.B. Jorgensen and T.H.Blackburn, 1983. Microelectrode studies of the photosynthesis and O₂, H₂S

- and pH profiles of a microbial mat. *Limnol. Oceanogr.* 28, 1062-1074.
- Richardson, K. J. Beardall and J.A. Raven, 1983. Adaptation of unicellular algae to irradiance: an analysis of strategies. *New Phytol.* 93, 157-191.
- Sand-Jensen, K., 1989. Environmental variables and their effect on photosynthesis of aquatic plant communities. *Aquatic Botany* 34, 5-25.
- Smith, E.L., 1936. Photosynthesis in relation to light and carbon dioxide. *Proc. Natl. Acad. Sci.* 22, 504-511.
- Steele, J.H., 1962. Environmental control of photosynthesis in the sea. *Limnol. Oceanogr.* 7, 137-150.
- Uhlmann, D., 1975. *Hydrobiologie, ein Grundriß für Ingenieure und Naturwissenschaftler* (in German). VEB Gustav Fischer Verlag Jena, 345 pp.
- Van Duin, E.H.S. and L. Lijklema, 1989. Modelling photosynthesis and oxygen in a shallow hypertrophic lake. *Ecol. Modelling* 45, 243-260.
- Van Duin, E.H.S., 1992. Sediment transport, light and algal growth in the Markermeer. Ph.D. Thesis Agricultural University Wageningen, the Netherlands, 273 pp.
- Vincent, W.F., 1990. The dynamic coupling between photosynthesis and light in the phytoplankton environment. *Verh. Internat. Verein. Limnol.* 24, 25-37.

Chapter 6

Estimation of primary production in macrophyte dominated ditches from continuous dissolved oxygen signals

key-words:

eutrophication - submersed macrophytes - primary production
- dissolved oxygen - parameter estimation

based on: Estimation of primary production in macrophyte dominated ditches from continuous dissolved oxygen signals, by R. Portielje, K. Kersting and L. Lijklema. submitted to Water Research.

6. ESTIMATION OF PRIMARY PRODUCTION IN MACROPHYTE DOMINATED DITCHES FROM CONTINUOUS DISSOLVED OXYGEN SIGNALS

ABSTRACT

In test ditches receiving three different levels of external nutrient (N,P) loading, primary production by the ditch community was estimated from continuously measured dissolved oxygen concentrations. The plant community in the ditches was dominated by submersed macrophytes. Processes affecting dissolved oxygen (primary production, respiration + decomposition) were estimated for individual days for a two-years period (March 1st 1990 - Feb 29th 1992). Reaeration was calculated from an empirical relation between the incident wind velocity and the reaeration coefficient.

For periods with O₂-stratification a two-layer model has been developed, for which it is assumed that primary production occurs in the top layer only. For these periods, which occur during the summer half year, it improves the best obtainable fit and provides a more realistic description of the system than a conventional one-box model.

Daily gross production rates and total oxygen consumption rates, which is the sum of respiration, decomposition and sediment oxygen demand, show a distinct seasonal fluctuation.

Cumulative gross production over two years increases with the level of external nutrient supply. The cumulative net production shows an irregular pattern. During the first half year it is related to the level of nutrient supply, but after two years the ditch receiving the intermediate nutrient loading rate (ditch B), dominated by *Elodea nuttallii*, had the highest cumulative net production. In the highest loaded ditch (C), also dominated by *Elodea nuttallii*, a significant decrease in net production occurred during the second year. The ditch receiving the lowest nutrient input (A) and dominated by Characeae had the lowest cumulative net production during the first year. In all ditches the net production was lower during the second year than during the first year.

The daily gross production rates plotted versus the daily total light irradiance for individual days over a two years period showed a saturation at high daily light irradiances. Least squares fitting showed that the maximum daily gross production was positively related to the level of external nutrient input. The light saturation constant was significantly higher in ditch A, dominated by Characeae, than in the two ditches with higher nutrient input, dominated by *Elodea nuttallii*, which had similar light saturation constants.

INTRODUCTION

Experiments have been performed in test ditches to study the

effects of nutrient loading on the structure and functioning of shallow aquatic ecosystems. This chapter deals with the estimation of primary productivity in ditches dominated by macrophytes. The results of similar parameter estimations in experimental ditches dominated by benthic algae or phytoplankton are described in chapter 5.

The photosynthetic activity of submerged macrophytes is directly reflected in, and can be estimated from, dissolved oxygen time series (Odum, 1956; Kelly et al., 1974; Fisher and Carpenter, 1976; Edwards et al., 1978; Marshall, 1981). The last two references deal with stagnant water bodies with similar vertical gradients as in our experimental ditches. In the case of strong vertical gradients a simple single-box model, assuming homogeneity, cannot be applied, as vertical transport starts to play a role. Edwards et al. (1978) developed a multi-layer model that generated realistic oxygen distributions over 24 hours. They applied their method to a few diurnal cycles.

Eutrophication of shallow waters can lead to a change in the structure of the macrophyte community favouring those species adapted to high nutrient conditions. Due to high productivity the vertical attenuation of light becomes high, and photosynthesis is mainly located in the upper part of the water column. Combined with a temperature stratification this can lead to steep vertical gradients of dissolved oxygen during the summer.

In this chapter primary productivity and total oxygen consumption, i.e. the sum of respiration, decomposition and sediment oxygen demand, are estimated from a model. This includes a parameter estimation routine on measured diurnal dissolved oxygen fluctuations. It has been applied to each individual day for a period of two years (March 1st 1990- Feb 29th 1992). The parameter estimation method is adapted from that described by Aalderink (1994). We used a two-layer model for those periods during which vertical mixing was not complete and a

single-layer model with average oxygen concentrations during vertical homogeneity. The method offers the possibility to study primary production and respiration by aquatic submerged macrophytes over longer periods under natural and undisturbed conditions.

Results are presented as daily gross and net primary production rates, as well as cumulatives over a two years period, and are related to the structure and external nutrient loading rate of the systems. The estimated gross and net production rates provide insight into the turn-over rate of the biomass, and the nutrient fluxes that are coupled to this.

The relation between daily gross production rates and cumulative daily light irradiance is also studied.

MATERIAL AND METHODS

Site studied

The location and the characteristics of the ditches are described in chapter 1.5 (p. 20-22).

The three ditches discussed in this chapter are the clay-ditches A, B and C. The clayish sediment layer of 25 cm originates from a mesotrophic fen near Wijchen in the Netherlands.

In all three ditches a vegetation had developed that consisted originally of mainly Characeae (coverage >95%). In ditch A, receiving no additional nutrients besides the atmospheric input and groundwater supply, the Characeae were slowly decreasing, but remained the dominant species during most of the considered period until they vanished just before the end of the research period (Portielje and Roijackers, 1994; chapter 3).

In the two ditches receiving an additional, manually added, external input of nutrients, referred to as ditch B and C, the original Characean vegetation was replaced by *Elodea nuttallii* filling up the water column from the bottom to the surface.

Nutrient addition

The levels of external nutrient loading and the method of nutrient addition is described in chapter 1.6 (p. 22-24).

The nutrient additions give rise to an instantaneous increase in the dissolved phosphorus concentrations of 0.53 and 1.71 mg P.l⁻¹ in ditch B and C respectively. After an addition the concentration drops back to its original background level in a period of about three weeks, due to biotic and sedimentary uptake.

The nutrient loading programme was started in May 1989, ten months before the simulation period considered in this chapter.

Measurements

Dissolved oxygen is measured at two water depths, 10 and 40 cm below the water surface. Water temperature is measured at the same depths as the oxygen concentration and in addition at mid-depth. Light irradiance is measured with a quantum sensor in the air. Wind speeds are obtained from a weather station at the experimental site. All measurements are taken at 30 second intervals and averaged over 15 minutes before storage in a data logger. A detailed description of the experimental ditches and the measuring equipment is given by Drent and Kersting (1993).

Standing crop

Standing crop was measured on two occasions by quantitative harvesting of the vegetation inside a 37.5 cm diameter cylinder on three locations in the ditches, and drying at 40°C. Internal phosphorus was measured as dissolved phosphorus, determined on a Scalar SA-40 Autoanalyser, using the modified molybdate-blue method according to Murphey & Riley (1962), after 2 hrs digestion of dried plant material in a H₂SO₄-Se-

lenium mixture at 340°C, with H₂O₂ as oxydator.

THEORY

For periods of complete vertical mixing the same model and parameter estimation method (Aalderink, 1994) have been applied to the ditches dominated by macrophytes as were used for ditches dominated by benthic algae (see chapter 5). As the attenuation of light in the water column is spatially and temporally inhomogeneous, productivity has been related directly to the incident irradiance at the water surface, disregarding light attenuation. Preliminary tests revealed that this does not influence the quality of the fit, or the estimated net and gross primary production rates, but it affects the values of the parameters of the photosynthesis-light function. These parameters therefore in this approach have no direct physiological meaning for individual light receptor sites, but they characterize the response of the system as a whole. When periods with only slight vertical gradients during the light period of the day occurred, reaeration was related to the measured concentrations at 10 cm depth, and parameters were estimated from least squares fitting to averaged concentrations.

The differential equation to describe the change in the oxygen concentration in time is:

$$\frac{dC}{dt} = k_A(C_s - C) + G_m F(I) - R_{20^\circ C} \theta^{(T-20)} \quad (1)$$

with:	C	O ₂ concentration (g.m ⁻³)
	C _s	saturation oxygen concentration (g.m ⁻³)
	k _A	reaeration coefficient (hr ⁻¹)
	G _m	maximum gross production rate (g O ₂ .m ⁻³ .hr ⁻¹)
	F(I)	light-production function (-)
	R _{20°C}	total oxygen consumption rate at 20°C (g O ₂ .m ⁻³ .hr ⁻¹)
	θ	temperature coefficient (-)

At each measurement interval *i* the simulated concentration, using a modification of the continuous solution approach by

Aalderink (1994), is calculated from:

$$C_i = C_0 + \sum_{j=1}^i k_{\lambda,j} (C_{s,j} - C_{j,m}) + \sum_{j=1}^i G_m F(I)_j - \sum_{j=1}^i R_{20^\circ C} \theta^{(T_j - 20)} \quad (2)$$

k_{λ} is a function of the incident wind velocity (Portielje et al., 1994; chapter 5). In the literature a number of relations between primary production and light can be found. In this study we used that of Smith (1936), which assumes saturation at high light irradiances:

$$F(I) = \frac{\frac{I}{I_k}}{\sqrt{1 + \left(\frac{I}{I_k}\right)^2}} \quad (3)$$

with I the incident light irradiance ($E.m^{-2}.s^{-1}$)
 I_k the light parameter according to Smith ($E.m^{-2}.s^{-1}$).

The model is linear in G_m and $R_{20^\circ C}$, but not in I_k . The best fit is obtained from applying a search routine on I_k , and solving the normal equations of the sum of squares at a given value for I_k with respect to $R_{20^\circ C}$ and G_m :

$$\frac{dSS}{dR_{20^\circ C}} = 0 \quad \frac{dSS}{dG_m} = 0 \quad (4)$$

with SS the sum of squares of the differences between measured (m) and simulated (s) concentrations at each measure time:

$$SS = \sum_{i=1}^n (C_{i,m} - C_{i,s})^2 \quad (5)$$

with n the number of samples per day.

The initial concentration for each day, C_0 , is calculated by linear regression of the first five measurements and extrapolation to $t=0$.

In case of a dense vegetation of *Elodea nuttallii* the vertical

oxygen gradient becomes too steep during the summer to allow the use of a one-box model with assumed complete vertical mixing. For these conditions, which only occurred in ditch B, a two-box model has been developed. Based on the observation in the ditches that *Elodea nuttallii* forms a dense biomass near the water surface with an almost 100% areal coverage (Portielje and Roijackers, 1994; chapter 3), it can be assumed that all primary production occurs near the water surface. In the lower layer only respiration and decomposition take place. The exchange between the upper and lower compartment is related to the vertical oxygen gradient. The oxygen concentration measured at 10 cm depth is assumed to represent a well mixed top layer of the water column, and the measured concentration at 40 cm to represent a bottom layer. The following model equations are used:

$$\frac{dC_t}{dt} = k_A(C_s - C_t) + G_m F(I) - E_{z,t} \cdot (C_t - C_b) - R_{20^{\circ}C,t} \theta^{(T-20)} \quad (6)$$

$$\frac{dC_b}{dt} = E_{z,b} (C_t - C_b) - R_{20^{\circ}C,b} \theta^{(T-20)} \quad (7)$$

with E_z the coefficient of dispersive exchange between the top and bottom layer (hr^{-1})

subscripts t and b refer to top layer and bottom layer respectively.

$E_{z,t}$ and $E_{z,b}$ are interconvertible by:

$$E_{z,t} = E_{z,b} \frac{V_b}{V_t} \quad (8)$$

with V_t and V_b the volumes of the upper and lower compartment respectively.

The simulated concentration in the lower box at time $t=i$, is calculated from:

$$C_{b,i} = C_{b,0} + \sum_{j=0}^{i-1} E_{z,b} (C_{t,j} - C_{b,j}) - \sum_{j=0}^{i-1} R_{20^{\circ}C,b} \theta^{(T_j-20)} \quad (9)$$

with $C_{b,0}$ the initial concentration in the lower box.

The concentration at time i in the top layer is calculated from:

$$C_{t,i} = C_{t,0} + \sum_{j=0}^{i-1} k_{A,j} (C_{s,j} - C_{t,jm}) + \sum_{j=0}^{i-1} G_m F(I)_j - \sum_{j=0}^{i-1} E_{z,t} (C_{t,jm} - C_{b,jm}) - \sum_{j=0}^{i-1} R_{20^{\circ}C,t} \theta^{(T_j-20)} \quad (10)$$

$E_{z,b}$ is estimated by fitting equation (9) to the oxygen concentration course in the bottom layer. After conversion of $E_{z,b}$ to $E_{z,t}$ with equation (8), $E_{z,t}$ is substituted in equation (10). The model is non-linear in I_k and a search routine is applied on I_k . The optimum values of the other parameters, G_m and $R_{20^{\circ}C,t}$, are obtained from solving the normal equations of the sum of squares with respect to each parameter, analogous to equation (4).

As $E_{z,b}$ is estimated from curve-fitting of the concentrations in the bottom layer, and then is used as an input variable for the top layer, it is not an additional free parameter for the latter.

The presented two-layer model is a simplification of the real situation. The division into two layers is an approximation of the real concentration gradient. For the calculation of primary production and total oxygen consumption an assumption has to be made about the volumes for which the measured concentrations are representative. These volumes V_t and V_b can be estimated by comparing to independent calculations of the net production for each day. The net production can be calculated as the difference between gross production and oxygen consumption:

$$NP_{model} = \sum_{i=1}^n \frac{V_t}{V_t+V_b} G_m F(I)_i - \sum_{i=1}^n \left[\frac{V_t}{V_t+V_b} R_{20^{\circ}C,t} \theta^{(T_i-20)} + \frac{V_b}{V_t+V_b} R_{20^{\circ}C,b} \theta^{(T_i-20)} \right] \quad (11)$$

It can also be calculated as the opposite of the total diffusive flux across the water-atmosphere interface plus the difference between initial and final oxygen concentration on the considered day:

$$NP_{diffusion} = \sum_{i=1}^n [k_{A,i} (C_s - C_{t,i})] + \frac{V_b}{V_t+V_b} (C_{b,n} - C_{b,0}) + \frac{V_t}{V_t+V_b} (C_{t,n} - C_{t,0}) \quad (12)$$

The two calculations have to lead to the same result. The estimates of $E_{z,b}$ and R_b are independent of the volume of the lower compartment (equation 7). Conversion of $E_{z,b}$ to $E_{z,t}$ and the contribution of R_b to the total oxygen consumption, on the other hand, depends on the ratio of the volumes of the two layers. Therefore after estimating $E_{z,b}$ and R_b from equation 9 a separate search routine for V_t was applied. For each value of V_t , $E_{z,t}$ is calculated from $E_{z,b}$ (equation 8), and the other parameters for the top layer are estimated from equation 10. The parameters are used to calculate NP_{model} (equation 11) and $NP_{diffusion}$ is calculated with equation 12. V_t is varied until NP_{model} equals $NP_{diffusion}$. Figure 6.1 provides a diagram of the procedure. Note that the criterium for the optimum value for V_t is the agreement between net production and diffusive flux (equations 11 and 12) and not the least squares sum.

As the reaeration coefficient has the dimension hr^{-1} , and was based on the volume of the whole ditch, the reaeration coefficients calculated from the original wind reaeration function have to be corrected for the volume of the top layer compared the total ditch volume.

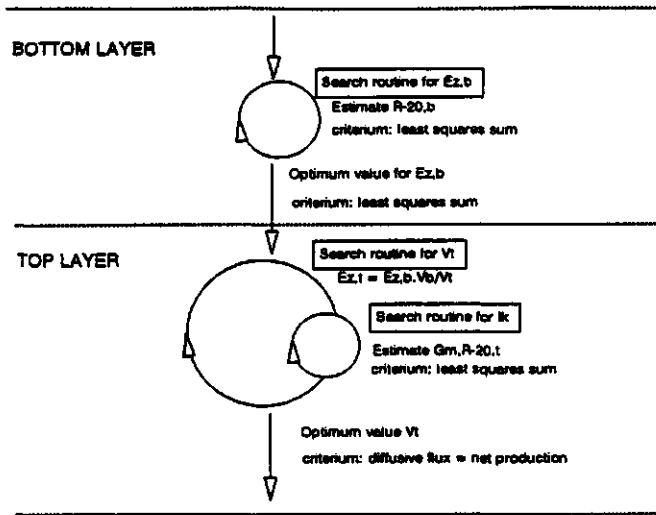


Figure 6.1. Schematization of the parameter estimation procedure of the two-box model.

The quality of the fit of the simulated to the measured concentration course is expressed as a model efficiency.

This model efficiency η is defined as:

$$\eta = \frac{\sum_{i=1}^n (C_{i,m} - \bar{C}_m)^2 - \sum_{i=1}^n (C_{i,s} - C_{i,m})^2}{\sum_{i=1}^n (C_{i,m} - \bar{C}_m)^2} \quad (13)$$

\bar{C}_m is the daily averaged measured concentration, subscripts s and m refer to simulated and measured respectively.

The frequency distribution of the model efficiencies for individual days provides insight into the general correspondence between measured and simulated diurnal oxygen courses, and of the ability of the model to estimate the processes affecting the oxygen household. The value of η is determined both by the quality of the model and the parameter estimation routine as by the quality (noise) of the measured oxygen data.

Confidence contours for the parameters describing daily gross production as a function of total daily light irradiance are calculated from (Draper and Smith, 1981):

$$SS_{cont} = SS_{min} \left[1 + \frac{p}{n-p} F(n, n-p, \alpha\%) \right] \quad (14)$$

with SS_{cont} the sum of squares at the $\alpha\%$ confidence contour, SS_{min} the minimum sum of squares, p the number of parameters, n the number of independent data and $F(n, n-p, \alpha\%)$ the F-distribution according to Fischer.

RESULTS

Two-box model

The two-box model was applied only to ditch B, which showed the most persistent stratification from half May until half October. In ditch C a vertical gradient was present regularly during daytime in the summer, but at night this gradient disappeared. For this ditch for ditch A, a one-box model, slightly modified in case of gradients during the day, was used for the whole period of two years.

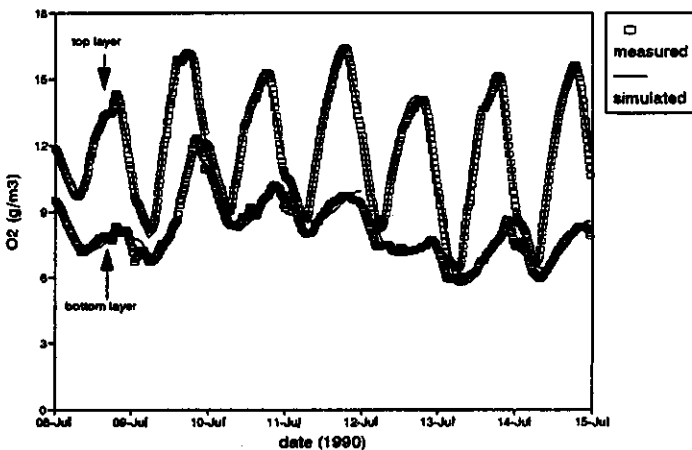


Figure 6.2. Measured and simulated dissolved oxygen concentrations in the top and bottom layer (ditch B, July 8th - July 15th, 1990).

Figure 6.2 illustrates the simulated and measured dissolved oxygen courses in top and bottom compartment (C_t and C_b) in ditch B during the period July 8th - July 14th 1990. During this period the model efficiency in the upper box varied between 0.966 (July 12th) and 0.993 (July 9th) and in the lower box between 0.542 (July 11th) and 0.946 (July 9th). The low model efficiency for the lower compartment on July 11th seems to be caused by a fluctuation in the measured concentration course leading to a poor estimation of the initial concentration $C_{b,0}$. Estimation of $C_{b,0}$ as an independent parameter can probably improve the fit. As can be seen from figure 6.2, the measured concentration of the lower compartment shows irregular fluctuations which are probably due to variations in the vertical transport that cannot be simulated with the present model. This, and the small daily amplitudes in the oxygen concentration during periods of low vertical exchange, cause lower model efficiencies for the bottom compartment. During periods of stratification, as in figure 6.2, the model efficiencies obtained with the two-box model for the top layer were an improvement with respect to the conventional one-box model. This is illustrated in figure 6.3, which displays the model efficiencies for the summer of 1990 and 1991 obtained with both models. At days when the model efficiency of the two-box model is much lower than that of the one-box model, the former is apparently not appropriate. For those periods in which an improvement was obtained, the results of the two-box model are used.

Figure 6.4 displays the vertical dispersion coefficient $E_{z,b}$ (hr^{-1}) in ditch B, for the summer of 1990 and 1991 respectively. Although the values for $E_{z,b}$ show large variations, they are usually low, and on average 0.06 and 0.05 hr^{-1} for 1990 and 1991 respectively.

Primary production by macrophytes

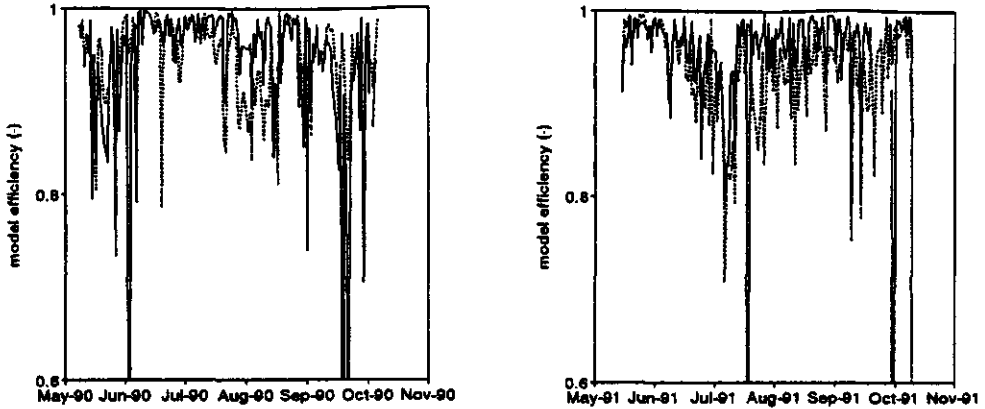


Figure 6.3. Model efficiencies in the top layer, obtained with one-box (-----) and two-box model (——), ditch B, summers of 1990 and 1991.

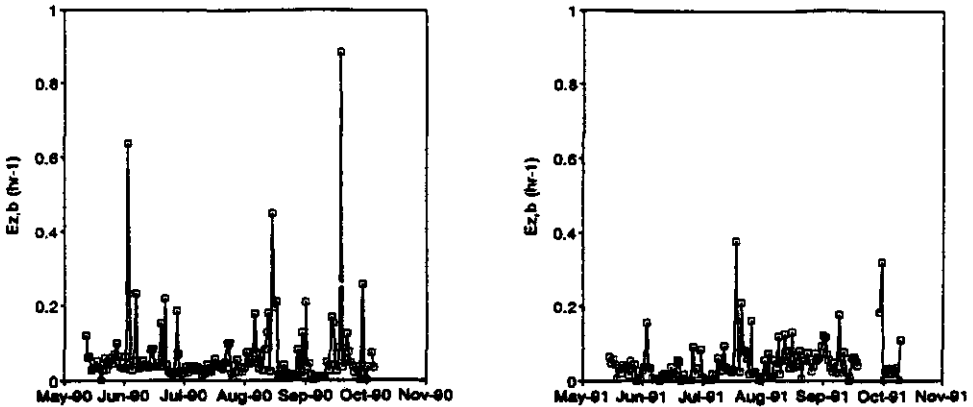


Figure 6.4. Estimated $E_{z,b}$ values (hr^{-1}), ditch B.

Overall results for the two years period

Figure 6.5 displays the frequency distribution of the model efficiency for all three ditches (for those days on which the two-box model was applied, model efficiencies of the top layer were used). A model efficiency of 0.90 is exceeded on 77, 75 and 76 % of all days for ditch A, B and C respectively.

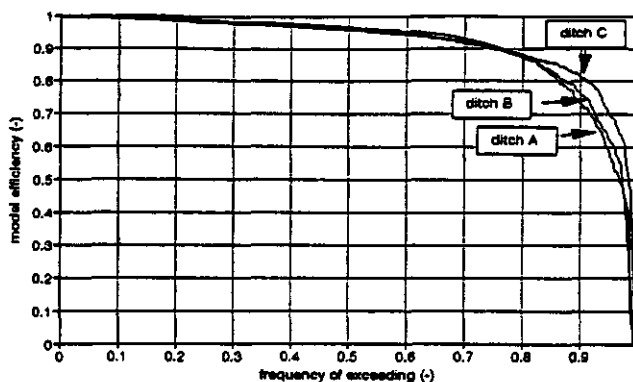


Figure 6.5. Frequency distribution of model efficiency values in ditch A, B and C .

Figure 6.6 displays the daily gross production rates for the two years period. The data are scattered during the summer in ditch B and C, but they show a positive relation with the level of nutrient input.

Figure 6.7 displays the daily total oxygen consumption rates of the three ditches. Again the scattering is large during the summer in the two *Elodea* dominated ditches. In case of the two-box model, the volume weighted sum of the oxygen consumption rates in the top and bottom layer is presented.

Figure 6.8 displays the daily net productions for the three ditches. Although there is a wide scattering between individual days, especially in ditch C, the seasonal fluctuations are apparent.

Figure 6.9 presents the cumulative gross production, cumulative oxygen consumption and cumulative net production for the three ditches. Both the cumulative gross productions and total oxygen consumptions are positively related to the level of external nutrient input. The initial increase in cumulative net production shows a correspondence with the level of external nutrient input, with the fastest initial increase in ditch C. On the other hand, it also decreases faster during autumn and winter than in the other two ditches.

Primary production by macrophytes

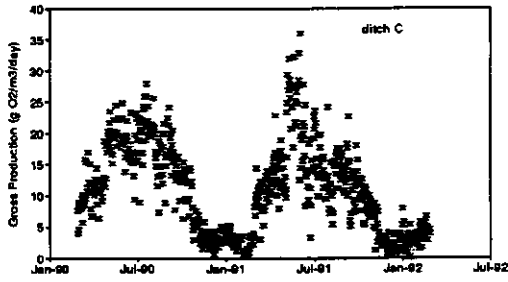
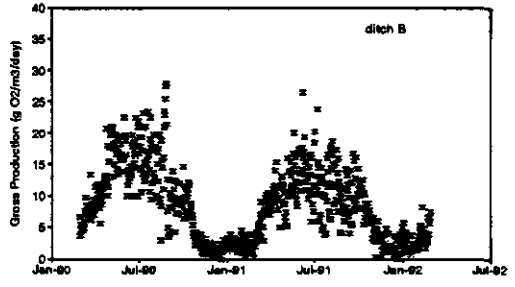
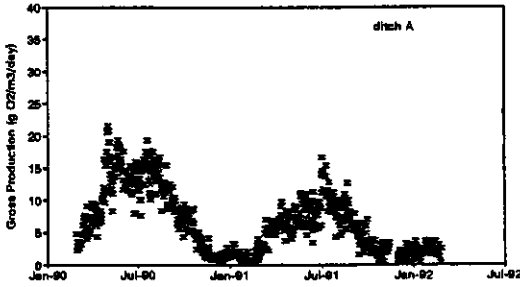


Figure 6.6. Estimated daily gross production rates. ($\text{g O}_2 \cdot \text{m}^{-3} \cdot \text{d}^{-1}$)

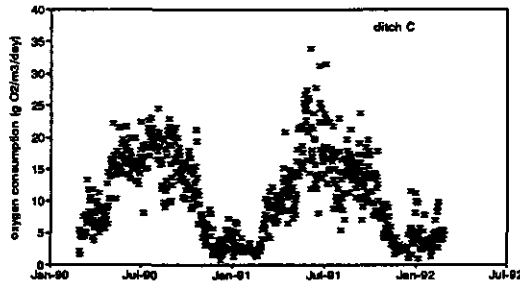
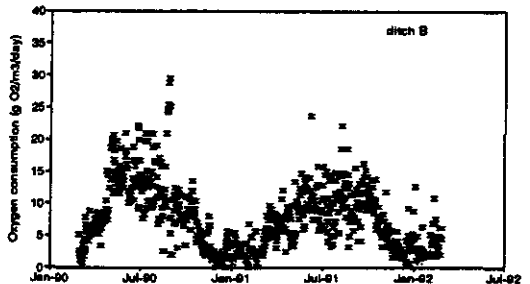
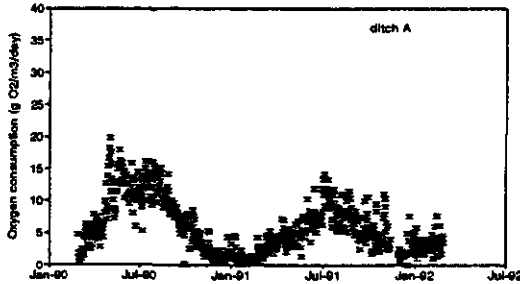


Figure 6.7. Estimated daily oxygen consumption rates. ($\text{g O}_2 \cdot \text{m}^{-3} \cdot \text{d}^{-1}$)

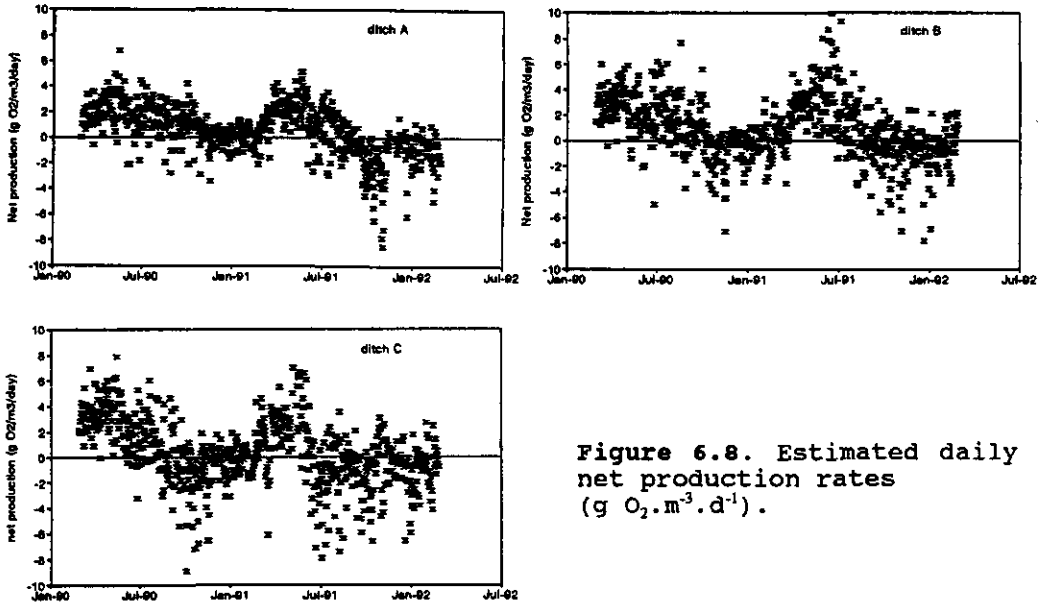


Figure 6.8. Estimated daily net production rates ($\text{g O}_2 \cdot \text{m}^3 \cdot \text{d}^{-1}$).

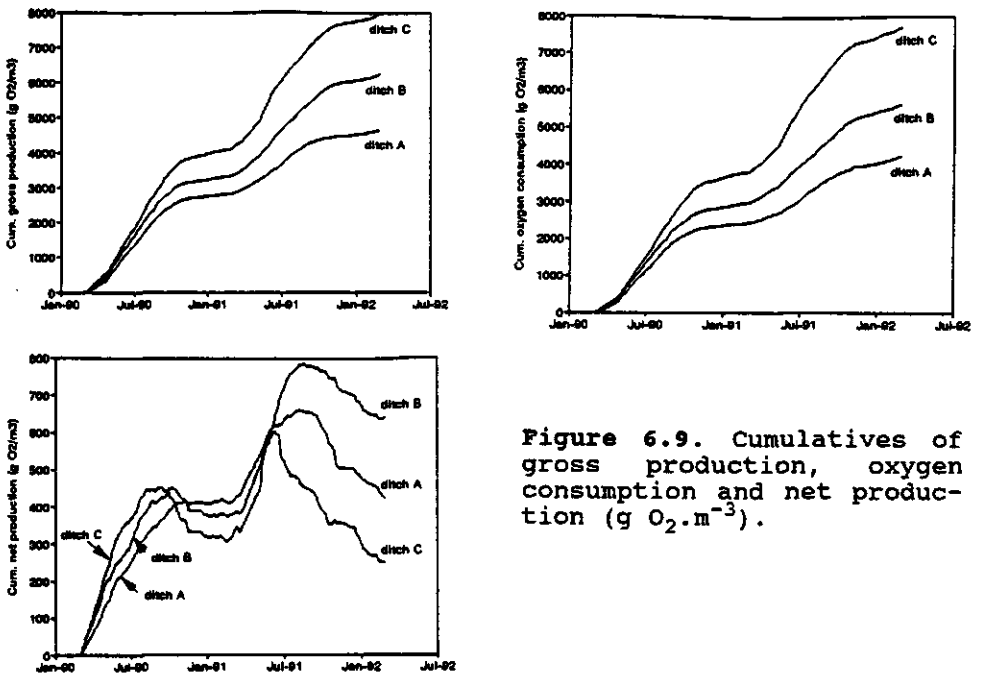


Figure 6.9. Cumulatives of gross production, oxygen consumption and net production ($\text{g O}_2 \cdot \text{m}^3$).

Primary production by macrophytes

In 1991, the decrease in the cumulative net production in autumn and winter is larger than in 1990 in all ditches. The cumulative net production in ditch C, after a steep increase in May (probably caused by the nutrient dosage), already starts to decline in June. After two years there is a large difference in cumulative net production between ditch B and C, although both have a virtually complete coverage with *Elodea nuttallii*.

The cumulatives per year (March 1st-February 28th) are given in table 6.1. It shows that both gross production and oxygen consumption were considerably lower in 1991 than in 1990 in ditch A and B. In ditch C the differences were much smaller, with a small increase in total oxygen consumption. The P/R ratios were lower in 1991 than in 1990 in all three ditches. Only in ditch C in 1991 was the P/R ratio smaller than one, resulting in a negative value for total net production during this year.

Table 6.1. Cumulatives of gross production (P), oxygen consumption (R), P/R ratio and net production per year ($\text{g O}_2 \cdot \text{m}^{-3}$). Percentual changes in 1991 compared to 1990 are given between brackets.

ditch		1990	1991
A, reference	gross production	2835	1814 (-36)
	oxygen consumption	2425	1802 (-26)
	P/R	1.17	1.01
	net production	410	12
B, medium	gross production	3345	2904 (-13)
	oxygen consumption	2968	2659 (-10)
	P/R	1.13	1.09
	net production	377	266
C, highest	gross production	4114	3848 (-6)
	oxygen consumption	3800	3913 (+3)
	P/R	1.08	0.98
	net production	313	-135

Table 6.2 presents measured standing crops and internal P-concentrations of the vegetation on two occasions in October 1990 and October 1991. It shows that the *Elodea* community of ditch

C has higher internal P-concentrations but a lower standing crop than that of ditch B.

Table 6.2. Standing crop SC (g dry matter \cdot [m² sediment]⁻¹) and intracellular P-concentrations (mg P. [g dry matter]⁻¹) of the macrophytes in the ditches.

ditch	SC Oct. '90	P _{int}	SC Oct'91	P _{int}
A, reference ^{*)}	408	1.42	323	1.19
B, medium	502	2.06	448	3.63
C, highest	394	3.18	364	4.53

^{*)} emergent species excluded.

In ditch C a cumulative gross production after two years of 8000 g O₂·m⁻³ was found. With a conversion factor from oxygen production to dry weight of 0.68, and a sediment area to volume ratio of 1.36, this equals 3995 g dry weight·m⁻². This is about 10.5 times the measured standing crops, and roughly indicates a turn-over rate of 5.3 year⁻¹, based on the standing crop in autumn. In ditch B this turn-over rate is roughly 3.3 year⁻¹ and in ditch A 3.2 year⁻¹.

In ditch A a gradual development of emergent *Scirpus acicularis* took place, with an average standing crop of 67 g dry matter·[m² sediment]⁻¹ in October 1991. The photosynthetic activity of this species is not reflected in dissolved oxygen fluctuations, but affects the dissolved oxygen concentration during periods of increased decomposition.

Direct comparison of the estimated cumulative net production with a change in standing crop is however not allowed as settling of a considerable amount of dead, undegraded plant material may have occurred, resulting in an increased organic matter content of the upper sediment layer. Losses of plant material through the discharge are low due to the construction of the overflow funnel. Anoxic and anaerobic decomposition of dead plant material in the sediments may also be an important process controlling the loss of plant material. Anaerobic

Primary production by macrophytes

decomposition could lead to a flux of methane to the atmosphere.

Figure 6.10 presents the daily gross production rates at 20°C versus total daily light irradiance.

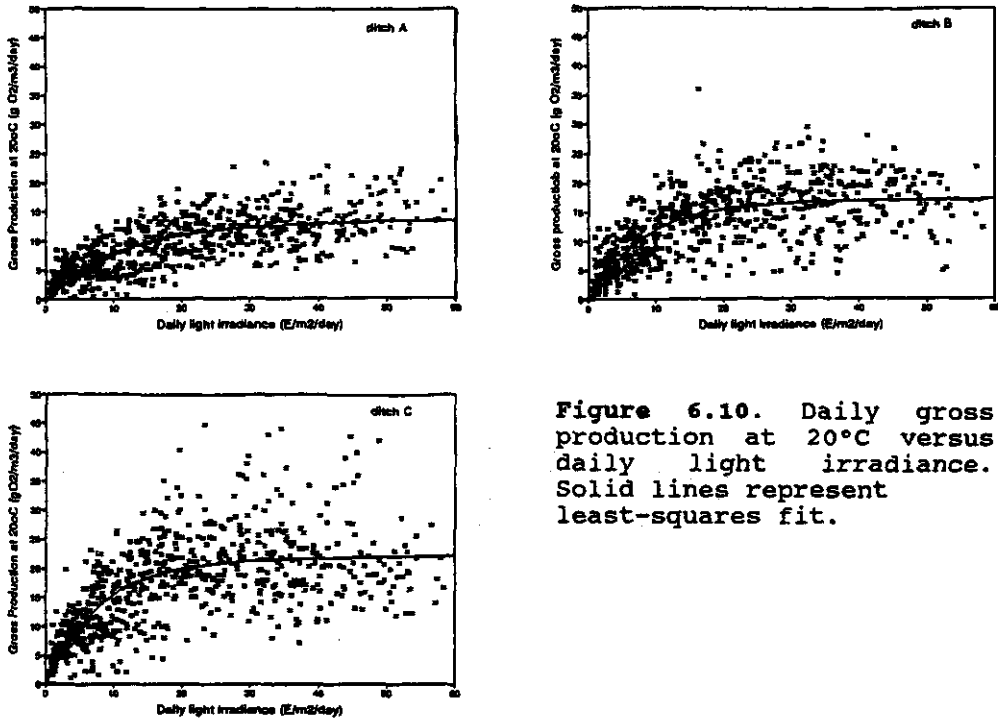


Figure 6.10. Daily gross production at 20°C versus daily light irradiance. Solid lines represent least-squares fit.

Temperature correction was performed using the relationship:

$$P_{20^{\circ}\text{C}} = \frac{P_T}{\theta^{(T-20)}}$$

with $\theta=1.06$ (-) and T the average water temperature of the current day. All three ditches show saturation at high light

intensities, and the behaviour resembles that of Smith' photosynthesis-light function. There is no evidence for the occurrence of photo-inhibition at high light intensities. Although the areal coverage of the macrophyte community varies within a year, and thereby also the fraction of light that is intercepted by the macrophytes, no particular seasonal pattern can be detected (not shown in figure). Fitting the data to a function relating daily gross production to daily total irradiance according to Smith (1936), and using least-squares optimization, yields as best estimates:

ditch	max. gross prod (g O ₂ .m ³ .day ⁻¹)	I _k (E.m ² .day ⁻¹)
A, reference	13.8	15.6
B, medium	17.5	10.8
C, highest	22.5	10.6

Figure 6.11 presents these estimated values and their 95% confidence contours. It shows a significant increase of daily maximum gross production rates with increasing level of nutrient loading. I_k is significantly higher in ditch A than in ditch B and C, for which the I_k values are about equal.

DISCUSSION

Field studies of photosynthesis in macrophytes communities often suffer from a number of imperfections. They provide momentary information, and due to natural variations in parameters extrapolation of experimental results to longer periods is difficult. Physical disturbances, inherent to field enclosure experiments with macrophytes, also influence the result. Continuous in situ oxygen measurements are labour intensive, but they are non-destructive, and it is relatively easy to automatize the method of data retrieval and subsequent parameter estimation.

Inaccuracies in parameter estimations from continuous dissolved oxygen measurements result from spatial inhomogeneities in

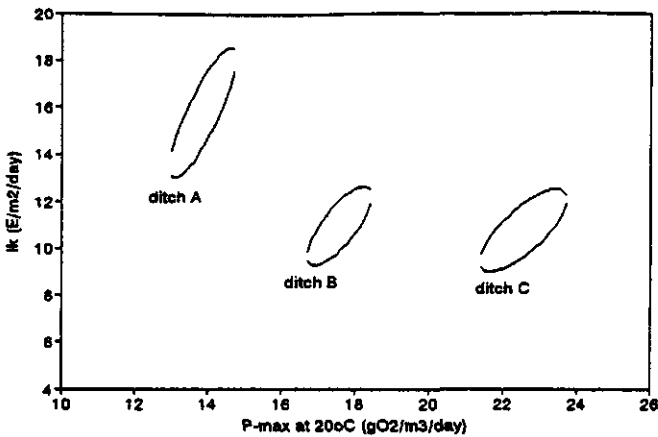


Figure 6.11. 95 % confidence contours of I_k versus the maximum daily production rate at $20^\circ C$.

the oxygen concentrations. The movement of the oxygen electrodes will locally affect the density of the vegetation, as a small area has to be kept free of macrophytes.

Production and oxygen consumption vary seasonally, but also daily depending on the weather conditions. This short term variability hampers extrapolation from production estimates during short periods to cumulative productions over longer periods (Kersting and Kouwenhoven, 1989).

The cumulative net production over longer periods is equal to the cumulative diffusion and consequently directly related to the wind-re-aeration relationship. For the calculation of the exchange of oxygen across the air-water interface an empirical relationship between re-aeration coefficient and continuously measured wind speed has been used. These measurements were performed in a ditch without a significant macrophyte community, but with the same geometry.

Vegetation reduces the turbulence which is generated by wind action at the water surface, and thereby affects the mass transfer at the air-water interface. The density of the vegetation fluctuates over the seasons, and concomitantly probably

does the wind-re-aeration relationship. For the summer periods, with an *Elodea* vegetation that filled up the zone near the water surface, this relationship may give an overestimation of the mass transfer rate. It is expected that this overestimation will be about the same in both ditch B and C.

Cumulative gross production is less sensitive to the wind-re-aeration function. A sensitivity analysis on the cumulative gross production in ditch A as a function of the mass transfer rate showed that a decrease in the mass transfer rate with 25 % at each time interval caused a decrease in the cumulative gross production over two years of only 6 %.

When large vertical gradients occur, and/or the light attenuation in the top layer is very high, the course of the dissolved oxygen concentration in the lower compartment is controlled by vertical transport and the total oxygen consumption rate. The vertical gradient in the dissolved oxygen concentration is always negative from surface to sediment. As the exchange between upper and lower layer is proportional to the vertical gradient, it varies significantly within a daily cycle. The oxygen consumption rate in the lower compartment also varies within a diurnal cycle, but in a way different from the vertical exchange, as it is a function of temperature. This allows generally an independent estimation of E_2 and $R_{20^\circ\text{C}}$, although a positive correlation between the two parameters is sometimes observed. E_2 has been assumed constant throughout a day, while in reality it will vary due to variations in wind speed. It will also be affected by variations in the vertical temperature gradient during a 24 hours cycle. The data allow no identification of a quantitative relationship between E_2 and environmental factors.

The thickness of the upper and lower box is estimated from the agreement between net production calculated from daily gross production and total oxygen consumption, and net production calculated from the diffusive flux of oxygen across the air-water interface and the difference between initial and final

O₂ concentration. This is, however, a simplification. Continuous measurements at a large number of fixed depths would of course allow a better estimate of the thickness of the layers in the two-box model, as the volumes of the boxes then can be related to the measured vertical gradient. These measurements however will put large demands on instrumentation and labour facilities. It might indicate the necessity to increase the number of boxes in the model.

Production has been related to the incident light intensity measured above the water surface. The vertical light profile in the water column has not been taken into account. This vertical light profile will vary in space and time, but cannot be quantified with sufficient accuracy in macrophyte dominated systems. Relating the production to the light intensity above the surface will affect the parameters of the light-production function, but preliminary tests showed that this does not appreciably affect the estimated gross production and oxygen consumption rates.

The concentrations of dissolved nutrients are low during most of the year (results not shown), and the level of external nutrient input is mainly reflected in internal concentrations. The cumulative gross production and oxygen consumption rates are related to the nutrient loading rate, but not in a direct proportional way. Ditch B only received extra phosphorus indicating that phosphorus was limiting the production in ditch A. Between October 1990 and October 1991 there was a decrease in standing crop in all ditches. Yet there was a positive net oxygen production in ditch A and B. Organic matter has probably accumulated in the sediment, or anaerobic degradation resulting in methane volatilization may have occurred.

Ditch B and C both have an almost 100% areal coverage with *Elodea nuttallii* during the summer period, but showed a large difference in cumulative net production over two years. The

cumulative net production was positive during the first year indicating the accumulation of organic matter. This stimulated the oxygen consumption in the second year in ditch C, but not in ditch B. Ditch A is slightly different, because some emergent vegetation developed in this ditch. This vegetation does not contribute to the gross oxygen production, but it does contribute to the oxygen consumption of the system. Nutrient enrichment affects the production in a complex way. Both gross production and oxygen consumption are stimulated, but the proportions are different and vary in time. This leads to a complex behaviour of the balance of these two processes, the net production. For this process the history of the system is important.

The maximum daily gross production rate is positively related to the level of external nutrient input. The light parameter according to Smith (1936) was not shown to differ in *Elodea* dominated ditches at two different levels of nutrient input, but was higher in the *Chara* dominated ditch. The effect of a transition from a *Chara* dominated system to an *Elodea* dominated system on gross production therefore is twofold: higher maximum production rates at high light intensities and a more efficient light-utilization at low light intensities.

CONCLUSIONS

- Estimation of primary production from continuously measured dissolved oxygen concentrations provides information on the productivity of a system over long periods, without disturbing the system.
- The two-box model provides a more realistic description than a one-box model for periods with a permanent vertical DO gradient.
- The cumulative gross production of the macrophyte communities is related to the level of external nutrient input.
- Net production was dependent on the nutrient load in a complex way. Cumulative net production over two years was

significantly higher in ditch B than in ditch A and C.

- The maximum daily production rate of the macrophyte communities is positively related to the level of external nutrient input.

REFERENCES

- Aalderink R.H., subm. Estimation of parameters describing primary production from continuously measured dissolved oxygen. (submitted to *Ecol. Modelling*)
- Draper, N.R. and H. Smith, 1981. *Applied regression analysis*, 2nd edition. John Wiley and Sons, New York, pp 458-474.
- Drent, J. and K. Kersting, 1993. Experimental ditches for research under natural conditions. *Water Research* 27 (9), 1497-1500.
- Edwards, R.W., Duffield, A.N. and Marshall, E.J., 1978. Estimates of community metabolism of drainage channels from oxygen distribution. *Proc. EWRS 5th Symp. on Aquatic Weeds*. 295-302.
- Fisher, S.G. and S.R. Carpenter, 1976. Ecosystem and macrophyte primary production of the Fort River, Massachusetts. *Hydrobiologia* 47, 175-187.
- Kelly, M.G., Hornberger, C.M., Cosby, B.J., 1974. Continuous automated measurements of rates of photosynthesis and respiration in an undisturbed river community. *Limnol. Oceanogr.* 19, 305-312.
- Kersting, K. and P. Kouwenhoven, 1989. Annual and diel oxygen regime in two polder ditches. *Hydrobiol. Bull.*, 23, 111-123.
- Marshall, E.J.P., 1981. The ecology of a land drainage channel-I. Oxygen balance. *Water Research* 15, 1075-1085.
- Murphy, J. and J.P. Riley, 1962. A modified single solution method for the determination of phosphate in natural waters. *Anal. Chim. Acta* 27, 31-36.
- Odum, H.T., 1956. Primary production of flowing water. *Limnol. Oceanogr.* 1, 102-117.

- Portielje, R. and R.M.M. Roijackers, *subm.* Primary succession in test ditches receiving different levels of external supply with nutrients. (submitted to Aquatic Botany)
- Portielje, R., K. Kersting and L. Lijklema, *subm.* Estimation of productivity by benthic algae from continuous oxygen measurements in relation to external nutrient input. (submitted to Water Research)
- Smith, E.L., 1936. Photosynthesis in relation to light and carbon dioxide. Proc. Natl. Acad. Sci. 22, 504-511.

Chapter 7

Sorption of phosphate by sediments as a result of enhanced external loading

keywords:

phosphorus - sediments - adsorption - dispersion
- solid-phase diffusion - Al-hydroxide

Based on: Sorption of phosphate by sediments as a result of enhanced external loading, by R. Portielje and L. Lijklema (1993). *Hydrobiologia* 253, 249-261.

7. SORPTION OF PHOSPHATE BY SEDIMENTS AS A RESULT OF ENHANCED EXTERNAL LOADING

ABSTRACT

In artificial test ditches, originally poor in nutrients, the effects of enhanced external loading with phosphorus were studied. An important term in the mass balance of phosphorus is retention by sediment. Parameters concerning the uptake of phosphorus by the sandy sediment of a ditch have been measured or were obtained from curve-fitting and were used in a mathematical model to describe diffusion into the sediment and subsequent sorption by soil particles.

On a time scale of hours uptake of phosphorus from the overlying water by intact sediment cores could be simulated well with a simple diffusion-adsorption model. Mixing of the overlying water resulted in an enhanced uptake rate caused by an increased effective diffusion coefficient in the top layer of the sediment.

Laboratory experiments revealed that after a fast initial adsorption, a slow uptake process followed that continued for a period of at least several months. This slow sorption can immobilize a substantial part of the phosphorus added. It may physically be described as an intraparticle diffusion process, in which the adsorbed phosphate penetrates into metal-oxides, probably present as sand grain coating, and thereby reaches sorption sites not immediately accessible otherwise.

The total sorption capacity of the soil particles is ca. 3.3 times the maximum instantaneous surficial adsorption capacity.

INTRODUCTION

Over the last decades eutrophication in surface waters has received ample attention in water research, resulting in numerous publications. The role of the sediments as a buffer for phosphorus has been a central issue. During periods of enhanced external loading the sediments can readily take up large amounts of phosphorus, thereby keeping bio-availability relatively low (Golterman, 1977). On the other hand, after a reduction of the external loading the sediments can release the sorbed phosphorus, thus counteracting beneficial effects (Lijklema, 1986; Ahlgren, 1977).

An important requirement for a realistic description and prediction of phosphorus fluxes across the sediment-water interface is a good apprehension of the underlying mechanisms.

These include physical processes that affect transport (diffusion, dispersion) and the factors controlling them and the kinetics and time scales of the physical/chemical processes involved (adsorption, desorption, precipitation; Lijklema, 1991).

In this chapter the accumulation of phosphorus in the sediment of a test ditch receiving a high external loading with nutrients (sand ditch D) is discussed. Following other authors (e.g. Kamp-Nielsen, 1982) a multi-layer sediment model has been used to simulate uptake and subsequent sorption by the sediment particles. The description is in terms of diffusive transport mechanisms, both in the interstitial water and in a solid phase consisting mainly of aluminum-hydroxides, where partial conversion of the hydroxides to Al-phosphates follows (Van Riemsdijk, 1984; Bolan et al, 1985; Van der Zee, 1988). The diffusive transport parameters are derived by fitting the model to observations.

SITES STUDIED

The location and characteristics of the ditch is described in chapter 1.5 (p. 20-22).

Most of the time the water can be assumed to be mixed well horizontally and vertically.

In this study bottom material from sand ditch A, receiving no additional P-input, has been used for uptake experiments. The results are used to simulate the uptake of P by the sediment in the ditch D, receiving the highest load, $12 \text{ g P} \cdot \text{m}^{-2} \cdot \text{yr}^{-1}$, supplied in monthly dosages as K_2HPO_4 dissolved in tap water and spread evenly in the overlying water. Each dosage corresponds to an instantaneous increase in the dissolved phosphorus concentration of 2.63 mg P/l .

MODEL CONCEPT

Following increased dissolved phosphorus concentrations in the

water, phosphorus will diffuse into the sediment as a result of the imposed vertical concentration gradient. In a situation with no vertical advective flow the resulting concentration change $\partial C_w / \partial t$ in the overlying water is:

$$\frac{\partial C_w}{\partial t} = D_{eff, z=0} \epsilon_{z=0} \left. \frac{\partial C}{\partial z} \right|_{z=0} \frac{A}{V} \quad (1)$$

For explanation of symbols see table 7.1.

The change of the concentration in the pore water C_z (Berner, 1980) is:

$$\frac{\partial C_z}{\partial t} = \frac{\partial (D_{eff, z} \epsilon_z \frac{\partial C_z}{\partial z})}{\epsilon_z \partial z} - R_z \quad (2)$$

The effective diffusion coefficient $D_{eff, z}$ is the sum of all diffusion processes involved in the vertical transport of solutes in sediments (Booij, 1989). It can be approximated by:

$$D_{eff, z} = \frac{(D_{mol} + D_{dis, z} + D_{bio})}{\theta^2} \quad (3)$$

Bioirrigation depends on the number and species of benthic fauna. Solid mixing is neglected, based on the observation that detritus on top of the sediment does not mix with the sand to an appreciable extent.

The tortuosity $1/\theta^2$ accounts for the slow-down of vertical transport caused by an extended pathway due to the travel around particles (Berner, 1980). It is related to the porosity by a formation factor that accounts for the ratio of the electrical resistivity of the sediment to that of the pore fluid (McDuff & Ellis, 1979), but the theoretical value for θ^{-2} of 0.7 is generally acceptable (Brinkman et al., 1987). The molecular diffusion coefficient is ion-specific and depends on temperature. For $H_2PO_4^-$ it is $7.34 \cdot 10^{-5} \text{ m}^2 \cdot \text{day}^{-1}$ at 20°C (Brinkman & Raaphorst, 1986).

Table 7.1. Summary of symbols.

Symbol	Explanation	Dimension
A	Area of sediment	L^2
C	Concentration in overlying water	$M.L^{-3}$
C_z	Conc. in porewater at depth z	$M.L^{-3}$
C_s	Conc. in solid	$M.L^{-3}$
C_{eq}	Equilibrium conc. (fast step) in porewater	$M.L^{-3}$
D	Water depth	L
$D_{eff,z}$	Effective diffusion coeff.	$L^2.T^{-1}$
D_{mol}	Molecular diffusion coeff.	$L^2.T^{-1}$
D_s	Solid-phase diffusion coeff.	$L^2.T^{-1}$
$D_{dis,z}$	Dispersion coefficient	$L^2.T^{-1}$
D_{bio}	Bioirrigation coefficient	$L^2.T^{-1}$
H	Wave height	L
K	Langmuir adsorption constant	$L^3.M^{-1}$
O	Specific surface area	$L^2.M^{-1}$ solid
R	Sources and sinks	$M.L^{-3}.T^{-1}$
S	Sum of squares of deviations	-
T	Wave period	T
V	Volume of overlying water	L^3
VM	Concentration of solids	$M.L^{-3}$
X_z	Amount of P adsorbed (fast step) at depth z	$M.M^{-1}$
X_m	Max. adsorption capacity (fast)	$M.M^{-1}$
h	Wave number	L^{-1}
k	Attenuation of D_{dir} over depth	L^{-1}
k_p	Permeability coefficient	$L.T^{-1}$
k_s	Rate of adsorption	$L^3.M^{-1}.T^{-1}$
$k_{s,act}$	Actual adsorption rate	T^{-1}
l	thickness of outer layer involved in surficial adsorption	L
r	Depth in Me-oxide coating	L
z	Depth in sediment	L
α_z	Mechanical dispersion	$L^2.T^{-1}$
ϵ	Porosity	$L^3.L^{-3}$
λ	Wave length	L
θ	Tortuosity	-

The effective vertical diffusion coefficient in the sediment can be enhanced by horizontal pressure gradients, caused by wind induced wave action or seiches. Rutgers van der Loeff (1981) gives an overview of the percolation of shallow sand beds caused by wave action and the resulting vertical dispersion in the sediments. In our column experiments pressure gradients were caused by aeration of the overlying water and

in the field-experiments in the ditches by wind. The resulting dispersion, $D_{dis,z}$, is assumed to decrease exponentially with depth, in accordance with the analysis by Rutgers van der Loeff, 1981):

$$D_{dis,z} = D_{dis,z=0} \exp(-kz) \quad (4)$$

in which the attenuation coefficient k depends on sediment characteristics like porosity and particle size distribution. The equilibrium of short-term sorption onto sediment particles is calculated using the Langmuir adsorption isotherm:

$$X_z = X_m \frac{KC_{eq,z}}{(1 + KC_{eq,z})} \quad (5)$$

X_m and K have to be determined experimentally for each type of sediment. X_z and $C_{eq,z}$ are time and depth dependent. A mass balance for the change in the amount of sorbed P has to be implemented in the model.

Short-term sorption equilibrium is not reached instantaneously, so in a short-term experiment adsorption processes are not at steady state. The sorption rate depends on the difference between actual porewater concentration C_z and the $C_{eq,z}$ calculated from (5). Thus, considering only adsorption, R_z can be described as (Brinkman et al., 1987):

$$R_z = k_{s,act}(C_z - C_{eq,z}) \quad (6)$$

The actual rate constant $k_{s,act}$ depends on the surface available for adsorption per volume pore water and, therefore, is a rate constant k_s , corrected for the concentration of adsorbents in the solid phase and the porosity:

$$k_{s,act} = k_s \frac{VM}{\epsilon} \quad (7)$$

An explicit numerical calculation of the time-porewater-concentration course is used. Discretization with respect to depth yields:

$$\frac{dC_i}{dt} = D_{eff}(i-1) \frac{(\epsilon_i + \epsilon_{i-1})}{2} \frac{(C_{i-1} - C_i)}{\epsilon_i (\Delta Z)^2} - D_{eff}(i) \frac{(\epsilon_i + \epsilon_{i+1})}{2} \frac{(C_i - C_{i+1})}{\epsilon_i (\Delta Z)^2} - R_i \quad (8)$$

Index *i* refers to a horizontal layer and increases with depth. The layers are chosen equidistant.

True equilibrium of sorption usually is not reached within a few days, and after a fast initial adsorption a slow step often follows (e.g. Barrow & Shaw, 1975). The slow step is assumed to result from diffusion of adsorbed P into the interior solid phase consisting of Fe- and Al-(hydr)oxides, and this assumption has been shown to explain experimental observations satisfactorily (Van Riemsdijk et al., 1984; Van der Zee, 1988).

Solid diffusion of adsorbed P can occur when the thickness of a metal-oxide particle or coating around the soil particles exceeds a threshold value at which not all the adsorbent is immediately accessible to adsorbing phosphate ions. Surficial adsorption induces a gradient towards the interior of the particles (Barrow, 1983). Although the exact chemical or physical mechanism by which ion-groups diffuse through a solid is not considered (solid phase or micropore diffusion), it is usually described as being analogous to diffusion in a liquid medium, hence :

$$\frac{\partial C_s}{\partial t} = D_s \frac{\partial^2 C_s}{\partial r^2} \quad (9)$$

Since the thickness of the coating is very small compared to the radius of the sand particles spherical geometry has not been employed. To be able to calculate the concentration

gradient in the coating, conversion of surficially adsorbed P, X_z , measured as g P.g⁻¹ dry matter, to an internal concentration $C_{s,z}$ (g P.m⁻³) in the outer layer of the coating involved in surficial adsorption, is needed. The conversion is executed by dividing X_z by the volume of the outer layer per unit of dry matter:

$$C_{s,z} = \frac{X_z}{O \cdot l} \quad (10)$$

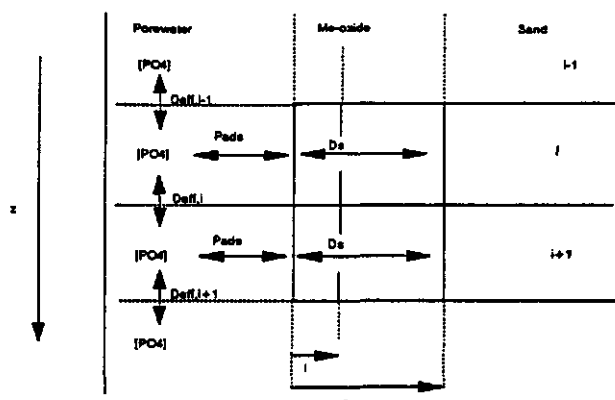
The time-concentration course is calculated numerically after dividing the inner part of the coating, not involved in surficial adsorption, in equidistant sublayers with thickness Δr :

$$\frac{dC_{s,j}}{dt} = D_s \frac{(C_{s,j-1} - C_{s,j})}{(\Delta r)^2} - D_s \frac{(C_{s,j} - C_{s,j+1})}{(\Delta r)^2} \quad (11)$$

Index j refers to the number of the layer in the coating. Combining (6), (9) and (10) yields a mass balance for the internal concentration in the outer layer of the coating involved in surficial adsorption ($j=1$):

$$\frac{dC_{s,j=1}}{dt} = -\frac{D_s}{l} \frac{(C_{s,j=1} - C_{s,j=2})}{1/2\Delta r} + \frac{k_{s,act}(C_z - C_{eq,z})}{O \cdot l} \frac{\epsilon}{VM} \quad (12)$$

in which the term ϵ/VM is again introduced to convert a pore-water concentration change to a change per amount of dry matter. $\frac{1}{2}\Delta r$ is the distance between the boundary between the layers $j=1$ and $j=2$ and the middle of the layer $j=2$. Figure 7.1 presents the processes implemented in the model for a horizontal layer in the sediment.



D_{eff} = Effective diffusion in porewater
 P_{ads} = Surficial adsorption
 D_e = Diffusion in Me-oxide coating

i Refers to number of horizontal layer
 z Depth in sediment
 r Total thickness of Me-oxide coating
 l Thickness of layer involved in surficial adsorption

the volume of the porewater (porosity) decreases with depth. The thickness of the coating is constant.

Figure 7.1. Schematization of the processes implemented in the model.

MATERIALS AND METHODS

Chemical analyses

Dissolved phosphorus was determined with the modified molybdate-blue method according to Murphey & Riley (1962) on a Skalar SA-40 Autoanalyser or on a Vitatron Photometer.

Total dissolved iron was measured after reduction with hydroxylammoniumchloride to Fe^{2+} with tripyridiltriazine as colour reagent on a Skalar SA-40 Autoanalyser.

Aluminum was determined on a Spectro Analytical Instruments

ICP type Spectroflame with inductively coupled plasma atomic emission spectrometry (ICP-AES) (Novozamsky et al., 1986).

Short-term adsorption characteristics

The maximal short-term adsorption capacity X_m and the adsorption constant K of the Langmuir equation (5) were determined by adding different amounts of dissolved phosphate to suspensions of the ditch sediment in filtered (0.45 μm) ditch water. After 48 hrs shaking at 20°C and pH 7 it was assumed that the fast equilibrium had been reached. The amount of adsorbed P (X) and dissolved P (C_{eq}) were determined. The native adsorbed P was estimated from extrapolation to $C_{\text{eq}} = 0$ and added to the measured additional sorption.

K and X_m were estimated by least-squares fitting of eq. (5) to the data. 90% confidence intervals for K and X_m were calculated from (Draper & Smith, 1966):

$$S + S_{\min} \left[1 + \frac{p}{(n-p)} F(p, n-p, 90\%) \right] \quad (13)$$

with S the sum of the squares at the 90% confidence contour, S_{\min} the minimum sum of the squares, n the number of samples, p the number of parameters and $F(p, n-p, 90\%)$ the F-distribution according to Fisher.

Short-term uptake experiments

To study the uptake of phosphorus by sand and to gain qualitative insight into the effect of mixing of the overlying water, intact sediment cores were collected in a polythene cylinder with a diameter of 5.3 cm and immediately transported to the laboratory. The overlying water and a watery benthic layer consisting of algae and detritus with a thickness of 1.5-2 cm were removed carefully without resuspending the sand and replaced by filtered (0.45 μm) phosphate-enriched (added as

K_2HPO_4) ditch water. The pH was adjusted to 7 with HCl and/or NaOH. The columns were incubated for two or three days. In one experiment the overlying water was not mixed, in another experiment it was mixed by moderate aeration.

The initial PO_4 -P concentrations in the overlying water of the non-mixed column and the aerated column were 1.71 mg.l^{-1} and 2.33 mg.l^{-1} respectively, somewhat lower than the highest loading in the field experiment in the ditches. The initial heights of the overlying water columns were 9.9 cm and 12.0 cm respectively.

The change in PO_4 -P concentration in the water was measured in 5 ml samples collected at regular time intervals.

The vertical profile of porosity and solid concentration in the sediment of the ditch was known from an inventory made after the construction of the ditches, in which intact sediment cores were used. The reference ditch (A), from which the cores were collected, has a very low primary production and virtually no macrophytes, so almost no changes had occurred.

Experiments on long-term sorption by sand particles

To study the long-term sorption of phosphorus by the sand, 5 g dried (40°C) sediment was incubated in 250 ml at 18°C . Phosphate was added as K_2HPO_4 up to 1, 2 and 5 mg P.l^{-1} respectively. Samples of 5 ml were collected over a period of 150 days, with a higher frequency during the first weeks after the start of the experiment than later, and analysed for dissolved phosphorus.

Determination of total sorption capacity

As total equilibration of the coated sand grains with the solution takes a long time due to the very slow second phase uptake, it is difficult to estimate the equilibrium solid phase concentration $C_{s,eq}$ corresponding to the ambient P concentration and pH. Hence, a direct estimation of the total

sorption capacity of the sand without the inconvenience of being dependent on the time scale of the solid-phase diffusion process has been applied. The method is based on the principle that dissolution of the Al- and Fe-(hydr)oxides in acid medium and subsequent homogeneous precipitation in the presence of phosphate at the original pH enables immediate occupation of all sorption sites present.

The metal-oxide coating was dissolved by shaking 1 g dried sediment during 48 hrs in 0.1 M HCl. After centrifugation (10 mins at 3500 rpm) Al was measured in the supernatant. Three series were prepared: in one the supernatant and the sand were not separated; from the second the supernatant was removed and replaced by demineralized water; the third consisted of the removed supernatant of series 2 only. After phosphate addition to all series (up to 0, 1, 2 and 5 mg P.l⁻¹ resp.) the pH was adjusted to 6.8 (the original value), so that formation of the Al-OH-phosphate complexes could occur. After two and three days Al and dissolved phosphorus were determined in the supernatant after centrifugation.

Simulation of vertical concentration profiles in the porewater

Since the start of the programme of monthly nutrient dosages in May 1989, the dissolved phosphorus concentration has been measured in the water regularly, usually at 1,3,6,10 and 20 days after each monthly dosage and on the day before the next dosage. The concentrations on intermediate days were obtained by linear interpolation. These concentrations have been used as a boundary condition: $c_{z=0} = c_w$. This might slightly over- or underestimate $c_{z=0}$ due to the presence of a benthic algae layer or a diffusive sublayer on top of the sand, but the very loose structure of this layer (porosity > 99%) and the relatively small rate at which P can be released from or taken up by the layer with respect to the high phosphate concentration and the turbulence in the overlying water most of the time makes this deviation negligible.

The amount of phosphorus adsorbed to the original sediment matter has been measured and used as an initial condition in the simulation of [P] in the porewater. Since aluminum, which is insensitive to changing redox conditions, is the main P-sorbing element in the ditches (see next section), redox conditions have not been incorporated into the model.

RESULTS

Adsorption characteristics

The short-term Langmuir adsorption isotherm is given in figure 7.2. The values for X_m and K , obtained from least-squares fitting are:

$$\begin{aligned} X_m &= 101 \text{ } \mu\text{g}\cdot\text{g}^{-1} \text{ dry matter} \\ K &= 0.57 \text{ m}^3\cdot\text{g}^{-1} \end{aligned}$$

The native adsorbed P was estimated at $3 \text{ } \mu\text{g}\cdot\text{g}^{-1}$ of dry matter. The boundaries of the 90% confidence intervals for both parameters are:

$$\begin{aligned} X_m &: 83 - 124 \text{ } \mu\text{g}\cdot\text{g}^{-1} \text{ dry matter} \\ K &: 0.32 - 1.03 \text{ m}^3\cdot\text{g}^{-1} \end{aligned}$$

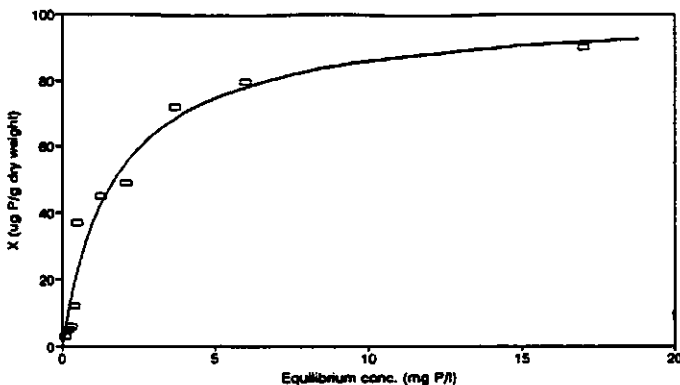


Figure 7.2. Langmuir isotherm of surficial adsorption.

Short-term column uptake experiments

Figures 7.3 and 7.4 present observed and simulated dissolved P in the overlying water for the short-term column uptake experiments. Simulations include the role of dispersion induced by aeration. In case of no mixing of the overlying water, a good agreement is obtained if, next to molecular diffusion, $D_{dis,z=0}$ is set equal to the low value of $4.7 \cdot 10^{-5} \text{ m}^2 \cdot \text{day}^{-1}$, which is about 65% of D_{mol} . The boundaries of the 90% confidence interval for $D_{dis,z=0}$ are $2.6 \cdot 10^{-5} - 7.0 \cdot 10^{-5} \text{ m}^2 \cdot \text{day}^{-1}$. At the aeration rate used in the second experiment a dispersion coefficient at the water-sediment interface $D_{dis,z=0}$ of $4.6 \cdot 10^{-4} \text{ m}^2 \cdot \text{day}^{-1}$ yields good results. The attenuation constant k in (4) has been set at 75 m^{-1} . The simulation results are relatively insensitive to k . $D_{dis,z=0}$ and k are positively correlated. The boundaries of the 90% confidence interval for $D_{dis,z=0}$ are $3.7 \cdot 10^{-4} - 5.9 \cdot 10^{-4} \text{ m}^2 \cdot \text{day}^{-1}$.

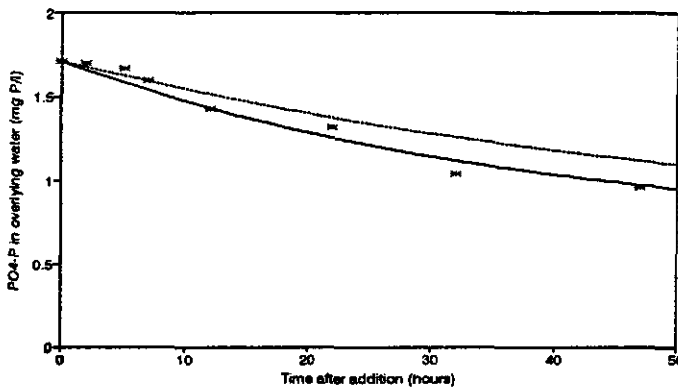


Figure 7.3. Dissolved phosphorus concentrations in overlying water of sediment column without mixing.
 ---- = simulated, $D_{dis,z=0} = 0$
 ——— = simulated, $D_{dis,z=0} = 4.7 \cdot 10^{-5} \text{ m}^2 \cdot \text{day}^{-1}$
 * = measured

The presence of a diffusive boundary layer may have reduced the phosphate fluxes in the non-aerated column. This would

lead to an underestimation of $D_{dis, z=0}$ in the non-aerated column. Erosion of the diffusive boundary layer by turbulence in the overlying water cannot explain the measured increase in uptake rate in the aerated column compared to the non-aerated, since in the simulation of the non-aerated column already a complete absence of this diffusive boundary layer was assumed.

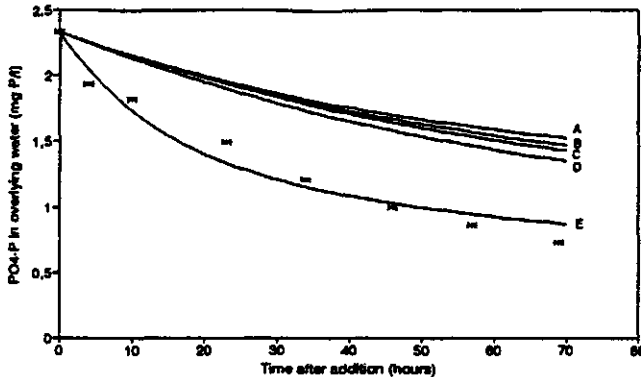


Figure 7.4. Dissolved phosphorus concentrations in overlying water with mixing by aeration.
(for values of parameters in A-E see table 7.2)

In table 7.2 the results of a sensitivity analysis are given, by comparing the simulated concentrations in the overlying water of the aerated column at $t = 69$ hr with the measured concentrations for different values of the parameters. The time-concentration courses for these different values are also presented in figure 7.4. It can be concluded that the uptake rate in the aerated column can only be explained with an enhanced effective diffusion coefficient caused by the aeration.

Long-term sorption experiments

Figure 7.5 illustrates the results of the long-term sorption experiments (averages of duplicates). They show, after a fast initial adsorption, a gradually decreasing sorption rate that

can be described adequately by the solid-phase diffusion model

Table 7.2. Sensitivity analysis for simulation of aerated column experiment. C_{sim} is simulated concentration at $t=69$ hr. Measured concentration at $t=69$ hr was 0.74 mg P/l.

PARAMETER:	$D_{dis,z=0}$	K	X_m	k_s	C_{sim}
	$10^{-4}m^2.day^{-1}$	$m^3.g^{-1}$	$\mu g.g^{-1}$	$m^3.g^{-1}.hr^{-1} * 10^6$	mgP.l ⁻¹
A (original)	0	0.57	101	2.59	1.53
B	0	0.57	126	2.59	1.48
C	0	1.03	101	2.59	1.43
D	0	1.03	126	5.18	1.36
E (optimal)	4.5	0.57	101	2.59	0.88

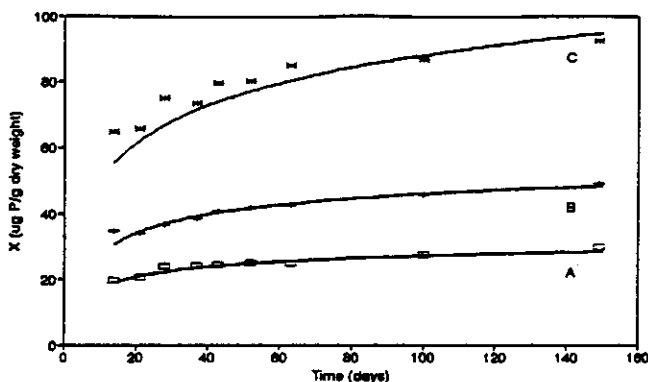


Figure 7.5. Long-term sorption experiments, as measured in suspensions and simulated.

(at $t=0$: A: 1 mg P/l; B: 2 mg P/l; C: 5 mg P/l. $D_s = 2.7 \cdot 10^{-19} m^2.day^{-1}$ and the total sorption capacity is $3.3 * X_m$)

(solid lines). The decreasing concentrations in the water have been taken into account.

D_s was obtained by curve-fitting, and in all three cases a value of $2.7 \cdot 10^{-19} m^2.day^{-1}$ gives reasonably good results. The

90% confidence intervals for D_g , calculated with (13) are:

series A :	$2.7 \cdot 10^{-19}$ - $3.8 \cdot 10^{-19}$	$m^2 \cdot day^{-1}$
series B :	$2.5 \cdot 10^{-19}$ - $2.8 \cdot 10^{-19}$	„
series C :	$2.0 \cdot 10^{-19}$ - $3.0 \cdot 10^{-19}$	„

The value of D_g , however, depends on the ratio between the thickness of the layer involved in the surficial adsorption and the total thickness of the metal-oxide coating. The estimation of this ratio will be explained in the next section.

In the simulations the surficially adsorbed phosphorus was used as an initial condition. This was calculated from the Langmuir adsorption isotherm and the measured concentrations after 7 days, assuming that at this time the fast surficial adsorption step had reached equilibrium.

This is, however, an arbitrary choice, since no clear distinction in time can be made between the fast initial step and the slow step.

Total sorption capacity

The amount of iron extracted from the sand in 0.1 M HCl was 71 $\mu g \cdot g^{-1}$ dry matter ($n=4$, $\sigma=6 \mu g \cdot g^{-1}$ dry matter) and comparable to the oxalate-extractable amount ($75 \pm 24 \mu g \cdot g^{-1}$ dry matter, $n=9$). The 0.1 M HCl extractable Al was 323 $\mu g \cdot g^{-1}$ dry matter ($n=15$, $\sigma=18 \mu g \cdot g^{-1}$ dry matter).

Lijklema (1980) found in homogeneous precipitation after addition of an aluminum solution to a phosphate solution a maximal molar ratio P/Al of 1.0 (pH 7). When assuming that the homogeneous sorption capacity of Al is twice that of Fe (Lijklema, 1991), it can be concluded that Al is the main P-sorbing element in the sediment considered (for about 95% of the total sorption capacity by Fe and Al). A maximal P/Al ratio of 1.0 and a maximal P/Fe ratio of 0.5 yields a total binding capacity of 391 $\mu g P \cdot g^{-1}$ dry matter (371 $\mu g \cdot g^{-1}$ dry matter Al-P and 20 $\mu g \cdot g^{-1}$ dry matter Fe-P), which is 3.87 times the estimated

maximal surficial sorption capacity X_m .

In figure 7.6 the amounts of P sorbed by the acid extracted and thereafter homogeneously precipitated Al-OH-phosphates are plotted versus the equilibrium concentrations and compared with the surficial Langmuir-adsorption isotherm. The plain sand without the metal-oxide coating (series 2) did not adsorb any phosphate and therefore is not displayed. The separated supernatant shows a larger P-sorption than the suspension that still contains sand grains. This may be caused by occupation of a part of the available sorption sites by the silicate surface. In the pure supernatant without phosphate addition the precipitation of the Al-hydroxides seems to be hampered. After three days only 60% of the dissolved Al was precipitated again. In samples with phosphate addition and/or in the presence of sand grains all Al was precipitated again.

The total sorption capacity of the supernatant+solid is about 3.3 times the surficial adsorption, and is slightly smaller than the potential sorption capacity calculated from the extractable Al + Fe content. The number of prints is insufficient to construct a 'total sorption isotherm', which displays the amount of sorbed P versus the equilibrium concentration of the slow step.

Simulation of vertical concentration profiles in the porewater

Figure 7.7 displays the concentrations of dissolved phosphorus in the water of the sand ditch with the highest P-loading. The monthly fluctuations result from the dosages. In the winter of 1990-1991 (days 550-650) no dosages could be given due to an ice cover. In figure 7.8 the simulated vertical profile of dissolved phosphorus in the interstitial water 660 days after the start of the dosages in May 1989, is fitted to the measured profile. $D_{dis,z=0}$ has been assigned values of 0, $1.5 \cdot 10^{-3}$ and $1.8 \cdot 10^{-3} \text{ m}^2 \cdot \text{day}^{-1}$. An average value of $D_{dis,z=0}$ of $1.8 \cdot 10^{-3} \text{ m}^2 \cdot \text{day}^{-1}$ gives a good agreement. This is about 3.9 times the value found for the aerated column experiment and indicates

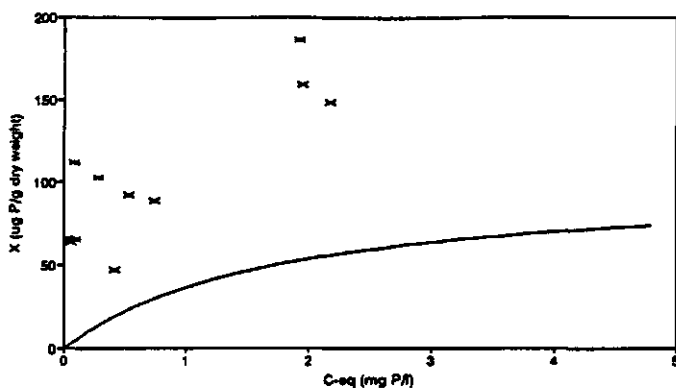


Figure 7.6. Sorption of series 1 and 3 after three days in precipitation experiments compared to surficial adsorption isotherm.

(— = surficial adsorption, X = series 1, * = series 3)

that on the average pressure gradients in the ditch are larger than in the column experiment. The simulated porewater profile at $D_{dis,z=0} = 0$ shows bad agreement. The attenuation constant k in equation (4) has been assigned a value of 50 m^{-1} . The sensitivity to k is quite low.

The estimated dispersion coefficient $D_{dis,z=0}$ can be compared to theoretical values calculated as a function of water depth, wave length and amplitude and grain size. Two theories are used, the first (Rutgers van der Loeff, 1981), gives:

$$D_{dis,z=0} = \frac{\pi k_p^2 T H^2}{2 \lambda^2 \cosh^2(hD)} \quad (14)$$

with k the permeability coefficient (L.T^{-1}), T the wave period, λ the wave length, H the wave height ($= 2 \cdot \text{amplitude}$), h the wave number ($= 2\pi/\lambda$) and D the water depth. k_p can be related to the grain size according to (Harrison, 1983):

$$k_p = cd^2 \quad (15)$$

with d the grain size and c a constant. c has a value of $1.84 \cdot 10^4 \text{ (m.s)}^{-1}$ for a porosity of 0.4 and at 20°C .

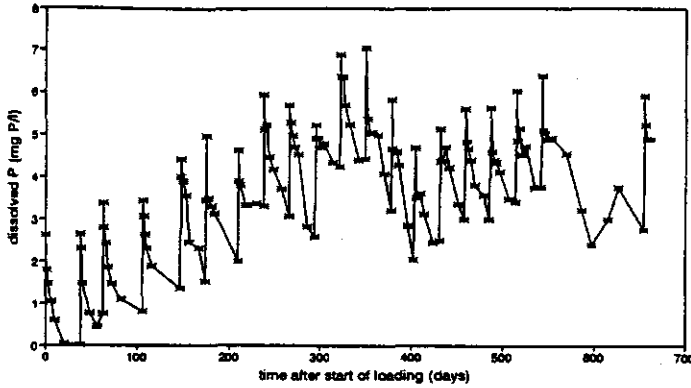


Figure 7.7. Dissolved phosphorus concentrations in the ditch.

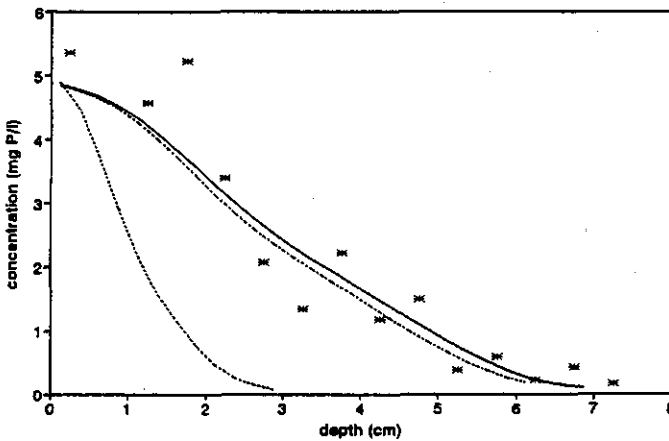


Figure 7.8. Measured and simulated vertical concentration profile of phosphorus in the porewater after 660 days.

(* = measured, --- = simulated, $D_{dis,z=0} = 0$,
 - - - = simulated, $D_{dis,z=0} = 1.5 \cdot 10^{-3} \text{ m}^2 \cdot \text{day}^{-1}$,
 ————— = simulated, $D_{dis,z=0} = 1.8 \cdot 10^{-3} \text{ m}^2 \cdot \text{day}^{-1}$)

In figure 7.9 $\ln D_{dis,z=0}$ is plotted versus wave length for two values of H and d . The thick solid line represents molecular diffusion and the thin solid line the $D_{dis,z=0}$ estimated from

fitting to the measured phosphate porewater concentration profile (see figure 7.8). It is clear that $D_{dis,z=0}$ strongly depends on wave length as well as grain size and wave amplitude.

In the second theory, Harrison (1983) used the term "mechanical dispersion" for wave-induced dispersion in the sediment. This dispersion becomes significant when the Peclet number $Pe (=v.d/D_{mol}) \gg 1$, with v the resulting velocity in the sediment. The mechanical dispersion $\alpha_{z=0} (= v.d = Pe.D_{mol})$, can be calculated from:

$$\alpha_{z=0} = \frac{0.5cd^3hH}{\cosh(hD)} \quad (16)$$

The vertical component usually is about 10% of the total, and is assumed to represent $D_{dis,z=0}$. Figure 7.10 presents $\ln \alpha_{z=0}$ plotted versus wave length. It again strongly depends on wave-length, grain size and wave amplitude, but exhibits higher values than calculated according to Rutgers van der Loeff (figure 7.9).

The wave length and wave amplitude required for a value of $D_{dis,z=0}$ of $1.8 \cdot 10^{-3} \text{ m}^2 \cdot \text{day}^{-1}$ are in the range of 0.6-1.0 m and 0.025 - 0.05 m respectively. Visual observations showed that these values are on the average lower. $D_{dis,z=0}$ estimated from fitting the simulated vertical phosphate profile in the porewater to measured data is higher than theoretical values derived from Rutgers van der Loeff (1981) and Harrison (1983). Due to strong non-linearity of the behaviour of the dispersion coefficient the variation in time will be considerable, but when considering longer periods the use of an average value seems, at least for the moment, justified.

Furthermore, the simulation indicated that after 660 days about 60% of the sorbed phosphorus in the sediment of the ditch had diffused into the interior of the aluminum-hydroxide layer.

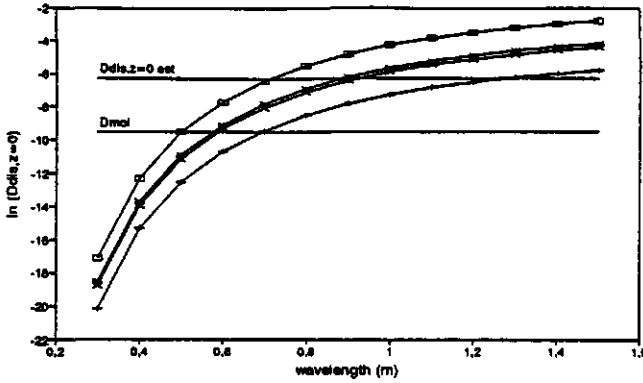


Figure 7.9. $\ln (D_{dis, z=0})$, as calculated according to Rutgers van der Loeff (1981), plotted versus wave length and compared to D_{mol} and $D_{dis, z=0}$ estimated ($1.8 \cdot 10^{-3} \text{ m}^2 \cdot \text{day}^{-1}$). (\diamond : $H=10 \text{ cm}$, $d=1.5 \text{ mm}$, $*$: $H=5 \text{ cm}$, $d=1.5 \text{ mm}$, X : $H=10 \text{ cm}$, $d=1 \text{ mm}$, $+$: $H=5 \text{ cm}$, $d=1 \text{ mm}$).

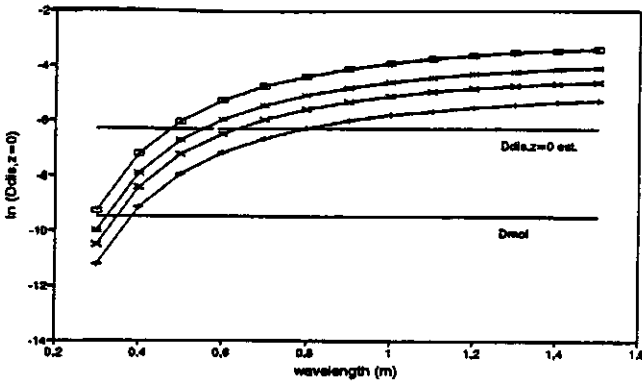


Figure 7.10. $\ln (D_{dis, z=0})$, as calculated from Harrison (1983), plotted versus wave length and compared to D_{mol} and $D_{dis, z=0}$ estimated ($1.8 \cdot 10^{-3} \text{ m}^2 \cdot \text{day}^{-1}$). (\diamond : $H=10 \text{ cm}$, $d=1.5 \text{ mm}$, $*$: $H=5 \text{ cm}$, $d=1.5 \text{ mm}$, X : $H=10 \text{ cm}$, $d=1 \text{ mm}$, $+$: $H=5 \text{ cm}$, $d=1 \text{ mm}$).

CONCLUSIONS AND DISCUSSION

- Mixing of the overlying water has been demonstrated to enhance the flux of phosphate across the sediment-water interface. In column uptake experiments without mixing the overlying water, the simulation matched the data, when the dispersion coefficient at the sediment-water interface was about 65% of the molecular diffusion coefficient. Part of this 65 % may result from underestimation of the tortuosity factor θ^{-2} in the top few millimeters of the sediment, which have the highest porosity (≈ 0.7) and play an important role in short-term column uptake experiments. From Ullman and Aller (1982) it can be calculated that θ^{-2} can be at maximum 0.89 in sandy sediments with a porosity of 0.7. In the simulations a constant value for θ^{-2} of 0.7 has been used. Mixing by aeration strongly increased the initial fluxes. A sensitivity analysis for all parameters in the model showed that this could only be attributed to an enhanced effective diffusion coefficient. A dispersion coefficient that was one order of magnitude larger than the molecular diffusion coefficient gave the best fit.

The attenuation of dispersion in the sediment is described as an exponential decrease, with a relatively low sensibility of the model for the attenuation constant k . A k -value of 75 m^{-1} generates an intensity of pressure gradient induced mixing equal to molecular diffusion at a sediment depth of 6 cm. Hesslein (1980) found enhanced mixing rates of porewater up to a sediment depth of 10 cm at overlying water depths of 0.75 and 3.85 m without mixing of the solid phase of the sediments. In stagnant shallow waters the effect of wind action is an enhanced effective diffusion coefficient in the sediment. After enhanced external loading its effect is an increased penetration rate of phosphorus into the sediment and, thereby, an increased retention in the sediment.

- In the simulation of the phosphate fluxes across the sediment-water interface over a period of 660 days, an average

dispersion coefficient, corrected for tortuosity, of $1.8 \cdot 10^{-3} \text{ m}^2 \cdot \text{day}^{-1}$ has been used and is satisfactory. This is about 35 times the molecular diffusion coefficient, corrected for tortuosity. Comparison with theoretical values calculated from wave characteristics indicated that the enhanced effective diffusion coefficient in the sediment could, for a substantial part, be attributed to wind induced pressure gradients. In shallow systems like the ditches, pressure gradients induced by congestion also might contribute to this enhancement.

When considering shorter time scales variations in wind velocity cannot be neglected. Wind velocity affects wave heights, which affect the pressure gradients in the sediment, and, as a result of that, affect D_{dis} . The attenuation constant of dispersion in the sediment, k , has been assumed to be constant over depth. It might increase slightly with depth because of decreasing porosity.

- A subsequent slow uptake process causes immobilization of a considerable part of the externally supplied phosphorus. This slow process can well be described as a diffusion process in which adsorbed P penetrates into a coating of Al-hydroxides.

In the situation considered, with aluminum as the main P-sorbing compound, the sensitivity for changing redox conditions is low, in contrast to sediments where iron is the dominating adsorbate. This allows a permanent storage of phosphate, gradually penetrating into deeper layers.

Considering the time scale of the solid phase diffusion process and the reversibility of the process suggested by the model, the release of phosphorus from the sediment after a reduction of the external loading with nutrients will be very long-lasting (see also Barrow, 1983). However, no direct evidence for the reversibility of the slow process has yet been obtained, and it may display other kinetics, although the model used assumes complete reversibility.

- Dissolution of the Al-hydroxide coating and subsequent

precipitation in the presence of phosphate yielded a total sorption capacity that is about 3.3 times the maximal surficial adsorption. It may be that the polymeric structures of the precipitated Al-hydroxo-phosphates are still partly a function of the initial conditions in the experiment, but comparison with data from Lijklema (1980) showed a reasonable correspondence. The observation that precipitation of the dissolved Al-hydroxide coating in the presence of the sand particles sorbed less P than in the absence of the sand grains, suggests that the precipitation in the first case was not completely homogeneous. Bolan et al. (1985) found similar results after precipitation of Al- and Fe-hydroxides in the presence and absence of kaolinite.

Mineralization in the sediment has been neglected in the simulation of the vertical dissolved phosphorus profile in the interstitial water. This is based on the visual observation that a layer of benthic algae and dead organic matter on top of the sand in the highest loaded ditch (D) does not mix into the sand to any appreciable extent. It may have caused variations in the dissolved phosphorus concentrations within this organic layer on top of the sediment, thereby affecting the flux. The living fraction in the benthic layer is continuously exposed to a relatively high dissolved P concentration and hence luxury uptake and other variations in P-content due to loading are small. The total P-content in the benthic material per m^2 is at its maximum towards the end of the simulated period, more or less equal to a monthly loading ($1 \text{ g P} \cdot m^{-2}$). Besides this, the effects of luxury uptake have a short time-constant as compared to the dosing interval. Conversely, mineralization in the benthic layer continuously may produce dissolved P and thus maintain a gradient at the interface, so that PO_4 -concentrations at $z=0$ are underestimated, which results in overestimation of $D_{dis,z=0}$. However, again the relative change induced by this process is small compared to the ambient concentration and the mixing rate will attenuate

such concentration gradients. Finally, uptake and mineralization have opposite effects. The total error caused by assuming the overlying water concentrations as representative for the concentration at $z=0$ will be small.

ACKNOWLEDGEMENTS

Martin Seidl of The Winand Staring Centre for Integrated Land, Soil and Water Research, Wageningen, the Netherlands, kindly supplied data on the vertical concentration profile of dissolved phosphorus in the interstitial water. Rein van Eck, Department of Soil Science and Plant Nutrition, Agricultural University, Wageningen, measured the Aluminum concentrations. The critical comments and suggestions of Wim van Raaphorst, Netherlands Institute for Sea Research, Bernie Boudreau and an anonymous reviewer are gratefully acknowledged.

REFERENCES

- Ahlgren, I., 1977. Role of sediments in the process of recovery of a eutrophicated lake. In: Golterman, H.L. (ed.): Interactions between sediments and freshwater, Junk Publ., The Hague, pp. 372-377.
- Barrow, N.J. & T.C. Shaw, 1975. The slow reactions between soils and anions: 2. Effect of time and temperature on the decrease in phosphate concentration in the soil solution. *Soil Science* 119 : 167-177.
- Barrow, N.J., 1983. A mechanistic model for describing the sorption and desorption of phosphate by soil. *J. Soil Sci.* 34: 733-750.
- Berner, R.A., 1980. Early diagenesis, a theoretical approach. Princeton Univ. Press.
- Bolan, N.S., N.J. Barrow & A.M. Posner, 1985. Describing the effect of time on sorption of phosphate by iron and aluminum hydroxides. *J. Soil Sci.* 36: 187-197.

- Booij, K., 1989. Exchange of solutes between sediments and water. PhD Thesis, University of Groningen.
- Brinkman, A.G. & W. van Raaphorst, 1986. De fosfaathuishouding van het Veluwemeer. PhD Thesis, Technical University Twente.
- Brinkman, A.G., W. van Raaphorst, L. Lijklema & G. van Straten, 1987. Enkele experimentele technieken bij de bestu-
dering van fosfaatuitwisselingsprocessen tussen meersedi-
ment en oppervlaktewater. *H₂O* 20, 664-668.
- Draper N.R. & H. Smith, 1981. Applied regression analysis, 2nd
edition. John Wiley & Sons, New York, pp 458-474.
- Golterman, H.L., 1977. Sediments as a source of phosphate for
algal growth. In: Golterman, H.L. (ed.): Interactions
between sediments and freshwater, Junk Publ., The Hague,
pp.286-293.
- Harrison, W.D., D. Musgrave and W.S. Reeburgh, 1983. A wave-
induced transport process in marine sediments. *J. of
Geophys. Res.* 88 (C12): 7617-7622.
- Hesslein, R.H., 1980. In situ measurements of pore water
diffusion coefficients using tritiated water. *Can. J.
Fish. aquat. Sci.* 37: 545-551.
- Kamp-Nielsen, L., H. Mejer & S.E. Jørgensen, 1982. Modelling
the influence of bioturbation on the vertical distribu-
tion of sedimentary phosphorus in Lake Esrom. *Hydrobio-
logia* 91: 197-206.
- Lijklema, L., 1980. Interaction of orthophosphate with iron-
(III) and aluminum hydroxides. *Envir. Sci. Technol.* 14 :
537-540.
- Lijklema, L., 1986. Phosphorus loading in sediments and inter-
nal loading. *Hydrobiol. Bulletin* 20(1/2): 213-224.
- Lijklema, L., 1993. Considerations in modeling the sediment-
water exchange of phosphorus. *Hydrobiologia* 253, 219-231.
- McDuff, R.E. & R.A. Ellis, 1979. Determining diffusion coef-
ficients in marine sediments: a laboratory study of the
validity of resistivity techniques, *Am. Jour. Sci.* 279:
666-675.

- Murphy, J. & J.P. Riley, 1962. A modified single solution method for the determination of phosphate in natural waters. *Anal. Chim. Acta* 27: 31-36.
- Novozamsky, I., R. van Eck, V.J.G. Houba & J.J. van der Lee, 1986. Use of inductively coupled plasma atomic emission spectrometry for determination of iron, aluminium and phosphorus in Tamm's soil extracts. *Neth. J. of Agric. Sci.* 34: 185-191.
- Rutgers van der Loeff, M.M., 1981. Wave effects on sediment-water exchange in a submerged sand bed. *Neth. J. of Sea Res.* 15: 100-112.
- Ullman, W.J. and R.C. Aller, 1982. Diffusion coefficients in nearshore marine sediments. *Limnol. Oceanogr* 27(3): 552-556.
- Van der Zee, S.E.A.T.M., 1988. Transport of reactive contaminants in heterogeneous soil systems. PhD Thesis, Agricultural University Wageningen: pp. 35-64.
- Van Riemsdijk, W.H., L.J.M. Boumans & F.A.M. de Haan, 1984. Phosphate sorption by soils I; A diffusion-precipitation model for the reaction of phosphate with metal-oxides in soils. *Soil Sci. Soc. Am. J.* 48: 537-540.

Chapter 8

Kinetics of luxury uptake of phosphate by algae dominated benthic communities

key-words:

benthic algae - phosphate - luxury uptake - eutrophication -
intracellular P

Based on: Kinetics of luxury uptake of phosphate by algae-dominated benthic communities, by R. Portielje and L. Lijklema, 1994. *Hydrobiologia* 275/276, 349-358.

8. KINETICS OF LUXURY UPTAKE OF PHOSPHATE BY ALGAE DOMINATED BENTHIC COMMUNITIES

ABSTRACT

The uptake of phosphate by benthic communities, dominated by living algae, previously exposed to different levels of external nutrient loading, exhibited first-order kinetics with respect to the intracellular P-deficit. This deficit is the difference between the maximum and the actual intracellular P-concentration.

The maximum storage capacity of P per unit of dry weight was positively correlated to the level of external nutrient loading, whereas the phosphate uptake rate constant was negatively correlated.

The observed internal P concentrations in the benthic layer of test ditches over a period of two and a half years, indicated a slight decrease towards a minimum value in a ditch with a low external P input (ditch A). In a medium loaded ditch (B) the internal P-concentration did not change significantly. In a high loaded ditch (C) increasing internal P-concentrations over time were observed, towards P-saturation of the benthic community.

INTRODUCTION

The control of growth of photo-autotrophic organisms by rate-limiting environmental factors has since long been a central issue in water research. Numerous publications have appeared on photosynthesis-light relationships (see e.g. Kirk (1983) for a review) and on the effects of nutrient limitation (e.g. Droop, 1974; Kunikane and Kaneko, 1984).

In natural waters often periodic changes in the phosphorus concentration occur. The efficiency at which a species is capable of uptake and storage of phosphorus during periods of enhanced availability, for use during periods of limitation, determines its competitive ability.

After addition of dissolved phosphorus to a P-limited community of algae a considerable uptake can follow (Bierman, 1976; Riegman, 1985) far in excess of the immediate needs for growth and maintenance. An internal feedback mechanism, that restricts the uptake rate progressively when the intracellular P concentration increases is responsible for an asymptotic

approach towards internal P-saturation of the cells.

In contrast to the fairly large number of experiments performed with pure cultures of one single species (e.g. Okada et al., 1982; Kunikane et al., 1984; Riegman, 1985), information on phosphate uptake kinetics in natural communities is rather scarce. Extrapolation of parameter values obtained in the laboratory on single species to natural systems with a variety of species under fluctuating environmental conditions is often questionable.

Different species may perform different uptake kinetics and therefore contribute to a different extent to the phosphate uptake kinetics of the whole community. Furthermore, the composition of the natural community itself may change following the level of phosphate supply.

It has since long been recognised that growth rates are controlled by internal rather than extra-cellular nutrient concentrations (Droop, 1974; Nyholm, 1978). Depending on the biomass present in a system and its nutritional status, luxury uptake, which is nutrient uptake in excess of the amount immediately needed for growth, may cause the extracellular dissolved phosphorus concentration to return fast to a low level after a step-wise phosphorus addition. The effects of the nutrient dosage remain visible in an increased primary productivity over a much longer period (Portielje et al. 1994; chapter 5), caused by the availability of the internally stored phosphorus for growth.

This chapter presents the results of laboratory experiments on the kinetics of phosphorus-uptake by algae dominated natural benthic communities. Parameters derived from these experiments, combined with field data on the accumulation of biomass and internal phosphorus in artificial ditches subject to different rates of external nutrient loading, are subsequently used to estimate the phosphate uptake capacity of the benthic communities of these ditches after step-wise nutrient dosages. The aim of the study is to gain insight into the role of the benthic community in the nutrient household of the whole

system. The phosphate uptake capacity of the benthic community and the kinetics of phosphate uptake in relation to the level of external phosphorus input are studied. The immediate phosphorus uptake by the benthic community after a dosage acts as a buffer of the system to step-wise phosphorus loadings. Due to this buffering capacity the dissolved phosphate concentration decreases rapidly to low values. This may to a substantial extent determine the resistance of the ecosystem towards transition to a higher trophic state. After saturation of this buffer capacity the increasing phosphorus concentrations in the water phase will enable phytoplankton to become the dominant primary producers.

THEORY

After addition of phosphorus to a P-limited culture of algae, the algae can readily take up significant amounts of the added phosphorus. The uptake rate V (g P.[g dry matter.hour]⁻¹) is usually described using Michaelis-Menten kinetics:

$$V = V_{\max} \frac{[P]}{(K_p + [P])} \quad (1)$$

in which V_{\max} is the maximum uptake rate, $[P]$ the external dissolved phosphorus concentration and K_p the concentration at which the uptake rate is at half-maximum. V_{\max} depends on the P-deficiency of the cells, expressed as the difference between the maximum intracellular P-content $P_{\text{int,max}}$ and the actual intracellular P-content P_{int} , and a first-order rate constant k , also defined as an adaptation rate constant (Riegman, 1985). This thus defines the rate at which a P-deficiency can be eliminated as:

$$V_{\max} = k (P_{\text{int,max}} - P_{\text{int}})^n \quad (2)$$

n is the order of the process.

Both n and k are parameters that reflect the enzymatically controlled uptake system, which may comprise more than one step. Bierman (1976) used a two-step mechanism to describe the uptake of phosphate by cyanobacteria. The first step represented the transport across the cell membrane by means of an assumed membrane carrier. The driving force for this transport is the gradient from external dissolved phosphate to internal dissolved phosphate. The second step is the intracellular storage of excessive P as a solid compound, usually polyphosphates (Nyholm, 1978). The level of the internal dissolved phosphate concentration is determined by the internal stored phosphate.

$P_{int,max}$ may be subject to long-term adaptation and selection mechanisms of the community to environmental conditions. For convenience the difference between $P_{int,max}$ and P_{int} is expressed as a deficit D , and the decrease of the deficit during a period of enhanced uptake, is :

$$\frac{dD}{dt} = -V \quad (3)$$

At high external concentrations the Michaelis-Menten term approaches unity, so $V \approx V_{max}$. The solution of equation (3), after substitution of (1) and (2), with initial conditions $t=0: D=D_{t=0}$, is:

$$D_t = [D_{t=0}^{1-n} + (n-1).kt]^{-\frac{1}{1-n}} \quad (4)$$

In case of a first-order uptake proces, with $n=1$, the solution is simply:

$$D_t = D_{t=0}e^{-kt} \quad (5)$$

The values of the parameters k, n and $P_{int,max}$ can be estimated through least-squares optimization from the changes in the intracellular P-concentration as calculated from measured

extra-cellular P concentrations. For each parameter the 90 % confidence contours are calculated using (Draper and Smith, 1966) :

$$S = S_{\min} \left[1 + \frac{p}{n-p} F(p, n-p, 90\%) \right] \quad (6)$$

with S the sum of squares at the 90 % confidence contour and S_{\min} the minimum sum of squares. n is the number of samples and p the number of parameters to be estimated. $F(p, n-p, 90\%)$ is the F-distribution according to Fisher.

MATERIALS AND METHODS

Uptake experiments were performed using benthic communities from three test ditches (sand ditches A, B and C), receiving three different levels of external P- and N-loading.

The location and characteristics of the ditches are described in chapter 1.5 (p. 20-22).

Initially the conditions in all three ditches were identical. The sediments had a low phosphorus content of about 0.10 mg P.[g dry matter]⁻¹. This was measured as the sum of the individual steps of the extraction scheme according to Hieltjes and Lijklema (1980). Since May 1989 the ditches received different levels of external phosphorus loading. The levels of external nutrient input and the method used for nutrient addition are described in chapter 1.6 (p.22-24).

On top of the sand a benthic layer consisting mainly of living algae has developed in all three ditches. Because macrophytes and phytoplankton are virtually absent, this layer is the main source of primary production in ditch A and B (Portielje et al., 1994; chapter 5). In ditch C also a bloom of filamentous algae, mainly *Cladophora*, occurred, but this vanished by a sudden transition to a phytoplankton dominated system in the spring of 1991.

The species composition of the benthic community was determi-

ned microscopically as the visually estimated fraction of total biomass for individual species.

Phosphate uptake experiments

Samples of the benthic communities were collected from three intact sediment cores per ditch, each with a diameter of 5.3 cm. The cores were pushed into the sand to a depth of at least 10 cm. A benthic layer consisting of mainly living algae was present as a clearly distinct layer on top of the sand. It was removed by means of resuspension and decantation of the algal suspension after settling of the sand. This was repeated several times until all the algal material was removed and only the clear sand remained in the core. The algal material of the three cores was mixed for each ditch.

In the mixtures the dry weight (105°C) concentrations were determined as the dry rest after evaporation of a subsample of the mixture.

The initial intracellular P-content was determined by drying a subsample of the mixture at 40°C, complete destruction of the dried material with a H_2SO_4 -Se mixture, using H_2O_2 as an oxidator, and subsequent P analysis (Novozamsky et al., 1983).

Phosphorus uptake experiments were conducted in moderately stirred 250 ml suspensions (dilutions of the original suspension) with a known dry weight concentration at room temperature, allowing exposure to the daily light variation as experienced in the laboratory. After addition of phosphate to a concentration of 6 mg P/l, added as dissolved K_2HPO_4 and pH adjustment to 7, samples of 10 ml were taken at regular time intervals. These were immediately filtered through a 0.45 μm membrane filter, and dissolved phosphorus was determined in the filtrate on a Skalar SA-40 Autoanalyser, using the modified molybdate-blue method according to Murphy and Riley (1962). The choice of the initial ratio of the dry weight and P concentration was based on the results of preliminary experiments (not included here), and chosen in such a way that an

accurate measurement of the time course of the phosphate concentration was possible. Furthermore, the P-concentrations were chosen high enough to allow omission of the Michaelis-Menten term in equation (1) for the whole duration of the experiments. This enhances the quality of the parameter estimation for k and P_{max} . However, K_p is not estimated. The tailing-off of the uptake at low phosphate concentrations as expressed by the Michaelis-Menten term therefore is not considered, but it is felt (and can be shown by simulation) that for long term changes this term hardly affects the results. The results of the experiments are used to estimate the contribution of the benthic layer to the removal of dissolved phosphorus from the water phase after a dosage.

RESULTS

Algal species composition

Visual observation revealed that the benthic material consisted for the major part of living algae, and that detritus and bacteria only contributed a small fraction.

In ditch A the dominant species in the algal community was *Gloeocystis*, which was estimated to cover about 80% of the total algal biomass. Other species present in appreciable amounts (estimated at >1% of the total algal biomass) were *Oscillatoria limnetica* (≈10-15%), *Coelosphaerium* (5%) and *Closterium* (2%).

In ditch B, *Gloeocystis* was also the dominant species and estimated at about 60-70 %. *Aphanocapsa delicatissima* contributed an estimated 20 % of the total algal biomass, and *Oscillatoria limnetica* about 10 %. Further on, there were a few percents of diatoms (pennales).

In ditch C *Dimorphococcus* made up about 65 % of the biomass. *Gomphosphaerium* was estimated at 25 % and *Monoraphidium* at 5 %. Present at low abundancies (< 1 %) were *Astasia fasmus*, *Phacus helicoides*, several species of *Euglena*, *Pediastrum*

duplex and *Scenedesmus spp.*

Most species are of planktonic origin but in the ditches they are present in the benthic layer, which is most probably due to the stagnant conditions in the water and an enhanced nutrient availability in the near bottom region.

Gloeocystis, *Aphanocapsa delicatissima*, *Dimorphococcus* and *Gomphosphaerium* are present in the benthic layers as colonies of cells surrounded by mucus.

Phosphate uptake experiments

The amounts of dry weight in the benthic layer in the three ditches and the initial intracellular P-concentrations within this layer are given in table 8.1.

Table 8.1. Dry weight and initial intracellular P-concentrations in the benthic layer of the three ditches.

ditch	g DW.m ⁻²	mg P. [g DW] ⁻¹
- A, reference	352	0.57
- B, medium	460	1.70
- C, highest	563	4.09

Figure 8.1 shows the results of the uptake experiments. The experiments were performed in duplo and the averages of P_{int} are plotted versus time.

Fitting of equation (4) versus the measured data revealed that the parameters k and n are strongly correlated, which is reflected in wide confidence contours (data are not included). Therefore the simplified equation (5) was used. The simulated course of P_{int} with the optimum parameter set is represented in figure 8.1 by the lines. The optimum parameter set obtained by fitting of (5) is given in table 8.2.

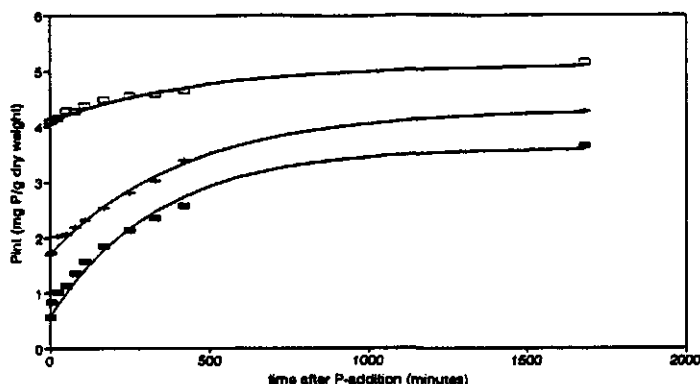


Figure 8.1. Changes in internal P-concentrations after a pulse addition of 6 mg P/l to suspensions of benthic algae originating from the three ditches.

(■ = ditch A, + = ditch B, □ = ditch C)

Table 8.2. Optimum parameter set obtained from least-squares optimization of the measured data.

	k $\text{min}^{-1} \cdot 10^4$	$P_{\text{int,max}}$ $\text{mg P.} [\text{g dm}^{-3}]^{-1}$
- A, reference	30	3.60
- B, medium	24	4.29
- C, highest	22	5.14

Figure 8.2 presents the optimum values for k and $P_{\text{int,max}}$ and the 90% confidence contours. The quality of the best fit, in terms of the least-squares sum, using two parameters (k and $P_{\text{int,max}}$, with n arbitrarily set at 1), did not deteriorate much as compared to the three parameter model (equation 4), in which n is also estimated.

Figure 8.3 displays the measured time-course of the dissolved phosphorus concentration in ditch C after a dosage in April 1992. It is compared with the simulated uptake by the benthic community, using the estimated optimum values of the parameters ($k = 22 \cdot 10^{-4} \text{ min}^{-1}$, $P_{\text{int,max}} = 5.14 \text{ mg P.} [\text{g dry weight}]^{-1}$).

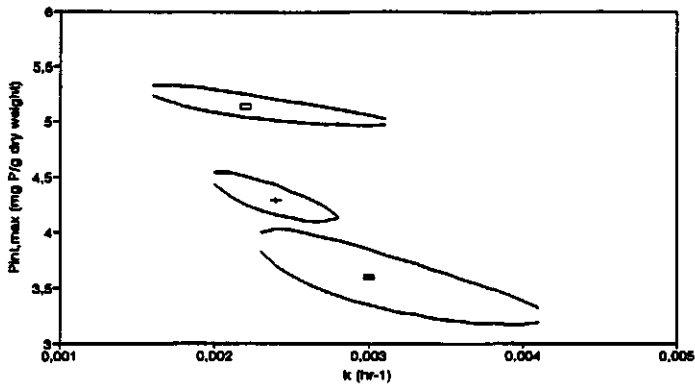


Figure 8.2. Optimum values and 90% confidence contours for k and $P_{int,max}$ as estimated from least-squares optimization. (■ = ditch A, + = ditch B, □ = ditch C)

The initial external dissolved phosphorus concentration at $t=0$ was, as calculated from the supplied dosage, 1.80 mg P.l^{-1} . The figure shows that the simulated uptake by the benthic community is responsible for a major part of the fast decrease in dissolved phosphorus concentrations during the first day after the dosage. After that no significant additional uptake by the benthic layer is likely to take place. Sedimentary uptake, by the underlying sand, is responsible for the remaining decrease in dissolved phosphorus which continues after the first day, as shown by the lower line in figure 8.3. The model used for the simulation of sedimentary uptake is described by Portielje and Lijklema (1993), and describes vertical transport in the sediment and the dynamics of adsorption onto the sand particles. In figure 8.3 a K_p value of $100 \text{ } \mu\text{g P.l}^{-1}$ has been used, but the sensitivity for K_p and k is small, and affects the calculated concentration only during the first day.

Neglect of diffusion limitation in the benthic layer may have overestimated the uptake rate during the first day, as can be seen from figure 8.3. Inclusion would have shifted the curve slightly to the right. The thickness of the diffusive boundary layer strongly depends on the turbulent conditions

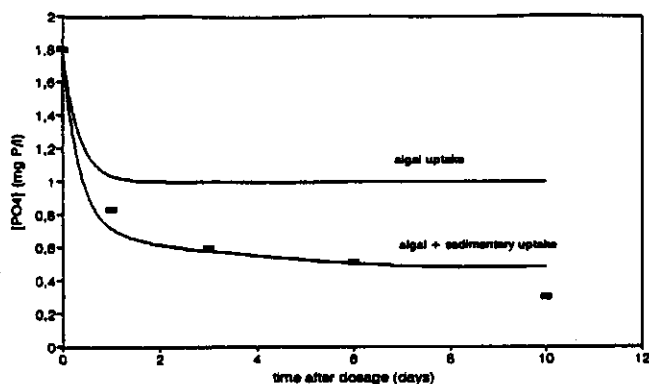


Figure 8.3. Simulated algal uptake and sedimentary uptake after a pulse loading of 1.80 mg P/l to ditch C in May 1992 and observed P concentrations.

in the water column and therefore varies in time. The fraction of phosphate taken up by the benthic community as compared to sedimentary uptake is however not affected to any appreciable extent by this imperfection.

Figure 8.4 presents the global change of the internal P-content of the benthic material in the three ditches since the start of the loading program in May 1989. In ditch C P_{int} is continuously increasing, despite the net production of biomass. The continuous increase of P_{int} and the small additional uptake capacity measured in the uptake experiments suggest that the benthic community will approach saturation with P upon continuation of the present level of external phosphorus input. In ditch B P_{int} remains more or less unchanged. In ditch A a slight but irregular decrease is observed, which may be due to a still on-going net production of cell material (Portielje et al., 1994; chapter 5), resulting in dilution of the internal P-pool. It should be noted however that this interpretation is slightly biased by the restricted number of observations and the fact that the last data were taken in May, whereas the others originate from

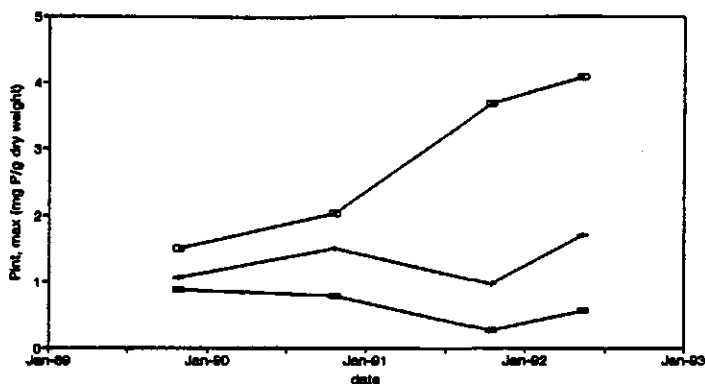


Figure 8.4. Change in measured internal P-concentrations in benthic algal communities at three different trophic levels. (■ = ditch A, + = ditch B, □ = ditch C)

October. All observations however were made just before a new semi-annual phosphorus dosage, so a steady state of the nutritional status of the algae with respect to the external loading at the time of sampling can be assumed.

CONCLUSIONS AND DISCUSSION

Measured kinetics of phosphorus uptake by algae dominated benthic communities can be described well as a function of the intracellular P deficit, defined as the difference between maximum storage capacity of phosphorus and the actual intracellular P-content.

In benthic communities previously exposed to different levels of external nutrient supply, and as a result with different composition and intracellular P-contents, the maximum storage capacity for phosphorus was found to be correlated to the initial intracellular P-content, indicating a shift in the maximum storage capacity of the community in relation to the ambient trophic level. This may also be partly due to species selection related to the availability of phosphate.

The uptake rate constant did not differ significantly for the

three communities, although there is a slight tendency for higher k -values at lower internal P-concentrations.

The species composition of ditch B is to a large extent ($\approx 75\%$) identical to that of ditch A. The main difference is an estimated 20% contribution to total algal biomass of *Aphanocapsa delicatissima* in ditch B, which was absent in ditch A. Adaptation in maximum storage capacity caused by adaptive mechanisms within a species is a possible explanation for the differences in the maximum P storage capacity between these two ditches. The species composition of ditch C is different from that of the other two ditches, and this may also cause the higher maximum storage capacity of phosphorus in ditch C.

Although algae contribute the largest part of the biomass in the benthic communities, bacteria may also to a certain extent determine the kinetics of phosphate uptake and the phosphate storage. Some bacterial species can reach very high internal P-concentrations (Marais et al., 1983). Redox conditions determine storage or release of P by bacteria (Fuhs and Chen, 1975). Anaerobic conditions and the resulting microbial mediated P-release may cause a decrease in the P-pool of the sedimentary top layer of well over 30% during a few weeks (Boström et al., 1985). Calculations on the oxygen budget of the ditches revealed that anaerobic conditions due to oxygen consuming processes within the benthic layers only occur at very low vertical dispersion coefficients (results will be published elsewhere), but that during most of the year the O_2 -depletion within the benthic layer during night is too small to cause anoxia. The benthic layers have a very loose structure (porosities are well over 90 %).

The mucilage surrounding the algal colonies may be a growing site for bacteria (Bronberg and Boström, 1992), and interactions between algae and attached bacteria may determine the survival of the algal colonies, but possibly also the kinetics of P-uptake.

Reported values for the uptake rate constant k are an order of

magnitude lower than those published by Riegman (1985) for cyanobacteria. He found for seven phosphorus starved species k values ranging from 120 to $370 \cdot 10^{-4} \text{ min}^{-1}$. This may be due to differences in algal species composition. Cyanobacteria are known to exhibit the largest uptake rates under P-limited conditions. As in the present experiments the major part of the algae (*Gloeocystis*, *Aphanocapsa delicatissima*, *Dimorphococcus*, *Gomphosphaerium*) was present as colonies surrounded with mucus, this may have reduced diffusion in the boundary layer around the cells.

Although there is no proven law that first order kinetics apply to phosphorus uptake mechanisms, it is generally used and shown to describe observed uptake satisfactory. The simplification of the model to first-order kinetics ($n=1$ in equation (4)) did not significantly deteriorate the accuracy of the description with respect to the optimal parameter set with $n \neq 1$. This is in agreement with Riegman (1985) who also found first-order kinetics to work satisfactory.

Luxury uptake by an the algae dominated benthic community is responsible for most of the fast decrease in the dissolved phosphorus concentration in the water phase, observed during the initial phase after a dosage in ditch C. After the first day no significant additional uptake by the benthic community will take place, and from that time on the observed decrease in the dissolved phosphorus concentration is mainly due to uptake by the sandy sediment, where adsorption processes determine the phosphate storage.

The value of K_p affects the tailing off of phosphate uptake after a step-wise addition but is not important for long term simulations. Bierman (1976) suggests a value for K_p of about $30 \mu\text{g P.l}^{-1}$ for cyanobacteria and $60 \mu\text{g P.l}^{-1}$ for diatoms and green algae. Riegman (1985) reported values of approximately $7 \mu\text{g P.l}^{-1}$ for the cyanobacteria *Oscillatoria limnetica* and *Anabaena flos-aquae*.

Benthic microbial layers often perform a high activity per unit of volume. In natural systems of benthic microbial layers

often distinct horizontal layers have been distinguished (Revsbech et al., 1983). Differences between different species in uptake kinetics combined with their spatial separation makes application of measured mixed culture kinetics to field situations more difficult, as physical transport starts to play a role.

On a longer term the increased intracellular P-concentrations cause a higher net production of cell material if no other factors are limiting. This then results again in 'dilution' of the internal P-concentrations.

From extrapolation in time of the internal P-concentrations in the benthic communities of the three ditches, it may be inferred that at the level of phosphorus loading in ditch A, net production of biomass will continue until the internal P-concentration reaches a minimum value. Our measured internal P-concentrations in ditch A are lower than those calculated from data from Bierman (1976): 2.3 mg P.[g dry matter]⁻¹ for green algae and 0.7 mg P.[g dry matter]⁻¹ for non N-fixing blue-green algae. The mucus surrounding the colonies may have added to the total amount of dry weight in the ditches, thereby lowering the P-fraction, and a small contribution of dead organic matter with lower P-content can also not be precluded. In ditch B the internal P-concentrations are rather constant, while in ditch C they are increasing and likely to reach saturation upon continued external loading, given the reduced uptake capacity after a phosphate addition as shown by phosphate uptake experiments. The benthic and phytoplankton community will then lose its function as a buffer site for pulse loadings of phosphate. In this ditch a transition from a system dominated by benthic algae to a system dominated by phytoplankton has been observed. The reason for this transition may be due to the competitive advantage of phytoplankton species over benthic algal species in light limited systems. Another explanation may be that the replacement of P-limitation by light and/or inorganic carbon limitation can induce mechanisms by which algae can perform

active vertical movement by means of buoyancy regulation. In the literature (e.g. Booker and Walsby, 1981) evidence has been provided for a positive effect of a nutrient dosage on the buoyancy of P-limited cyanobacteria. Klemer et al. (1982) showed that C-limitation and N-limitation have opposite effects on the buoyancy of *Oscillatoria*, with respectively an increase and a decrease. It can not be proven that these mechanisms have caused the transition towards a phytoplankton dominated system in ditch C, but it may be an explanation. The ability of alternating presence in the euphotic zone and in nutrient-richer deeper layers is of ecological advantage.

ACKNOWLEDGEMENTS

The authors wish to thank Rudi Roijackers and Rob Suijkerbuijk for the identification of the algal species, and two anonymous reviewers for their valuable comments.

REFERENCES

- Bierman, V.J., 1976. Mathematical model of the selective enhancement of blue-green algae by nutrient enrichment. In: R.P. Canale (ed), Modeling biochemical processes in aquatic ecosystems. Ann Arbor Science Publishers, Michigan, USA.
- Booker, M.J. and A.E. Walsby, 1981. Bloom formation and stratification by a planktonic blue-green alga in an experimental water column. Brit. Phycol. J. 16, 411-421.
- Boström, B. I. Ahlgren and R. Bell, 1985. Internal nutrient loading in a eutrophic lake, reflected in seasonal variations of some sediment parameters. Verh. Internat. Verein. Limnol. 22, 3335-3339.
- Brunberg, A-K. and B. Boström, 1992. Coupling between benthic biomass of *Mycrocystis* and phosphorus release from the sediments of a highly eutrophic lake. Hydrobiologia 235/236, 375-385.

- Drent, J. and K. Kersting, 1993. Experimental ditches for research Under natural conditions. *Water Res.* 27 (9), 1497-1500.
- Droop, M.R., 1974. The nutrient status of algal cells in continuous culture. *J. Mar. Biol. Assoc. U.K.*, 54, 825-855.
- Fuhs, G.W. and M. Chen, 1975. Microbiological basis of phosphate removal by in the activated sludge process for the treatment of wastewater. *Microbial Ecol.* 2, 119-138.
- Hieltjes, A. and L. Lijklema, 1980. Fractionation of inorganic phosphates in calcareous sediments. *J. Envir. Qual.* 9, 405-407.
- Kirk, J.T.O., 1983. Light and photosynthesis in aquatic ecosystems. University of Cambridge, 401 pp.
- Klemer, A.R., J. Feuillade and M. Feuillade, 1982. Cyanobacterial blooms: carbon and nitrogen limitation have opposite effects on buoyancy of *Oscillatoria*. *Science* 215, 1629-1631.
- Kunikane, S., M. Kaneko and R. Maehara, 1984. Growth and nutrient uptake of green alga, *Scenedesmus dimorphus*, under a wide range of nitrogen/phosphorus ratio-I Experimental study. *Water Research* 18, 1299-1311.
- Kunikane, S. and M. Kaneko, 1984. Growth and nutrient uptake of green alga, *Scenedesmus dimorphus*, under a wide range of nitrogen/phosphorus ratio-II Kinetic model. *Water Research* 18, 1313-1326.
- Marais, G.v.R, R.E. Loewenthal and I.P. Siebritz, 1983. Observations supporting phosphate removal by biological excess uptake - A Review. *Wat. Sci. Tech.* 15, 15-41.
- Murphy, J. and J.P. Riley, 1962. A modified single solution method for the determination of phosphate in natural waters. *Anal. Chim. Acta* 27, 31-36.
- Novozamsky, I., V.J.G. Houba, R. van Eck and W. van Vark, 1983. A novel digestion technique for multi-element plant analysis. *Comm. Soil Sci. Plant Anal.* 14, 239-249.

- Nyholm, N., 1978. Dynamics of phosphate limited algal growth: simulation of phosphate shocks. *J. Theor. Biol.* 70 415-425.
- Okada, M., R. Sudo and S. Aiba, 1982. Phosphorus uptake and growth of blue-green alga, *Microcystis aeruginosa*. *Biotechnol. Bioengng* 18, 1043-1056.
- Portielje, R. and L. Lijklema, 1994. The effect of reaeration and benthic algae on the oxygen balance of an artificial ditch (accepted for publication by *Ecol. Modeling*).
- Portielje, R., K. Kersting and L. Lijklema, subm. Estimation of productivity by benthic algae from continuous oxygen measurements in relation to external nutrient input (submitted to *Water Research*).
- Portielje, R. and L. Lijklema, 1993. Sorption of phosphate by sediments as a result of enhanced external loading. *Hydrobiologia* 253, 249-261.
- Revsbech, N.P., B.B. Jørgensen and T.H. Blackburn, 1983. Microelectrode studies of the photosynthesis and O₂, H₂S and pH profiles of a microbial mat. *Limnol. & Oceanogr.* 28, 1062-1074.
- Riegman, R., 1985. Phosphate-phytoplankton interactions. PhD Dissertation Univ. of Amsterdam, 135pp.

Chapter 9

Carbon dioxide fluxes across the air-water interface and its impact on carbon availability in aquatic systems.

Keywords:

**CO₂-mass transfer - C-assimilation - eutrophication -
aquatic macrophytes - benthic algae**

Based on: Carbon dioxide fluxes across the air-water interface and its impact on carbon availability in aquatic systems, by R. Portielje and L. Lijklema. Submitted to Limnology & Oceanography.

9. CARBON DIOXIDE FLUXES ACROSS THE AIR-WATER INTERFACE AND ITS IMPACT ON CARBON AVAILABILITY IN AQUATIC SYSTEMS.

ABSTRACT

The enhancement of diffusion limited CO₂-exchange across the air-water interface by chemical reaction has been analyzed using a model simulating transport and reaction of CO₂ in a stagnant boundary layer at the air-water interface. The atmospheric C-influx has been studied in relation to a number of environmental conditions: pH, total dissolved inorganic carbon, temperature and the thickness of the stagnant boundary layer as related to the ambient wind velocity.

From this model the influx of carbon dioxide from the atmosphere into six experimental ditches was calculated for a period of six or eight months, starting in early spring. Three of the six ditches are dominated by aquatic macrophytes and three by benthic algae, each series receiving three different levels of external nitrogen and phosphorus input. Comparing the results with the net C-assimilation during the same period, as estimated from continuously measured oxygen data, showed that a considerable fraction of the carbon requirements during this period can be obtained from atmospheric carbon dioxide. This was especially the case in the ditches dominated by submersed macrophytes.

In the ditches dominated by benthic algae the percentage of the cumulative net C-assimilation that was covered by atmospheric C-influx was considerably less, but substantial, and it was related to the level of N and P loading.

Enhanced primary production due to enhanced external loading with nitrogen and phosphorus, resulted in an increased atmospheric C-input due to higher pH-values. This indicates that the trophic state with respect to nitrogen and phosphorus on one hand and the availability of carbon on the other are to a certain extent interrelated.

INTRODUCTION

The rate of photosynthesis by aquatic plants in surface waters is determined by a limitation imposed by any of the ingredients needed for photosynthesis: inorganic carbon, inorganic nutrients (N,P and, in case of diatoms, Si), micro-nutrients and light irradiance (Kirk, 1983; Sand-Jensen, 1989).

Eutrophication of surface waters has enhanced primary production due to the alleviation of P- and/or N-limitation. During periods of high primary production and under saturating light conditions, the availability of dissolved inorganic carbon

(DIC) may become the rate-limiting factor. Adams et al. (1978) found photosynthesis of *Myriophyllum spicatum* to follow Michaelis-Menten kinetics with respect to DIC.

As many highly productive systems have a large vertical attenuation of light the major part of primary production occurs just below the water surface. The flux of CO_2 across the air-water interface therefore may be an important source for carbon. Organisms can adapt to this locally enhanced carbon availability by vertical migration towards the water surface, as shown by Klemer et al. (1982), who found that cyanobacteria under C-limitation form near-surface blooms by increasing their buoyancy. Submersed macrophytes such as *Elodea* can form a dense biomass immediately below the water surface.

Replenishment of dissolved inorganic carbon (DIC) from the atmosphere will occur when the dissolved CO_2 concentration ($\text{CO}_{2,aq}$) is below the equilibrium at the air-water interface. Lowering of dissolved CO_2 concentrations is due to both carbon uptake by the organisms and the resulting increase in pH, causing a shift in chemical equilibrium towards HCO_3^- and CO_3^{2-} . The flux of CO_2 across the air-water interface and subsequent transport to the bulk water phase is limited by diffusional transport across the stagnant boundary layer. The driving force for this transport is a concentration gradient. For a chemical reactive compound such as CO_2 , this gradient varies with the depth in the boundary layer due to the combined effect of diffusion and reaction, when DIC species are not at chemical equilibrium.

Absorbed CO_2 is converted into H_2CO_3 or HCO_3^- and under steady-state conditions the CO_2 concentration gradient is the steepest immediately below the interface. The flux across the interface of a reactive compound like CO_2 will thus be larger than that of a chemical inert species.

To calculate the CO_2 -flux, the enhancement due to reaction must be known. Calculation of the acceleration factor can be done by simulating the transport and reaction of all chemical species involved in the equilibrium reactions between the

different DIC compounds in the stagnant boundary layer (Emerson, 1975). This also includes the transport and reaction of H⁺ and OH⁻, which as reactants control the rate-limiting steps and influence chemical equilibria.

As each ion has its specific diffusion coefficient, transport will also induce a gradient in the electrical potential in the boundary layer (Ben-Yaakov, 1972). Transport of other (inert) ions due to this electrical gradient also has to be taken into account, as this in turn influences the electrical gradient.

Calculation of the acceleration factor is performed with a numerical procedure (Emerson, 1975). Hoover and Berkshire (1969) presented equations for an analytical solution of the acceleration factor, but they had to assume a constant pH throughout the whole boundary layer.

In this chapter calculated values for the acceleration factor obtained from the simulation are used to estimate the C-flux across the air-water interface under varying environmental conditions. The estimated atmospheric CO₂ input rates into three experimental ditches dominated by macrophytes (*Elodea nuttallii*, *Chara spp.*) and three experimental ditches dominated by benthic algae are compared to estimated net C-assimilation (Portielje et al., 1994a,b) during the growth season from March to August or October 1990. In the framework of a eutrophication research, each series of three ditches received three different levels of nutrient loading.

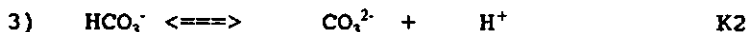
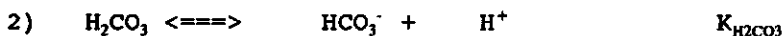
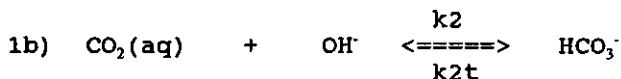
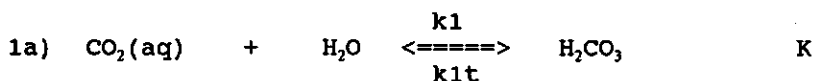
The rationale of this study is to establish the extent to which atmospheric C-influx can contribute to the carbon needs of aquatic communities, and to evaluate its ecological significance. Schindler et al. (1972) found an enhancement with a factor 3-4 for CO₂ input in an artificially eutrophied lake, and concluded that atmospheric C-input generally may be sufficient to satisfy the carbon needs of phytoplankton communities at saturating N and P conditions.

THEORY

Transport across the boundary layer at the air-water interface is represented by the Whitman film-model: a laminar boundary layer in which transport is controlled by molecular diffusion. The diffusion coefficient therefore is assumed to be constant throughout the whole thickness of the boundary layer. A numerical procedure is used in which the boundary layer is divided in a number of sublayers with equal thickness (Emerson, 1975). The flux of carbon through the boundary layer is the combined result of chemical and physical processes.

Chemistry

The fractionation of inorganic carbon in water is determined by the following equilibrium reactions (Stumm and Morgan, 1981):



Reactions 2) and 3) are very fast, so equilibrium is reached instantaneously. The rate constant k_1 of reaction 1a) is 0.035 sec^{-1} at 25°C and 0.022 sec^{-1} at 20°C . As the time-scales of transport and reaction are of the same order of magnitude, both processes determine the concentration profile. Therefore to adequately describe the combined effect of diffusion and reaction the time step in the numerical calculations has to be chosen small enough as compared to these reaction rates.

At pH > 8.55 reaction 1b becomes the main pathway for the removal of free CO₂. The values for the rate constants as a function of temperature implemented in the model are summarized in table 9.1.

Table 9.1. Rate constants and their sources.

rate constant	Ref.
k1	10 ^(10.685 - 3618/T)
k1t	10 ^(13.770 - 3699/T) Sirs (1958)
k2	10 ^(13.590 - 2887/T) Sirs (1958)
k2t	10 ^(14.88 - 5524/T) Welch et al. (1969)

At equilibrium the different compounds constitute the fractions $\alpha(0)$, $\alpha(1)$ and $\alpha(2)$ of total inorganic carbon C_{tot}. These fractions are a function of the pH and the equilibrium constants at the ambient temperatures (table 9.2).

Table 9.2. Fractionation of inorganic carbon species.

[H ₂ CO ₃ *]	=	$\alpha(0) \cdot C_{tot}$	(H ₂ CO ₃ * = CO ₂ + H ₂ CO ₃)
[HCO ₃ ⁻]	=	$\alpha(1) \cdot C_{tot}$	
[CO ₃ ²⁻]	=	$\alpha(2) \cdot C_{tot}$	
with			
$\alpha(0)$	=	$1 / (1 + (K1/[H^+]) + (K1.K2/[H^+]^2))$	
$\alpha(1)$	=	$1 / (([H^+]/K1) + 1 + (K2/[H^+]))$	
$\alpha(2)$	=	$1 / (([H^+]^2/K1.K2) + ([H^+]/K2) + 1)$	
with K1	=	$[HCO_3^-] \cdot [H^+] / [H_2CO_3^*]$	

The pH in the sublayers is calculated iteratively at each time step from C_{tot}^{*} and the alkalinity, by solving equations (1) and (2) simultaneously. Neglecting the contribution of other ions, the alkalinity ALK is:

$$ALK = [HCO_3^-] + 2[CO_3^{2-}] + [OH^-] - [H^+] \quad (1)$$

and:

$$C_{tot}^* = [H_2CO_3] + [HCO_3^-] + [CO_3^{2-}] \quad (2)$$

From the ALK/C_{tot}^* ratio an initial estimation pH_0 for the pH is made:

if $ALK/C_{tot}^* \leq 1$ -----> $pH_0 = 7.0$
 if $1 < ALK/C_{tot}^* \leq 2$ -----> $pH_0 = 10.0$

if $ALK/C_{tot}^* > 2.0$ than the pH can be calculated directly from the concentration of free OH. The arbitrary choices of the initial pH estimations are based on practical applicability. The pH is usually calculated with an accuracy of three decimals within 8 iterations.

The concentration gradient in the boundary layer results from differences between the bulk concentration of CO_2 and the equilibrium at the air-water interface $CO_{2,eq}$. The latter is determined by the partial atmospheric pressure pCO_2 (atm) and Henry's constant ($g \cdot m^{-3} \cdot atm^{-1}$):

$$CO_{2,eq} = H_T \cdot pCO_2 \quad (3)$$

Henry's constant is temperature dependent. Temperature correction is made by:

$$H_T = H_{20} \cdot \frac{293}{(T + 273)} \quad (4)$$

Transport processes

From an initial estimation of the concentration profile within the boundary layer, the exchange between the sub-layers and the reactions within each sublayer are simulated for discrete time steps, each yielding a new concentration profile. The calculations are repeated until a stationary profile is reached. At steady-state the concentration profile of an ion i is determined by Fick's second law:

$$D_i \frac{\partial^2 C_i}{\partial x^2} = R_i \quad (5)$$

In case the ions considered represent more than a negligible

fraction of the total ionic strength, the effect of the electrical gradient induced by ionic diffusional transport cannot be neglected (Ben Yaakov, 1972) :

$$J_i = U_i \left[RT \frac{\partial C_i}{\partial x} + z_i C_i F \frac{\partial E}{\partial x} \right] \quad (6)$$

with J_i : the flux of ion i
 U_i : the mobility of ion i
 R : gas constant
 z_i : ionic charge
 C_i : concentration of ion i
 F : Faraday's constant
 $\partial E / \partial x$: Electrical gradient
 and: $U_i RT = D_i$

The first term is the classical Fickian diffusion, whereas the second term represents the effect of a gradient in the electrical potential on the flux. Emerson (1975) rewrote equation (6) to:

$$J_i = RTU_i \left[\frac{\partial C_i}{\partial x} - z_i C_i \frac{\sum U_k z_k \left(\frac{\partial C_k}{\partial x} \right)}{\sum U_k z_k^2 C_k} \right] \quad (7)$$

The mobilities U_k for individual ion species are calculated from:

$$U_k = \frac{\lambda_k^{\circ}}{|z_k|^2 F^2} \quad (8)$$

Values for the equivalent conductance λ_k° of all ion species at 20°C and their concentrations in the ditches are given in table 9.3.

In the CO₂ exchange model the term describing the effect of the electrical potential gradient on ion diffusion cannot be neglected, due to the relative high mobility of the OH⁻ ion (Emerson, 1975). This results in a lowering of the accelera-

Table 9.3. Equivalent conductance λ°_k of ionic species (from Robinson and Stokes, 1970) and their concentrations in the ditches.

ion species	λ° (mho.cm ² .eq ⁻¹)	Conc. (mM)
Ca ²⁺	60	0.50
Mg ²⁺	53	0.09
Na ⁺	50	0.03
K ⁺	74	0.24
SO ₄ ⁼	80	0.09
Cl ⁻	76	0.22
CO ₃ ⁼	69	var.
HCO ₃ ⁻	44	var.
H ⁺	350	var.
OH ⁻	198	var.

tion factor as compared to a situation with no electrical potential gradient. Reaction 1b induces concentration gradients of HCO₃⁻ and OH⁻ which have opposite directions. As the mobility of the OH⁻ ion is greater, the topmost sublayer becomes negatively charged compared to the one below, and thereby the diffusional transport of OH⁻ is hampered. The removal of free CO₂ by reaction 1b decreases as compared to a situation without electrical gradient, and concomitantly the steepness of the concentration gradient becomes smaller. In a stationary profile the total flux J of DIC is constant throughout the whole boundary layer:

$$J = D_{CO_2} \frac{\partial CO_2}{\partial x} + D_{HCO_3^-} \frac{\partial HCO_3^-}{\partial x} + D_{CO_3^{=}} \frac{\partial CO_3^{=}}{\partial x} \quad (9)$$

A schematization of chemical and physical processes and their interactions is given in figure 9.1.

Acceleration factor

The acceleration factor f_c of CO₂ transport across the air-water interface ($x=0$) in comparison with a linear concentra-

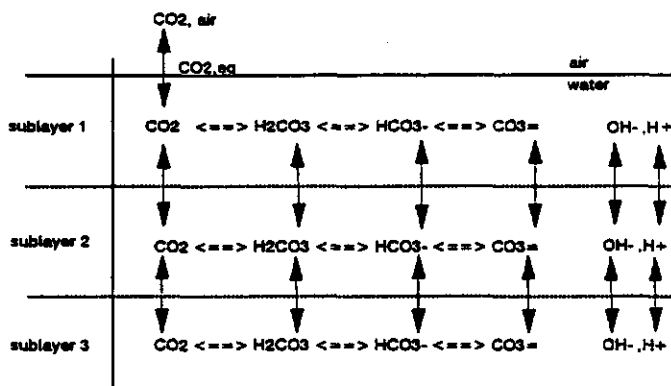


Figure 9.1. Schematization of physical and chemical processes in boundary layer.

on gradient throughout the boundary layer, can be defined as :

$$f_c = \frac{\lim_{x \rightarrow 0} \frac{dCO_2}{dx}}{\left(\frac{CO_{2,eq} - CO_{2,bulk}}{\delta} \right)} \quad (10)$$

with δ the thickness of the boundary layer (m).

From the steady-state CO₂(aq) profile in the diffusive boundary layer

$$\lim_{x \rightarrow 0} \frac{dCO_2}{dx}$$

can be approximated by the discretized concentration gradient in the topmost sublayer.

As f_c is determined by the ratio between diffusive transport and reaction for each component, it depends on a number of variables:

1- pH.

The pH determines the DIC-equilibria and the rate of the

reaction of CO_2 with OH^- to form HCO_3^- . This becomes the most important pathway for CO_2 conversion at high pH and its rate is directly controlled by the pH.

2- Total DIC

Total DIC determines the pH buffering capacity of the solution. A high DIC concentration reduces the lowering of the pH near the interface due to the absorption of CO_2 . Thus the decrease in the conversion rate of CO_2 with OH^- is counteracted by a high DIC concentration. A high total DIC concentration therefore has a positive effect on f_c .

3- Temperature.

Temperature affects the reaction rates and the chemical equilibria.

4- Thickness of the diffusive boundary layer.

The thickness of the diffusive boundary layer is determined by turbulence in the water phase, and therefore in stagnant waters mainly depends on wind stress. A greater thickness increases the acceleration factor since the time scale of transport through the boundary layer is greater and hence conversion towards equilibrium more complete.

Sites studied

The model for CO_2 -exchange was applied to six experimental ditches. The C-influx was calculated using continuously measured values for wind, pH and temperature. Total DIC was calculated from monthly measured alkalinities and has been assumed constant for that month. The six ditches considered in this study are the clay-ditches A, B and C, dominated by submersed macrophytes, and the sand ditches A, B and C, dominated by benthic algae. Each series receives three different levels of external N- and P-loading. The external nutrient loading rates and the method of nutrient addition are described in chapter

1.6 (p.22-24). The location and characteristics of the ditches are described in chapter 1.5 (p.20-22).

In all ditches pH is measured continuously at a depth of 0.25 m, and registered in a datalogger as fifteen minute averages. Water temperature is measured at three depths (0.10, 0.25 and 0.40 m) and also registered as fifteen minute averages. For the calculation of CO₂ exchange water temperatures at 0.10 m. have been used. Wind speed is measured continuously at an elevation of 2 m. A detailed technical description of the ditches and their instrumentation is given by Drent and Kersting (1993).

Thickness of the stagnant boundary layer

Knowledge of the relationship between the thickness of the stagnant boundary layer δ and the wind speed is needed. From tracer experiments with ethylene as a gas tracer, an empirical relationship between the mass transfer rate across the air-water interface and the wind speed W has been developed (Portielje and Lijklema, 1994):

$$K_{L,C2H4} = Z \cdot (0.034 \cdot W - 0.033) \quad (\text{m} \cdot \text{hr}^{-1})$$

with Z the average water depth (= 0.38 m). From the Whitman film-model it follows that $K_{L,C2H4} = D_{C2H4} / \delta$, with $D_{C2H4(20^\circ\text{C})} = 1.87 \cdot 10^{-9} \text{ m}^2 \cdot \text{s}^{-1}$ (Reid et al., 1977). So the thickness δ of the boundary layer is directly related to W . For instance at $W=2 \text{ m} \cdot \text{s}^{-1}$ it yields that $\delta \approx 500 \text{ }\mu\text{m}$ and at $W = 4 \text{ m} \cdot \text{s}^{-1}$ that $\delta \approx 170 \text{ }\mu\text{m}$. A value for δ of $750 \text{ }\mu\text{m}$ has been arbitrarily chosen as a maximum.

RESULTS

Figures 9.2 a-d display the acceleration factor f_c as a function of bulk pH for different values of total DIC, and for values for δ of 100, 250, 500 and $750 \text{ }\mu\text{m}$ respectively, all at

a temperature of 20°C. The range for δ corresponds to calculated values at occurring wind speeds. pH values below 8 are not displayed, as at these pH values the acceleration factor is always very close to 1. At pH=8 the enhancement as compared to a linear concentration gradient is always less than 10%. Schurr and Ruchti (1977) found in the river Aare at Bern, Switzerland that the relative exchange rate of CO_2 as compared to that of O_2 corrected for the molecular diffusion coefficient, was 1.034 while the pH varied between 7.8 and 8.6. At pH=11, 1000 μM DIC and a large boundary layer thickness (750 μm) the acceleration factor is more than 13. Emerson (1975) calculated a theoretical maximum for the acceleration factor

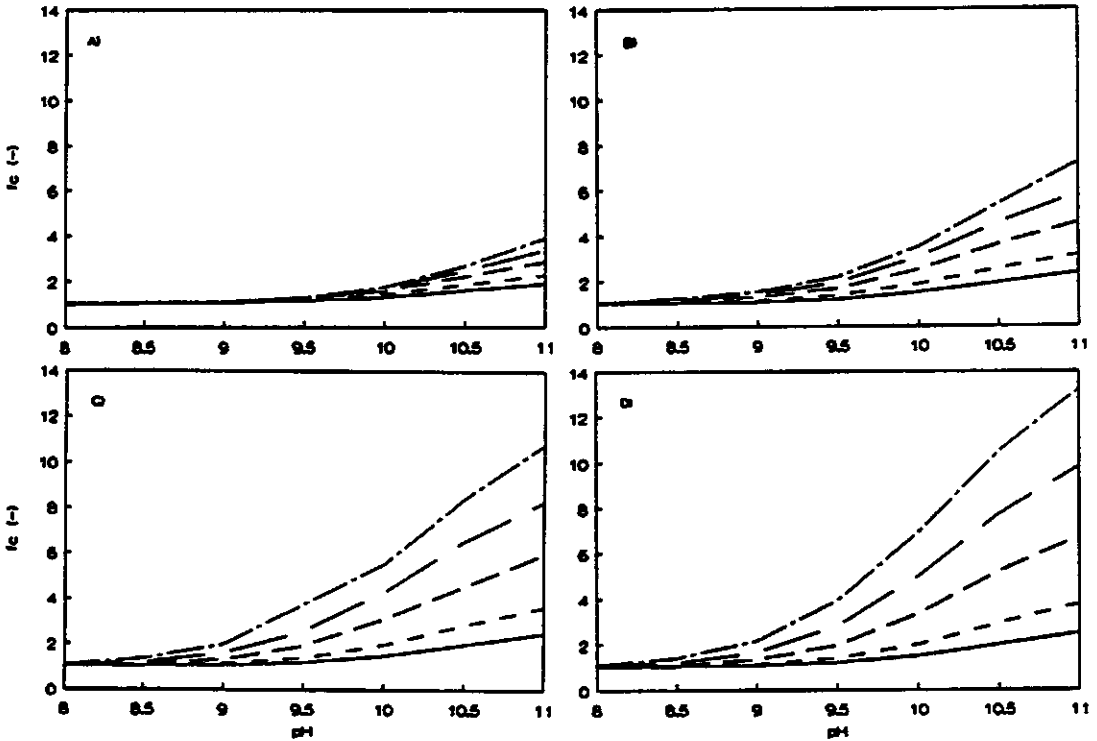


Figure 9.2. Acceleration factor f_c as a function of pH at different total DIC concentrations. a) $\delta = 100 \mu\text{m}$, b) $\delta = 250 \mu\text{m}$, c) $\delta = 500 \mu\text{m}$, d) $\delta = 750 \mu\text{m}$.

— $C_{\text{tot}}=50 \mu\text{M}$, - - - $C_{\text{tot}}=100 \mu\text{M}$, - - - $C_{\text{tot}}=250 \mu\text{M}$,
 - · - $C_{\text{tot}}=500 \mu\text{M}$, · · · $C_{\text{tot}}=1000 \mu\text{M}$.

CO₂-exchange across the air-water interface

of about 21, while assuming immediate equilibrium for all reactions.

Figures 9.3 a-d present the resulting atmospheric carbon influxes from the atmosphere as a function of pH for different values of total DIC and δ , all at 20°C. The figures show that, as a consequence of the counteracting effects of the acceleration factor and the equilibrium bulk CO₂ concentrations, the carbon flux is relatively insensitive to the total DIC concentration and bulk pH in a pH region of 8.5-9.5. At higher pH the acceleration factor determines the carbon flux, resulting in higher C-influxes at higher DIC concentrations.

Figure 9.4 displays the pH profile in a 500 μm boundary layer at a bulk pH of 10.5 for various total DIC concentrations. At

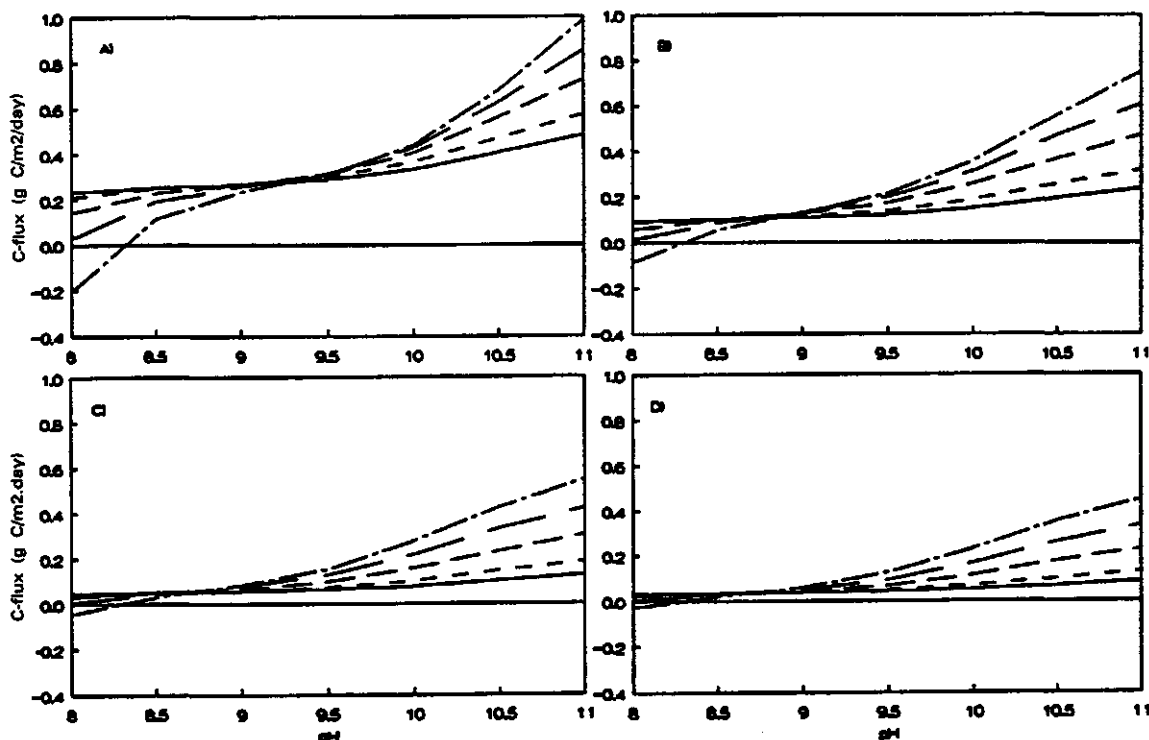


Figure 9.3. CO₂-flux across the air-water interface as a function of pH at different DIC concentrations.

a) $\delta = 100 \mu\text{m}$, b) $\delta = 250 \mu\text{m}$, c) $\delta = 500 \mu\text{m}$, d) $\delta = 750 \mu\text{m}$.
 —————: $C_{\text{tot}} = 50 \mu\text{M}$, - - - - -: $C_{\text{tot}} = 100 \mu\text{M}$, — — — —: $C_{\text{tot}} = 250 \mu\text{M}$,
 - . - . - .: $C_{\text{tot}} = 500 \mu\text{M}$, — - - - -: $C_{\text{tot}} = 1000 \mu\text{M}$.

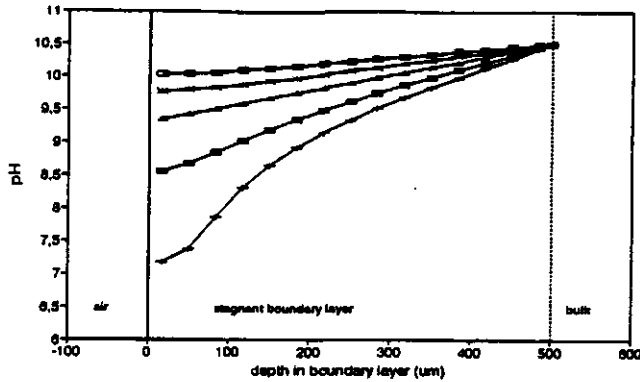


Figure 9.4. pH profile in the boundary layer at different total DIC concentrations and a bulk pH of 10.5 ($\delta = 500 \mu\text{m}$).
 +: $C_{\text{tot}} = 50 \mu\text{M}$, ●: $C_{\text{tot}} = 100 \mu\text{M}$, Δ: $C_{\text{tot}} = 250 \mu\text{M}$, ✖: $C_{\text{tot}} = 500 \mu\text{M}$, □: $C_{\text{tot}} = 1000 \mu\text{M}$.

low total DIC concentrations a considerable pH gradient exists in the boundary layer. The analytical solution for the acceleration factor as presented by Hoover and Berkshire (1969) assumes a constant pH throughout the whole boundary layer. This model requires considerable less computation time, but it seems appropriate only at total DIC concentrations of well over 1 mM.

The effect of temperature on the acceleration factor f_c and

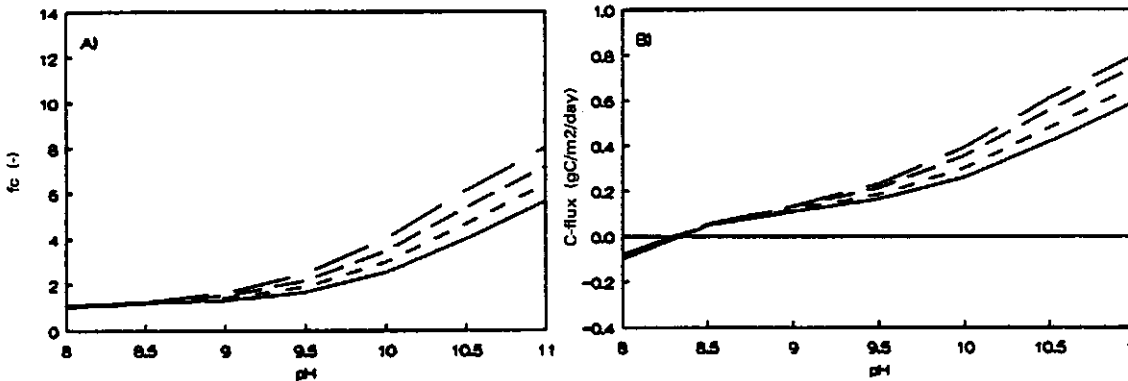


Figure 9.5. Temperature dependence of acceleration factor f_c (a) and CO_2 -flux (b), $\delta = 250 \mu\text{m}$, total DIC = 1 mM.
 —: 10°C; - - -: 15°C; - · - · -: 20°C; - - - - -: 25°C;

the resulting carbon influx across the air-water interface is illustrated in figures 9.5 a and b, for $\delta=250 \mu\text{m}$ and $C_{\text{int}}=1 \text{ mM}$. Figures 9.6 a-c present the cumulative atmospheric C-influx and the estimated cumulative net C-assimilation (from Portielje et al., 1994b) into the three macrophyte dominated ditches during the period March 1st-August 31st 1990. The results show that during this period atmospheric C-input covered 85, 97 and 58 % of the estimated net C-assimilation in the ditch C (Elodea), ditch B (Elodea) and ditch A (Chara) respectively. Figures 9.7 a-c present the cumulative atmospheric C-influx and the cumulative net C-assimilation (from Portielje et al., 1994a) in the three ditches dominated by benthic algae. In ditch A the C-influx is negative in March and April due to a low pH with subsequent oversaturation with respect to CO₂. After that the flux becomes positive following an increase in pH. For the whole period of March 1st - October 31st 1990 the cumulative atmospheric C-influx is 36 % of the estimated cumulative C-assimilation, but during the period May 1st - October 31st it was considerably higher: 65 %. In ditch B the cumulative atmospheric C-input is close to zero during the first three months, but after that increases due to an increased pH. For the whole period of March 1st - October 31st the cumulative atmospheric C-input covers 36 % of the cumulative net C-assimilation, and for the period June 1st - October 31st it is somewhat higher: 41 %. In ditch C the atmospheric C-input covers 58 % of the estimated net C-assimilation for the whole period. During March the atmospheric C-influx is close to zero, but from April on it is larger. Due to a pH near 10 a large portion of total DIC is present as carbonate, which cannot be taken up by the organisms.

In the macrophyte dominated ditches as well as the ditches dominated by benthic algae, both the cumulative C-influx and the cumulative net C-assimilation increase with increasing nutrient loading rate. The difference between both *Elodea* dominated ditches is only small.

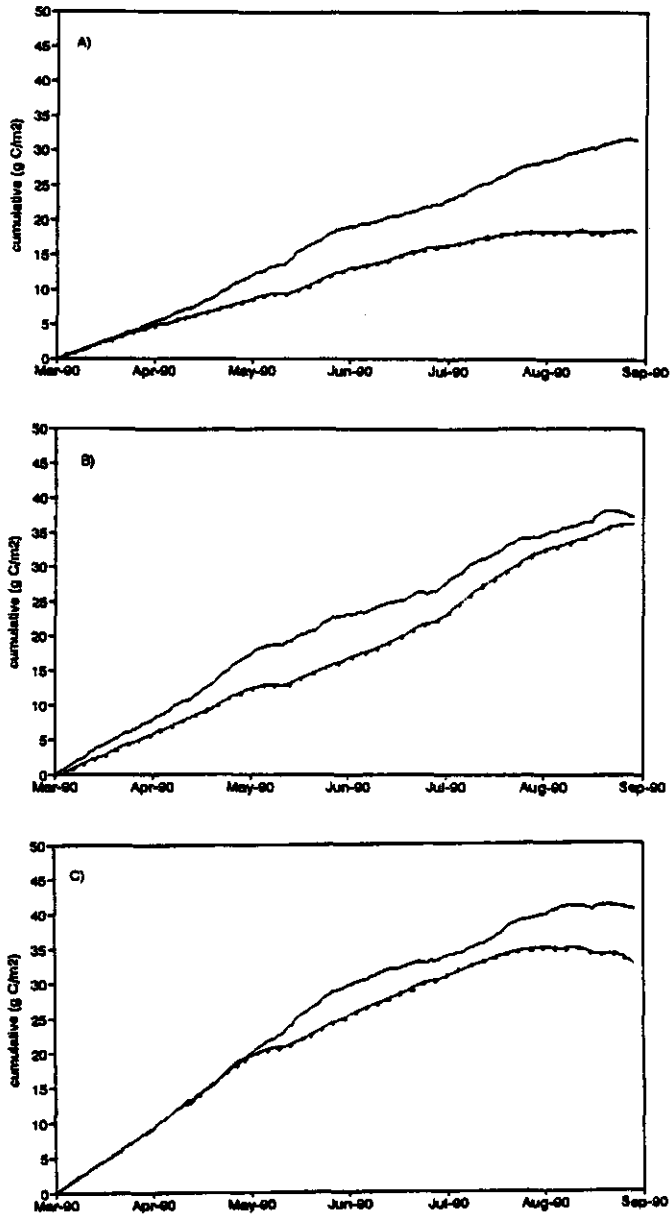


Figure 9.6. CO₂ influx and estimated net C-assimilation in the macrophyte dominated ditches over the period March 1st - August 31st 1990.

a) ditch A, b) ditch B, c) ditch C.

———— = C-assimilation, = C-influx.

CO₂-exchange across the air-water interface

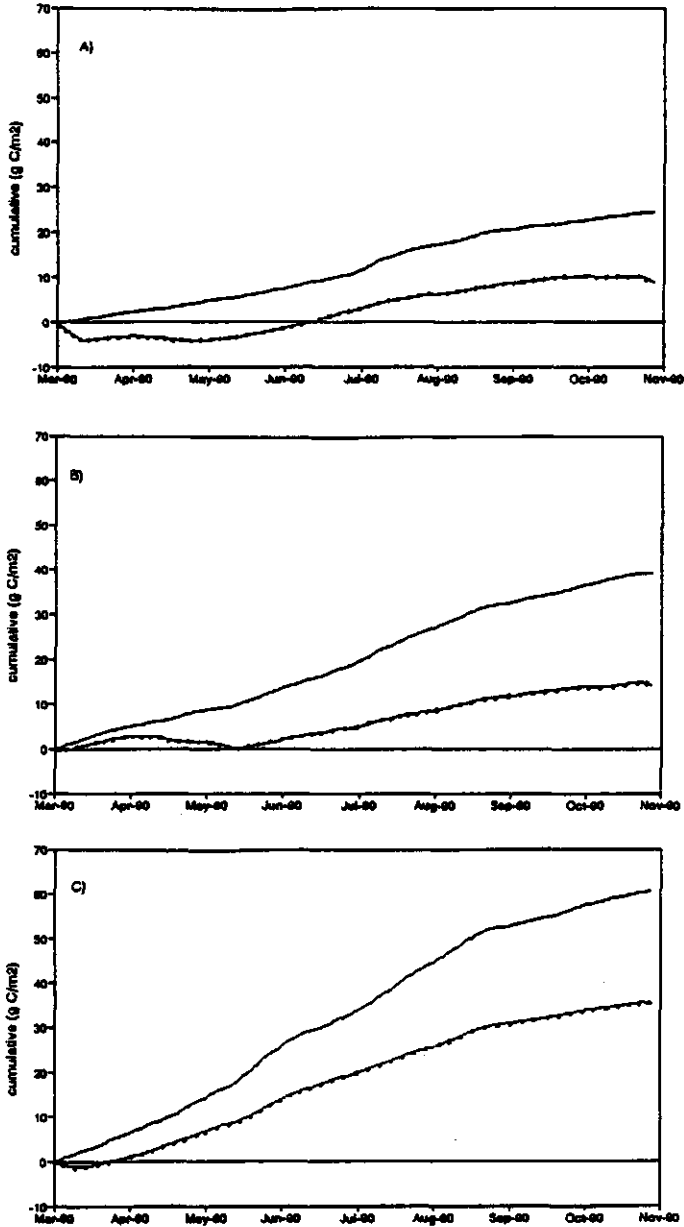


Figure 9.7. CO₂ influx and estimated net C-assimilation in the ditches dominated by benthic algae over the period March 1st - October 31st 1990.

a) ditch A, b) ditch B, c) ditch C

———— = C-assimilation, = C-influx.

CONCLUSIONS AND DISCUSSION

The calculated atmospheric C-influxes (see figures 9.3 a-d) show that at high pH there is a positive relation between DIC concentrations and the influx of atmospheric carbon. This implies a beneficial effect on primary production of high DIC concentrations in solution, as it increases the atmospheric carbon supply. As in a pH region of 8.5-10 most of the inorganic carbon is present as bicarbonate, this means a high compensation point, the concentration at which the net uptake rate (= uptake minus excretion) for HCO_3^- is zero. Allen and Spence (1981) found for a number of macrophyte species bicarbonate compensation points varying from 0.5-1.8 mM. Compensation points are susceptible to both short-term variations in time (in response to changing light, temperature and dissolved oxygen concentration) and to long-term seasonal variations (Maberly and Spence, 1983). In this study the bicarbonate concentration, as calculated from measured alkalinity and pH, was at maximum about 1.2 mM, and at minimum about 0.6 mM, with lower values during the summer.

The atmospheric carbon influx covered a relatively small, but substantial part of the carbon needs for assimilation in the ditches dominated by benthic algae. The cumulative atmospheric C-influx was related to the level of external N and P loading, with cumulative C-inputs of 8.7, 14.3 and 35.3 g C.m² in ditch A, B and C respectively over the period March-October 1990. The rest of the net C-assimilation was most probably derived from the sediments. Sedimentary CO₂ can serve as a complementary carbon source during periods in which atmospheric supply is insufficient (Boston et al., 1989; Raven, 1981). In spring, when the availability of recycled carbon from the sediments is higher, due to the dominance of decomposition and respiration over assimilation in autumn and winter, the relative contribution of atmospheric carbon was small in the ditches dominated by benthic algae. In ditch A it was even negative, due to oversaturation with CO₂. In the summer the

contribution of atmospheric carbon was generally higher. In the macrophyte dominated ditches the relative contribution of atmospheric carbon was greater than in the ditches dominated by benthic algae. This holds especially for ditch B and C, both dominated by *Elodea nuttallii*, which had a higher cumulative C-input over the period March-August 1990 (36.3 g C.m² in ditch B and 32.5 g C.m² in ditch C) than ditch A, which was dominated by *Chara* (18.4 g C.m²). For the use of sedimentary carbon by submerged macrophytes a short pathway from roots to leaves (< 0.20 m) seems a pre-requisite (Boston et al., 1989). Therefore sedimentary CO₂ is not economically beneficial for *Elodea nuttallii* in the summer, when it forms a dense vegetation near the water surface. The calculated atmospheric carbon flux from the atmosphere may have been underestimated due to higher pH bulk values immediately below the surface. During days of high productivity the pH can raise to values well over 10.5. Madsen and Sand-Jensen (1987) measured values of well over 11 in flow through systems with *Elodea canadensis* at bicarbonate concentrations ranging from 0.1-2.0 mM. Many species of macrophytes and phytoplankton can utilize bicarbonate, but a wide range of affinities exists (Allen and Spence, 1981). The mechanism of bicarbonate uptake by macrophytes involves extrusion of H⁺ on the lower sides of the leaves, which extracellularly converts HCO₃⁻ into H₂CO₃, and after dehydration CO₂ is transported across the cell membrane. On the upper side of the leaves OH⁻ is extruded (Prins et al., 1982). When these leaves are positioned immediately below the water surface, this will induce an enhancement of the atmospheric C-influx. In case CO₂ is the only carbon source and HCO₃⁻ cannot be taken up, the pH cannot raise beyond a certain point and as a result the atmospheric C-influx will be limited as well. Enhanced nutrient supply to N- or P-limited communities results in higher primary production. This results in a higher pH and thus has a positive effect on the atmospheric carbon input. Therefore C-limitation on one hand and N- or P-limitation on the other hand are not independent of each other, but

are to a certain extent interrelated. The atmospheric carbon supply to a system may determine the maximum primary production rate in eutrophied systems, especially in those that are dominated by submersed macrophytes.

The use of the Whitman film-model may have underestimated transport in the deeper part of the boundary layer. In this model a sharp transition between the ideally mixed bulk phase and the laminar boundary layer, with only molecular diffusion, is assumed. In reality, turbulent diffusion by eddies in the bulk phase is likely to gradually attenuate towards the air-water interface. The thickness of the boundary layer, as calculated from the measured mass transfer of a tracer and the film-model, therefore is a minimum value. In reality it is thicker, but with a higher effective diffusion coefficient in the deeper part of the boundary layer. However, no adequate experimental method to acquire accurate information on the in situ variation of the effective diffusion coefficient within the boundary layer, both in time and space, is available.

In this study the thickness of the stagnant boundary layer was calculated from a measured relationship between mass transfer across the air-water interface and ambient wind speed. This relationship is specific for the ditches used in this study. The mass transfer-wind dependency of any system will depend on several characteristics, e.g. its geometry, its exposure to the wind field. An error in this relationship affects both the cumulative net production estimated from continuous oxygen measurements (Portielje et al., 1994a) and the cumulative atmospheric C-influx.

ACKNOWLEDGEMENTS

The authors thank dr K. Kersting for the continuous pH measurements.

APPENDIX

SYMBOLS	DESCRIPTION	DIMENSIONS
fc	Acceleration factor	-
k1	Reaction rate of 1a), forwards	s ⁻¹
k1t	Reaction rate of 1a), backwards	s ⁻¹
k2	Reaction rate of 1b), forwards	moles ⁻¹ .m ³ .T ⁻¹
k2t	Reaction rate of 1b), backwards	
pCO ₂	Pressure of CO ₂ in atmosphere	atm
x	depth in boundary layer (x=0 at air-water interface)	m
z _i	Charge of ion i	eq
ALK	Alkalinity	eq.m ³
C _{tot}	Total DIC	moles.m ⁻³
C _{tot} [*]	Total DIC - free CO ₂	moles.m ⁻³
CO _{2,eq}	Equilibrium concentration of free CO ₂	moles.m ⁻³
C _i	Concentration of ion i	moles.m ⁻³
D _i	Diffusion coefficient of ion i	m ² .s ⁻¹
H	Henry's constant	moles.m ⁻³ .atm ⁻¹
J _i	Flux of ion i	moles.m ² .hr ⁻¹
K _L	Mass transfer rate	m.hr ⁻¹
U _i	Mobility of ion i	cm ² .mol ⁻¹ .J ⁻¹ .s ⁻¹
Z	Average water depth	m
α(0)	Fraction H ₂ CO ₃ [*] of total DIC	-
α(1)	Fraction HCO ₃ ⁻ of total DIC	-
α(2)	Fraction CO ₃ ⁼ of total DIC	-
δ	Thickness of boundary layer	m
λ ^o _i	Equivalent conductance of ion i	mho.cm ² .eq ⁻¹
F	Faraday	C.eq ⁻¹
R	Gas constant	J.°K ⁻¹ .mole ⁻¹

REFERENCES

- Adams, M.S., P. Guilizzoni and S. Adams, 1978. Relationship of dissolved inorganic carbon to macrophyte photosynthesis in some Italian lakes. *Limnol. and Oceanogr.* 23, 912-919.
- Allen, A.D. and D.H.N. Spence, 1981. The differential ability of aquatic plants to utilize the inorganic carbon supply in fresh waters. *New Phytol.* 87, 269-283.
- Ben-Yaakov, S., 1972. Diffusion of sea water in ions- I. Diffusion of sea water into a dilute solution. *Geochim. et Cosmochim. Acta* 36, 1395-1406.

- Boston, H.L., M.S. Adams and J.D. Madsen, 1989. Photosynthetic strategies and productivity in aquatic systems. *Aquatic Botany* 34, 27-57.
- Emerson, S. , 1975. Chemically enhanced CO₂ gas exchange in a eutrophic lake: A general model. *Limnol. and Oceanogr.* 20, 743-753.
- Drent, J. and K. Kersting, 1993. Experimental ditches for research under natural conditions. *Water Research* 27 (9), 1497-1500.
- Hoover, T.E. and D.C. Berkshire, 1969. Effect of hydration on carbon dioxide exchange across an air-water interface. *J. of Geophys. Res.* 74, 456-464.
- Kirk, J.T.O., 1983. Light and photosynthesis in aquatic ecosystems. University of Cambridge, 401 pp.
- Klemer, A.R., J. Feuillade and M. Feuillade, 1982. Cyanobacterial blooms: carbon and nitrogen limitation have opposite effects on buoyancy of *Oscillatoria*. *Science* 215, 1629-1631.
- Maberly, S.C. and D.H.N. Spence, 1983. Photosynthetic inorganic carbon use by freshwater plants. *J. of Ecology* 71, 705-724.
- Madsen, T.V. and K. Sand-Jensen, 1987. Photosynthetic capacity, bicarbonate affinity and growth of *Elodea canadensis* exposed to different concentrations of inorganic carbon. *Oikos* 50, 176-182.
- Portielje, R., K. Kersting and L. Lijklema, 1994a. Estimation of productivity by benthic algae from continuous oxygen measurements in relation to external nutrient input. *submitted to Water Research*.
- Portielje, R., K. Kersting and L. Lijklema, 1994b. Estimation of primary production in macrophyte dominated ditches from continuous dissolved oxygen signals. *submitted to Water Research*.
- Portielje, R. and L. Lijklema, 1994. The effect of reaeration and benthic algae on the oxygen balance of an artificial ditch. *accepted by Ecol. Modelling*.

- Prins, H.B.A., J.F.H. Snel, P.E. Zandstra and R.J. Helder, 1982. The mechanism of bicarbonate assimilation by the polar leaves of *Potamogeton* and *Elodea*. CO₂ concentrations at the leaf surface. *Plant. Cell and Environment* 5, 207-214.
- Raven, J.A., 1981. Nutritional strategies of submerged benthic plants: the acquisition of C, N and P by rhizophytes and haptophytes. *New Phytol.* 88, 1-30.
- Reid, R.C., J.M. Prausnitz and T.K. Sherwood, 1977. The properties of gases and liquids, 3rd ed. McGraw-Hill Inc., New York.
- Robinson, R.A. and R.H. Stokes, 1970. Electrolyte solutions, second edition. Butterworths, 571 pp.
- Sand-Jensen, K., 1989. Environmental variables and their effect on photosynthesis of aquatic plant communities. *Aquatic Botany* 34, 5-25.
- Schindler, D.W., G.J. Brunshill, S. Emerson, S. Broecker and T.H. Peng, 1972. Atmospheric carbon dioxide, its role in maintaining phytoplankton standing crop. *Science* 177, 1192-1194.
- Schurr, J.M. and J. Ruchti, 1977. Dynamics of CO₂ and O₂ exchange, photosynthesis and respiration in rivers from time-delayed correlations with ideal sunlight. *Limnol. and Oceanogr.* 22, 208-225.
- Sirs, J.A., 1958. Electrometric stopped flow measurements of rapid reactions in solutions. *Trans. of the Faraday Soc.* 54, 201-212.
- Stumm W. and J.J. Morgan, 1981. *Aquatic Chemistry*, second edition. Wiley Interscience, 780 pp.
- Welch, M.J., J.F. Lifton and J.A. Seck, 1969. Tracer studies with radioactive ¹⁵O. *J. Phys. Chem.* 73, 3351-3356.

Chapter 10

Summary

SUMMARY

Eutrophication of surface waters leads to a decline of water quality, which becomes manifest as an impoverishment of the aquatic community. Insight into the effects of eutrophication on the structure and functioning of these communities and knowledge on underlying interactions is needed to quantify the required reduction of nutrient input.

To investigate the effects of nutrient loading on the receiving water, it is important that environmental conditions that influence the response of a system to the level of nutrient input, are either controllable or measurable. This also holds for the initial conditions. These have to be identical to facilitate mutual comparison of different experimental systems.

In this research the effects of the level of nutrient loading are studied in experimental ditches. The emphasis on the internal cycling of phosphorus and the productivity of the system. With respect to scale, the ditches form a link between experimental set-ups in the laboratory and research on a full natural scale. In the first category the conditions can be well controlled, but extrapolation to a larger scale is often difficult, whereas in the second category the hydrology and environmental conditions cannot be controlled or measured with sufficient accuracy. Besides this, ditches also account for an important fraction of the Dutch surface waters.

Eight ditches have been used, four of which have sand as bottom material. The other four have a clayish sediment. Initially, all sand ditches were dominated by benthic algae, and had virtually no macrophytes. The clay ditches were dominated by submersed aquatic macrophytes. The initial nutrient contents in both sediment types were low. For each sediment type four different levels of external nitrogen and phosphorus input were established, varying from as low as possible to

extremely high. The levels are referred to as A (reference), B (second level), C (third level) and D (highest level).

In the clay-ditches the development of the macrophyte communities after the start of the nutrient loading programme has been monitored (see chapter 3). This concerns the species composition and the relative areal coverage of individual species. Initially the species composition was virtually identical. The ditches were dominated by Characeae, with areal coverage percentages of over 90% in all four. Gradually, the Characeae were replaced by *Elodea nuttallii* in all ditches, and the rate of the transition was positively related to the level of nutrient input. At the lowest level of nutrient input *Elodea* still exhibited a vertical growth strategy at the end of the investigation period, whereas at the two intermediate levels the growth strategy of *Elodea* was horizontal. Here it formed a dense vegetation near the water surface with areal coverage percentages of almost 100% during the summer period. In the highest loaded ditch *Elodea* was in turn replaced by *Lemna minor*, which forms a dense bed on the water surface during the summer. Later on, a generally terrestrial species (*Senecio congestus*) showed up as a pleustophyte. The location of the production zone remained in the bottom part of the water column in the reference ditch. It shifted to the top part of the water column at the second and third trophic state, and to the water surface (and above) at the highest trophic state.

In small systems the fluxes across the boundaries play a relatively large role. For gases the exchange between the air-water interface is important. This exchange is determined by the mass transfer coefficient, which depends on environmental conditions. In stagnant waters wind plays an important role. For the study of primary production the exchange of oxygen and carbon dioxide are of importance. Analysis of diurnal dissolved oxygen curves can provide information on the

productivity of the aquatic ecosystem. To be able to estimate primary production and oxygen consumption with sufficient accuracy, the reaeration term in the oxygen mass balance must be known.

Chapter 4 describes experiments in which mass transfer across the air-water interface as a function of wind speed is measured with the use of a tracer gas. The obtained wind-reaeration relationship is subsequently implemented in a model to simulate the dissolved oxygen concentration in the reference sand ditch. The other model parameters, describing primary production and oxygen consumption, were measured. This resulted in a fairly good agreement between measured and simulated dissolved oxygen during a period of four days.

Extrapolation to longer periods is not possible, as the values of the model parameters that describe primary production and oxygen consumption are not constant. To estimate primary productivity over longer periods, a parameter estimation routine was used to fit the oxygen model to measured daily oxygen curves. This was done for each individual day for a period of two years. Reaeration was again calculated from the wind-reaeration relationship. Gross production and oxygen consumption were subsequently estimated on a daily basis and as cumulatives over the two years period. Results are compared to the level of external nutrient loading.

The application of the model and parameter estimation routine to the sand-ditches are described in chapter 5, and in chapter 6 it is applied to the clay-ditches. Due to frequent and long-lasting anaerobia the method could not be applied to the highest loaded ditches (D) in both series.

In the sand-ditches, dominated by benthic algae, both gross and net production were positively related to the level of external nutrient input. In the reference ditch, the accumulation of dry weight in the layer of benthic algae, as calculated from the oxygen mass balance and the stoichiometry of the photosynthesis reaction, showed good agreement with the measured increase. At the second and third level the measured

accumulation was less than calculated.

For application of the method to the ditches dominated by macrophytes the model was extended to a two layer model for those periods during which steep vertical gradients in the dissolved oxygen concentration occurred. Those vertical gradients occurred during the summer periods when *Elodea nuttallii* formed a dense vegetation near the water surface. Each layers is supposed to be ideally mixed. Due to the strong vertical attenuation of light, primary production is assumed to occur exclusively in the top layer. In the bottom layer only oxygen consumption, resulting from respiration, decomposition and sediment oxygen demand, occurs. The exchange between the top and bottom layer is driven by the vertical concentration gradient.

The cumulative gross production is again positively related to the nutrient input. Cumulative net production shows an irregular pattern. Initially it was the highest in ditch C, but during the second year the cumulative net production declined in this ditch due to an increased oxygen consumption.

In the clay-ditches total gross production was smaller in the second than in the first year, whereas in the sand-ditches this was the other way round.

In case of an enhanced phosphate loading to an oligotrophic system, the sediment can take up a considerable part of the extra phosphate. The flux of phosphate from the water column to the sediment consists of the settling of particulate P, and a diffusive exchange of dissolved P between the water column and the interstitial water. The driving force for the diffusive exchange is a vertical concentration gradient. After enhanced phosphate input to the overlying water, the vertical concentration in the interstitial water is negative with depth, due to the sorption of P by sediment particles. The transport of ions along the concentration gradient is proportional to the effective dispersion coefficient D_{eff} , which is the sum of molecular diffusion D_{mol} , bioirrigation D_{bio} , and a

dispersion term D_{dis} . The latter results from pressure gradients, induced by formation of waves by wind stress at the water surface, resulting in an oscillating horizontal flow. Due to the presence of particles this flow has a vertical component which becomes manifest as an additional dispersion term D_{dis} in the sediment. It is at maximum at the sediment-water interface and attenuates with depth in the sediment. D_{dis} varies on a small time-scale due to variations in wave length and amplitude. In this study, and generally in shallow waters, D_{dis} at the surface boundary dominates in D_{eff} , and can be one to two orders of magnitude larger than D_{mol} . A sediment model that describes the diffusive transport of dissolved phosphorus from the overlying to the interstitial water and subsequent sorption by the sediment particles (see chapter 7), was calibrated on a measured vertical concentration profile in the porewater, almost two years after the start of the nutrient loading program. The results indicate that for this period D_{eff} at the sediment-water interface was on average about 35 times D_{mol} .

The sorption of phosphate by the sediment particles contains a fast reversible step, which is adsorption onto the surface of the particles, and is followed by a slow step. The latter can be described as an internal diffusion of adsorbed P into the solid phase. This solid phase was modelled as a coating of metal(hydr)oxides (in this study the metal was mainly aluminum) surrounding the sand particles. Removal of the coating resulted in a virtually complete disappearance of the ability of the particles to sorb P. From experiments in which the coating was dissolved and subsequent (co)-precipitated with phosphate, it was estimated that the total sorption capacity of the whole coating was about 3.3 times the maximum surficial adsorption capacity. Diffusion into the solid phase can be described analogous to diffusion in a fluid. The diffusion coefficient of phosphate in the Al-(hydr)oxide coating, experimentally estimated from the kinetics of phosphate sorption, was $2.7 \cdot 10^{-19} \text{ m}^2 \cdot \text{day}^{-1}$, which is between 10^{-14}

and 10^{15} times the molecular diffusion coefficient of phosphate in water. This shows that solid phase diffusion is a slow process. It has a time scale of several months. For the long term storage of phosphate in the sediment it is important, as ultimately ca. 70 % of the phosphate is internally stored in the metal-(hydr)oxide coating.

After a phosphate dosage to the sand-ditches part of the added phosphate is rapidly taken up by the benthic algae. The uptake is in excess of the amount immediately needed for the assimilation of cell material. The kinetics of this phosphate uptake can be described well as a first order process (see chapter 8). The internal P-deficit, defined as the difference between the maximum and the actual internal P content of the cells, is the driving force. The first order uptake rate did not differ among three benthic populations, previously exposed to different levels of external nutrient loading (from the sand-ditches A, B and C). The maximum internal P concentrations $P_{int,max}$ on the other hand were positively related to the trophic state, indicating mechanisms that regulate the phosphate storage capacity. The additional uptake capacity, i.e the initial P deficit, was smaller after exposure to higher levels of nutrient loading, but is somewhat extensible due to adaptation of $P_{int,max}$. This has consequences for the long term stability of dominance by benthic algae. An upward movement of the production zone from the sediment top layer to the water column can occur when the nutrient availability in the water column is enhanced. This means that the uptake capacity of the benthic algae and sediment must have become insufficient to compensate for the external nutrient input.

An increased productivity, and concomitantly an upward movement of the production zone, following enhanced nutrient loading, results in an enhancement of the carbon dioxide flux from the atmosphere. At high pH values the concentration of free $CO_2(aq)$ is generally lower than the equilibrium

concentration following from its solubility. Due to chemical equilibrium reactions the concentration gradient in the boundary layer is steeper near the air-water interface, than it would be due to purely physical processes. This results in an enhanced CO_2 mass transfer across the air-water interface compared to that of a chemical inert gas. The acceleration factor depends on pH, thickness of the laminar boundary layer, total inorganic carbon and temperature. With a model that calculates the acceleration factor from these variables, the atmospheric carbon dioxide flux and its contribution to the net carbon assimilation have been estimated (see chapter 9). The cumulative flux during the growth season increased with increasing levels of nutrient loading in the ditches dominated by benthic algae. From the ditches dominated by submersed macrophytes, the two ditches dominated by *Elodea nuttallii* (ditch B and C) had similar cumulative C-fluxes. These were estimated at 85 and 97 % of the cumulative net C assimilation during the same period, indicating the importance of atmospheric CO_2 for the carbon supply of these communities. In the ditch dominated by Characeae (ditch A), this fraction smaller.

The fraction of the net C assimilation during the growth season that was covered by the atmospheric C-influx was substantially less in the ditches dominated by benthic algae than in the ditches with macrophytes.

SAMENVATTING

Eutrofiëring van oppervlaktewateren leidt tot een achteruitgang van de waterkwaliteit, die zich manifesteert in een verarming van aquatische leefgemeenschappen. Om inzicht te krijgen in de effecten van eutrofiëring op de structuur en het functioneren van deze levensgemeenschappen, en om te komen tot een goede onderbouwing van beheersmaatregelen die de instroom van nutriënten in oppervlaktewateren moeten indammen, is kennis van de onderliggende interacties noodzakelijk.

Voor de interpretatie van onderzoeksresultaten naar het effect van het nivo van de nutriëntenbelasting, is het van belang dat de omgevingscondities, die de respons van het systeem op het nivo van de nutriëntenbelasting mede beïnvloeden, zoveel mogelijk beheersbaar, dan wel meetbaar zijn. Dit geldt ook voor de initiële condities. Deze moeten, om onderlinge vergelijking mogelijk te maken, voor de verschillende deelsystemen zoveel mogelijk identiek zijn.

In deze studie is onderzoek uitgevoerd naar het effect van het nivo van de externe nutriëntenbelasting op de respons van het ontvangende systeem, met nadruk op de interne cyclus van fosfor en de produktiviteit van het ontvangende systeem. Het onderzoek is uitgevoerd in proefsloten. Wat betreft de schaal vormt onderzoek in proefsloten een schakel tussen onderzoek op laboratoriumschaal en onderzoek onder volledig natuurlijke omstandigheden. In de eerste categorie zijn de omstandigheden goed controleerbaar, maar is extrapolatie naar grootschaliger systemen dikwijls zeer moeilijk. In de tweede categorie zijn de omstandigheden veelal niet controleerbaar of voldoende nauwkeurig meetbaar. Bovendien maken slootsystemen een belangrijk deel uit van de Nederlandse oppervlaktewateren.

Er zijn acht sloten gebruikt. Vier daarvan hebben een zandbodem, de andere vier een kleibodem. De zandsloten werden alle

initieel gedomineerd door benthische algen, en bevatten vrijwel geen macrofyten. De kleislotten werden gedomineerd door ondergedoken waterplanten. De oorspronkelijke nutriëntengehalten van beide sedimenttypen waren laag. Per bodemtype zijn vier nivo's van externe belasting met N en P vastgesteld, variërend van zo laag mogelijk tot extreem hoog. De vier nivo's worden aangeduid met A (referentie), B (tweede nivo), C (derde nivo) en D (hoogste nivo).

In de kleislotten is de ontwikkeling van de vegetatie na de start het programma m.b.t. de externe nutriëntentoevoer gevolgd (zie hoofdstuk 3). Dit betreft de soortensamenstelling en de relatieve bedekkingsgraad van individuele soorten. Initieel was de soortensamenstelling vrijwel identiek. De gemeenschappen werden gedomineerd door Characeae, met bedekkingspercentages van meer dan 90 % in alle sloten. Sindsdien zijn de Characeae in alle sloten verdrongen door *Elodea nuttallii*. De snelheid van deze overgang was positief gerelateerd aan het belastingsnivo. In de referentiesloot vertoonde *Elodea* aan het einde van de onderzochte periode nog steeds een verticale groei strategie, terwijl deze bij het tweede en derde belastingsnivo horizontaal was. Hier vormde ze een hechte vegetatie nabij het wateroppervlak, met een bedekkingsgraad van bijna 100 % gedurende de zomerperioden. Op het hoogste belastingsnivo is *Elodea* op zijn beurt verdrongen door *Lemna minor*, dat gedurende de zomerperiode een vrijwel gesloten bed op het wateroppervlak vormt. Later verscheen een in het algemeen terreestische soort (*Senecio congestus*) als pleustofyt. In de sloot A bleef de produktieve zone in het onderste deel van de waterkolom. Ze verschoof bij het tweede en derde nivo naar de toplaag van de waterkolom, en bij het hoogste nivo naar op en boven het wateroppervlak.

In kleine watersystemen spelen de systeemgrenzen een relatief grote rol. Voor gassen is de uitwisseling tussen de waterkolom en de atmosfeer van groot belang. De evenredigheidsfactor die

deze uitwisseling bepaalt is de stofoverdrachts-coëfficiënt, die afhangt van omgevingscondities. In stagnante wateren is de windsnelheid van grote invloed. Voor de bestudering van primaire produktie is met name de uitwisseling van zuurstof en kooldioxide van belang. Analyse van gemeten zuurstofcurven verschaft informatie over de produktiviteit van een aquatisch ecosysteem. Om primaire produktie en afbraak (zuurstofverbruik) nauwkeurig te kunnen schatten, is kwantificering van de reaëratie van groot belang.

In hoofdstuk 4 worden experimenten beschreven waarin de stofoverdrachtcoëfficiënt in relatie tot de windsnelheid is gemeten m.b.v. een tracergas. De verkregen relatie is vervolgens geïmplementeerd in een model waarmee de zuurstofhuishouding van zandsloot A gesimuleerd is. De overige modelparameters, die primaire produktie en zuurstofverbruik beschrijven, zijn gemeten. Dit resulteerde in een goede overeenkomst tussen gemeten en gesimuleerd zuurstofverloop gedurende een periode van vier dagen.

Extrapolatie naar langere perioden is echter niet mogelijk, daar de parameters die produktiviteit en zuurstofverbruik beschrijven kunnen variëren. Om de produktiviteit over langere perioden te kunnen kwantificeren is gebruik gemaakt van een parameterschattingsmethode waarmee het zuurstofmodel gefit wordt op gemeten dagelijkse zuurstofcurven. Dit is gebeurd voor alle individuele dagen gedurende een periode van twee jaar. Reaëratie is wederom berekend m.b.v. de wind-reaëratie relatie. Vervolgens zijn bruto produktie en zuurstofconsumptie per dag berekend, en als cumulatieven over de gehele periode van twee jaar. De resultaten zijn gerelateerd aan het nivo van de nutriëntenbelasting.

Hoofdstuk 5 beschrijft de toepassing van het model en de parameterschattingsmethode op de zandsloten. Hoofdstuk 6 doet hetzelfde voor de kleislotten. Door regelmatige en dikwijls langdurige anaërobie kon de methode niet toegepast worden op de hoogst belaste sloten (D) van beide series.

In de zandsloten, gedomineerd door benthische algen, zijn

zowel de bruto als de netto produktiviteit positief gerelateerd aan het nivo van de externe nutriëntenbelasting. In zandsloot A kwam de uit de zuurstofbalans en de stoichiometrie van de fotosynthesereactie berekende gewichtstoename in de benthische laag goed overeen met de gemeten toename; in de zandsloten B en C was de gemeten toename kleiner dan berekend. Voor toepassing op de sloten gedomineerd door macrophyten is, in geval van sterke verticale zuurstofgradiënten, het model uitgebreid tot een twee lagen model. Deze verticale gradiënten kwamen voor tijdens de zomerperioden, wanneer *Elodea* een dichte vegetatie vormde in de toplaag van de waterkolom (met name in kleisloot B). Elke laag wordt verondersteld ideaal gemengd te zijn. Op grond van de sterke verticale uitdoving van licht wordt verondersteld dat primaire produktie uitsluitend in de toplaag plaatsvindt. In de onderlaag vindt alleen zuurstofconsumptie (respiratie, decompositie en sediment zuurstof verbruik) plaats. De drijvende kracht van de uitwisseling tussen boven- en onderlaag is de verticale zuurstofgradiënt. De cumulatieve bruto produktie is wederom positief gerelateerd aan de nutriëntenbelasting. De cumulatieve netto produktiviteit vertoont echter een onregelmatig beeld. Aanvankelijk was deze het hoogst in kleisloot C, maar tijdens het tweede jaar nam de cumulatieve netto produktie hier sterk af t.g.v. een toegenomen zuurstofconsumptie.

In de sloten gedomineerd door macrophyten was de bruto produktiviteit gedurende het tweede jaar kleiner dan gedurende het eerste jaar, terwijl dit in de sloten gedomineerd door benthische algen juist andersom was.

Na een toename van de externe fosfaatbelasting op een oligotroof systeem, kan het sediment een belangrijk deel van het extra fosfaat opnemen. De P-flux van het water naar het sediment bestaat zowel uit particulier P, in de vorm van sedimentatie van deeltjes en het daaraan gebonden fosfaat, als uit opgelost P, in de vorm van een diffusieve uitwisseling tussen het bovenstaande en het interstitieel water. De

drijvende kracht voor de diffusieve uitwisseling is een verticale concentratiegradiënt. Na een toegenomen fosfaatbelasting van het bovenstaande water, zal de concentratie in het interstitieel water lager zijn dan die in het bovenstaande water door de sorptie van P aan bodemdeeltjes. Het transport van ionen langs de concentratiegradiënt is evenredig aan de effectieve dispersiecoëfficiënt D_{eff} , die gelijk is aan de som van moleculaire diffusie D_{mol} , bioirrigatie D_{bio} en een dispersieterm D_{dis} . De laatste wordt veroorzaakt door drukgradiënten. Golfvorming aan het wateroppervlak, veroorzaakt door wind, induceert een horizontale drukgradiënt die een horizontale oscillerende beweging aan en vlak onder het grensvlak tot gevolg heeft. Deze stroming leidt in het sediment, door de aanwezigheid van deeltjes, tot een verticale fluctuerende stroming die zich als dispersie manifesteert. Ze is maximaal is aan het sediment-water grensvlak, en neemt af met de diepte in het sediment. Deze D_{dis} varieert op korte tijdschaal door variaties in golflengte en -amplitude. In de proefsloten, en in het algemeen in ondiepe wateren, is D_{dis} veelal de belangrijkste component van D_{eff} , en kan een tot twee orden van grootte hoger zijn dan D_{mol} . Een sediment model dat de diffusieve uitwisseling van opgelost fosfaat tussen het bovenstaande water en het sediment en de daarop volgende sorptie aan de bodemdeeltjes beschrijft (hoofd-stuk 7), is gecalibreerd op het gemeten verticale concentratieprofiel in het interstitieel water, bijna twee jaar na de start van de nutriëntenbelasting. Gedurende deze periode was de effectieve dispersiecoëfficiënt aan het sedimentoppervlak gemiddeld 35 maal D_{mol} .

De sorptie van fosfaat aan sedimentdeeltjes bestaat uit een snelle reversibele stap, die een oppervlakkige adsorptie aan de deeltjes betreft, en een daaropvolgende langzame stap. De laatste betreft de inwendige diffusie van het oppervlakkig geadsorbeerde fosfaat in de vaste fase. Deze vaste fase kan worden voorgesteld als een coating van metaal(hydr)oxiden (in dit geval voornamelijk aluminium), die de zanddeeltjes

omgeeft. Verwijdering van deze coating resulteerde in het vrijwel volledig verdwijnen van het vermogen om fosfaat te adsorberen. Vanuit experimenten waarbij de coating opgelost is, en vervolgens met fosfaat wederom ge(co-)-precipiteerd, is de maximale sorptiecapaciteit van de gehele coating geschat op 3.3 maal de maximale oppervlakkige adsorptiecapaciteit. Diffusie in de vaste fase kan beschreven worden analoog aan diffusie in een vloeistof. De diffusiecoëfficiënt van fosfaat in de Al-(hydr)oxide coating, experimenteel bepaald uit de kinetiek van de fosfaatsorptie, was $2.7 \cdot 10^{-19} \text{ m}^2 \cdot \text{dag}^{-1}$, hetgeen 10^{-14} tot 10^{-15} maal die in water is. Dit maakt dat vaste fase diffusie een traag proces. Het heeft een tijdschaal van enkele maanden. Voor de oplading van de zandbodem met fosfaat op lange termijn is het een belangrijk proces, daar uiteindelijk ca. 70% van het opgeslagen fosfaat inwendig vastgelegd wordt in de coating.

Na een fosfaat dosering aan de zandsloten wordt een deel van het toegevoegde fosfaat snel opgenomen door de benthische algen. Deze opname overtreft de hoeveelheid die direkt benodigd is voor de assimilatie van celmateriaal. De kinetiek van deze fosfaatopname kan goed beschreven worden als een eerste orde proces (zie hoofdstuk 8). Het interne P-deficiet, gedefinieerd als het verschil tussen het maximale en het actuele interne P-gehalte, is de drijvende kracht. De eerste orde opnamesnelheden van een drietal benthische populaties, die voorheen blootgesteld waren aan verschillende externe nutriëntenbelastingen (afkomstig uit de referentie, tweede nivo en derde nivo zandsloten) verschilden niet significant. De maximale interne P-gehalten waren positief gerelateerd aan de externe nutriëntenbelasting, hetgeen duidt op mechanismen die de fosfaat opslagcapaciteit aanpassen aan de trofiegraad. De additionele opnamecapaciteit, ofwel het initiële P-deficiet, was kleiner bij hogere fosfaatbelastingen, maar is door dit mechanisme enigszins rekbaar. Dit heeft gevolgen voor de stabiliteit van dominantie door benthische algen. Een

verschuiving van de produktieve zone van de bodemtoplaag naar de waterkolom, zal dan optreden wanneer de nutriëntenbeschikbaarheid in de waterkolom verbetert. Dit houdt in dat de opnamecapaciteit van benthische algen en sediment onvoldoende moet zijn om de externe nutriëntentoevoer te compenseren.

Een verhoogde produktiviteit, en een daarmee gepaard gaande opwaartse verplaatsing van de produktieve zone, resulteert in een verhoging van de kooldioxideflux vanuit de atmosfeer. Bij hoge pH is de concentratie van vrij CO_2 in het algemeen lager dan de evenwichtsconcentratie met de atmosfeer, die volgt uit de oplosbaarheid van het gas. Bovendien is de concentratiegradiënt van CO_2 in de laminaire grenslaag tussen water en atmosfeer steiler t.g.v. chemische evenwichtsreacties dan ingeval uitsluitend fysisch transport zou optreden. Hierdoor treedt een versnelling in de uitwisseling van kooldioxide op t.o.v. die van een chemisch inert gas. De versnellingsfactor hangt af van de pH, het totaal anorganisch koolstofgehalte, de dikte van de laminaire grenslaag en de temperatuur. Met behulp van een model dat de versnellingsfactor en de atmosferische C-flux berekent, is haar bijdrage aan de netto C-assimilatie gedurende een groeiseizoen geschat (zie hoofdstuk 9). In de sloten gedomineerd door benthische algen neemt de cumulatieve flux gedurende een groeiseizoen toe met toenemende nutriëntenbelasting. In de sloten gedomineerd door ondergedoken waterplanten, was de cumulatieve koolstofflux in de twee sloten gedomineerd door *Elodea nuttallii* (kleisloot B en C) ongeveer even groot, en bedroeg respectievelijk 85 en 97 % van de geschatte cumulatieve C-assimilatie gedurende dezelfde periode. Dit geeft aan dat atmosferische kooldioxide een aanzienlijke bijdrage levert aan de koolstofvoorziening van deze systemen. In de sloot gedomineerd door Characeae (kleisloot A) was deze bijdrage lager.

In de sloten gedomineerd door benthische algen was de fractie van de netto C-assimilatie gedurende het groeiseizoen die

gedekt wordt door de atmosferische koolstof flux aanzienlijk kleiner dan in de sloten met waterplanten.

ABSTRACT

Eutrophication has since long been a major concern in water quality management. Eutrophication control primarily involves a reduction of the external input of nutrients. The relationship between the external nutrient input and the response of shallow, stagnant aquatic ecosystems were investigated in experimental ditches with two sediment types: clay and sand. Particularly the following subjects were adressed:

- The composition of the macrophytes communities in time and the effects of the loading rate on the primary succession rate.
- The effects of the loading rate on gross and net primary production: these were estimated from a model describing dissolved oxygen, using continuous oxygen measurements and a parameter estimation routine. Reaeration was calculated from a measured relationship between wind speed and the mass transfer coefficient, derived from experiments with a tracer gas (ethylene).
- The role of sediment uptake: a deterministic model was developed to describe sediment uptake in a ditch with a sandy sediment, with emphasis on transport mechanisms and sorption by the sediment particles. The effective vertical dispersion coefficient at the interface is mainly determined by dispersion resulting from horizontal pressure gradients caused by wind stress. Sorption of phosphate by the sand particles involves a fast step (adsorption onto a coating of mainly Al-(hydr)oxides on the surface) and a slow step, which can be described as solid-phase diffusion into the coating.
- The capacity and kinetics of phosphate uptake by benthic communities in which algae dominated: the maximum internal P concentration was positively related to the trophic state and the uptake exhibited first-order kinetics.
- The flux of carbon dioxide across the air-water interface as a function of pH, alkalinity, temperature and wind speed: calculated fluxes were compared to the cumulative net production as estimated from the oxygen model, and were shown to be positively related to the level of external nutrient input.

Key-words:

eutrophication - experimental ditches - nutrient loading - phosphorus - primary production - reaeration - sediments

DANKWOORD

Het doen van wetenschappelijk onderzoek en het schrijven van een proefschrift is niet mogelijk zonder de hulp van velen.

Als eerste dank ik mijn promotor, Bert Lijklema, voor zijn enthousiasme en toewijding bij de begeleiding van dit onderzoek. Hij heeft mij een ruime vrijheid gegeven bij de invulling en uitvoering van mijn onderzoek, en zijn opbouwende kritiek was van grote waarde.

Rudi Roijackers dank ik voor zijn bijdrage aan de onderzoeksopzet, en voor zijn bijdrage aan het totstandkomen van hoofdstuk 3, en het kritisch doornemen van het manuscript.

Jan Drent dank ik voor zijn vele inspanningen m.b.t. de organisatie en operationele zaken rond het proefslotencomplex 'De Sinderhoeve', en voor de nauwe en prettige samenwerking bij het opzetten en uitvoeren van het onderzoek.

Kees Kersting en de overige betrokken medewerkers van het IBN in Leersum dank ik voor het vergaren van de gigantische datasets die voor dit onderzoek gebruikt zijn. Al jarenlang worden continue metingen uitgevoerd in de proefsloten. Tevens dank ik Kees Kersting voor de prettige samenwerking die heeft geleid tot het tot stand komen van de hoofdstukken 5 en 6.

Arie van Heesen bedank ik voor zijn zorgen rondom het dagelijks beheer van 'De Sinderhoeve', en Antoni van de Toorn en Jaap Pankow voor de samenwerking bij bemonsteringen en voor het uitvoeren van het programma m.b.t. het toedienen van nutriënten aan de sloten.

Hans Aalderink dank ik voor zijn adviezen en ter beschikking gestelde kennis m.b.t. de analyse van continue zuurstofsignalen, en voor het kritisch doorlezen van hoofdstuk 4.

Theo IJwema, Fred Bransen en Frits Gillissen dank ik voor hun diverse inspanningen op het lab, de laatste met name voor het beheer van de auto-analyser. Voorts dank ik de studenten Ingrid Bremmer en Claire Holland.

Alle collega's van de (voormalige) vakgroep Natuurbeheer en de huidige vakgroep Waterkwaliteitsbeheer en Aquatische Oecologie dank ik voor de prettige tijd en een leuke werksfeer.

Mijn ouders en verdere familie dank ik voor hun steun en meelevens.

LIST OF PUBLICATIONS

- Portielje, R. and L. Lijklema (1993). Sorption of phosphate by sediments as a result of enhanced external loading. *Hydrobiologia* 253, 249-261.
- A.A. Koelmans, L. Lijklema and R. Portielje (1993). Water quality impacts of sediment pollution and the role of early diagenesis. *Wat. Sci. Tech.* 28 (8/9), 1-12.
- Portielje, R. and L. Lijklema (1994). Kinetics of luxury uptake of phosphate by algae-dominated benthic communities. *Hydrobiologia* 275/276, 349-358.
- Portielje, R. and L. Lijklema. The effect of reaeration and benthic algae on the oxygen balance of an artificial ditch. (accepted for publication by *Ecological Modelling*)
- Portielje, R. and R.M.M. Roijackers. Primary succession of aquatic macrophytes in experimental ditches in relation to nutrient input. (submitted for publication to *Aquatic Botany*)
- Portielje, R. and L. Lijklema. Carbon dioxide fluxes across the air-water interface and its impact on carbon availability in aquatic systems. (submitted for publication to *Limnology and Oceanography*)
- Portielje, R. K. Kersting and L. Lijklema. Estimation of productivity from continuous oxygen measurements in ditches dominated by benthic algae in relation to the level of external nutrient input. (submitted for publication *Water Research*)
- Portielje, R. K. Kersting and L. Lijklema. Estimation of primary production in macrophyte dominated ditches from continuous oxygen signals. (submitted for publication to *Water Research*)
- De Best, J., H.J. Danen-Louwerse, R. Portielje and L. Lijklema. Reduction of artificial iron(III)-phosphate complexes by hydroxylammonium chloride. (submitted for publication to *Water Research*)

CURRICULUM VITAE

Robert Portielje werd geboren op 14 september 1964 te Rotterdam. In juni 1982 werd het Gymnasium-B diploma behaald aan het Erasmiaans Gymnasium te Rotterdam. Van 1982 tot 1988 studeerde hij Milieuhygiëne aan de Landbouwhogeschool (vanaf 1986 Landbouwniversiteit) te Wageningen, met als specialisatie Waterkwaliteitsbeheer. Gedurende deze studie, van 1 februari tot 1 juli 1988, liep hij stage aan het Limnologisch Veldlaboratorium van het EAWAG in Kastanienbaum, Zwitserland. Het ingenieursdiploma werd behaald in september 1988.

Van november 1988 tot november 1992 werkte hij als Assistent in Opleiding aan onderzoek naar de effecten van eutrofiëring op oppervlaktewater, waarvan dit proefschrift het resultaat is. Het onderzoek werd uitgevoerd in dienst van de Sectie Waterkwaliteitsbeheer (eerst als onderdeel van de Vakgroep Waterzuivering; sinds mei 1989 als onderdeel van de Vakgroep Natuurbeheer).

Van 1 januari 1993 tot 15 augustus 1993 werkte hij, achtereenvolgens als plaatsvervangend Universitair Docent en als projectmedewerker in dienst van de Sectie Waterkwaliteitsbeheer van de Vakgroep Natuurbeheer aan verschillende projecten op het gebied van waterkwaliteitsmodellering.

18 OKT. 1994

UB-CARDEX

STELLINGEN

- 1 In ondiepe watersystemen is de beschikbaarheid van koolstof voor fotosynthese gerelateerd aan die van stikstof en fosfor
(dit proefschrift)
- 2 Het gebruik van de instantane sorptiecapaciteit van sedimenten met betrekking tot fosfaat voor de berekening van de ontwikkeling van de P-distributie in het sediment op lange termijn levert aanzienlijke fouten op
(dit proefschrift)
- 3 Het slecht experimenteel kwantificeerbaar zijn van een parameter zegt niets over de juistheid van de modelbeschrijving waarin deze parameter is opgenomen
- 4 De Europese eenwording zal slechts dan succesvol kunnen zijn wanneer de besluitvorming niet vertroebeld wordt door te vereffenen oude rekeningen
- 5 In de ecologie leidt het vervangen van de vraagstelling 'hoe werkt iets?' door 'hoe zou iets moeten werken, om optimaal te functioneren?' veelal op snellere wijze tot hetzelfde resultaat
- 6 Het ontstuimige verloop van de democratisering in voorheen door dictatuur geregeerde landen, is vergelijkbaar met de traagheid die de slinger van een klok doet doorslaan naar de andere zijde
- 7 De veronderstelling levend bij een groot aantal wetenschappers dat natuurlijke processen geheel te verklaren zijn uit de thans bekende natuurwetten, is, mede gezien de snelle ontwikkelingen in het recente verleden, voorbarig.
- 8 Om de objectiviteit van de beoordeling van ter publicatie aangeboden wetenschappelijke manuscripten te bevorderen, zou het recht op anonimiteit van referee naar auteur ook in omgekeerde richting moeten gelden
- 9 Een afname van de verhouding tussen het aantal werkenden en het aantal niet werkenden nu t.o.v. die van enige decennia geleden, zegt op zich niets over het vermogen van het productieapparaat om in de behoeften van de gehele bevolking te voorzien
- 10 Productie dient om in een behoefte te voorzien, en produkten waarvoor (door middel van reclame) de behoefte gecreëerd moet worden, zijn derhalve overbodig

Stellingen behorende bij het proefschrift van R. Portielje:
Response of shallow aquatic ecosystems to different nutrient loading levels.

Wageningen, 19 oktober 1994.